NASA Contractor Report 178061

NASA-CR-178061
19860019501

Near-Field Testing of the 15-Meter Model of the Hoop Column Antenna

Volume III— Near- and Far-Field Plots for the JPL Feed Final Report

Martin Marietta Denver Aerospace
Denver, CO 80201

Contract NAS1-18016
March 1986

NASA
National Aeronautics and Space Administration

Langley Research Center
Hampton, Virginia 23665

86N28973*# ISSUE 20 PAGE 3136 CATEGORY 15 RPT#: NASA-CR-178061 NAS 1.26:178061 MCR-85-640-VOL-3 CNT#: NAS1-18016 86/03/00 147 PAGES
UNCLASSIFIED DOCUMENT
UTTL: Near-field testing of the 15-meter model of the hoop column antenna. Volume 3: Near- and far-field plots for the JPL feed
AUTH: A/HOOVER, J.; B/KEFAUVER, N.; C/CENCICH, T.; D/OSBORN, J.
CORP: Martin Marietta Corp., Denver, CO.
SAP: Avail: NTIS HC A07/MF A01
CIO: UNITED STATES
MAJS: /*ANTENNA RADIATION PATTERNS/*HOOP COLUMN ANTENNAS/*LARGE SPACE STRUCTURES /*PARABOLIC ANTENNAS
MINS: / ANTENNA DESIGN/ GOLD/ MOLYBDENUM/ PERFORMANCE TESTS/ WIRE CLOTH
ABA: Author

MCR-85-640
Contract No. NAS1-18016

Volume III

Final
Report

March 1986

Near- and Far-Field Plots
for the JPL Feed

NEAR-FIELD TESTING OF THE 15-METER MODEL OF THE HOOP COLUMN ANTENNA

To

NASA Langley Research Center
Antenna and Microwave Research Branch

Authors:

John Hoover
Neill Kefauver
Tom Cencich

Jim Osborn
Program Manager and Author

Joe Osmanski
Manager
Environmental & Test Technologies

MARTIN MARIETTA
DENVER AEROSPACE
P.O. Box 179
Denver, Colorado 80201

FOREWORD

This report, prepared by Martin Marietta Denver Aerospace, is submitted to the NASA Langley Research Center, Antenna and Microwave Research Branch, in response to Contract No. NAS1-18016, Near-Field Testing of the 15-Meter Model of the Hoop Column Antenna, CDRL Line Item I.D. Our report consists of three volumes:

Volume I Technical Report

Volume II Near- and Far-Field Plots for the L&RC Feeds

Volume III Near- and Far-Field Plots for the JPL Feed

CONTENTS

Figures

Tables

GLOSSARY

HCA	Hoop Column Antenna
JPL	Jet Propulsion Laboratory
LaRC	NASA Langley Research Center
LHCP	Left-Hand Circularly Polarized
NFTL	Near-Field Test Laboratory
RHCP	Right-Hand Circularly Polarized

1.0 INTRODUCTION

This report is Volume III in a three-volume final report for Contract NAS1-18016 between NASA Langley Research Center and Martin Marietta Denver Aerospace. The contract, "Near-Field Testing of the 15-Meter Model of the Hoop Column Antenna," calls for a series of tests on this antenna based on a predetermined test plan. The contract had two objectives: to demonstrate that high-performance space-deployable antennas can be built and to demonstrate that the antenna performance can be accurately measured. Data contained in the report show that these objectives have been achieved.

Because of the extensive data produced by the program the report has been divided into three volumes. During the tests, NASA Langley Research Center (LaRC) and the Jet Propulsion Laboratory (JPL) supplied feed systems for the antenna, the basis for dividing the report. Under this division, each volume provides different data to the total report. Volume I, the technical summary, contains information essential to achievement of the test objectives; Volume II contains a complete set of graphical data using the LaRC feeds; Volume III contains corresponding data on the JPL feed.

Many types of tests were performed in the Near-Field Test Laboratory (NFTL). They included optical/electrical measurements of surface trueness, acceleration measurements of mechanical stability, and electrical measurements of the radiation performance of the antenna. This volume covers the data obtained from the electrical tests of the JPL feed. This feed was based on a previous design by JPL to meet the requirements of the Land Mobile Satellite System. The measurements performed on the JPL feed at the NFTL should not be considered a test of the reflector performance, which was already established using the feeds provided by LaRC.

This volume follows the test plan of the JPL feed chronologically. Analysis of the data will show separately the effects of the feed and reflector on antenna performance. The analysis emphasizes the performance of the JPL feed; the previous volumes established the quality of reflector. This volume compiles the test results used to analyze the effects of the JPL feed on antenna performance. Properties of the feed covered in the analysis include aperture illumination, cross-pol, and direct radiation from the feed.

This Page Intentionally Left Blank

2.0 TEST PLAN

The difficult first step in the test plan was to deploy the 15-Meter Hoop Column Antenna into a free-standing structure. Figure 1 shows the counterbalance system used to deploy the antenna. After deployment, the counterbalance structure was removed to permit movement of the antenna. Because the structure was virtually undamped, acceleration tests were used to determine maximum acceptable scan speed with a load equivalent to the JPL feed. During the near-field measurements, the antenna was translated 40 ft and rotated by the turntable in the scanning operations. For these tests it remained freestanding as shown in Figure 2; all other structures were removed to minimize RF reflections.

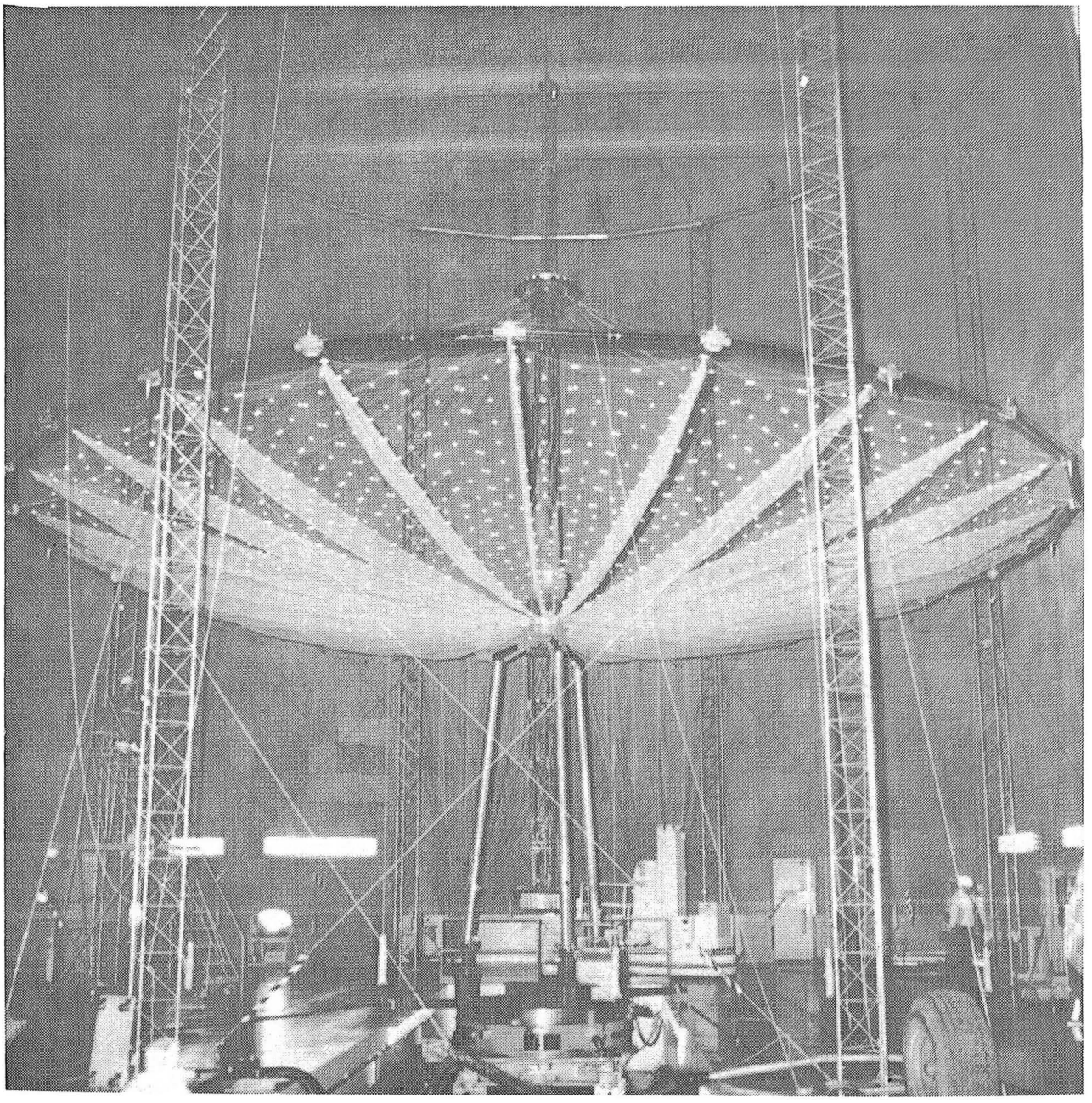

Figure 1 Antenna during Deployment

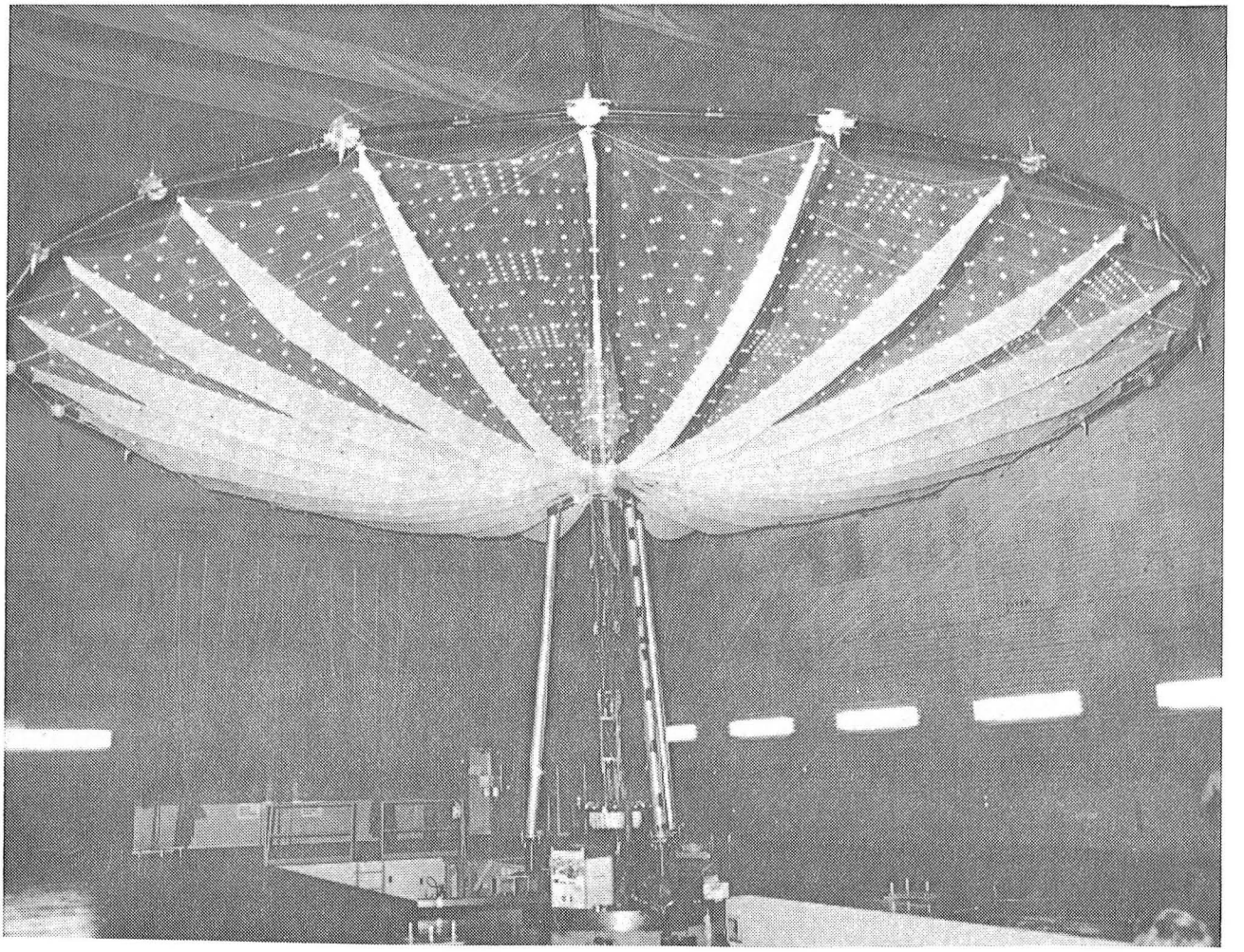

Figure 2 Freestanding Antenna

Table 2-1 shows the test plan, the sequence of tests performed with the JPL feed. All tests for the JPL feed were performed with the feed positioned over Quadrant 4 of the hoop column antenna (HCA). JPL specified a test frequency for the feed of 2.225 GHz, slightly lower in frequency than the 2.27-GHz LaRC feed which was tested just prior to the installation of the JPL feed.

The feed was a microstrip array driven by a multiport stripline network as shown in Figure 3. The panel supporting the array required counterbalancing to minimize the torque loading on the antenna column. The array elements were designed to radiate primarily with right circular polarization. Multiple ports on the feed allowed the generation of many beams from the single array. To allow closer spacing of the different beams generated by the array, the individual subarrays were overlapped so that several shared the same space on the panel.

Table 2-1 JPL Test Plan

Test	Page No.	Freq, GHz	Feed Port No.	Far-Field Polarization	Illum Quad	Beamscan, Beamwidths
8	15-22, 28-31	2.225	8	RHCP§	4	0
9	23-27, 32-35	2.225	8	LHCP§	4	0
10	36-44, 50-53	2.225	2	RHCP	4	2
11	45-49, 54-57	2.225	2	LHCP	4	2
11a	58-66, 72-75	2.225	4	RHCP	4	1
11b	67-71, 76-79	2.225	4	LHCP	4	1
11c	80-88, 94-97	2.225	5	RHCP	4	1
11d	89-93, 98-101	2.225	5	LHCP	4	1
11e*	102-110, 116-117	2.225	8	RHCP	4	0
11f*	111-115, 118-119	2.225	8	LHCP	4	0
11g*	120-128, 134-135	2.225	2	RHCP	4	2
11h*	129-133, 136-137	2.225	2	LHCP	4	2

* Abbreviated scans.

§ RHCP and LHCP are standard abbreviations for "right-hand circularly polarized" and "left-hand circularly polarized," respectively.

These tests assumed the feed was focused correctly because the feed assembly had no provision for positioning relative to the reflector focal point. Because of the large f/d ratio, any defocusing would have minimal effect on the far-field pattern. Also, because the feed was circularly polarized and because the measurement probe, an open-ended waveguide, had an extremely linear polarization, the feed required two collections to measure the co-pol response. The far-field patterns generated with this probe were the vertical and horizontal field components. Another processing step was required to determine the right- and left-hand circular far-field components.

The processing of the data from the near field to the far field occurred after the data collection. Antenna data collection involved an open-ended waveguide positioned in a scan plane to measure the complex fields of the antenna. These field points were then placed in an array. The array was discrete Fourier transformed to yield the plane-wave spectrum of the antenna. When polarization was expressed in azimuth and elevation, the probe had an extremely low-level cross-pol component. Therefore, the plane-wave spectrums generated by the two collections are orthogonal and can, when processed, yield the right- and left-hand circularly polarized components of the antenna far-field pattern.

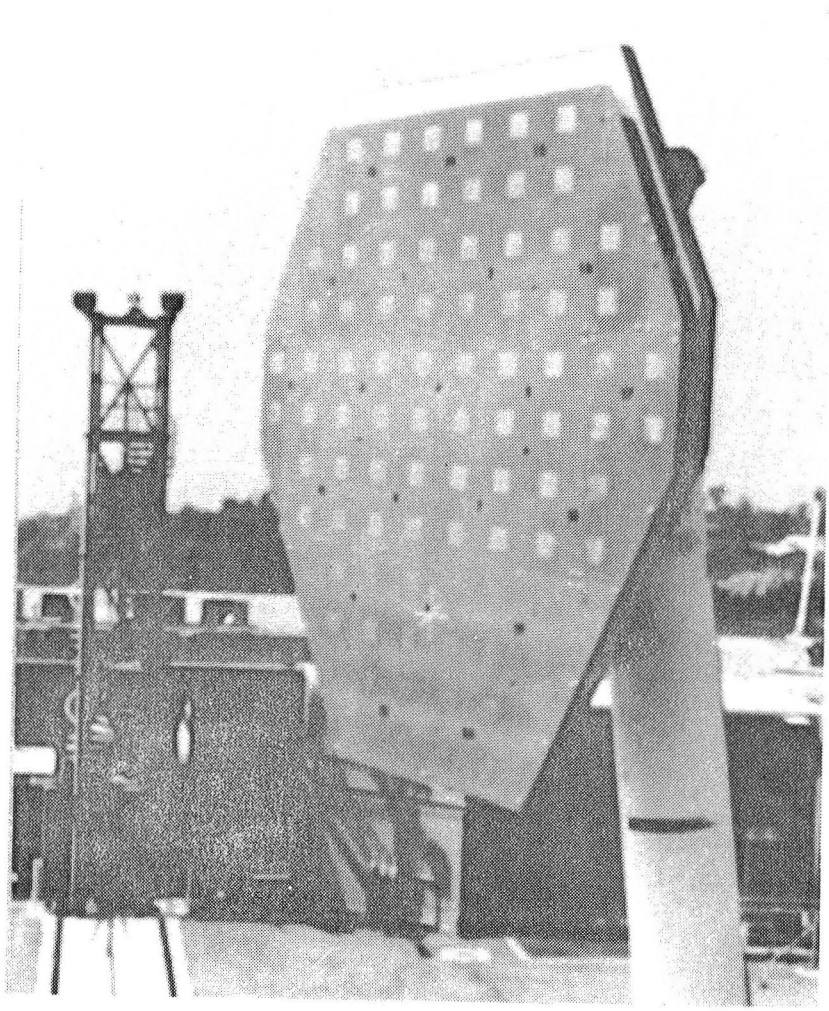

Figure 3 JPL Feed

this page intentionally left blank

3.0 NEAR- AND FAR-FIELD PATTERN PLOTS

The data in this volume are in the same sequence as the test plan in Table 2-1. To facilitate comparisons between tests, the same set of plots was generated for each test pair. The plots describe the antenna patterns, including beamwidths, sidelobe structures, and envelopes. This description leads to the analysis of the sources of pattern degradation in the antenna design. Additional information in Volume I, Section 5 will aid in the interpretation of the data shown by the plots.

Figure 4 shows the geometry used to plot the far-field data. There is a direct trigonometric relationship between the plane-wave spectrum generated by the data processing and the azimuth elevation coordinate system. The antenna was aligned with the center radial of the illuminated aperture parallel to the y-axis in Figure 4. A plane of constant elevation angle (E) was parallel to this radial in the near-field. A plane of constant azimuth angle (A) was parallel to the principal chord of the quadrant, which chord was parallel to the x-axis of Figure 4 but offset from the center of rotation. Future references to a position in azimuth elevation coordinates will be written "(A,E)." Boresight for the antenna is (0,0). Principal planes were plotted through the main beam of the antenna when it was steered off boresight.

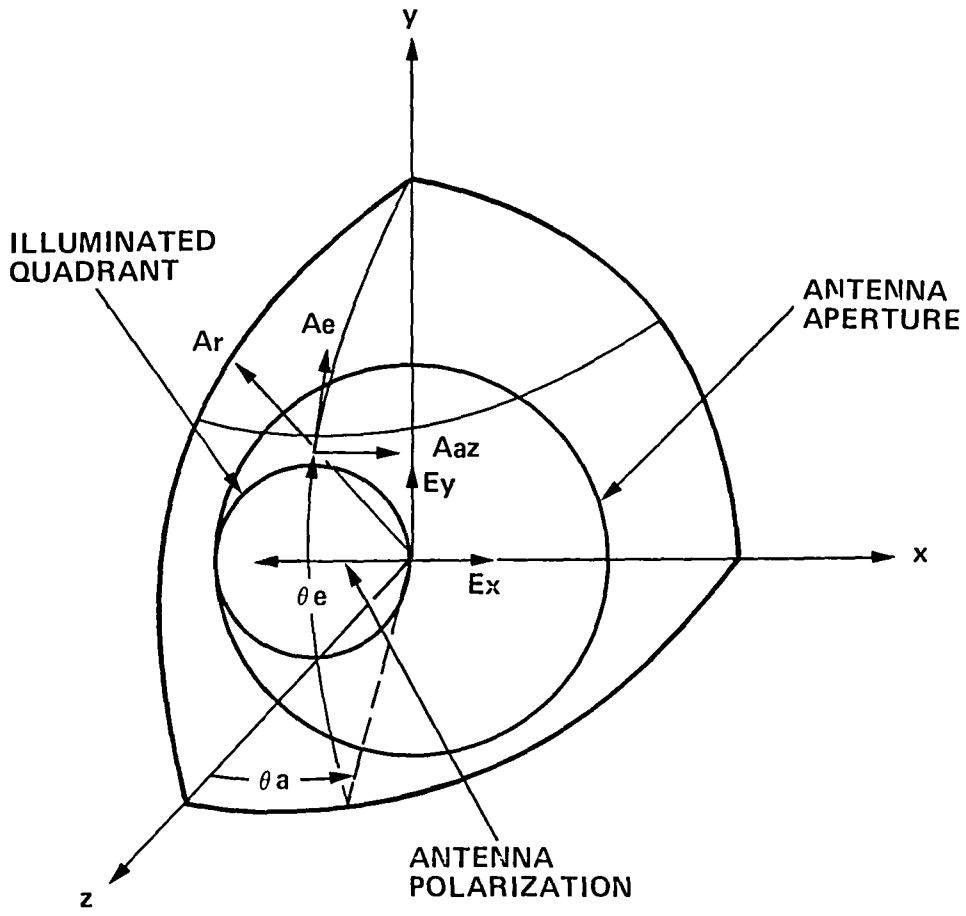

Figure 4 Far-Field Coordinate System

Because two tests performed with linearly polarized probes generated the circularly polarized far-field data, the plots for this pair of tests were the same as for any other pair of similarly polarized tests. The test pairs are, sequentially, 8 and 9, 10 and 11, 11a and 11b, 11c and 11d, 11e and 11f, and 11g and 11h. The set of plots generated for each pair of tests is given in Table 3-1. These data were sufficient to establish the performance of the antenna with this feed. However, decoupling the feed response from the reflector requires further data analysis.

Table 3-1 Plotting Format for Test Pair

Plot Type	Pattern Type	Range	
	Far-Field Plot	Dynamic, dB	Spatial Angle, °
	Co-pol		
1	Constant Elevation	-80 to 0	-30 to 30
2	Constant Azimuth	-80 to 0	-30 to 30
3	Constant Elevation	-60 to 0	-10 to 10
4	Constant Azimuth	-60 to 0	-10 to 10
5	Contour (Ranges)	-40,-30,-20,-10	Determined by Far-
6	Contour (Ranges)	-30,-20,-10,-3	Field Amplitude
7	Three-Dimensional	-40 to 0	-10 to 10
	Cross-pol		
8	Constant Elevation Overlay	-80 to 0	-30 to 30
9	Constant Azimuth Overlay	-80 to 0	-30 to 30
10	Constant Elevation	-80 to 0	-30 to 30
11	Constant Azimuth	-80 to 0	-30 to 30
12	Contour (Ranges)	-40,-30,-20	-10 to 10
	Near-Field Plot		Length of Plot
	y-Polarized Component		
13	Principal Chord	-80 to 0	Total Aperture
14	Center Radial	-80 to 0	Total Aperture
15	Principal Chord	-80 to 0	Active Quadrant
16	Center Radial	-80 to 0	Active Quadrant
	x-Polarized Component		
17	Principal Chord	-80 to 0	Total Aperture
18	Center Radial	-80 to 0	Total Aperture
19	Principal Chord	-80 to 0	Active Quadrant
20	Center Radial	-80 to 0	Active Quadrant

Each type of plot contains different information regarding the antenna performance. The far-field principal plane plots, Types 1 through 4, facilitate examination of the sidelobe envelope, first sidelobe level, half-power beamwidth, and main beam definition. However, these plots can be misleading about true far-field performance, especially when the antenna has an asymmetrical geometry like that of the 15-Meter Hoop Column Antenna. To avoid this problem, other methods were necessary for displaying far-field information.

Two methods for plotting far-field data are the contour and three-dimensional plots. The contour plot contains all of the far-field pattern inside a chosen angle from boresight. The levels are shaded from dark to light on the contour plot. For Plot Types 5 and 15 the darkest contour is -40 dB; for Type 6, -30 dB. All the area in the plot outside the darkest contour is lower than the levels mentioned previously. The other shading intensities correspond to levels given in Table 3-1. However, this plotting format gives information by discrete levels and does not allow the interpolation of information between these levels. The 3-D plot avoids the discreteness of data of the contour plot, but many sidelobes are hidden by both the main beam and major sidelobes because of the aspect angle chosen by the software. However, visible sidelobes can be checked for their true value--a feature not available on contour plots.

The near-field plots, Types 13 through 20, are in an amplitude and phase format. Plot Types 13, 14, 17, and 18 show the data collected across the entire scan (78 ft). The amplitude of the plot identifies the major energy sources over the entire antenna, and the phase shows the location of the major phase front that dominates the far-field pattern. Plot Types 15, 16, 19, and 20 contain data only on the fields directly above Quadrant 4. The amplitude on these plots shows the aperture illumination; when plots of the two near-field polarizations are compared, they should overlay. If the plots do not overlay well, there is a sizable linear component in the illumination which will result in a large cross-pol. The phase of the two polarizations should also differ by 90° for the optimum circular polarization. With these data on the near field, the feed and reflector performance may become isolated from each other.

3.1 UNSTEERED TESTS 8 AND 9

Figures 5-24 show the data collected using Port 8 of the JPL feed. This port has a predicted peak gain in the far field at (0,0). The measured pattern had the same result; therefore, the feed was not significantly defocused in the lateral direction. The far-field principal plane RHCP plots, Figures 5-9, show an asymmetric sidelobe envelope in the constant elevation plane and a main beam distorted by the first sidelobes in the orthogonal plane. The half-power beamwidth of these patterns averages 1.6°.

Figures 9 and 10 show a major pair of sidelobes caused by the adjacent apertures, which sidelobes peak at -15 dB. Because the feed was designed to illuminate a single aperture without regard for feed spillover, a major portion of the feed energy fell on the other three quadrants, causing the high sidelobes in the far-field pattern. Loss of this energy from the proper aperture had two effects on boresight: reducing peak gain and causing distortion in the main beam in the plane of constant azimuth. However, the far-field envelope, excluding those sidelobes which were caused by the other apertures, was relatively symmetrical and was caused mostly by surface errors in the reflector.

The peak cross-pol of the antenna was -17.7 dB. This level was mainly due to the imbalance of the linear polarized near-field components. This imbalance can easily be seen by comparing Figures 19 and 20 to Figures 23 and 24. These figures show approximately 1 dB of difference over the entire aperture. In previous cross-pol tests of the LaRC feeds, the dominant effect on the cross-pol near the co-pol main beam had been the feed illumination, and the dominant effect on the cross-pol for the JPL feed was the same. The cross-pol contour on Figure 16 shows no dominant sidelobes due to the other apertures, suggesting a major difference from the LaRC feeds in aperture illumination by the cross-pol.

A major part of the feed power radiates directly into the scan plane, causing the pronounced interference pattern of Figure 24 from the major grating lobe of the feed. This power radiates virtually parallel to the scan plane. While this power had no effect on the narrow-angle performance of the antenna, it may produce lobes in the far-field at wide angles off boresight. The existence of this wide-angle lobe could cause misleading signals in some applications of this feed with a multiple aperture antenna.

3.2 STEERED TESTS 10-11d

The predicted steered angles of the original test plan given in the statement of work differed 25% from the measured steered angles recorded in the tests. (Figures 25-84 show the data obtained from the tests.) However, as in previous tests with the LaRC feeds, this difference in beam steering caused no significant pattern degradation.

A major new sidelobe did appear in collections for all three steered ports at a 3.2° greater azimuth angle than the main beam. Because all of these collections steered the main beam (and hence the feed illumination) toward the back quadrant of the antenna, this sidelobe could have been generated by the increased illumination from the feed of the back quadrant. The gain, the half-power beamwidth, and the remaining sidelobe envelope appeared completely unaffected by the beam steering.

The antenna cross-pol, which was dominated by the feed cross-pol, showed only minor changes with the different ports, the changes probably due to the slightly different elements used by each port. The cross-pol peak steered with the main beam and was always less than -16 dB. Steering the cross-pol generated no major new sidelobes; therefore, the back quadrant illumination of the cross-pol was much lower than that of the co-pol. Overall, steering of the main beam of the antenna has had little measurable effect on antenna performance.

3.3 ABBREVIATED SCANS, TESTS 11e-11h

In an attempt to eliminate the effects of radiation from the adjacent and opposite quadrants on the far-field antenna pattern, the near-field scan area was reduced to include only the illuminated quadrant. Figures 85-116 show the results of this procedure. The collections did reduce the effects of radiation from outside the illuminated aperture, but the attempt to isolate the illuminated aperture also caused an increase in the relative far-field cross-pol. Because the adjacent and opposite quadrants have different illuminations for the two polarizations, the reduced scan changed the far-field pattern of each polarization differently. The peak level of the far-field cross-pol increased relative to the co-pol peak by 3dB, largely because of truncation of the co-pol near-field data. No other major change in the co-pol or cross-pol patterns resulted from these reduced scans.

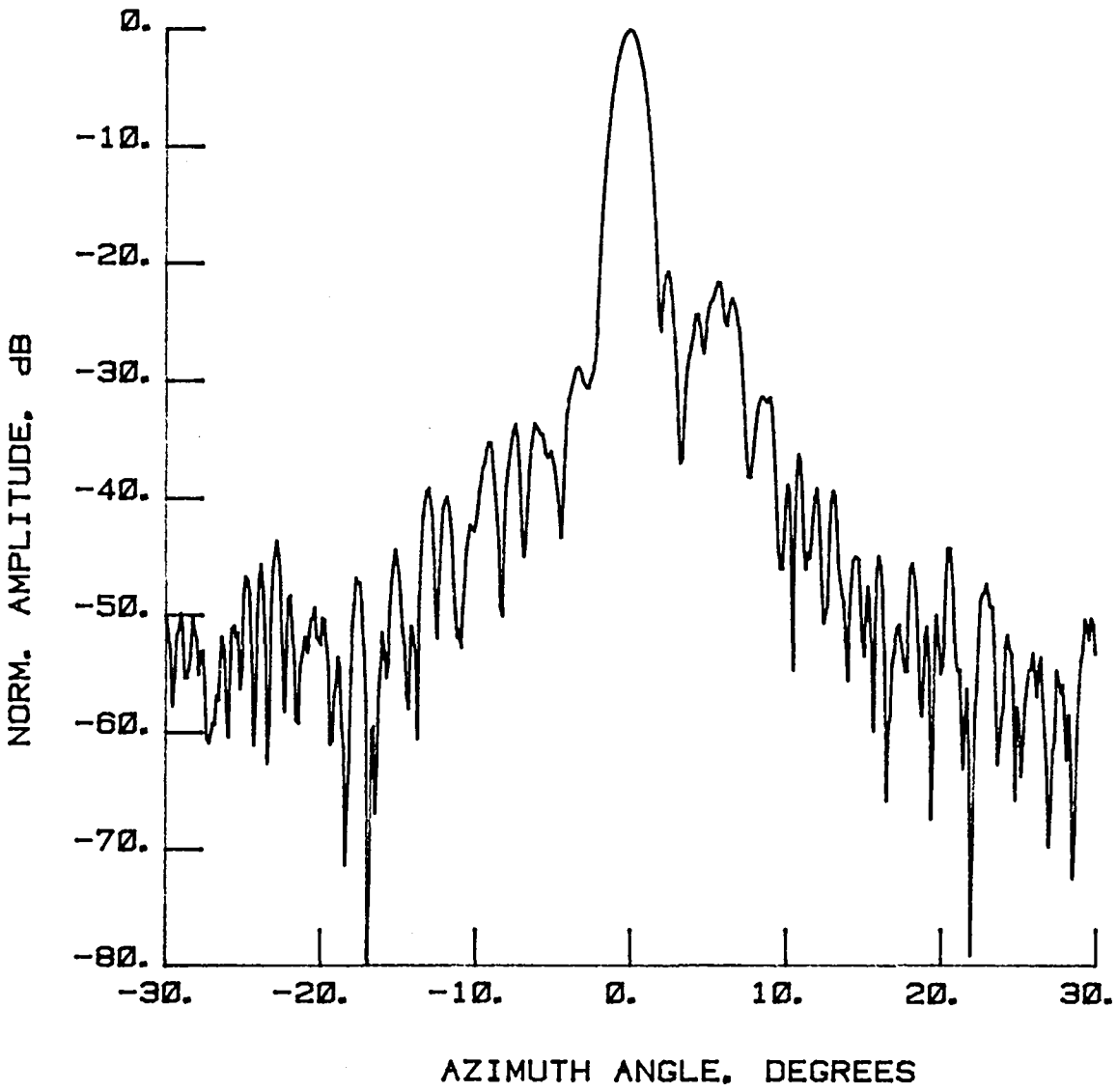

Figure 5 Test 8, E = 0°, Port 8, Type 1

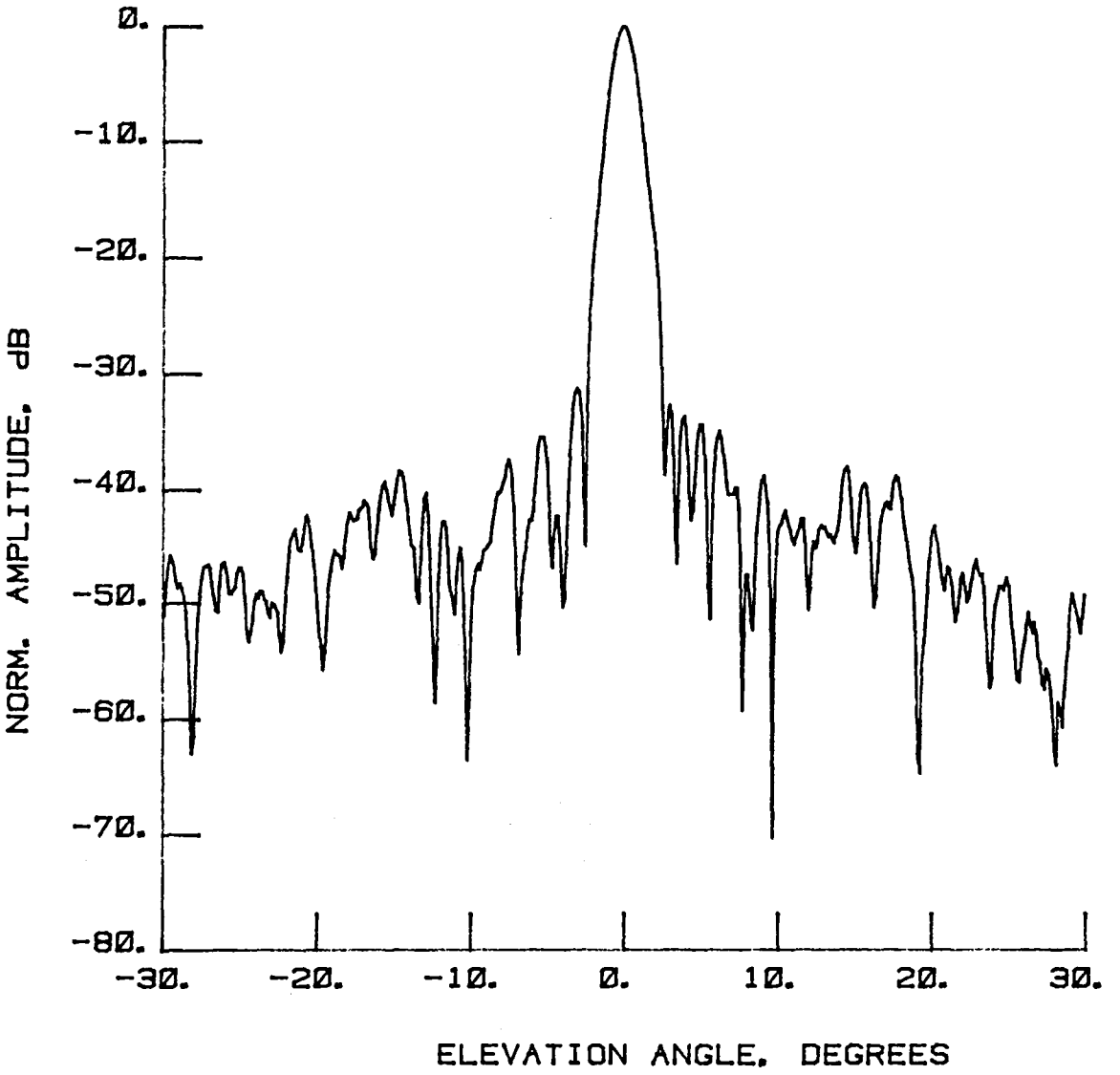

Figure 6 Test 8, A = 0°, Port 8, Type 2

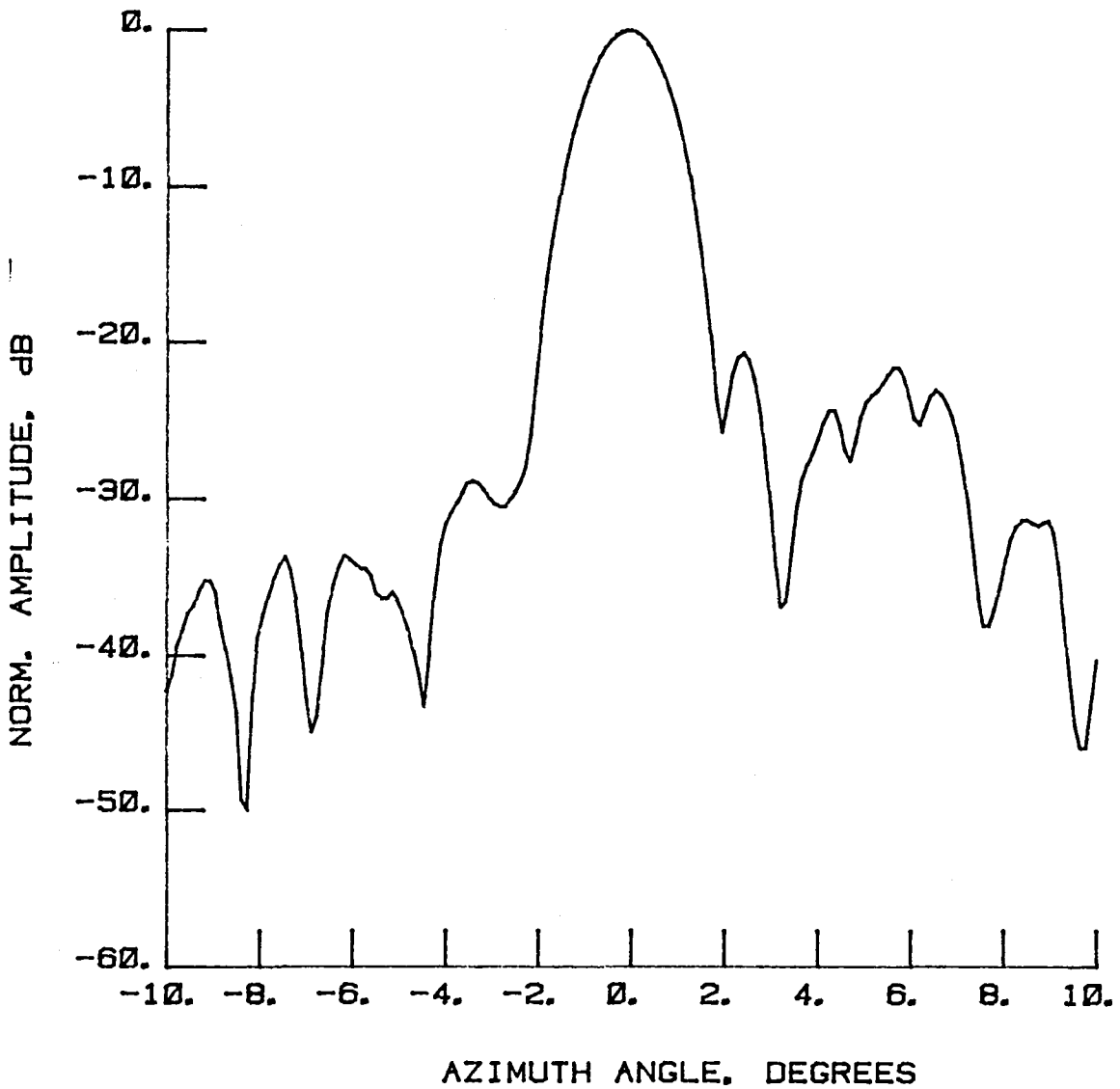

Figure 7 Test 8, E = 0°, Port 8, Type 3

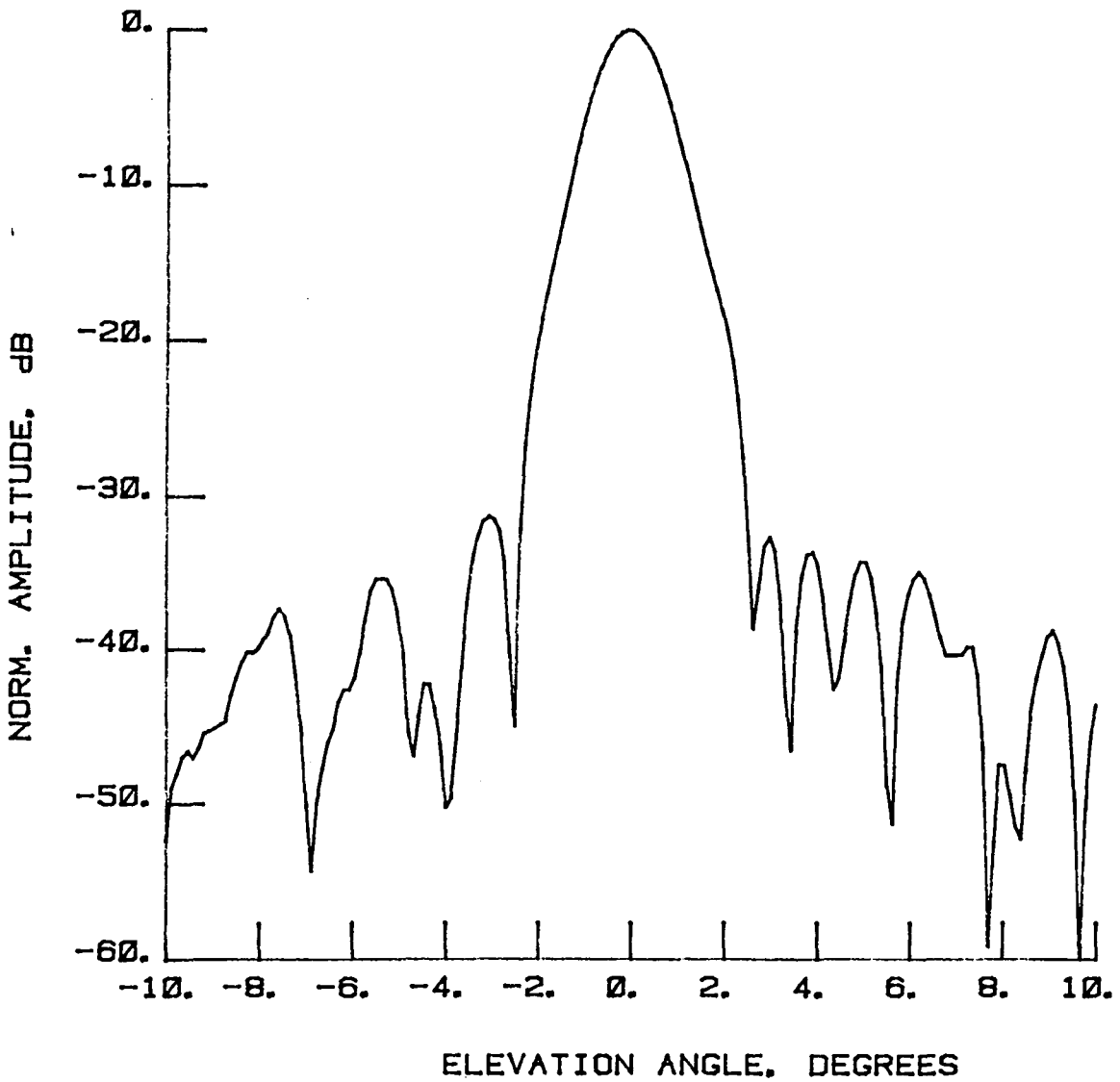

Figure 8 Test 8, A = 0°, Port 8, Type 4

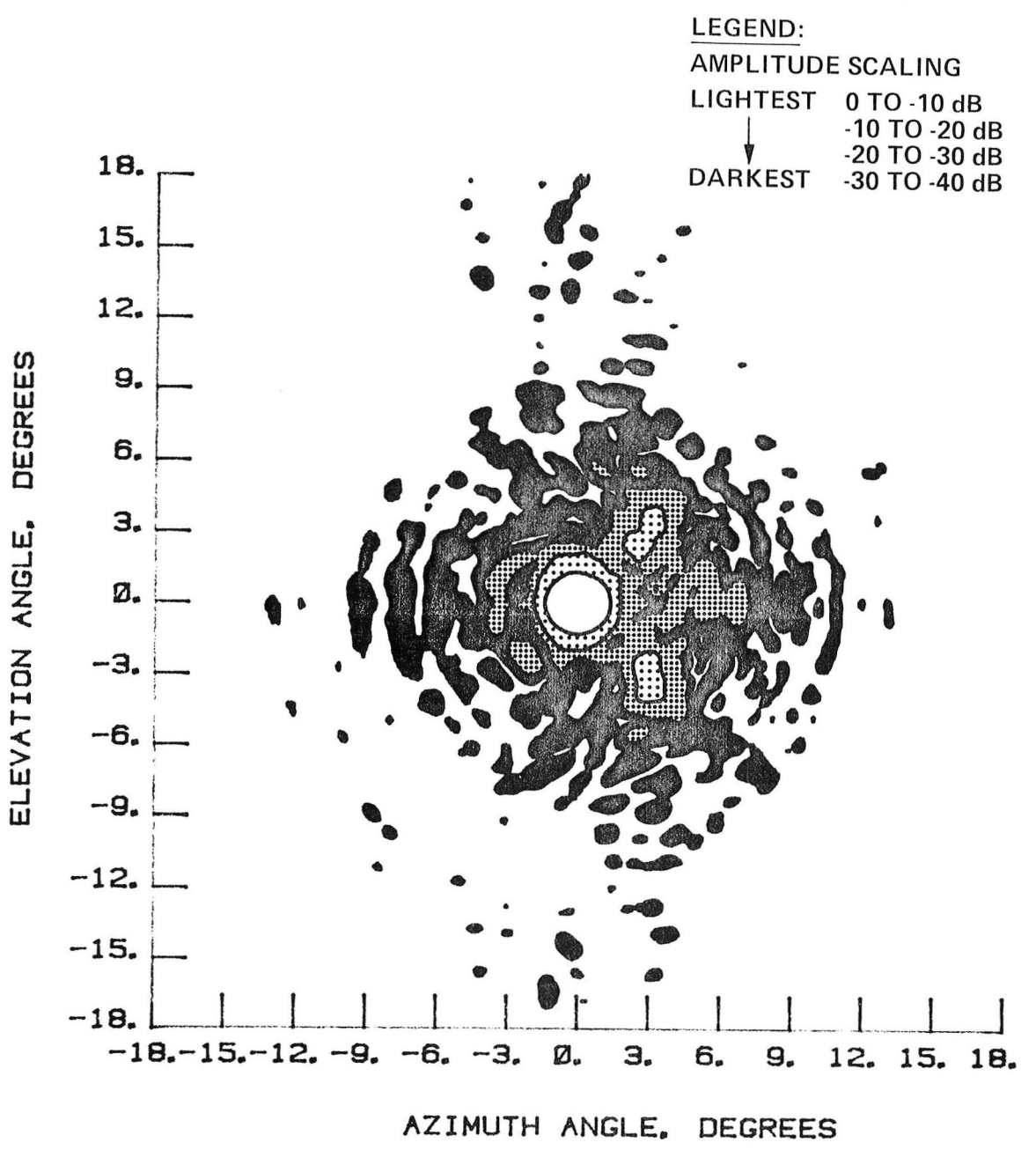

Figure 9 Test 8, Contour, Port 8, Type 5

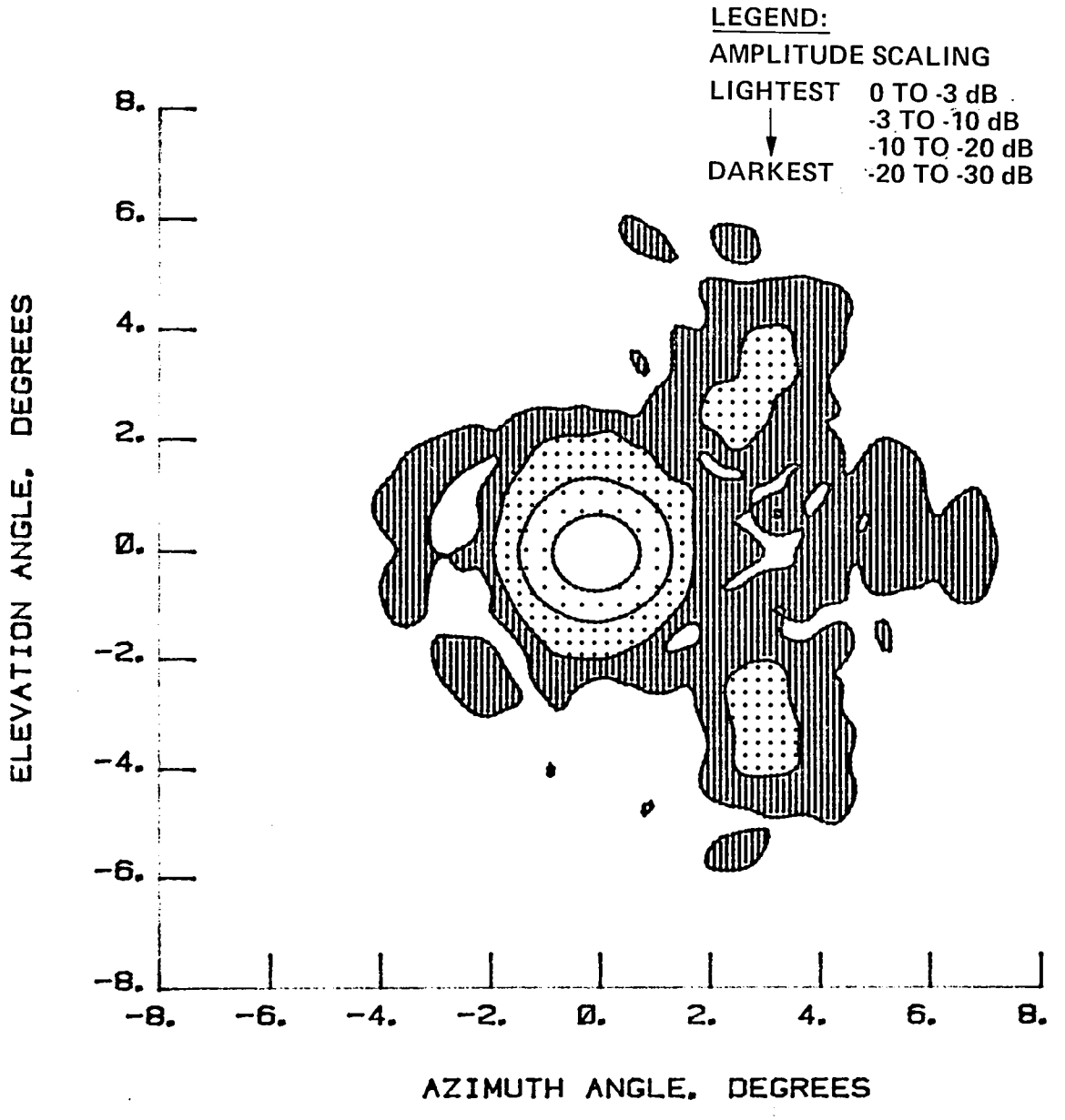

Figure 10 Test 8, Contour, Port 8, Type 6

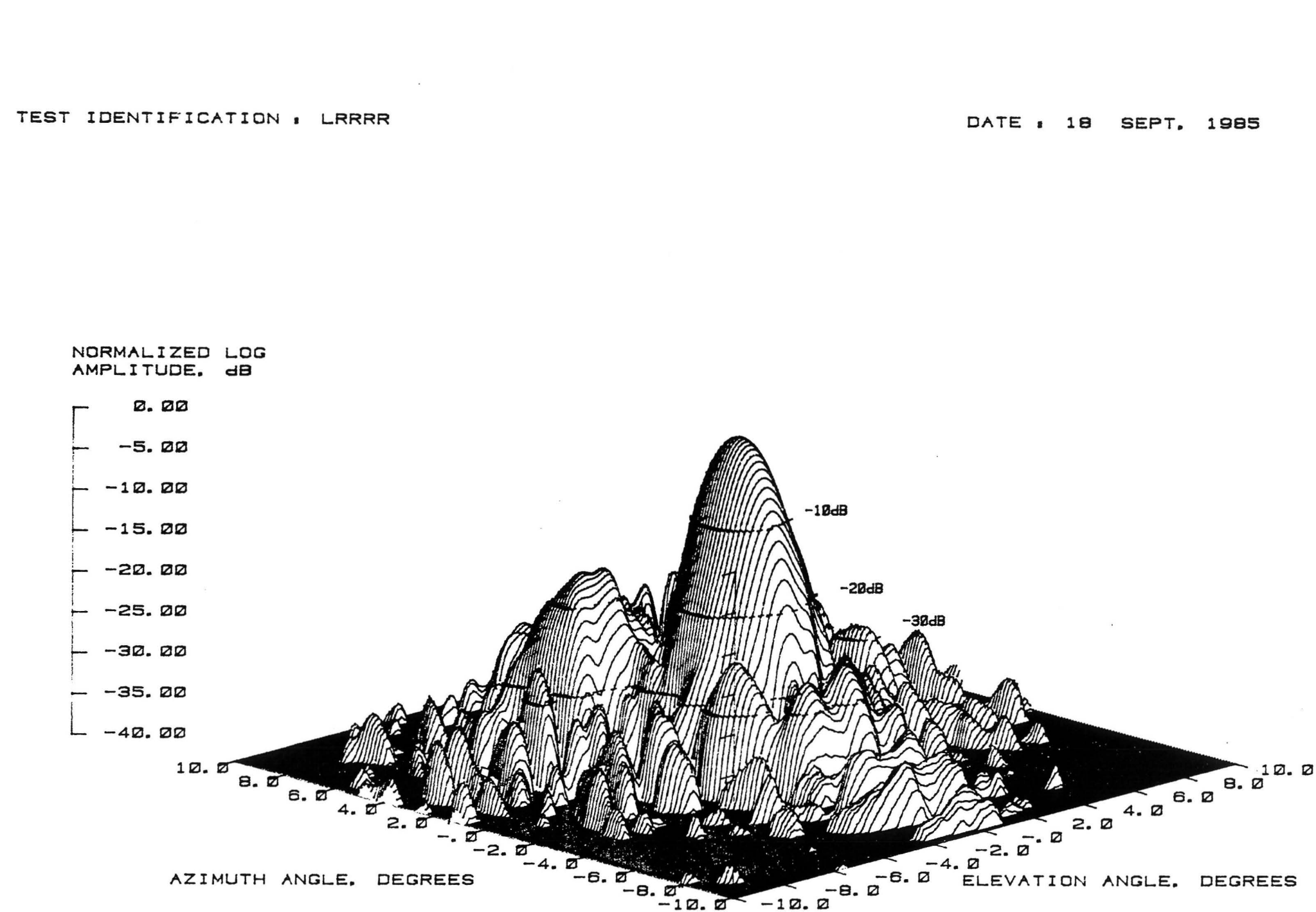

Figure 11 Test 8, 3-D, Port 8, Type 7

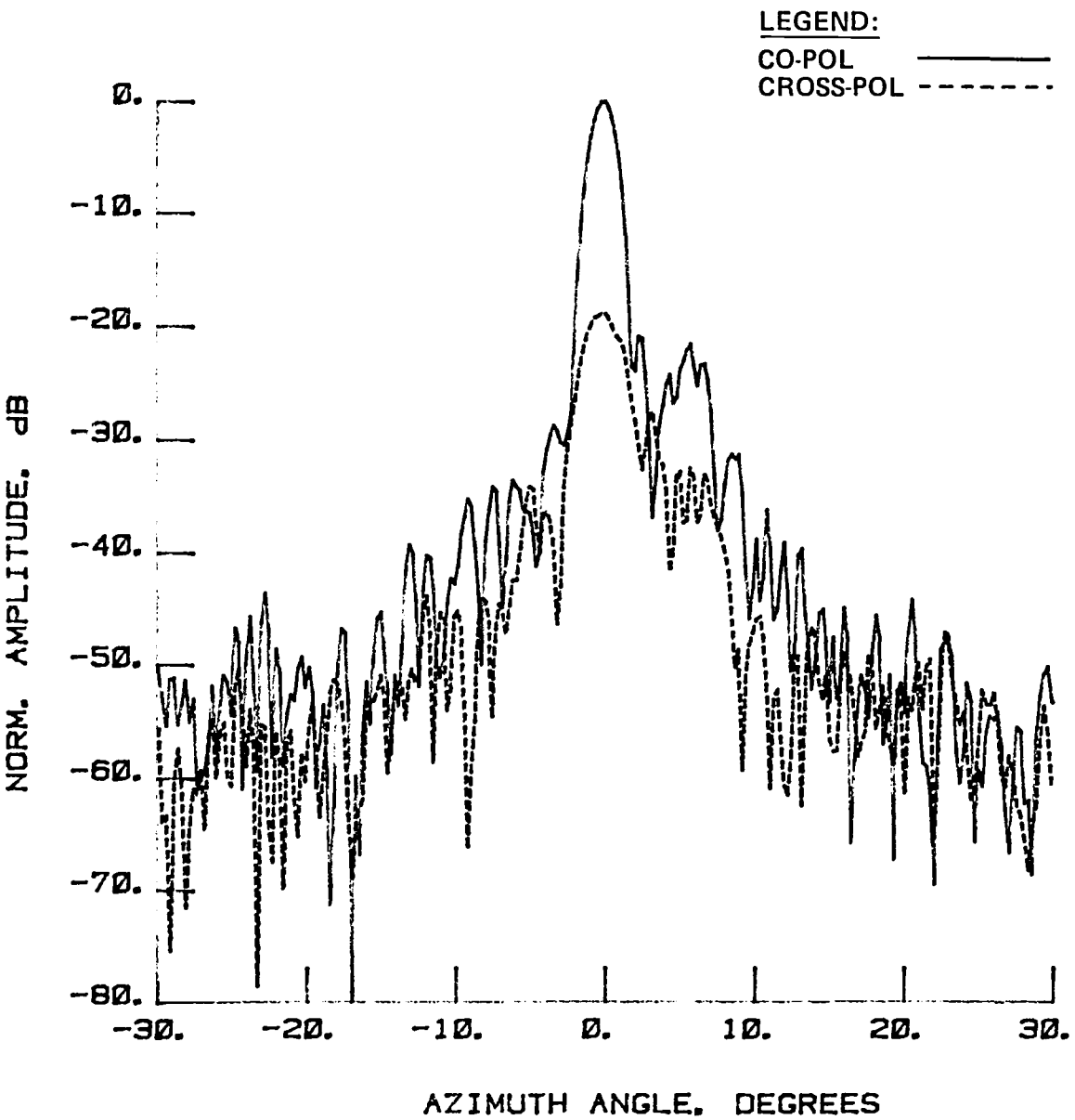

Figure 12 Test 9, E = 0°, Port 8, Type 8

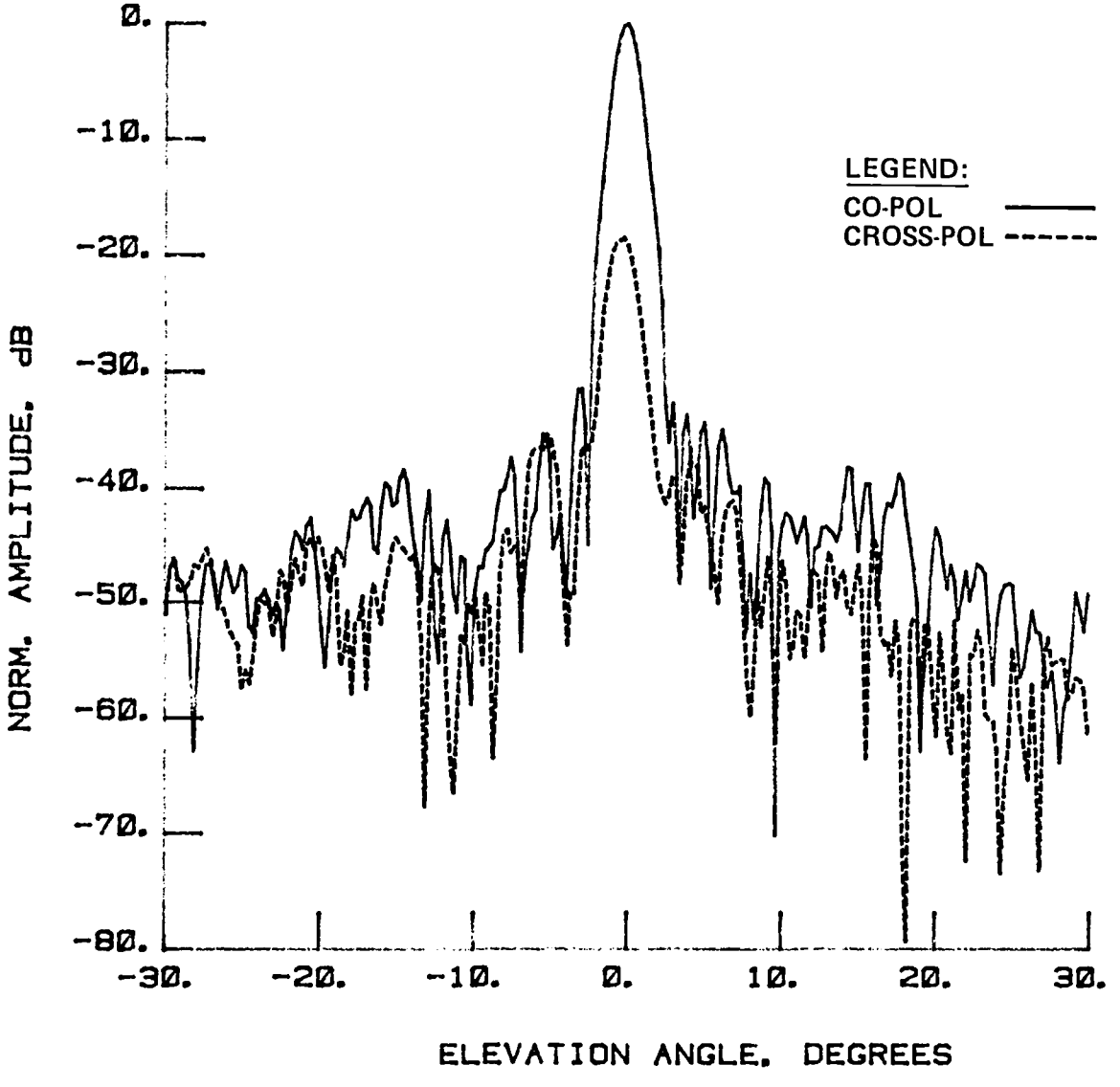

Figure 13 Test 9, A = 0°, Port 8, Type 9

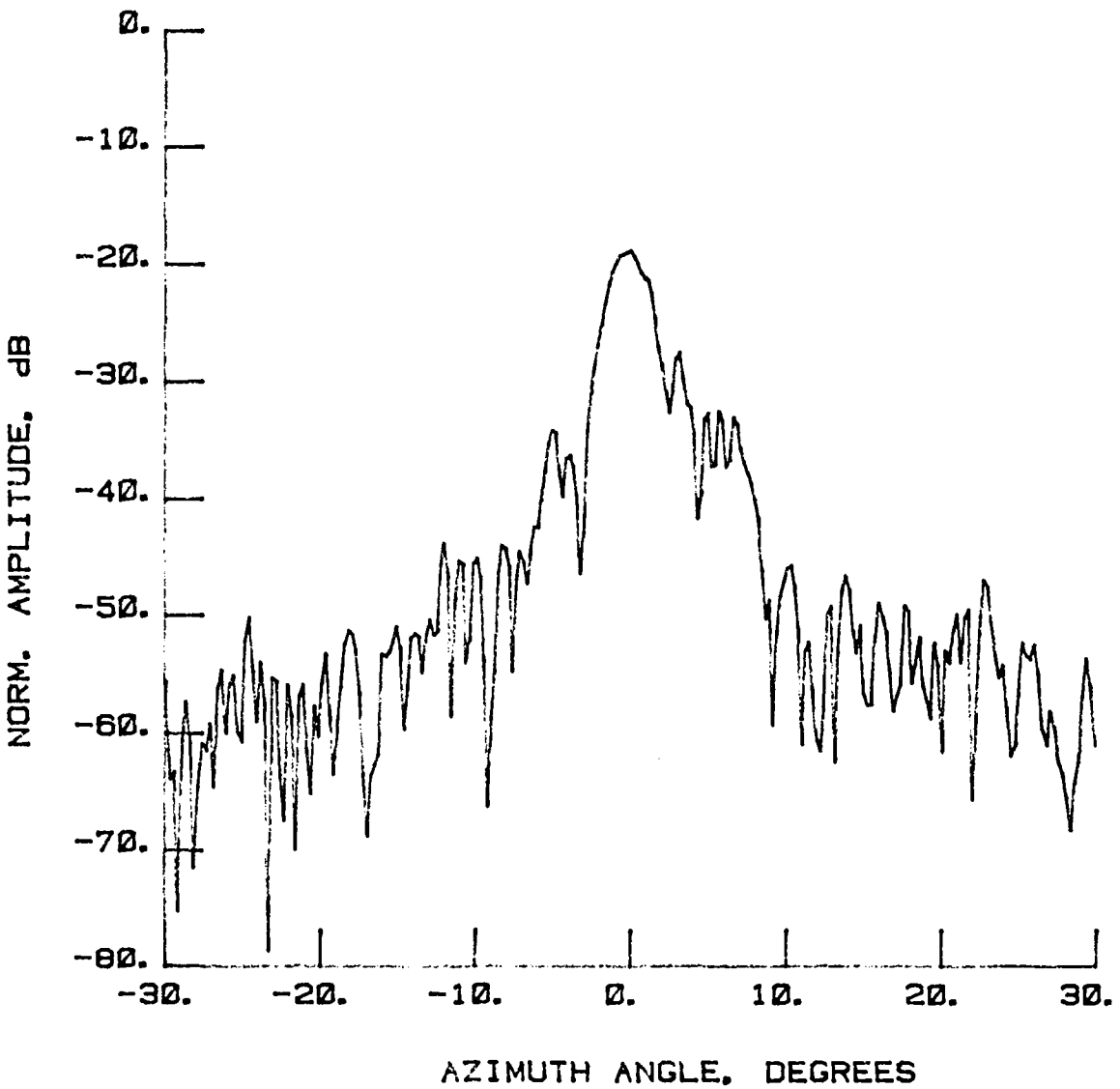

Figure 14 Test 9, E = 0°, Port 8, Type 10

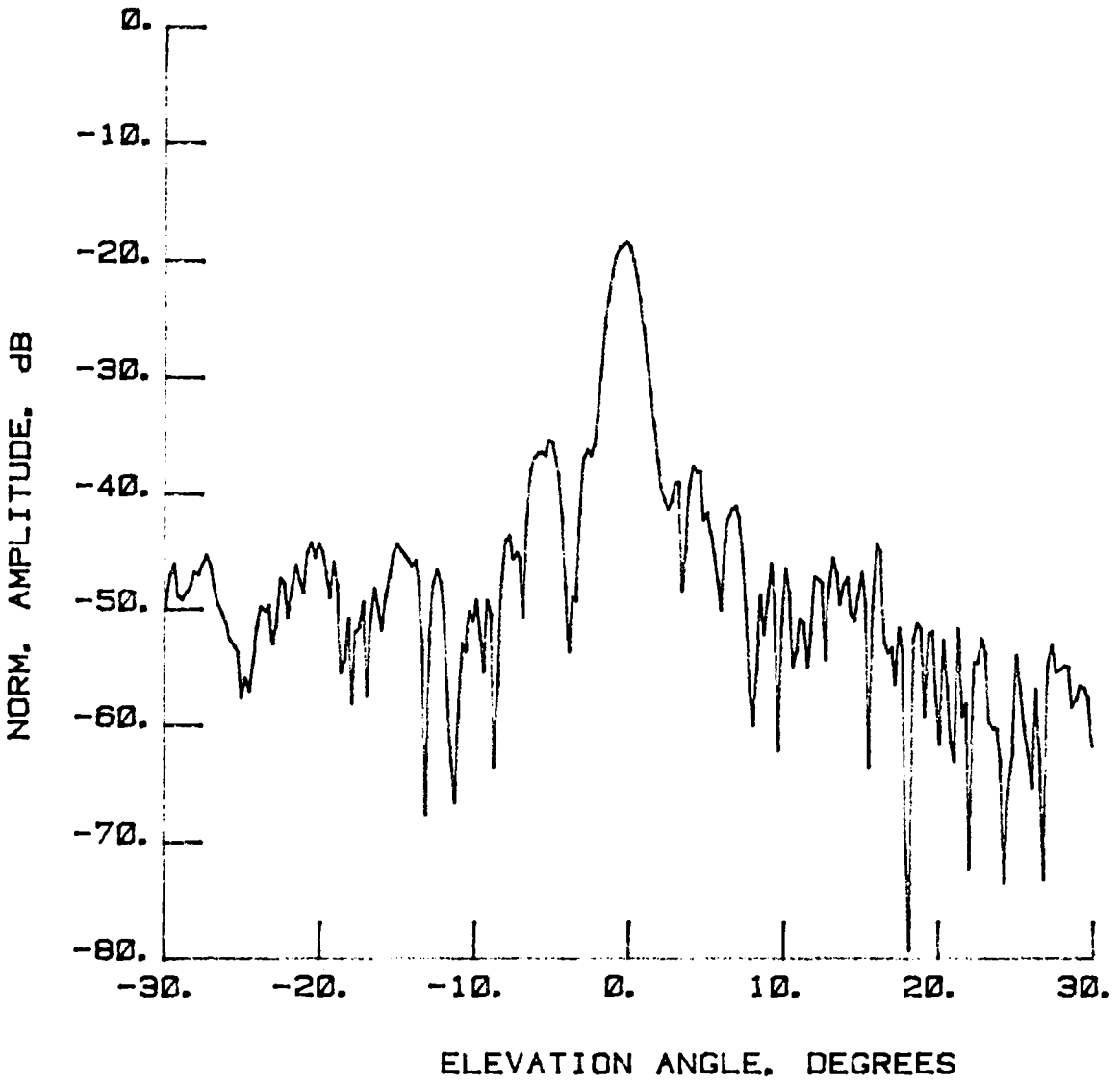

Figure 15 Test 9, A = 0°, Port 8, Type 11

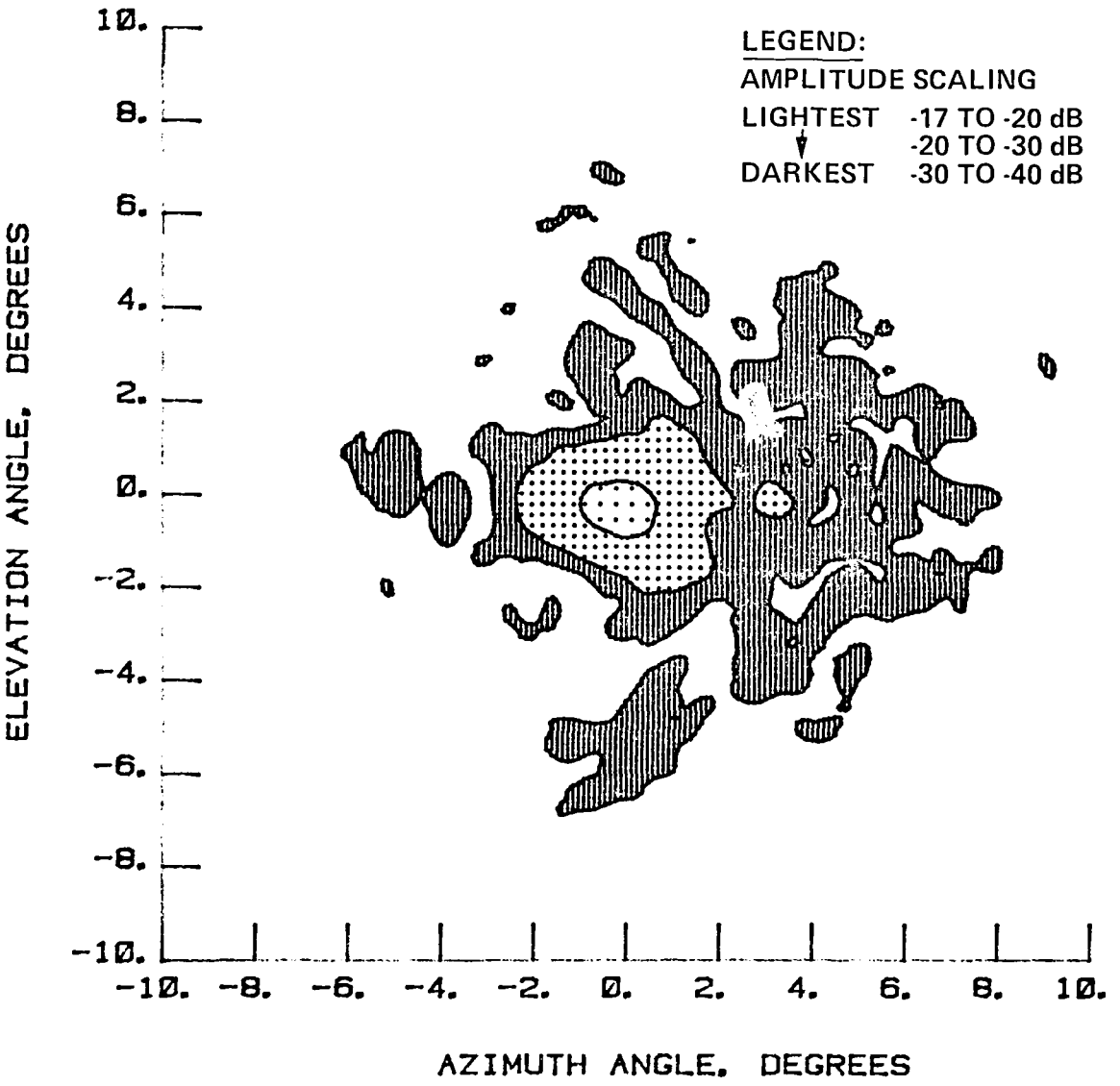

Figure 16 Test 9, Contour, Port 8, Type 12

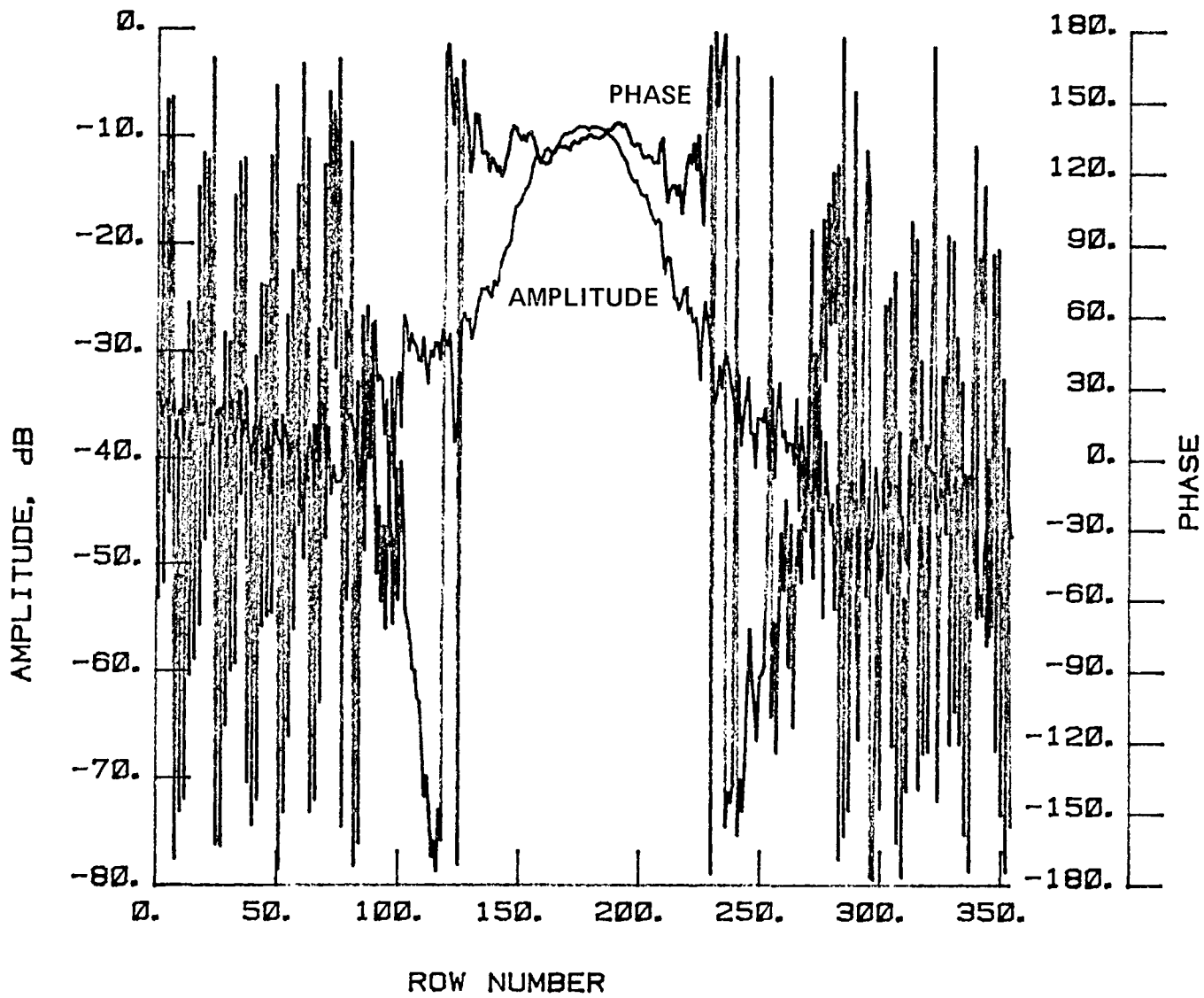

Figure 17 Test 8, Chord, Port 8, Type 13

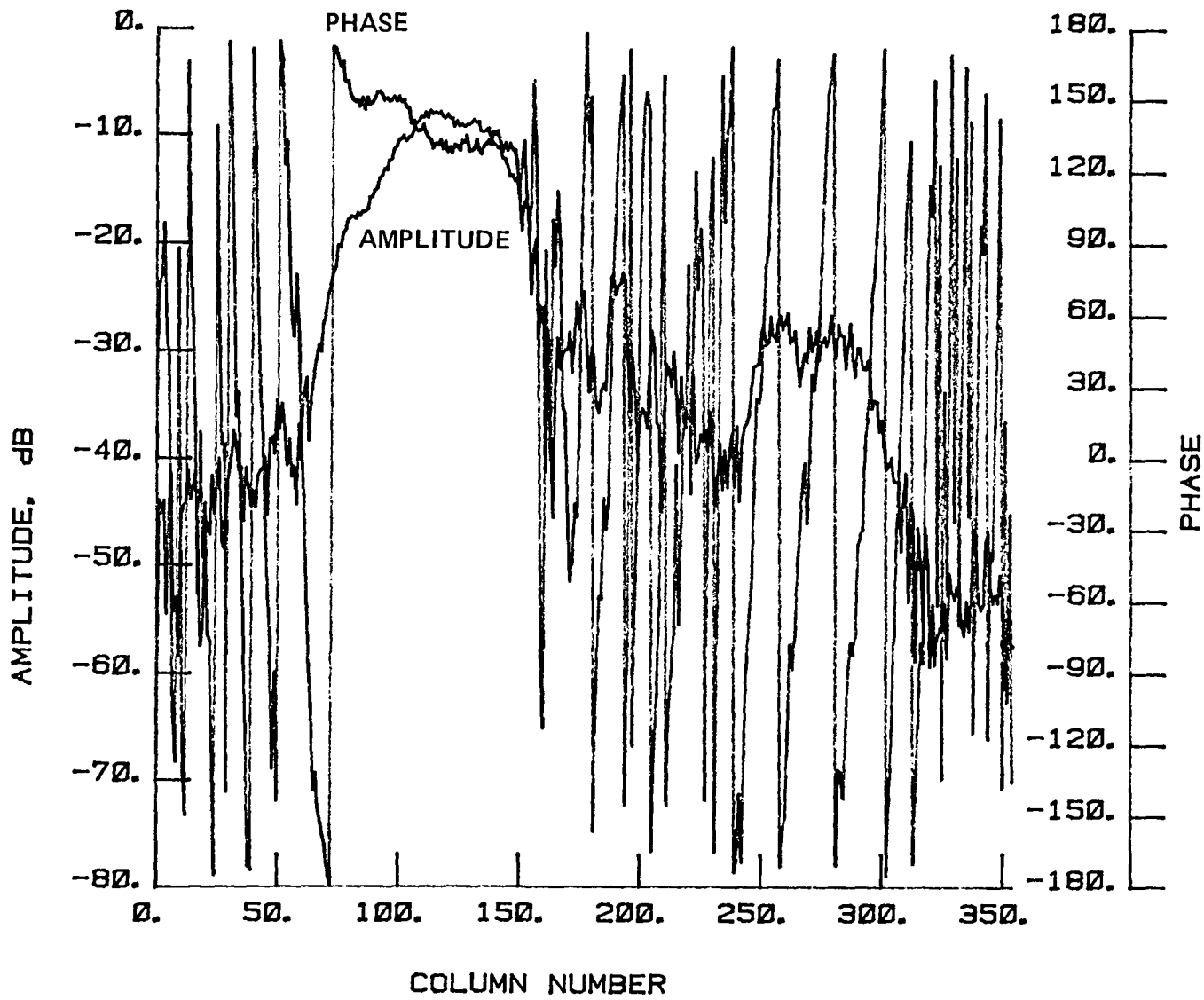

Figure 18 Test 8, Radial, Port 8, Type 14

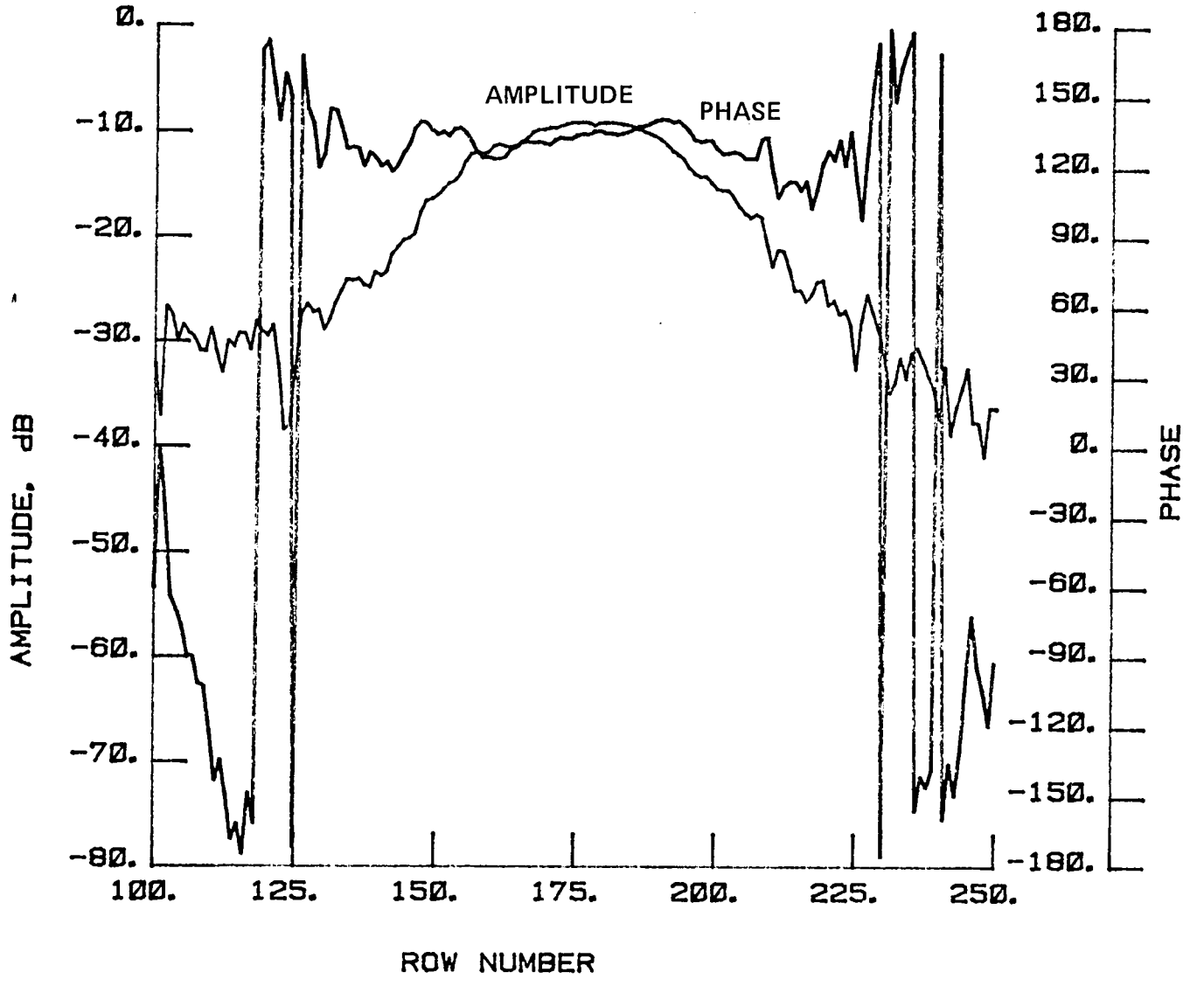

Figure 19 Test 8, Chord, Port 8, Type 15

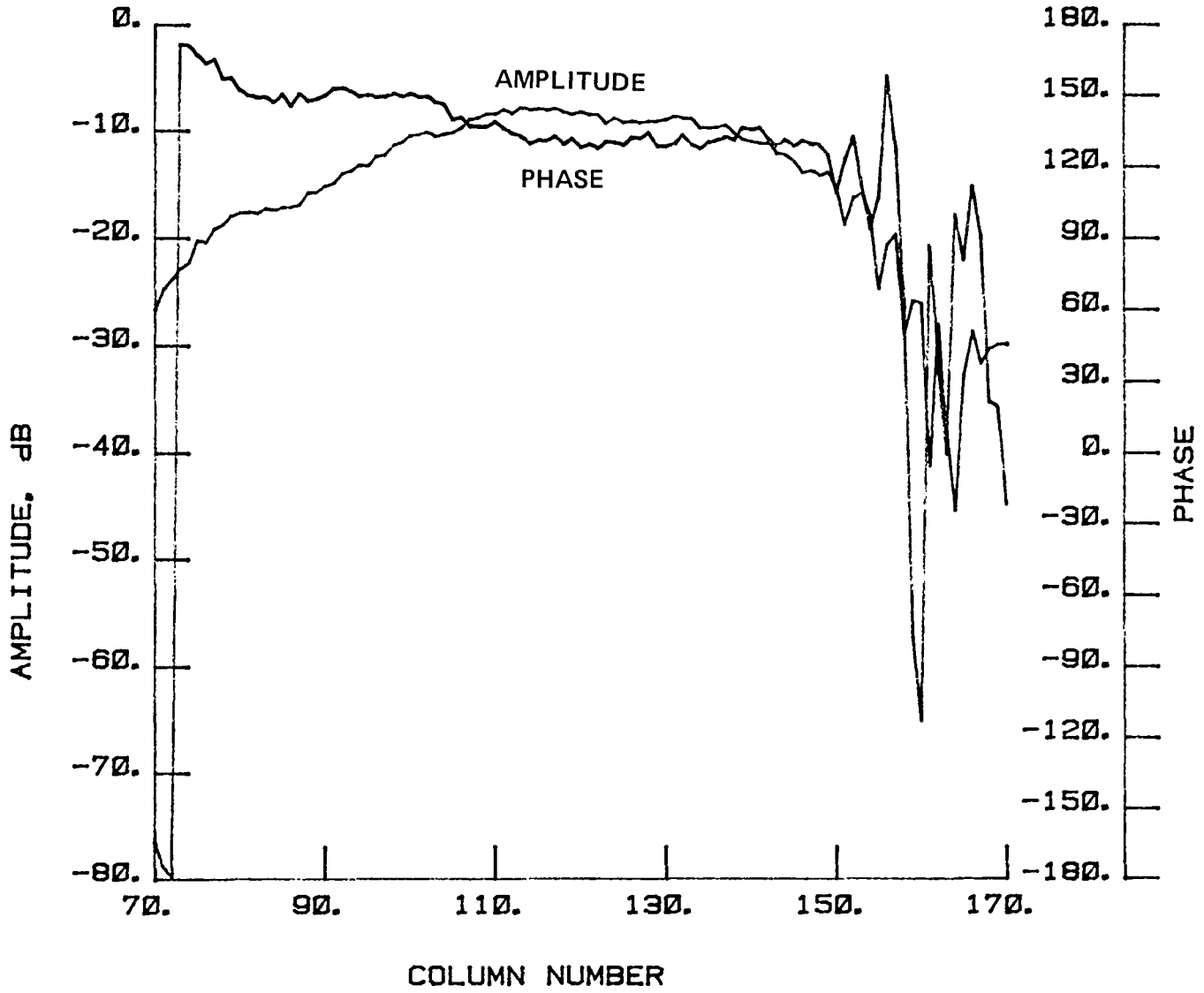

Figure 20 Test 8, Radial, Port 8, Type 16

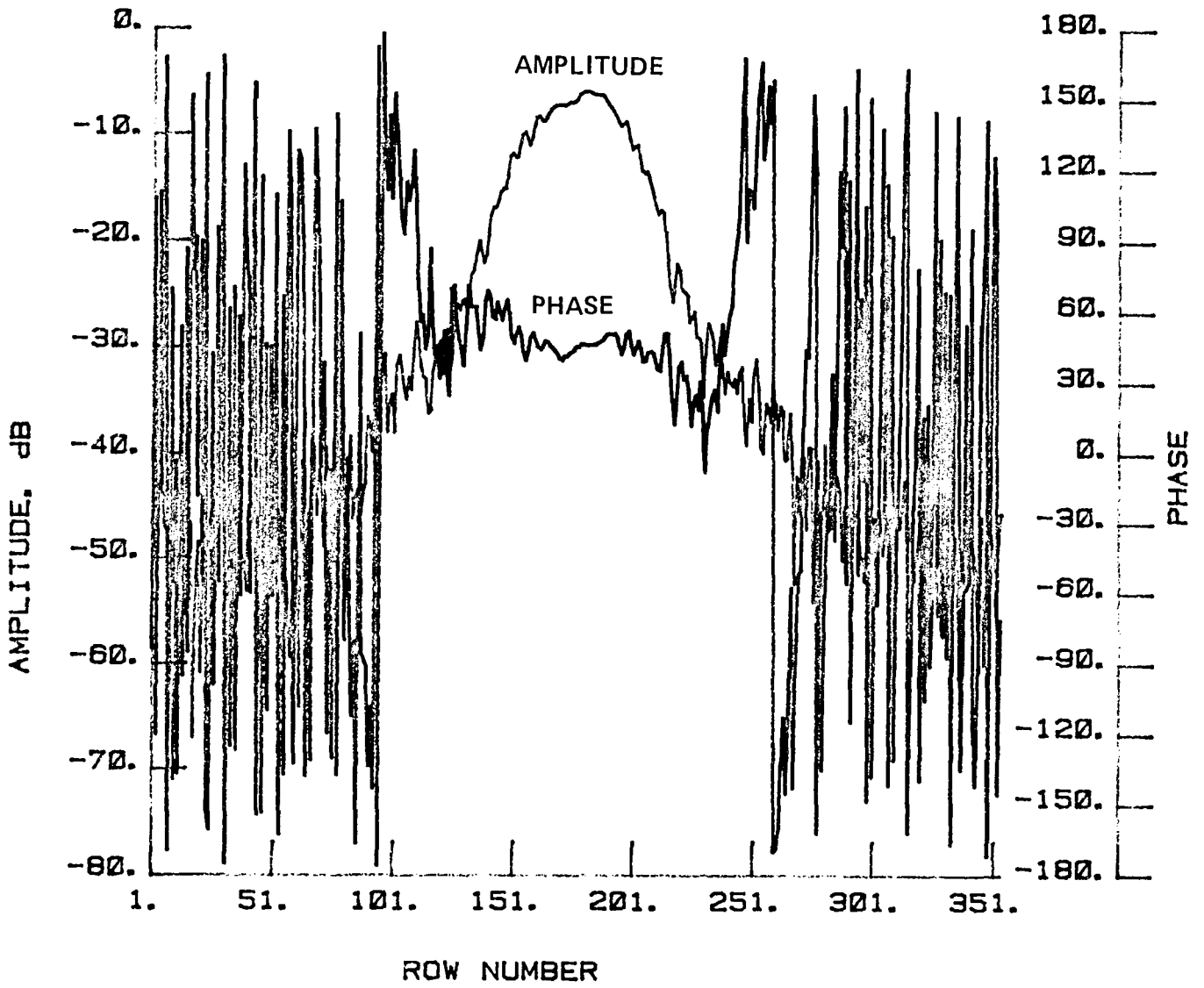

Figure 21 Test 9, Chord, Port 8, Type 17

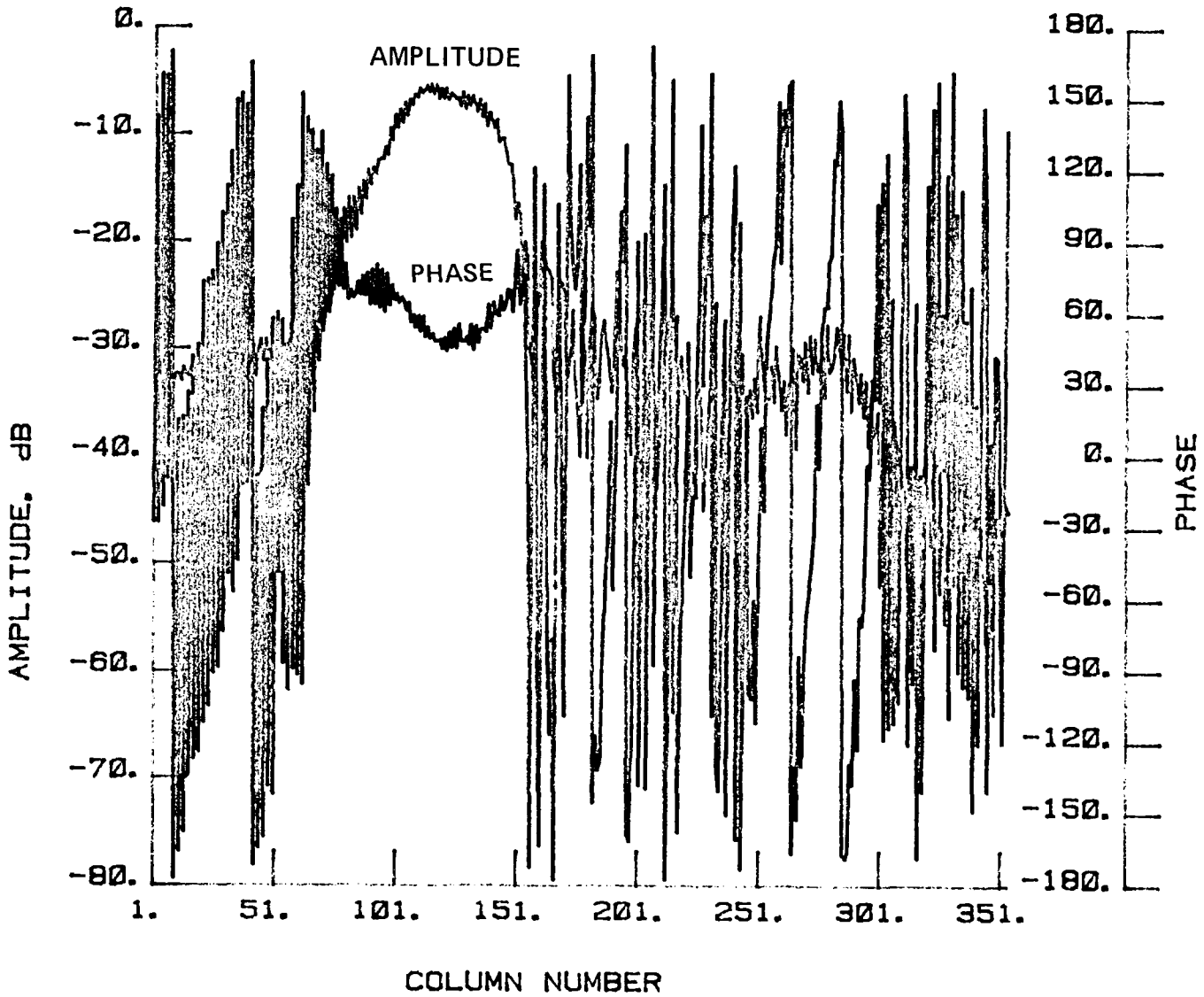

Figure 22 Test 9, Radial, Port 8, Type 18

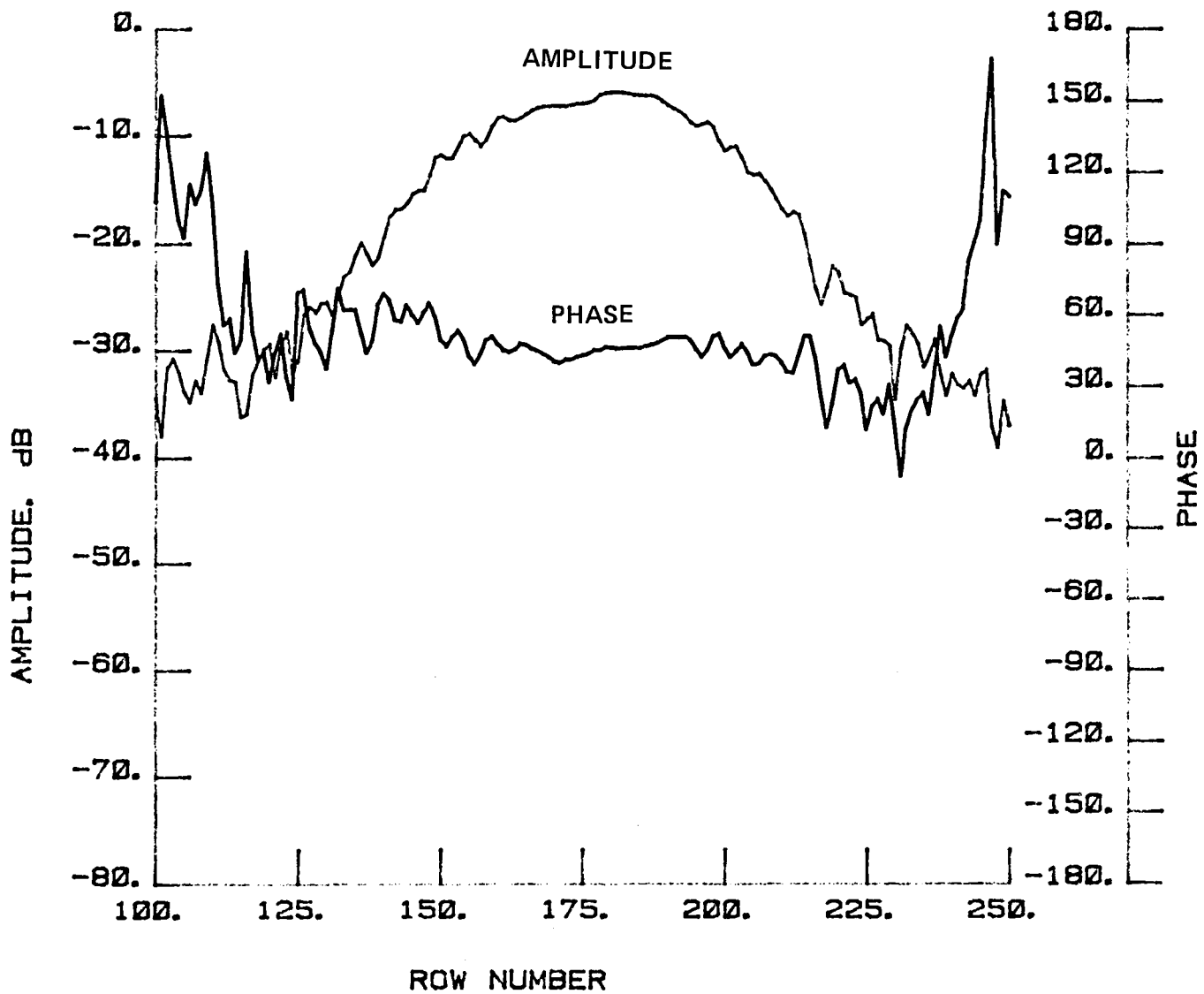

Figure 23 Test 9, Chord, Port 8, Type 19

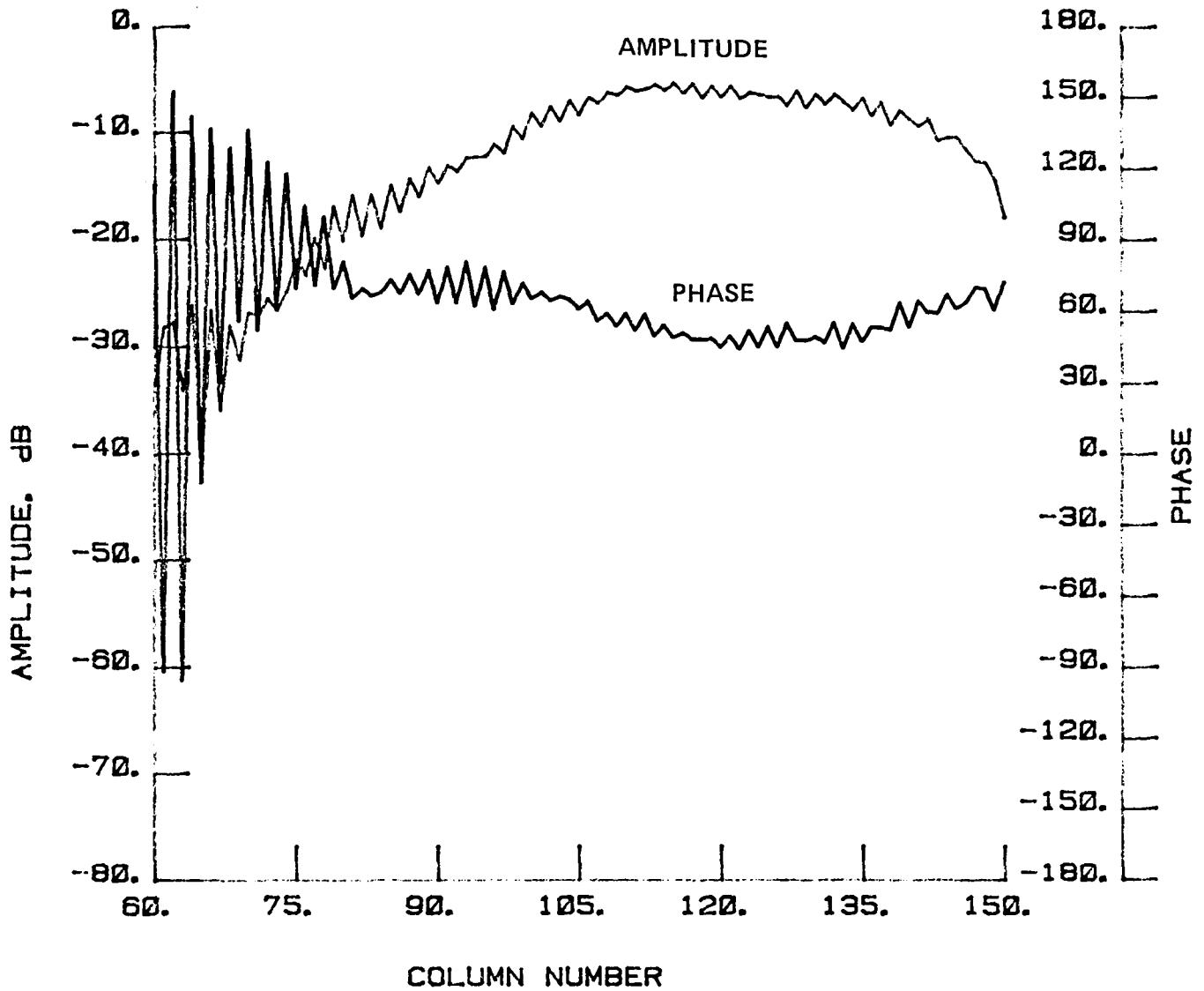

Figure 24 Test 9, Radial, Port 8, Type 20

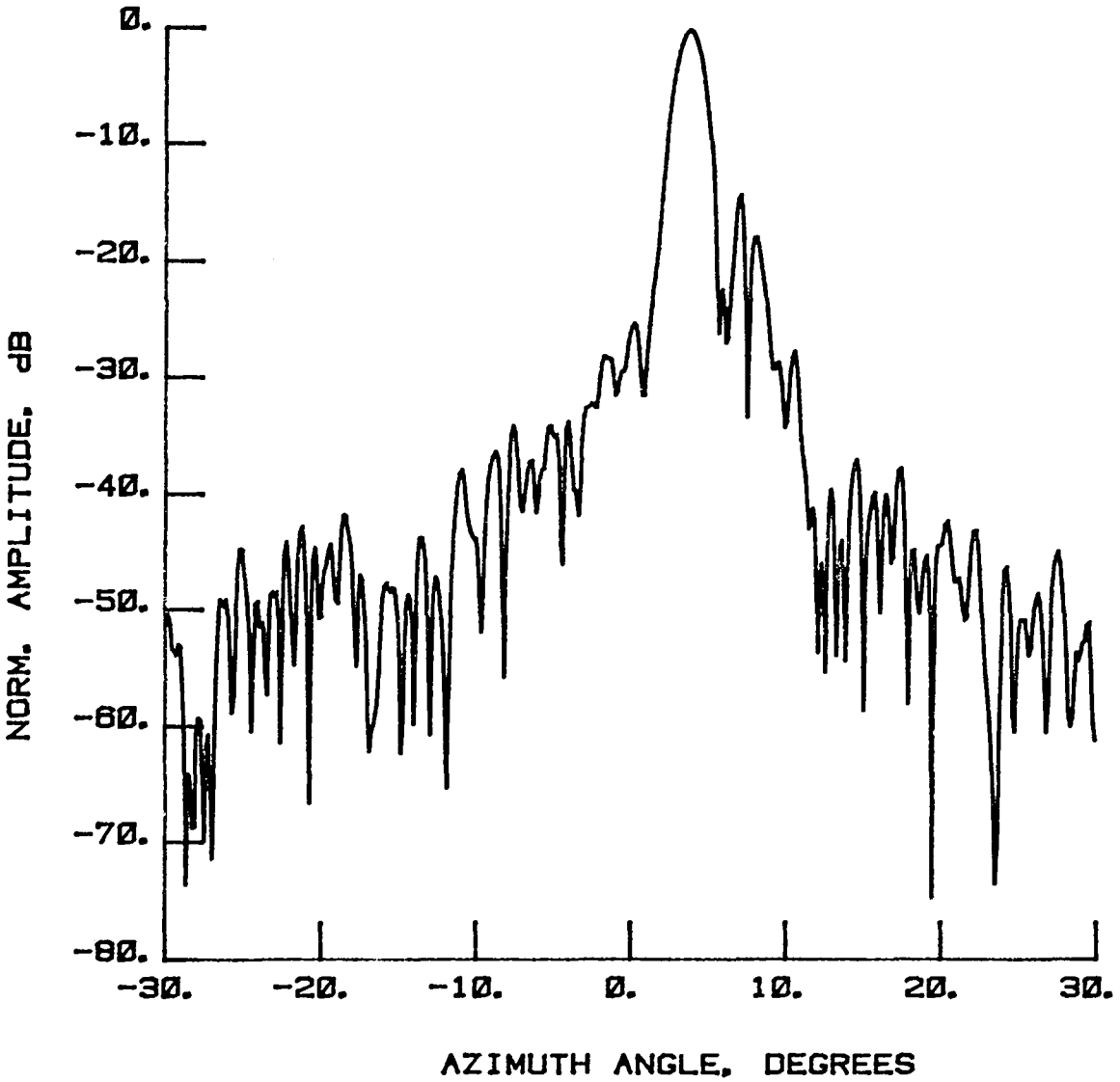

Figure 25 Test 10, E = 0.9°, Port 2, Type 1

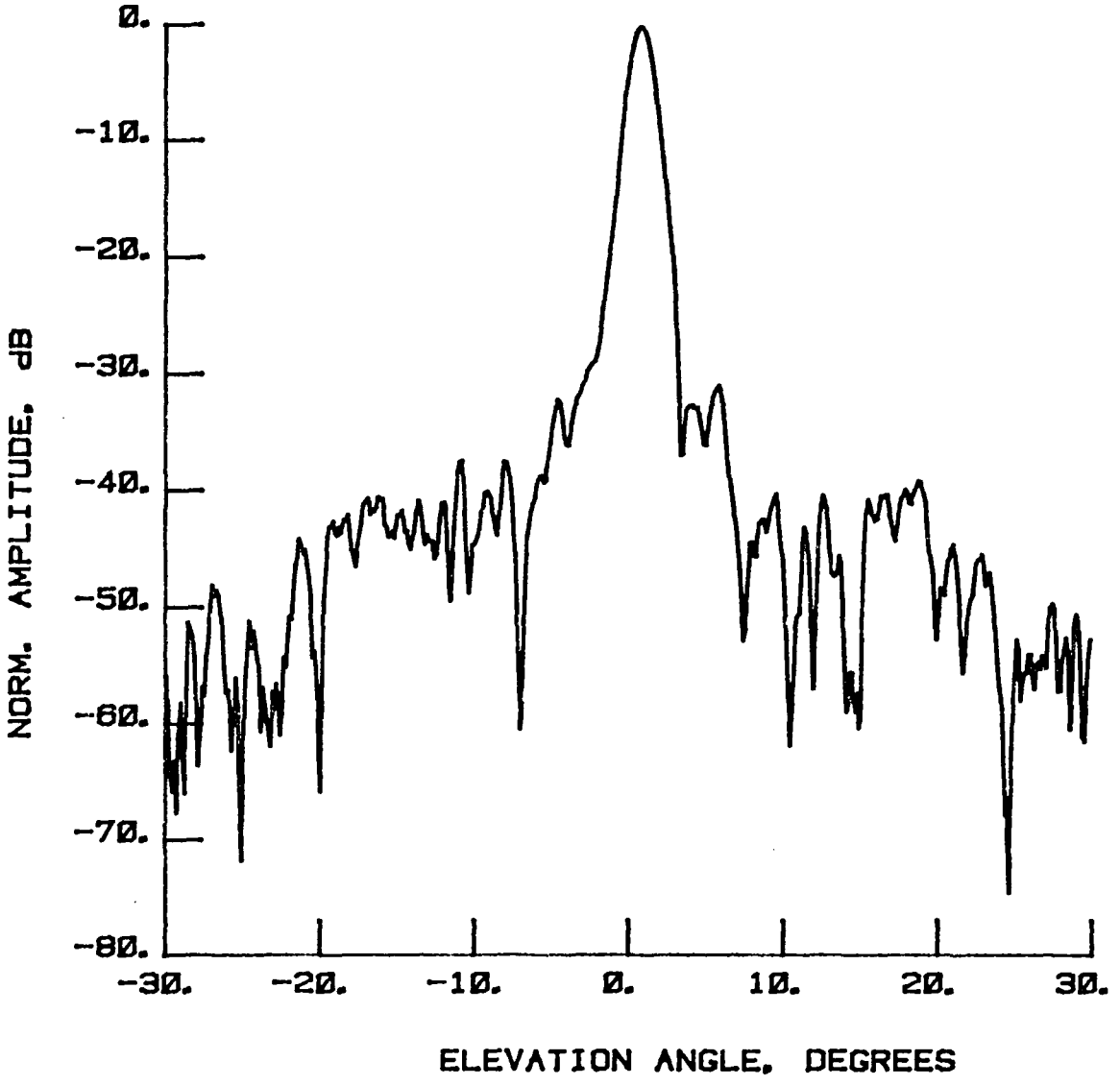

Figure 26 Test 10, A = 3.8°, Port 2, Type 2

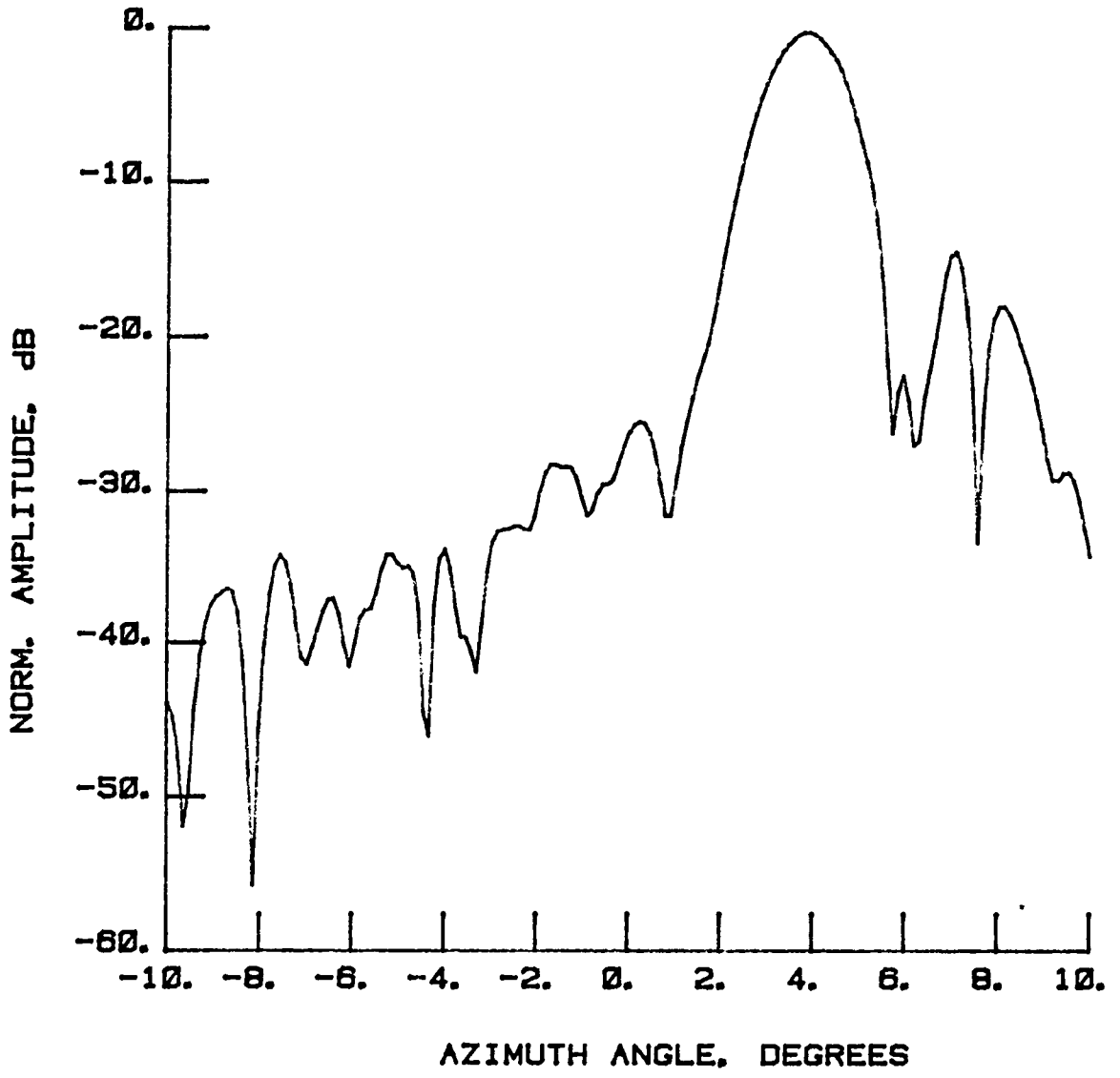

Figure 27 Test 10, E = 0.9°, Port 2, Type 3

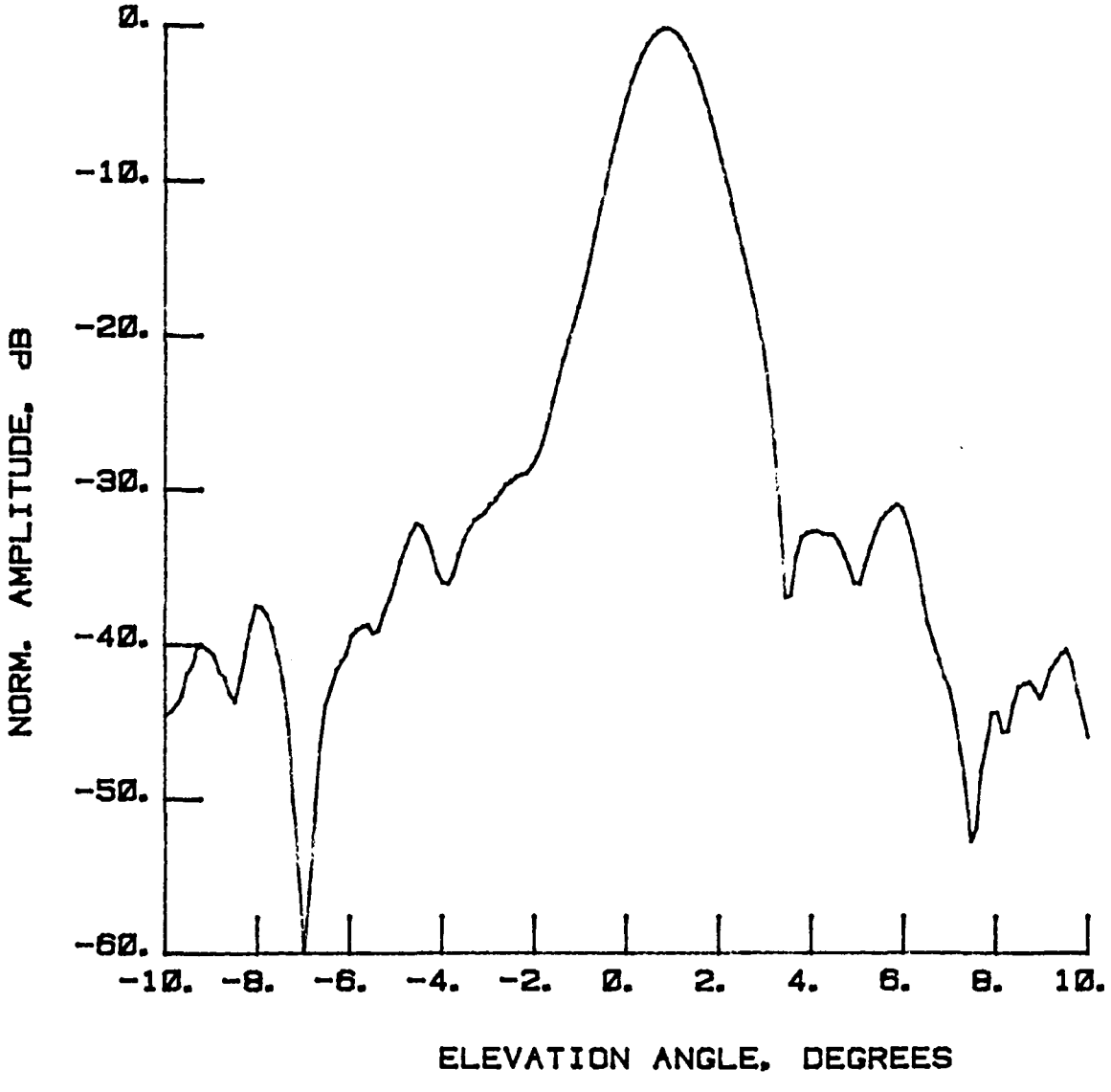

Figure 28 Test 10, A = 3.8°, Port 2, Type 4

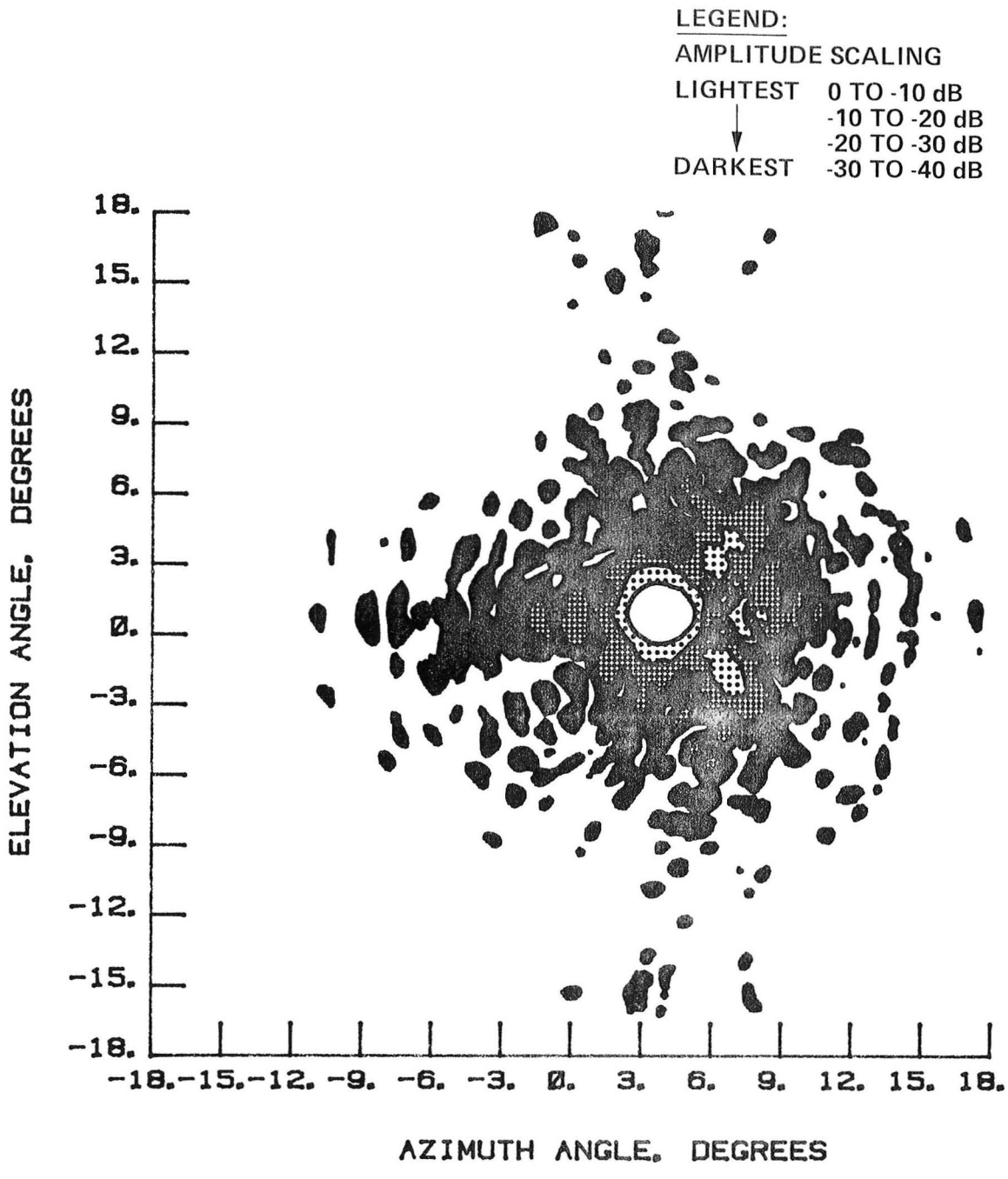

Figure 29 Test 10, Contour, Port 2, Type 5

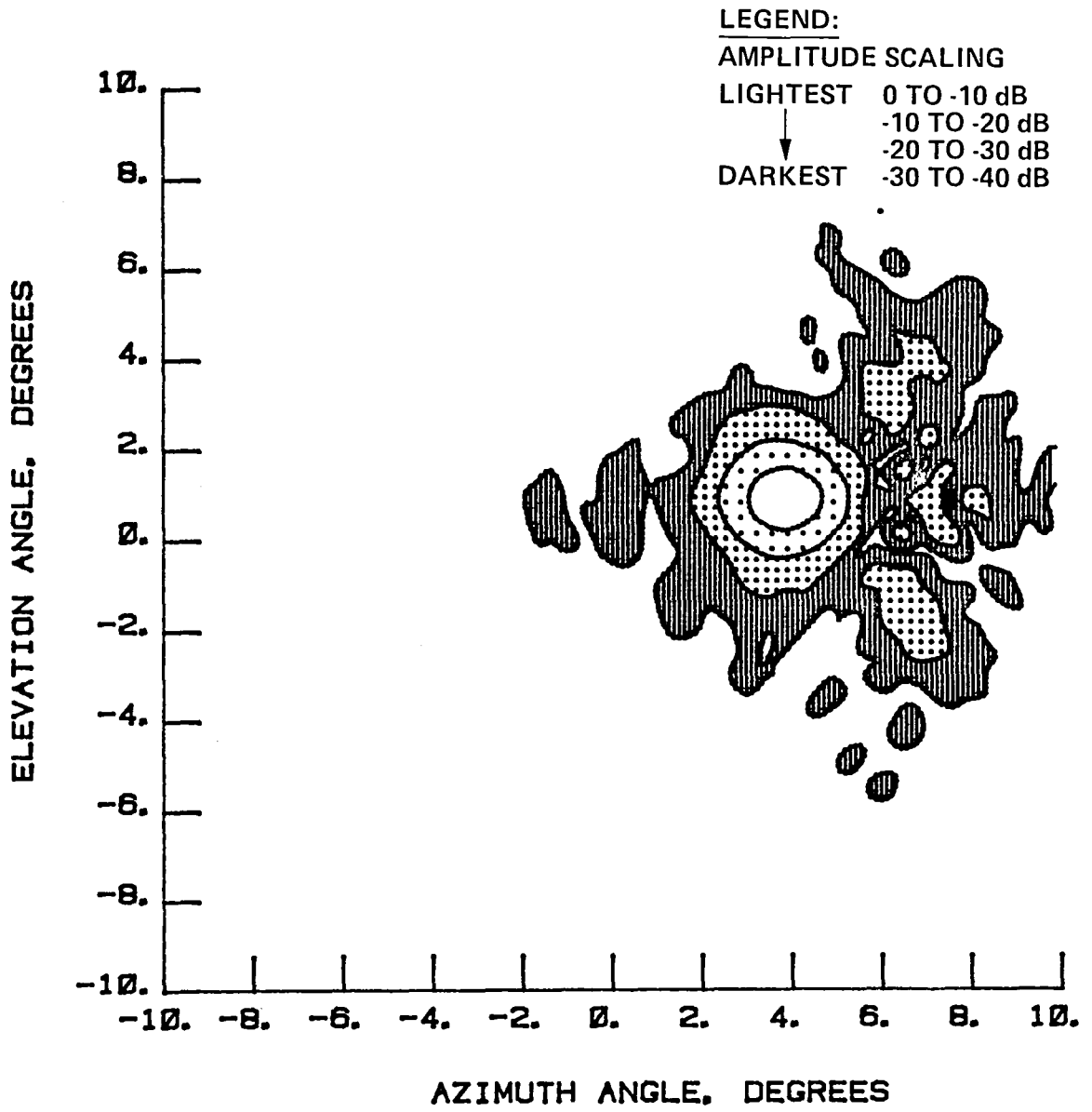

Figure 30 Test 10, Contour, Port 2, Type 6

This Page Intentionally Left Blank

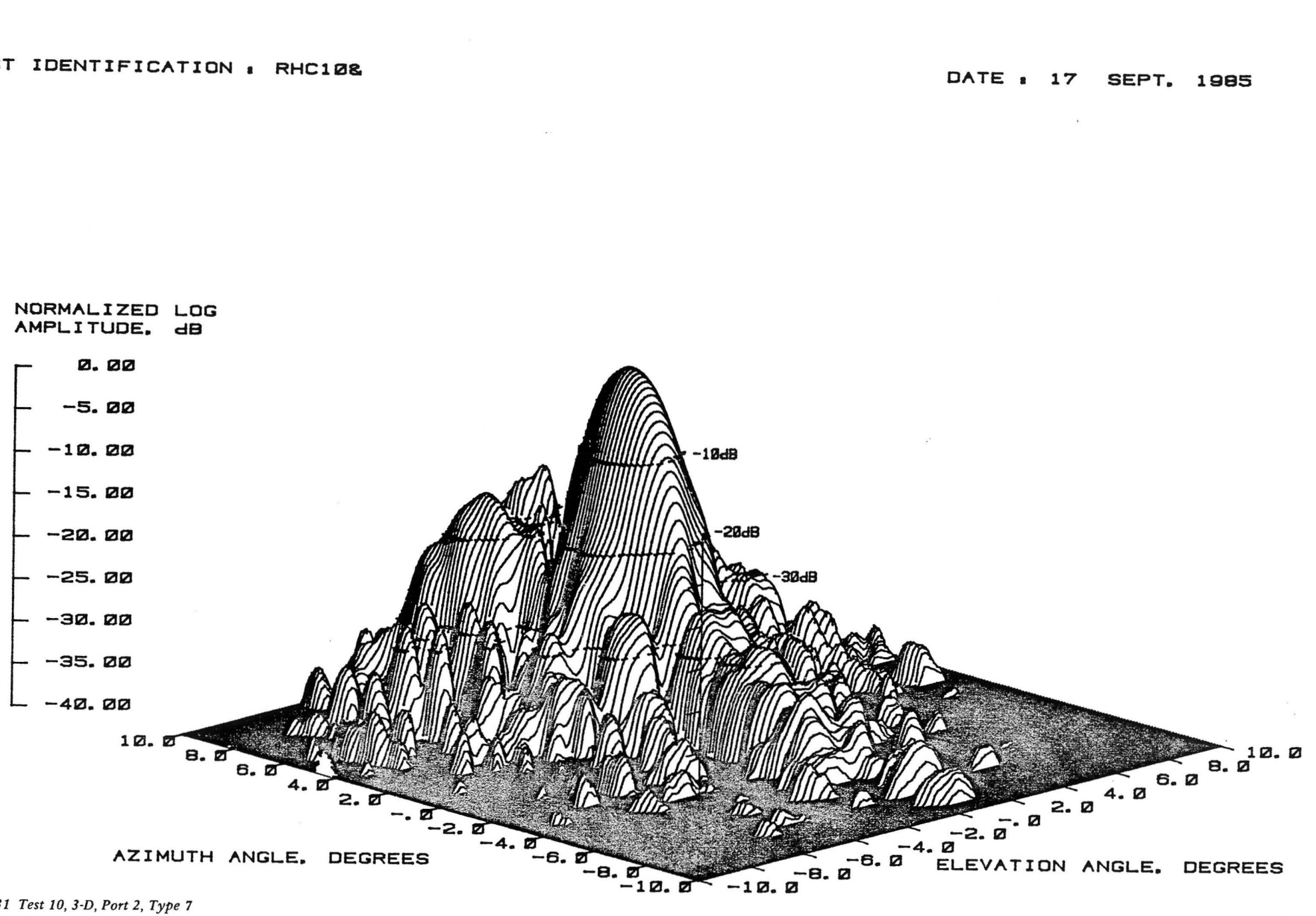

Figure 31 Test 10, 3-D, Port 2, Type 7

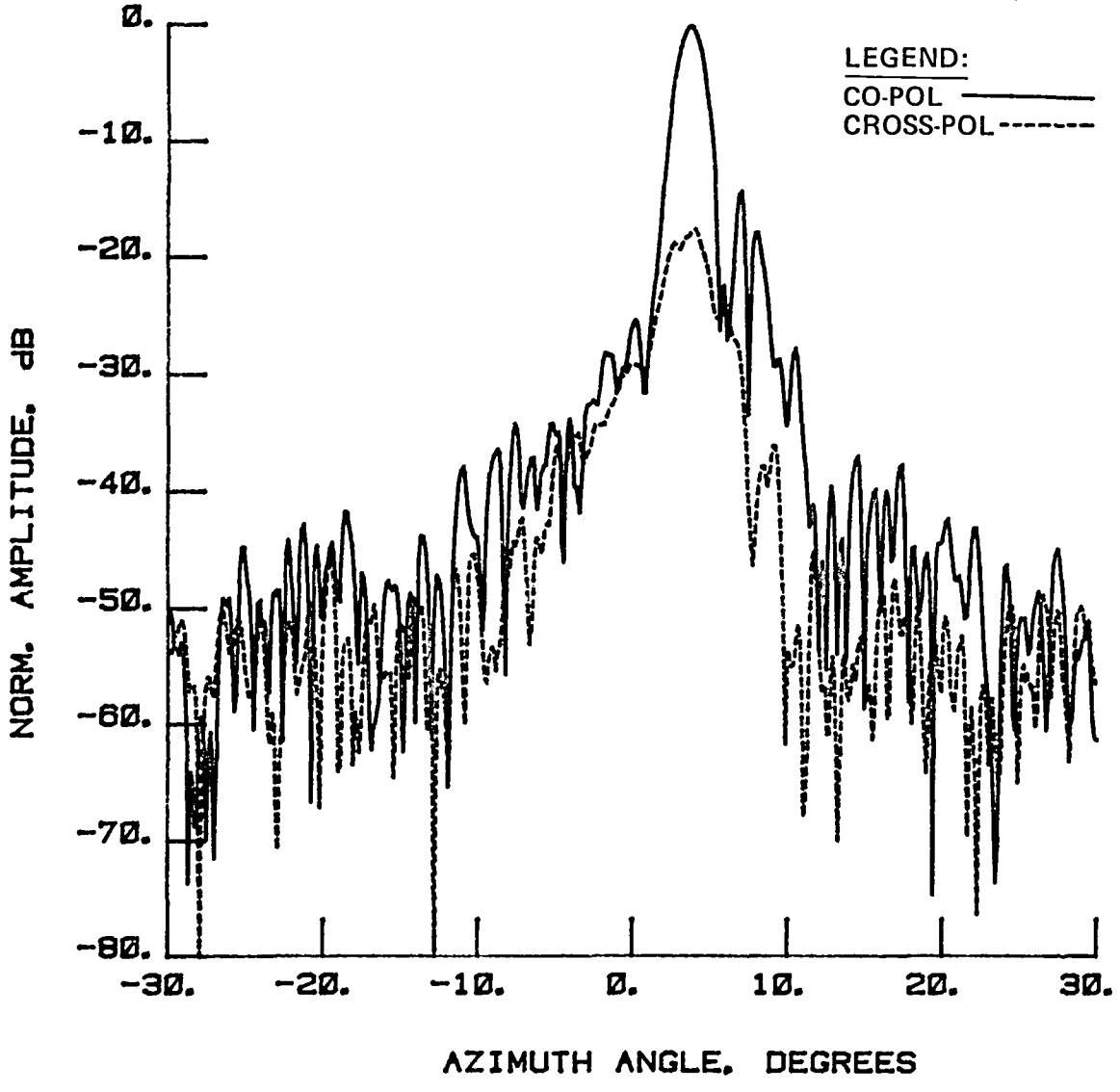

Figure 32 Test 11, E = 0.9°, Port 2, Type 8

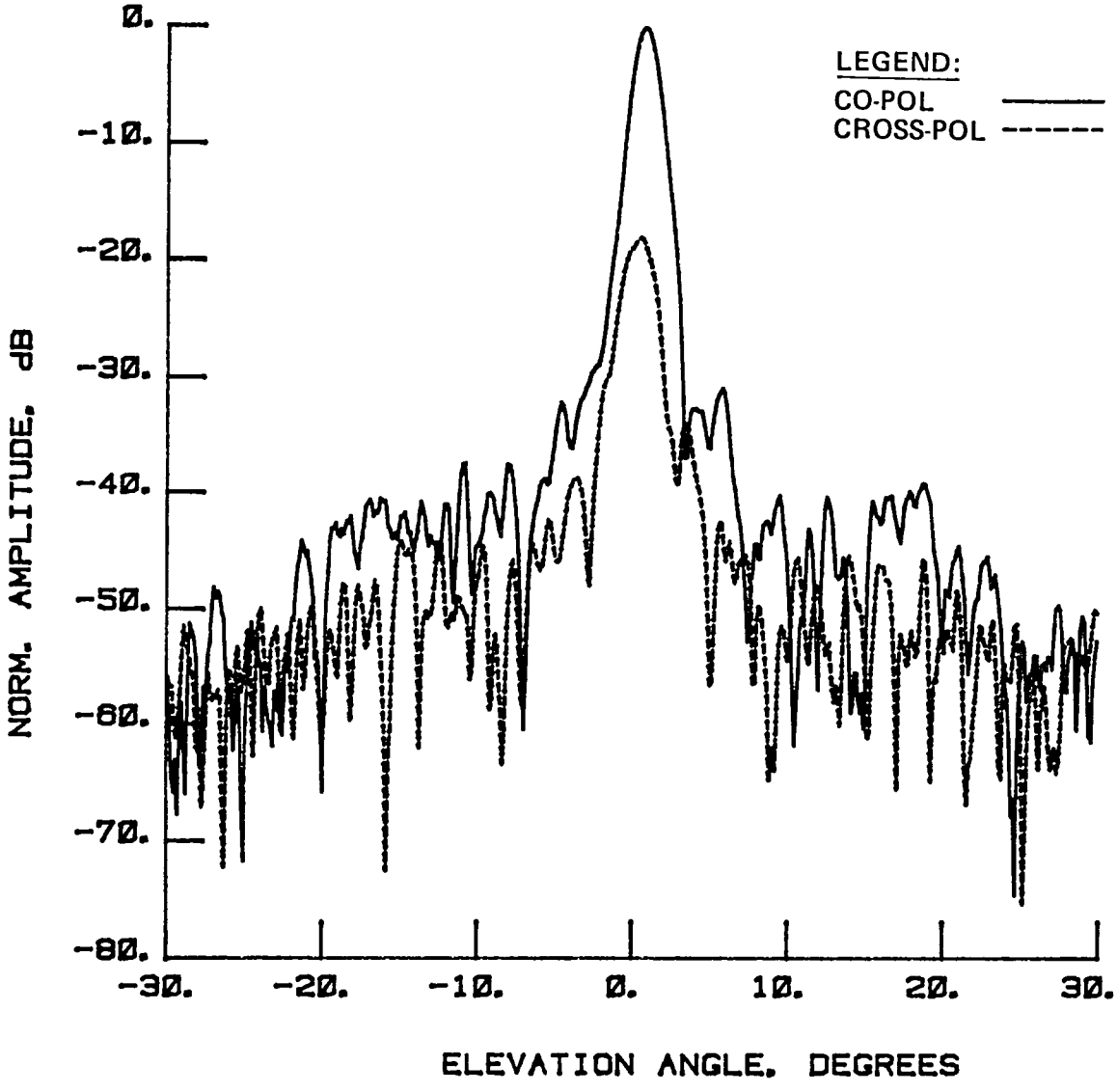

Figure 33 Test 11, A = 3.8°, Port 2, Type 9

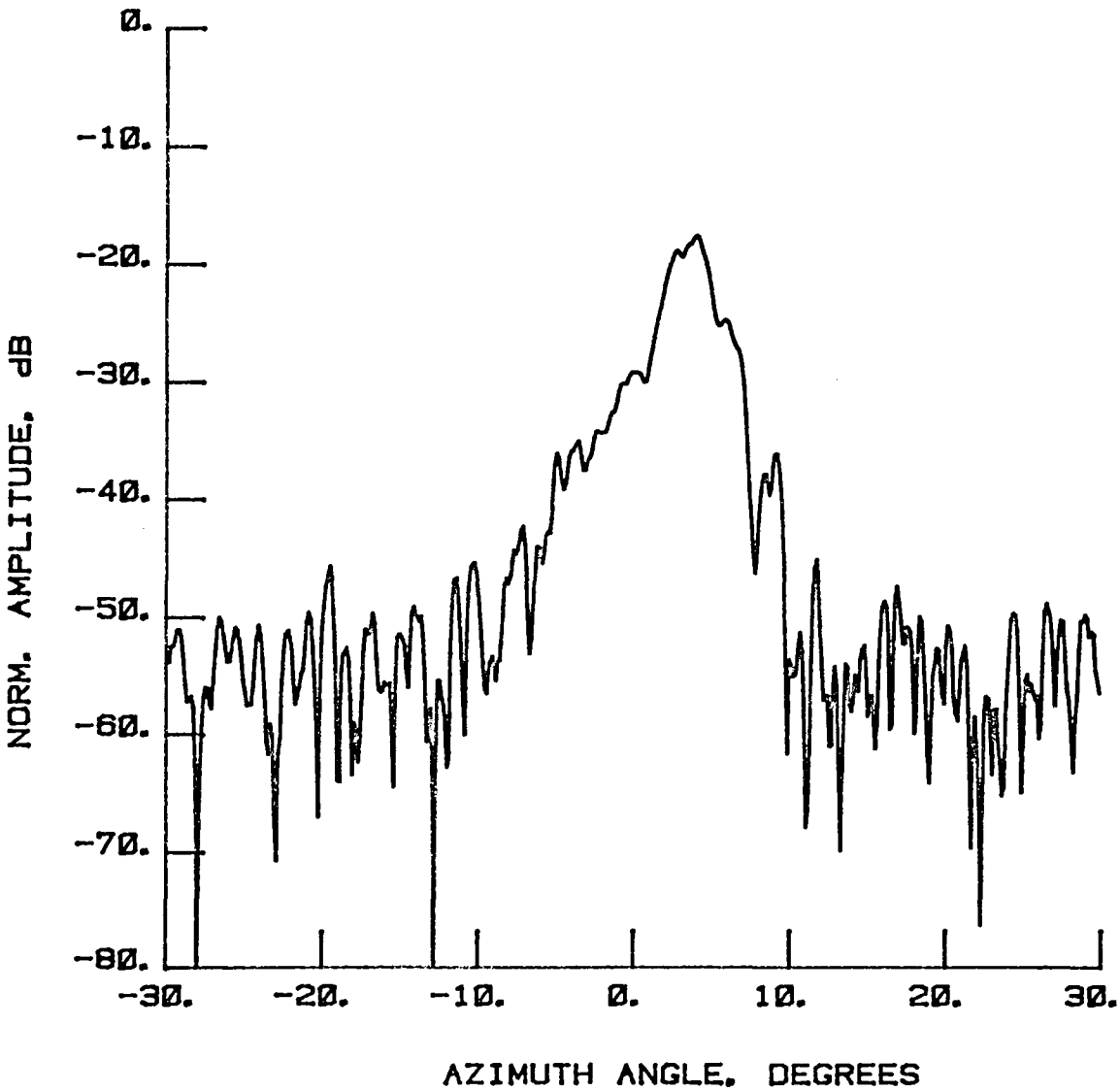

Figure 34 Test 11, E = 0.9°, Port 2, Type 10

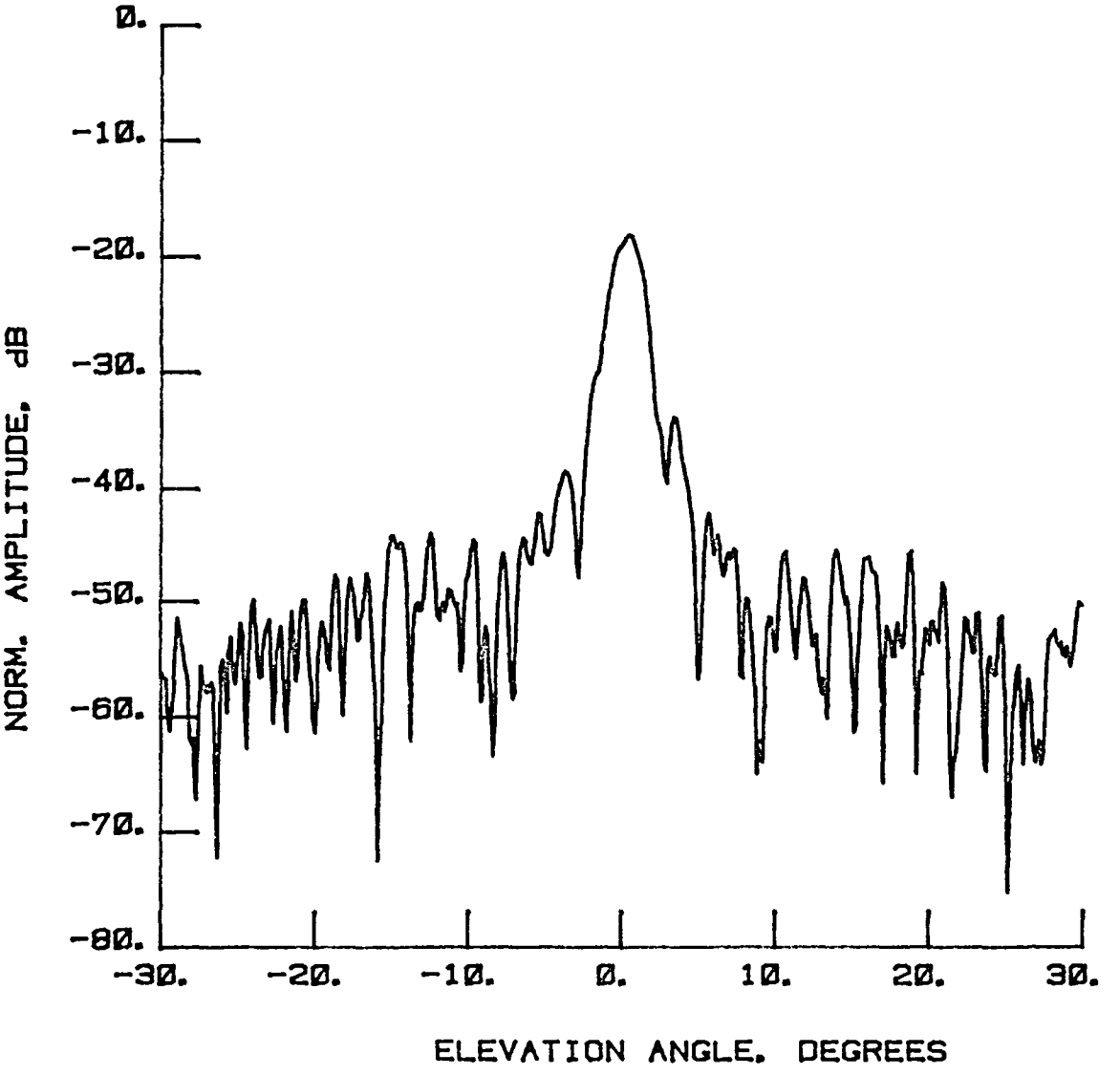

Figure 35 Test 11, A = 3.8°, Port 2, Type 11

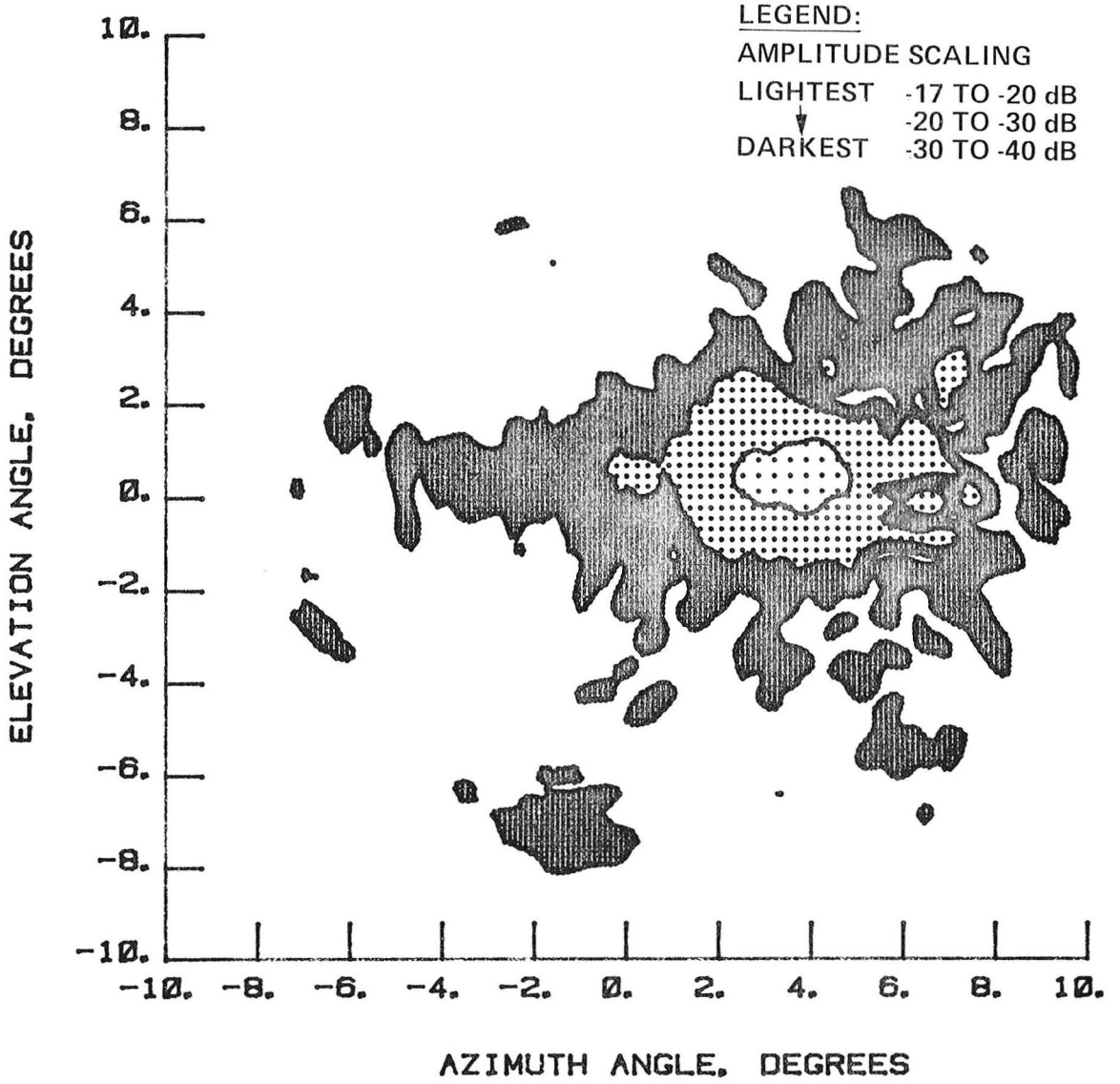

Figure 36 Test 11, Contour, Port 2, Type 12

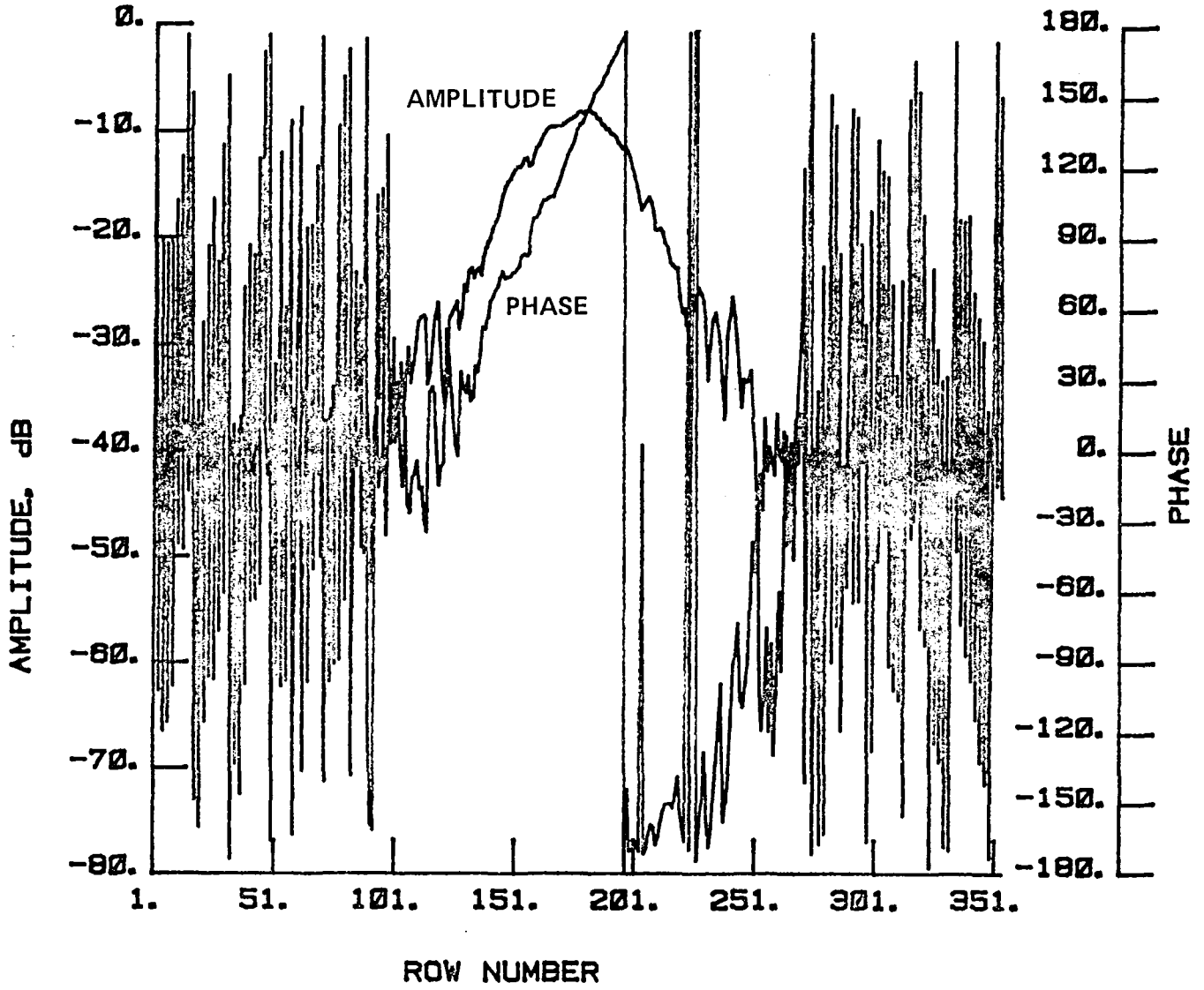

Figure 37 Test 10, Chord, Port 2, Type 13

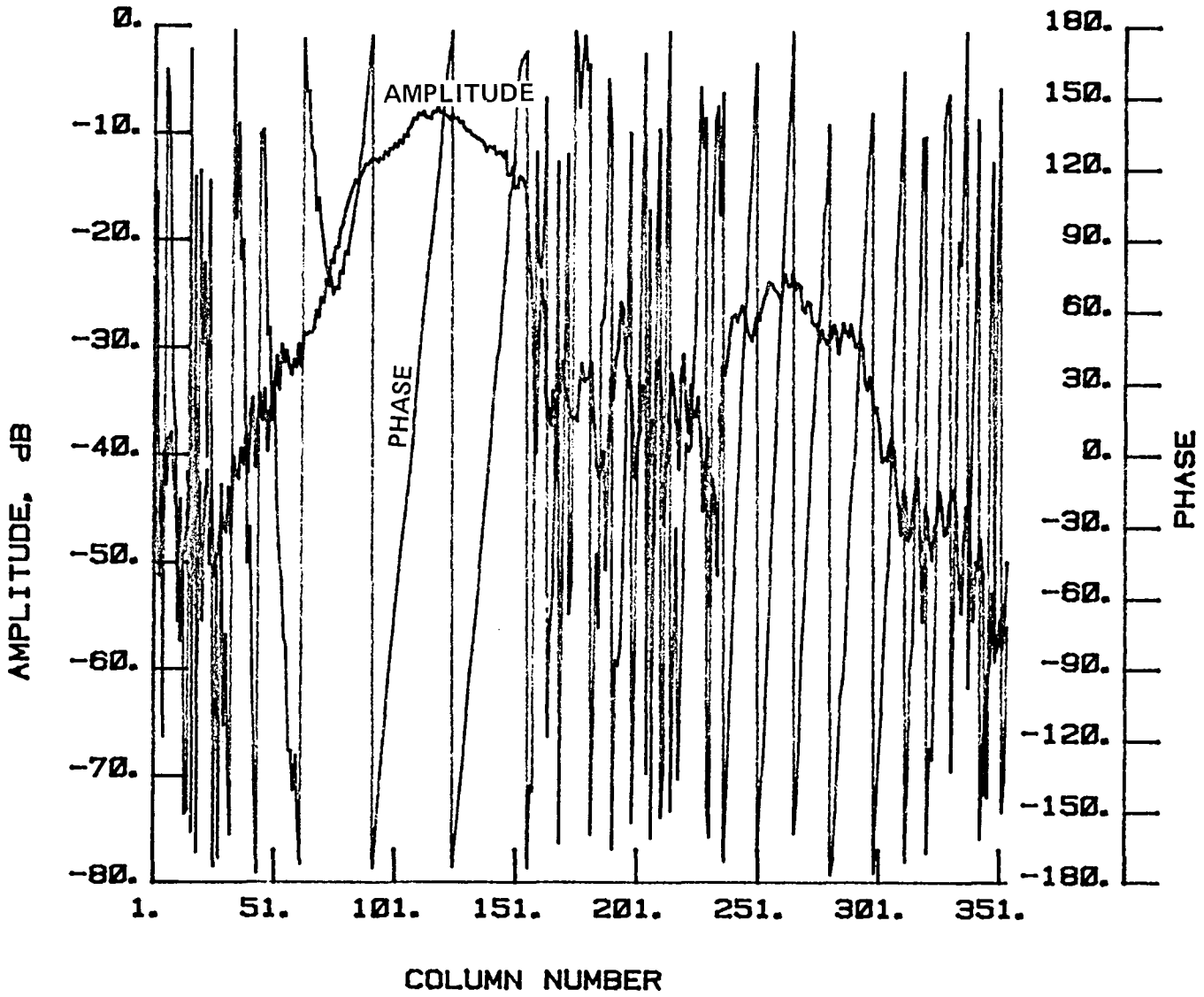

Figure 38 Test 10, Radial, Port 2, Type 14

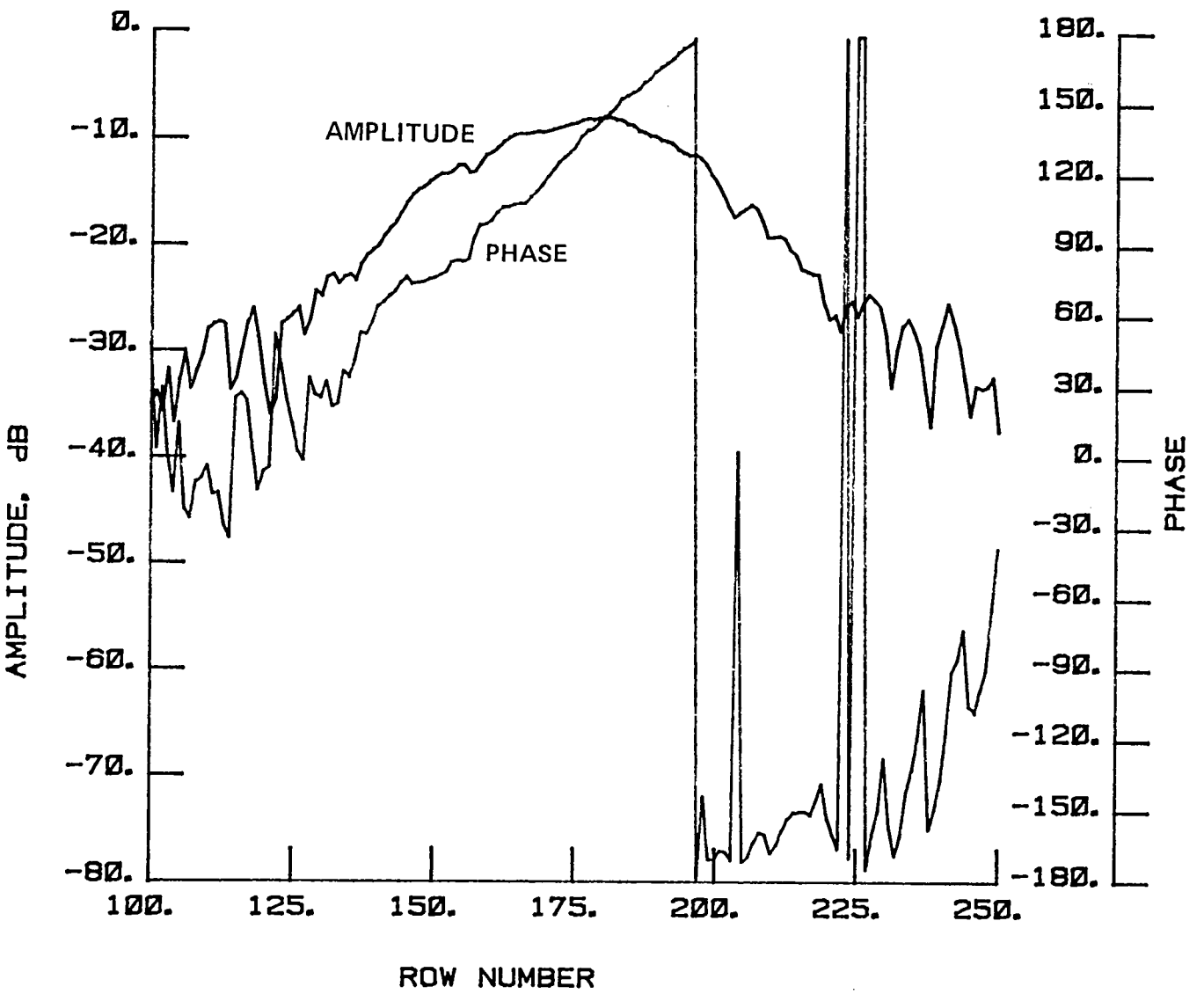

Figure 39 Test 10, Chord, Port 2, Type 15

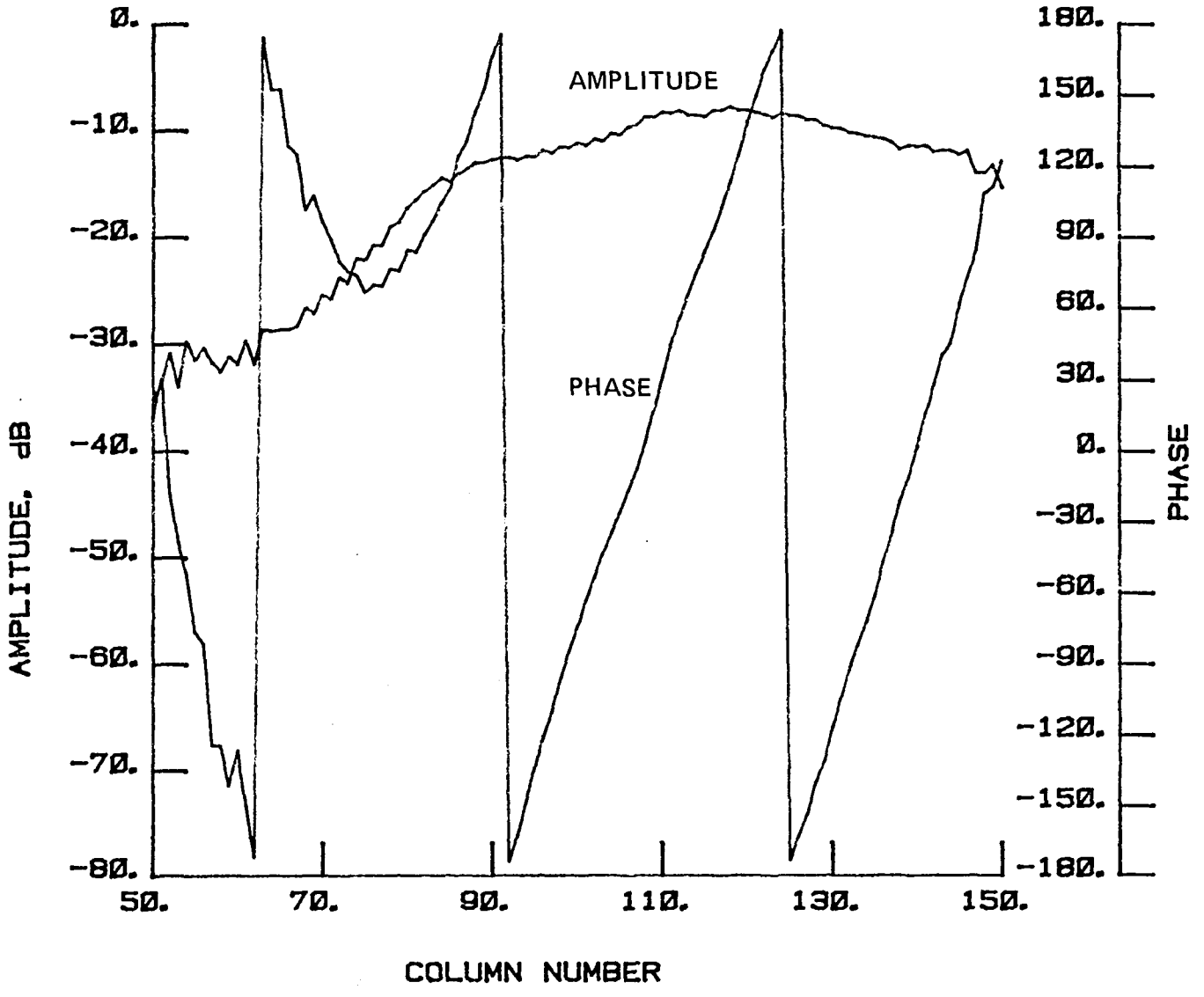

Figure 40 Test 10, Radial, Port 2, Type 16

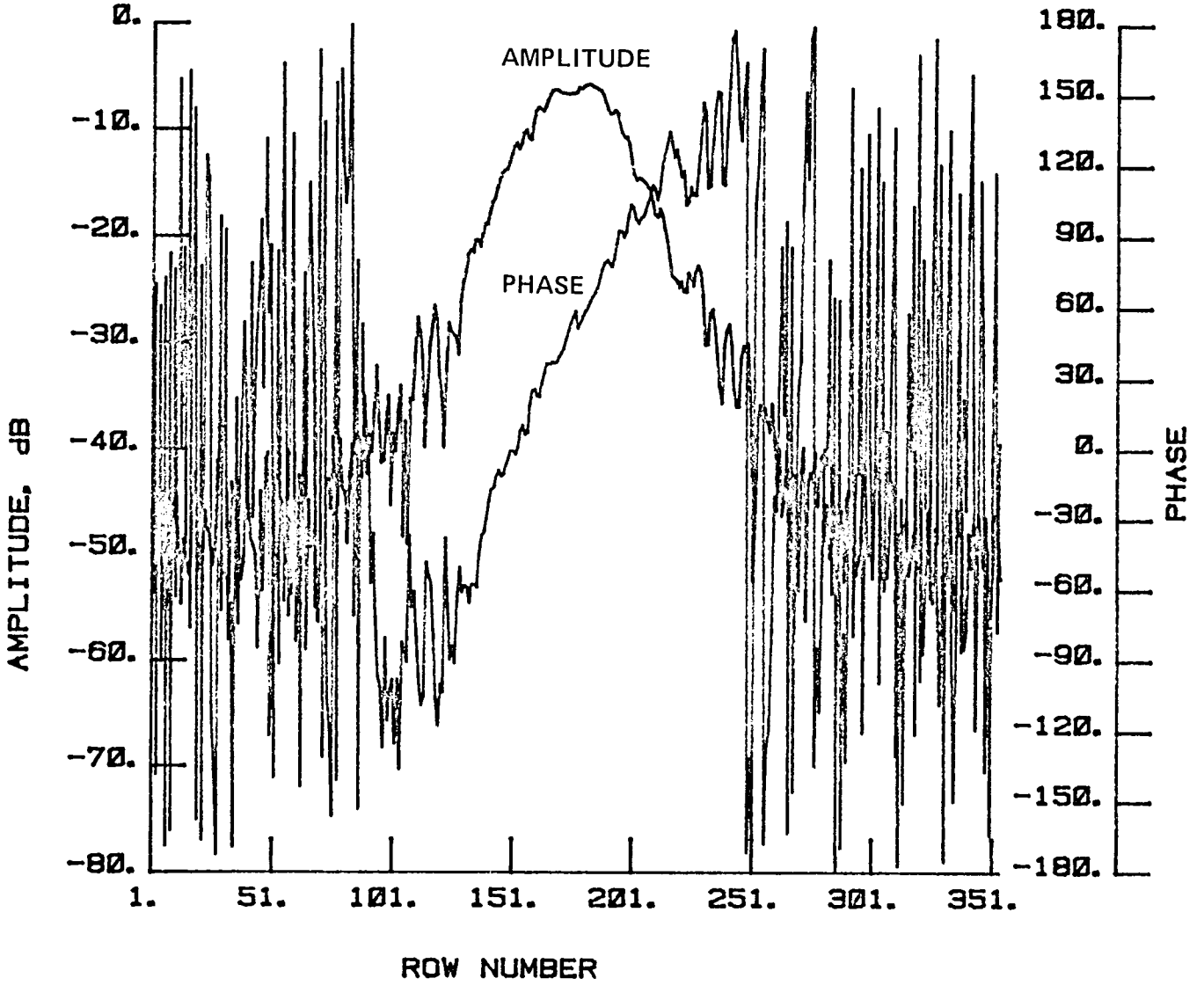

Figure 41 Test 11, Chord, Port 2, Type 17

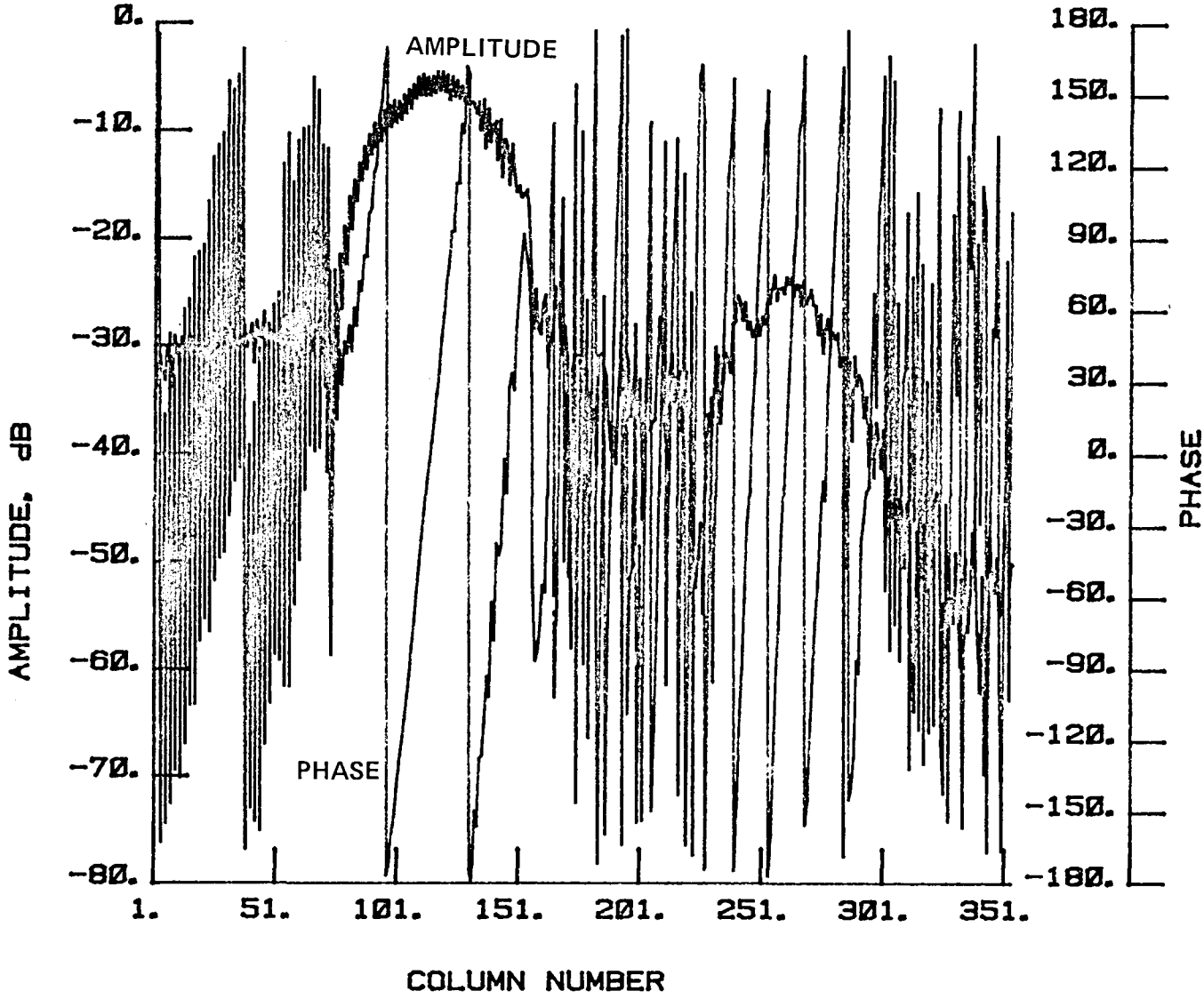

Figure 42 Test 11, Radial, Port 2, Type 18

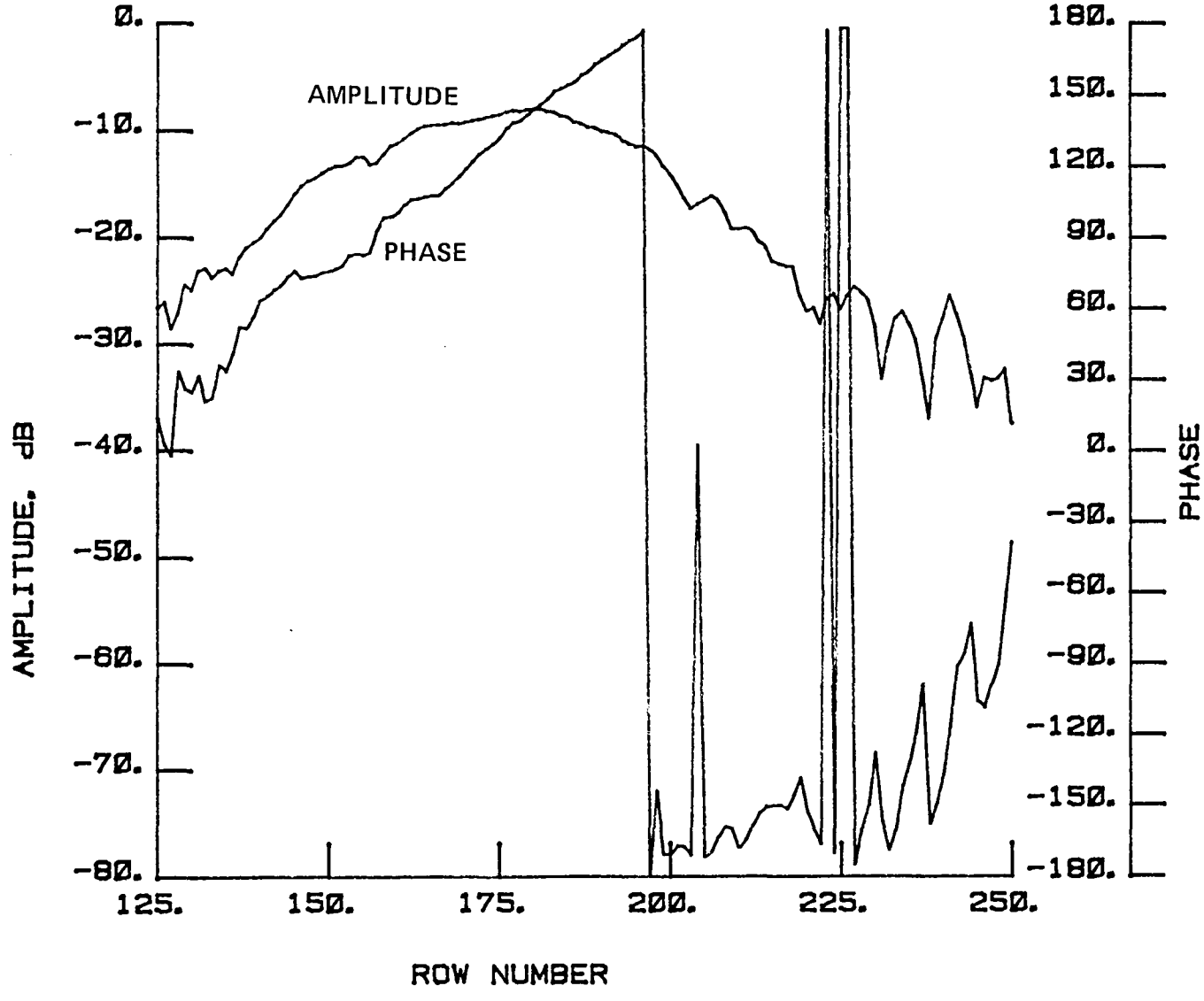

Figure 43 Test 11, Chord, Port 2, Type 19

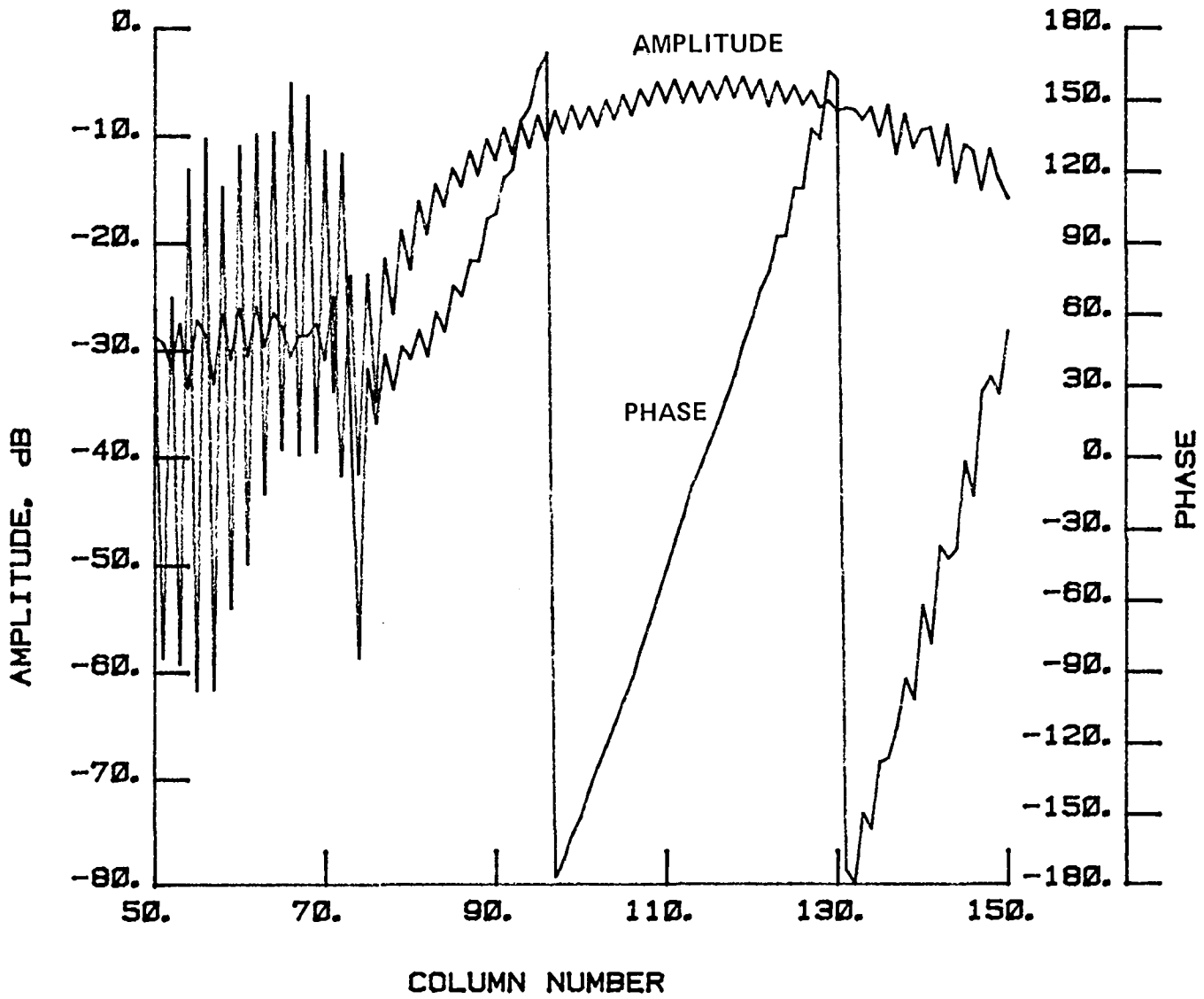

Figure 44 Test 11, Radial, Port 2, Type 20

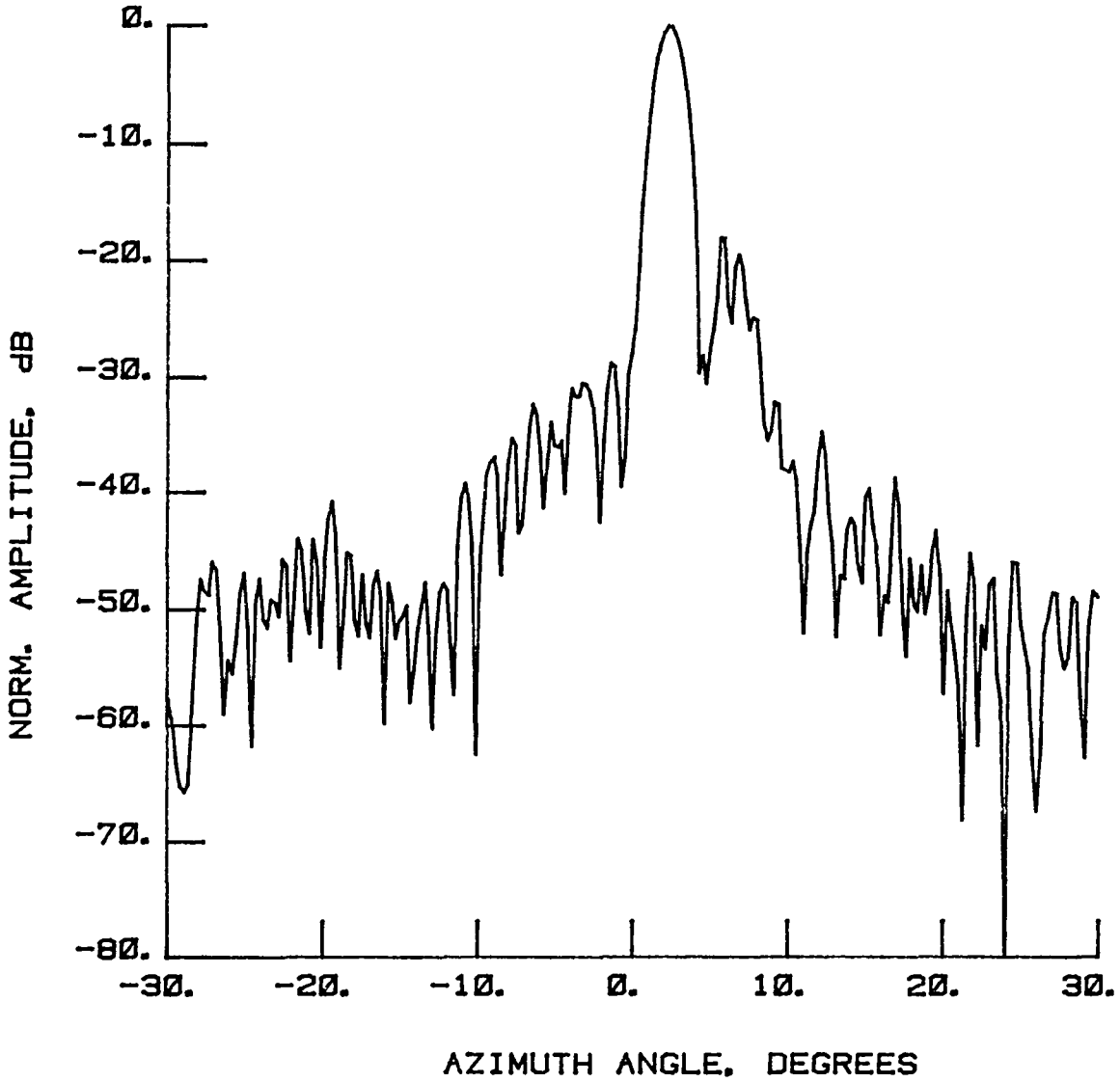

Figure 45 Test 11a, E = 0°, Port 4, Type 1

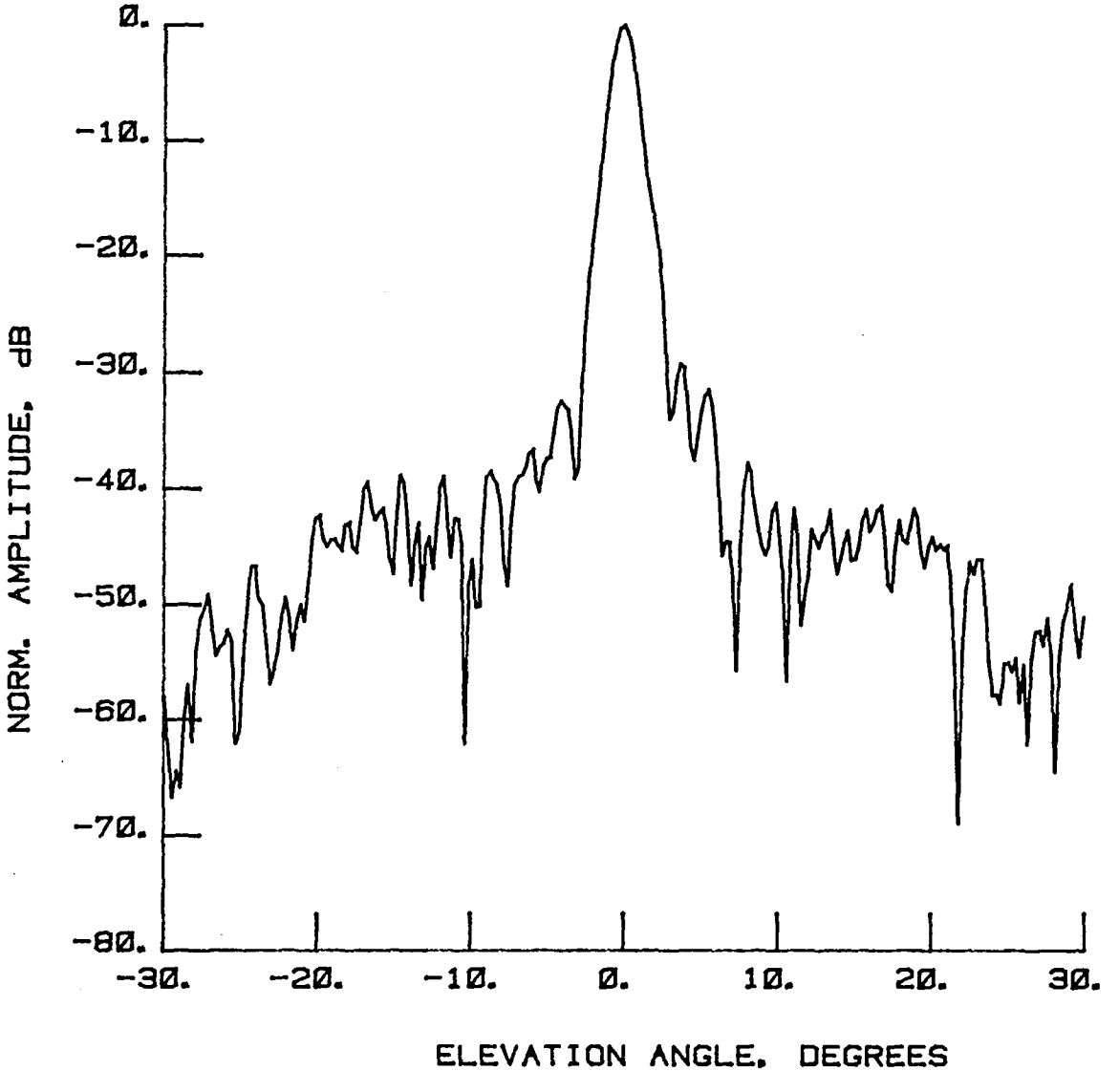

Figure 46 Test 11a, A = 2.6°, Port 4, Type 2

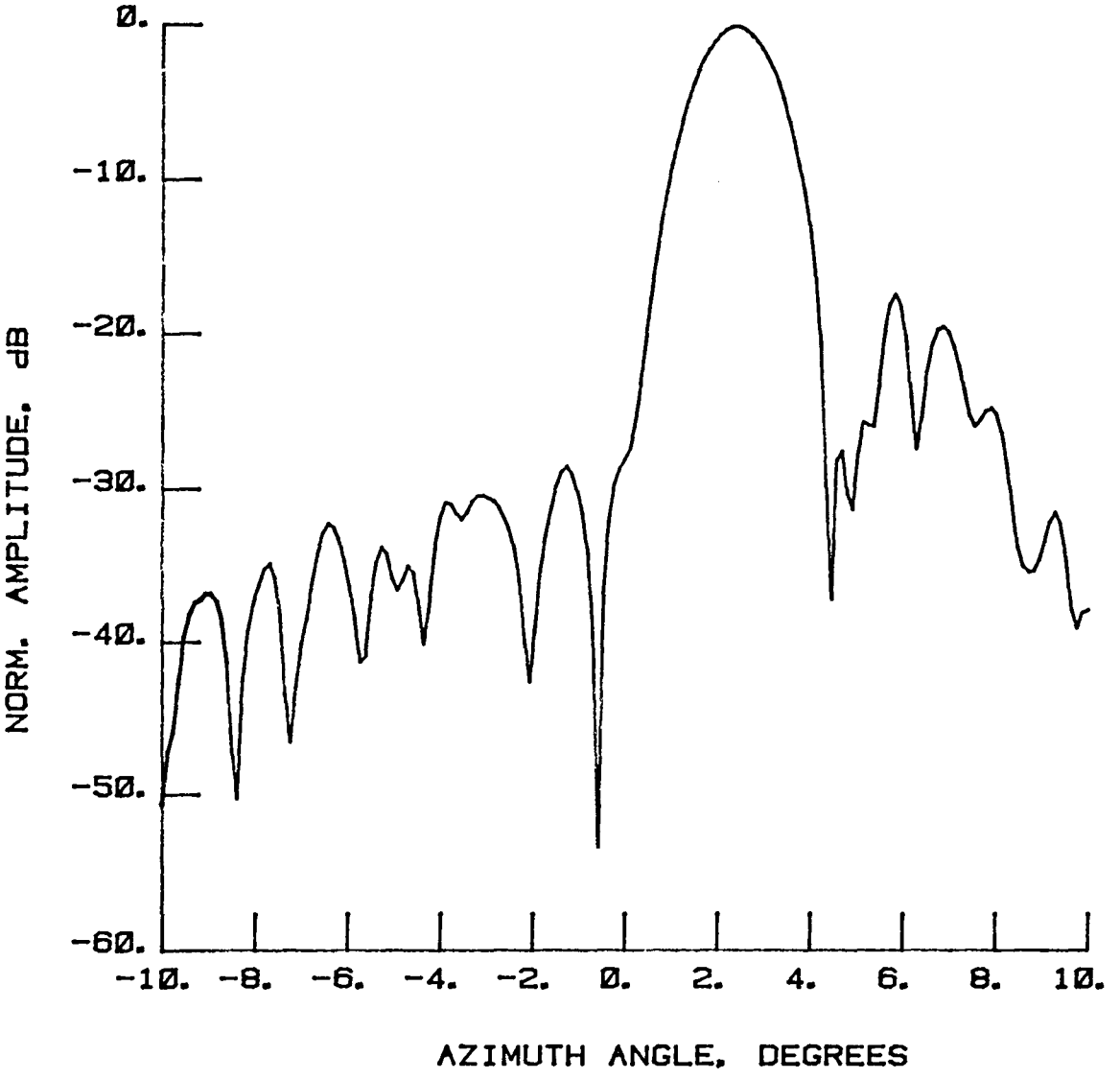

Figure 47 Test 11a, E = 0°, Port 4, Type 3

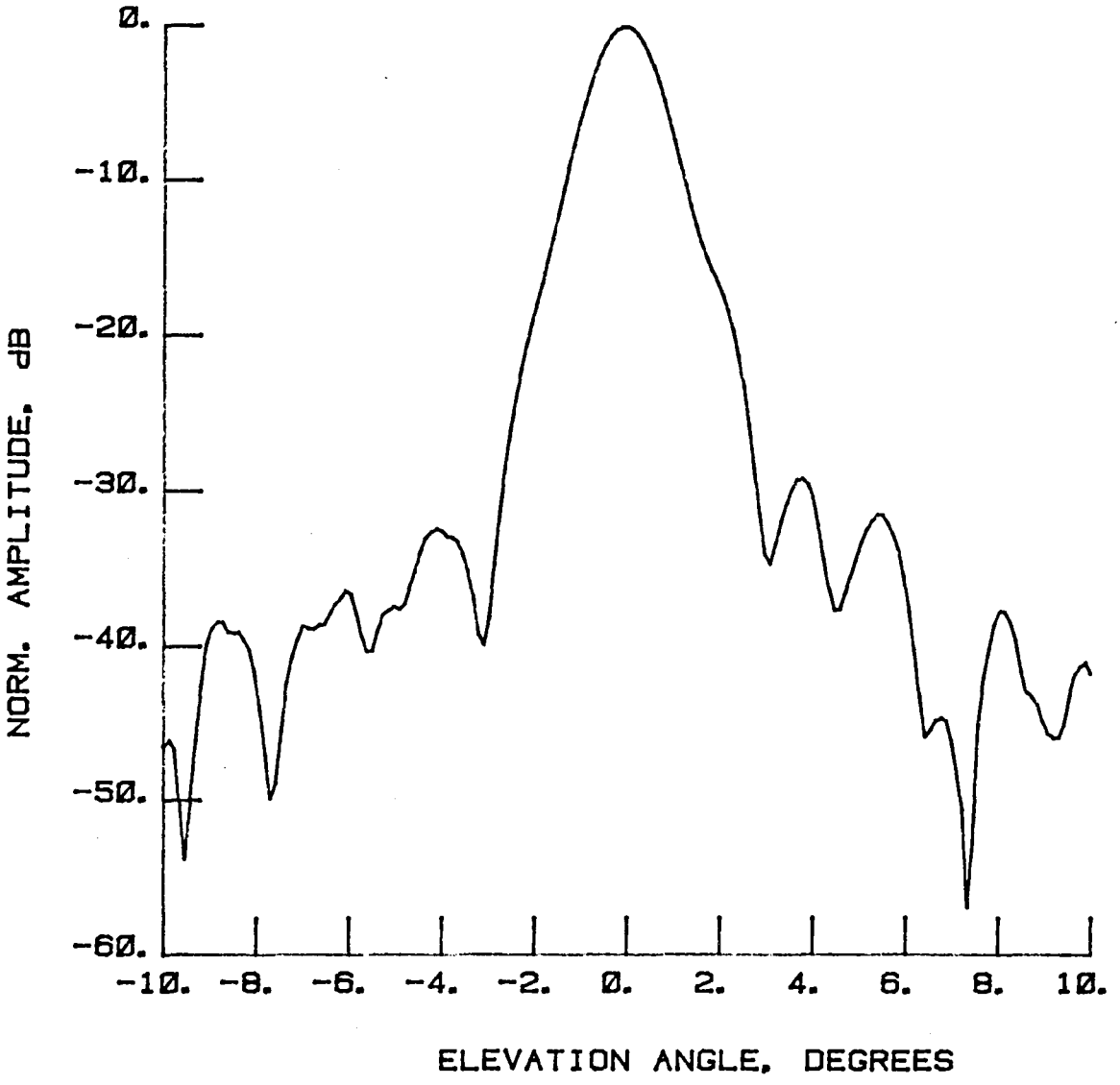

Figure 48 Test 11a, A = 2.6°, Port 4, Type 4

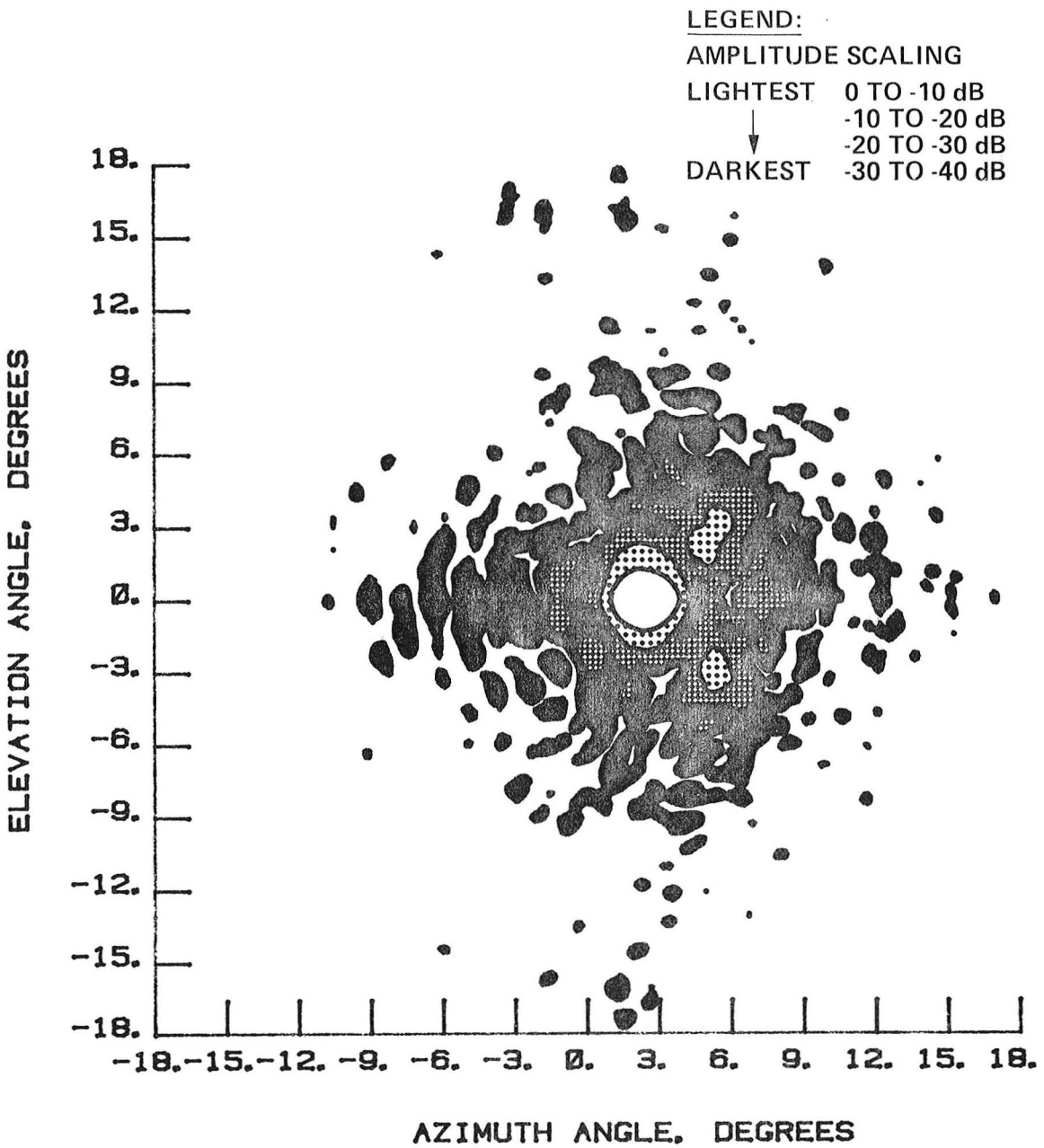

Figure 49 Test 11a, Contour, Port 4, Type 5

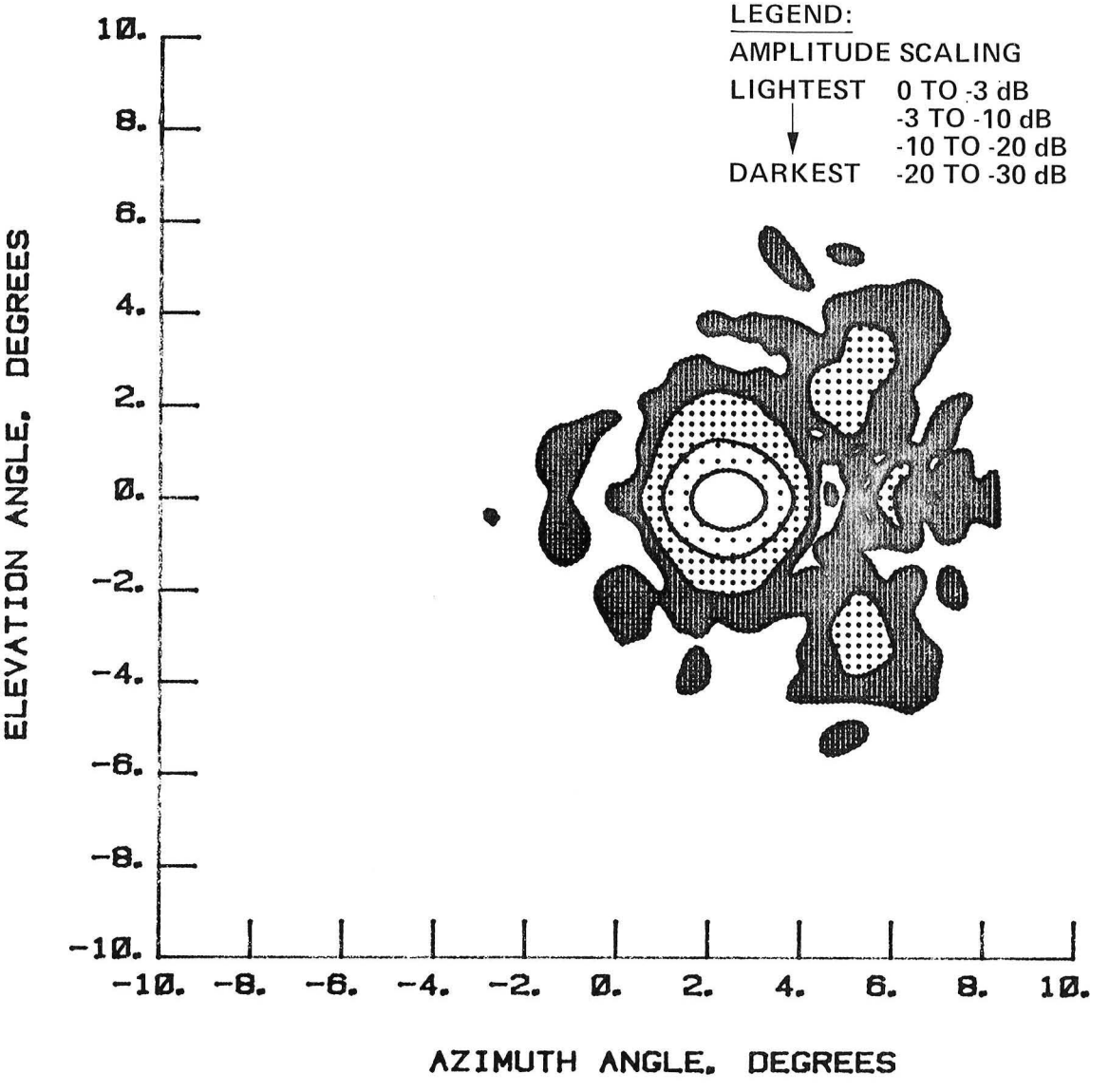

Figure 50 Test 11a, Contour, Port 4, Type 6

This Page Intentionally Left Blank

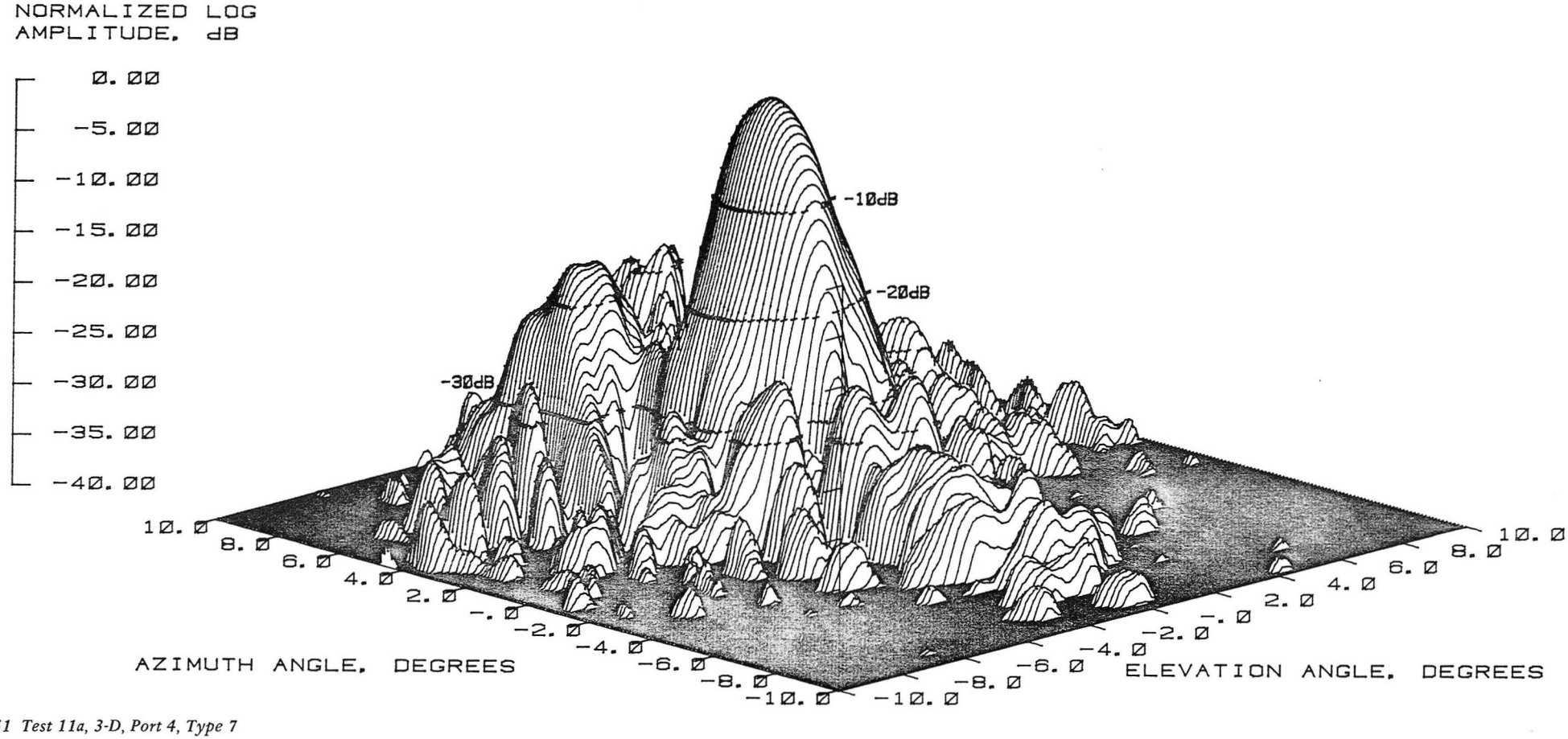

Figure 51 Test 11a, 3-D, Port 4, Type 7

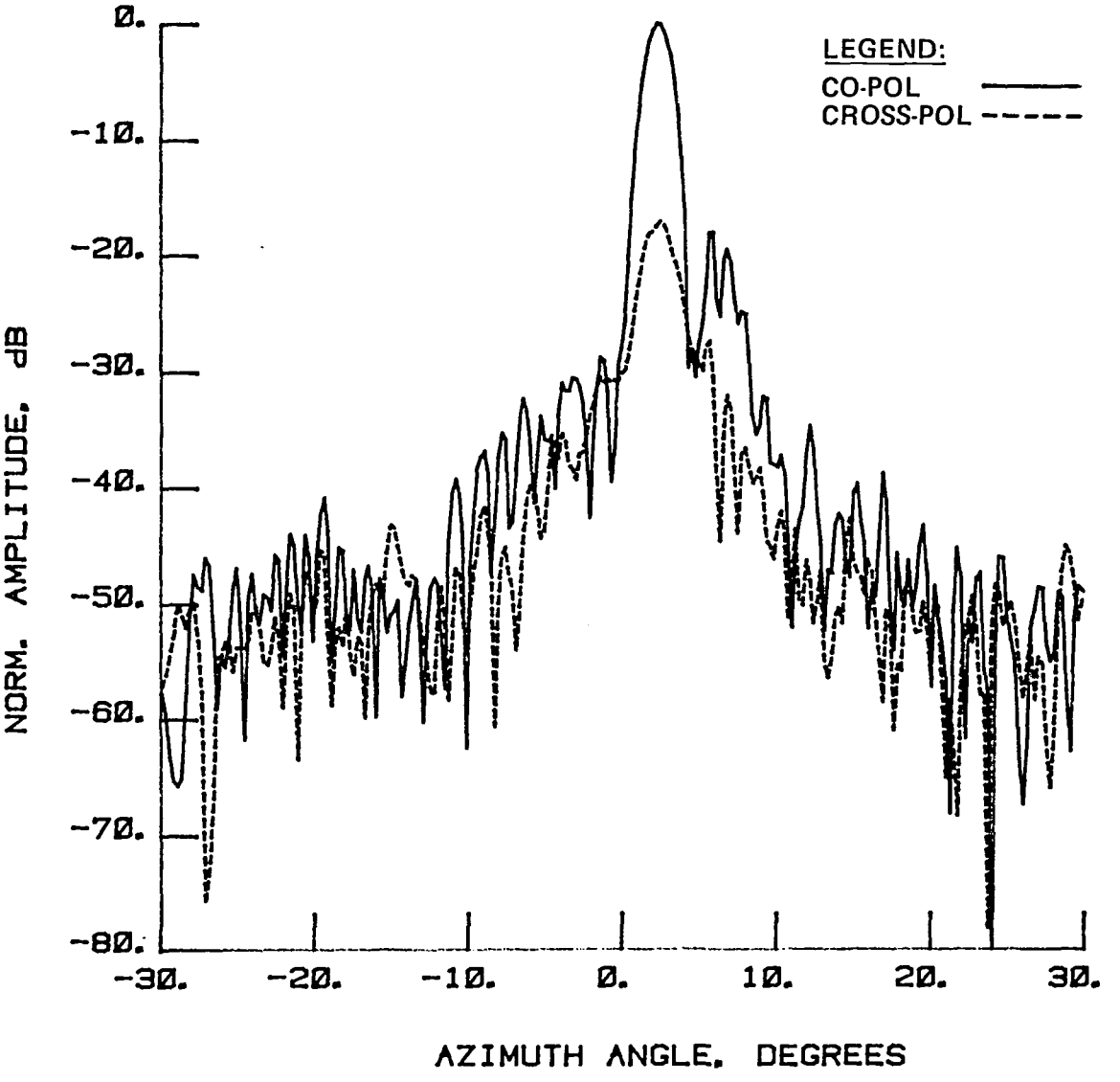

Figure 52 Test 11b, E = 0°, Port 4, Type 8

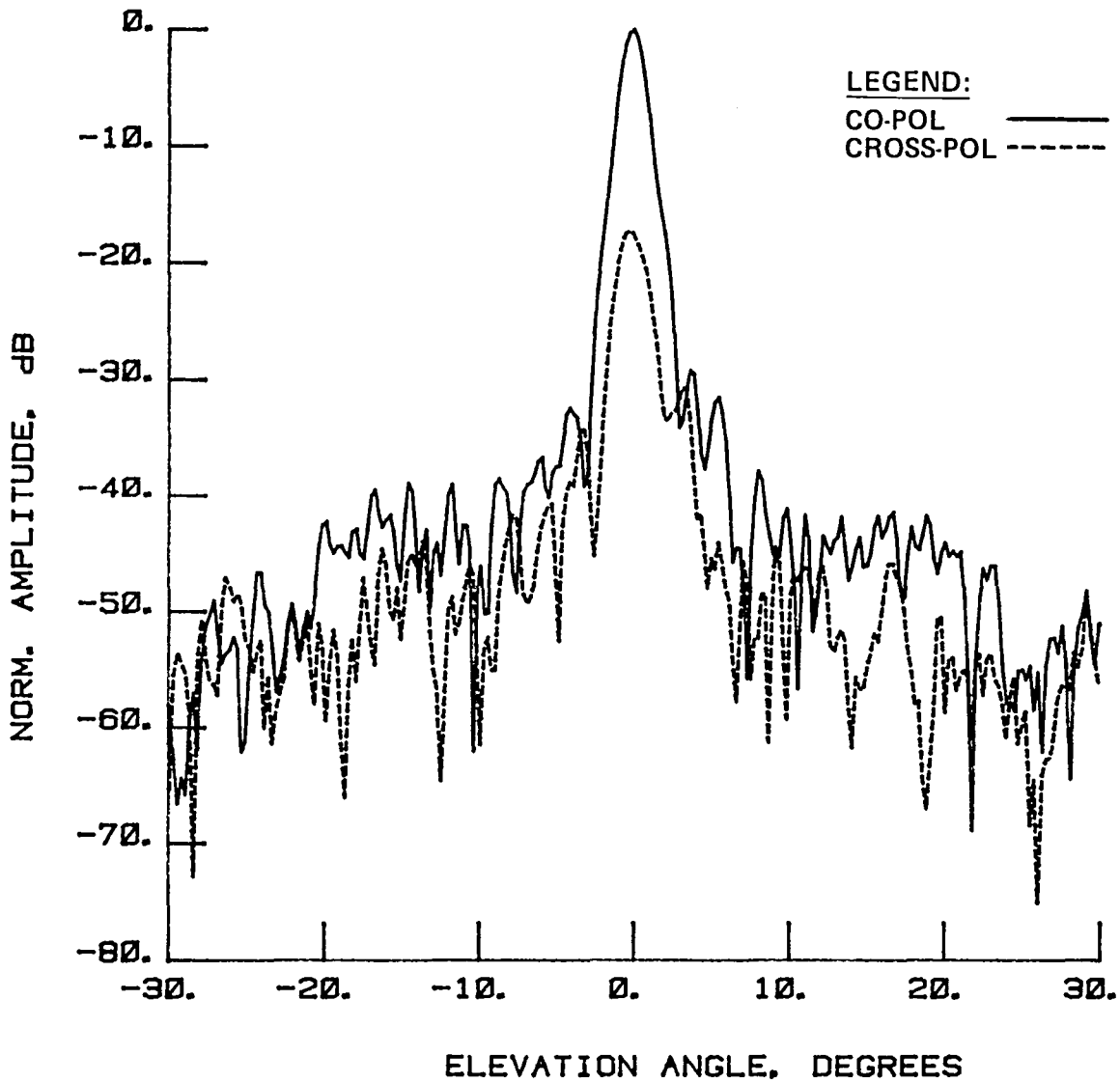

Figure 53 Test 11b, A = 2.6°, Port 4, Type 9

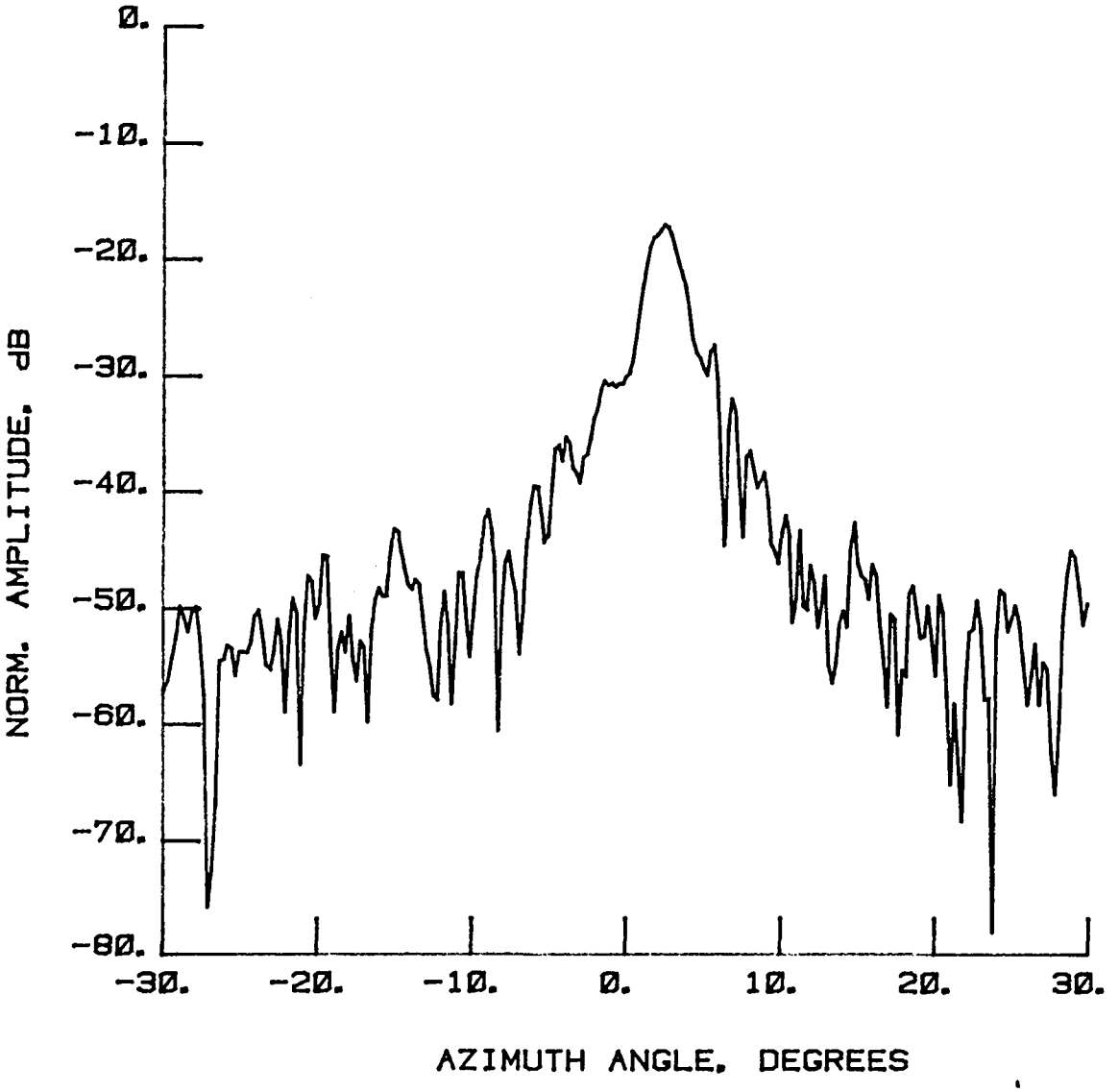

Figure 54 Test 11b, E = 0°, Port 4, Type 10

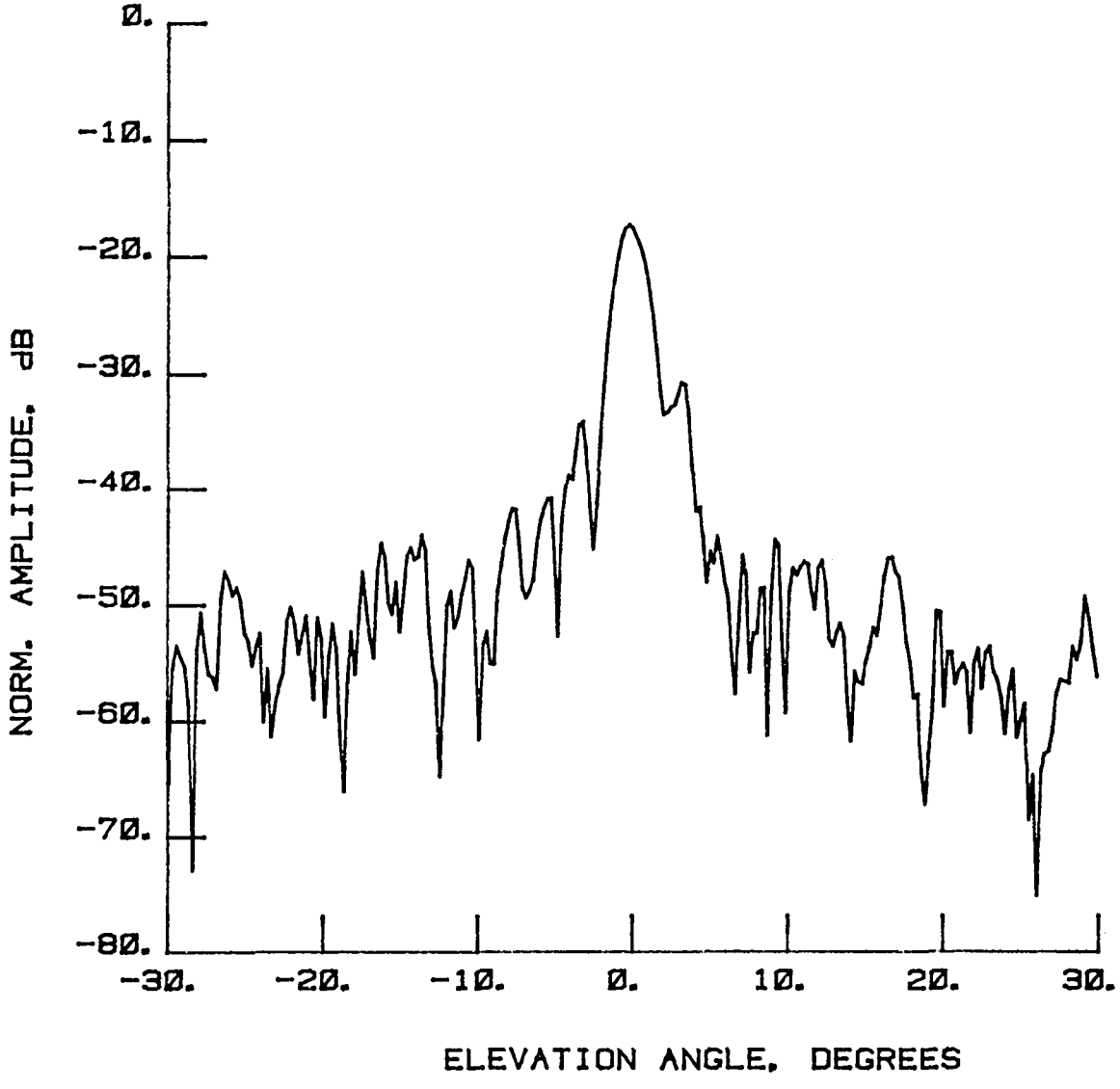

Figure 55 Test 11b, A = 2.6°, Port 4, Type 11

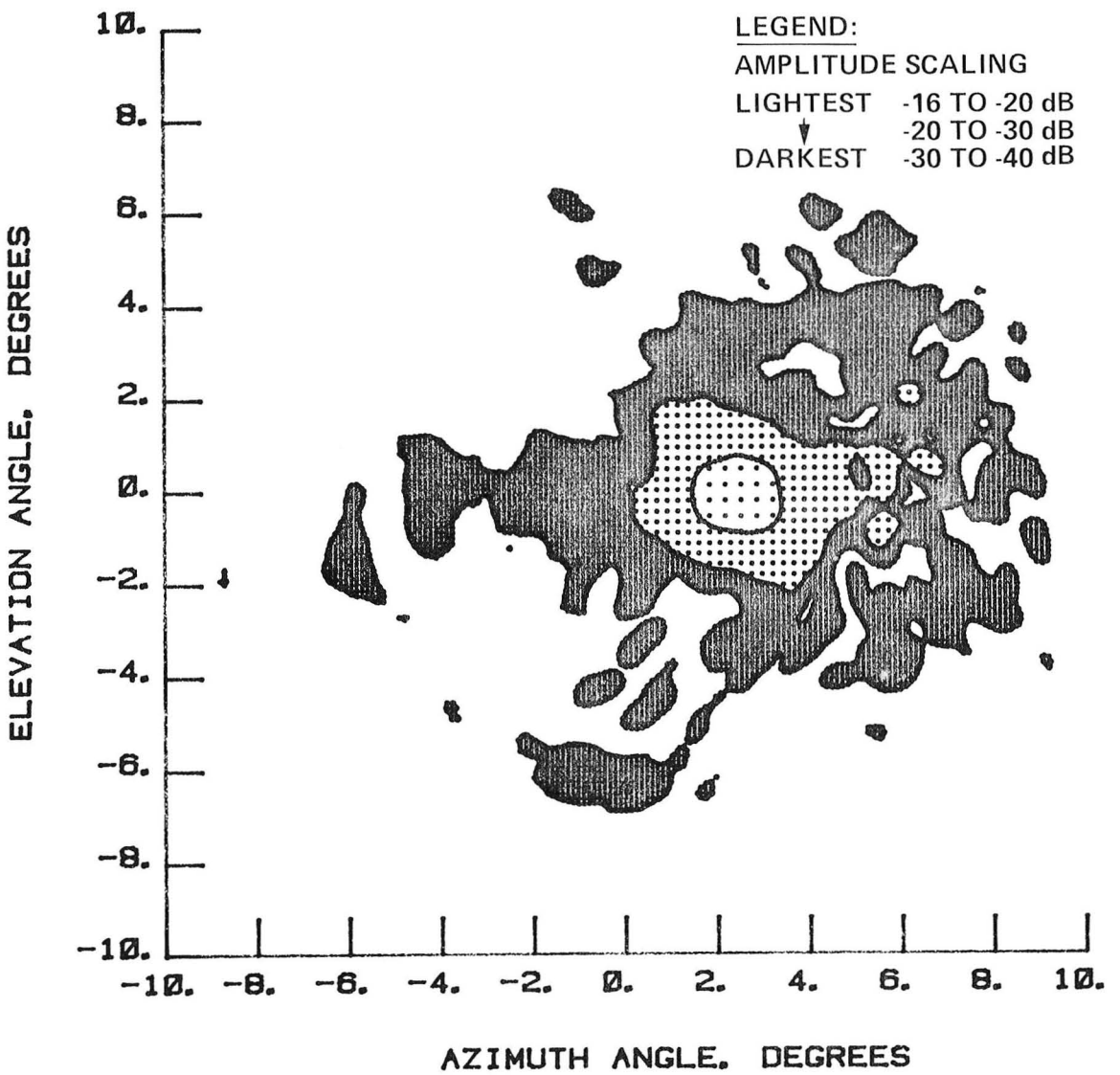

Figure 56 Test 11b, Contour, Port 4, Type 12

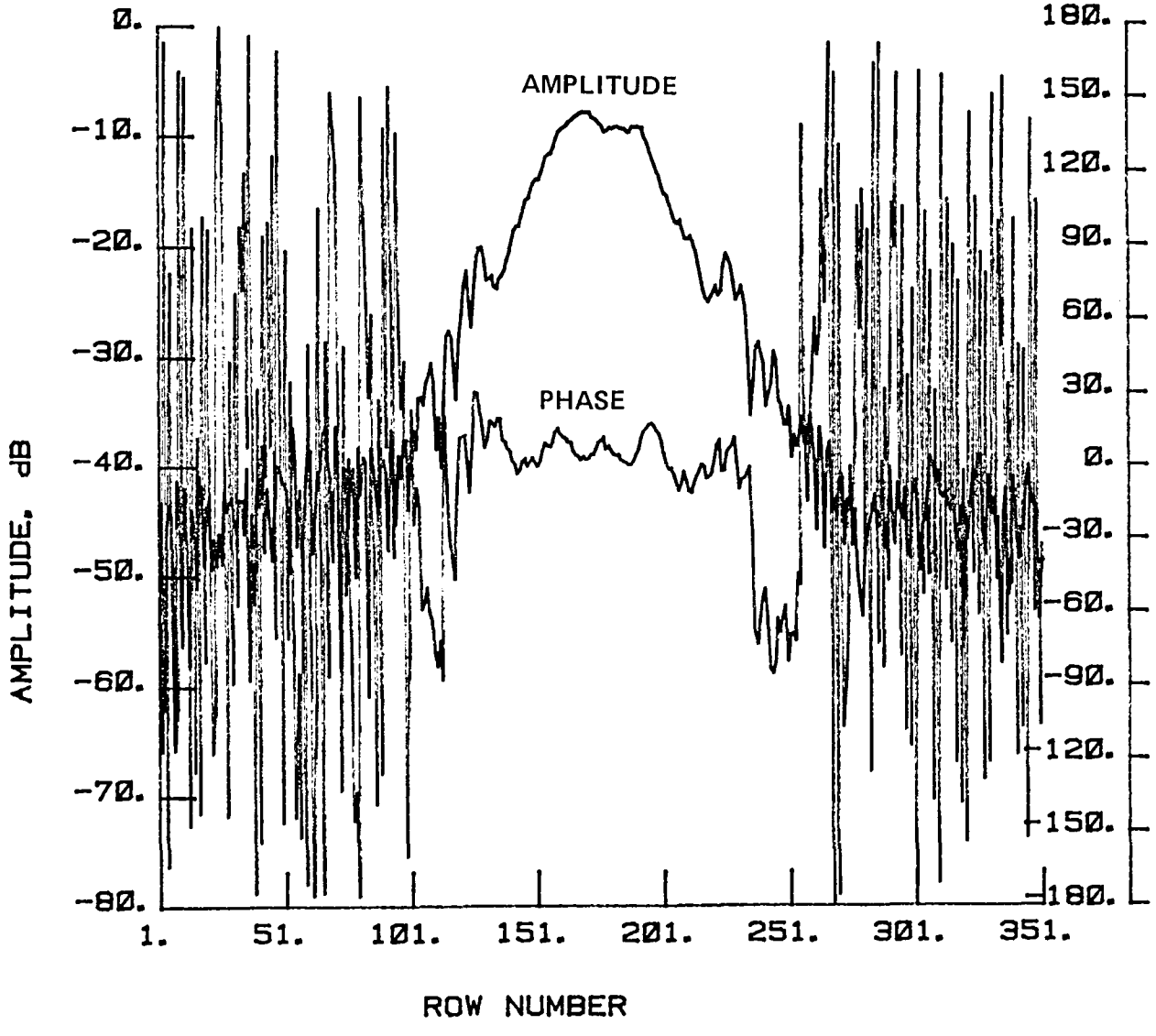

Figure 57 Test 11a, Chord, Port 4, Type 13

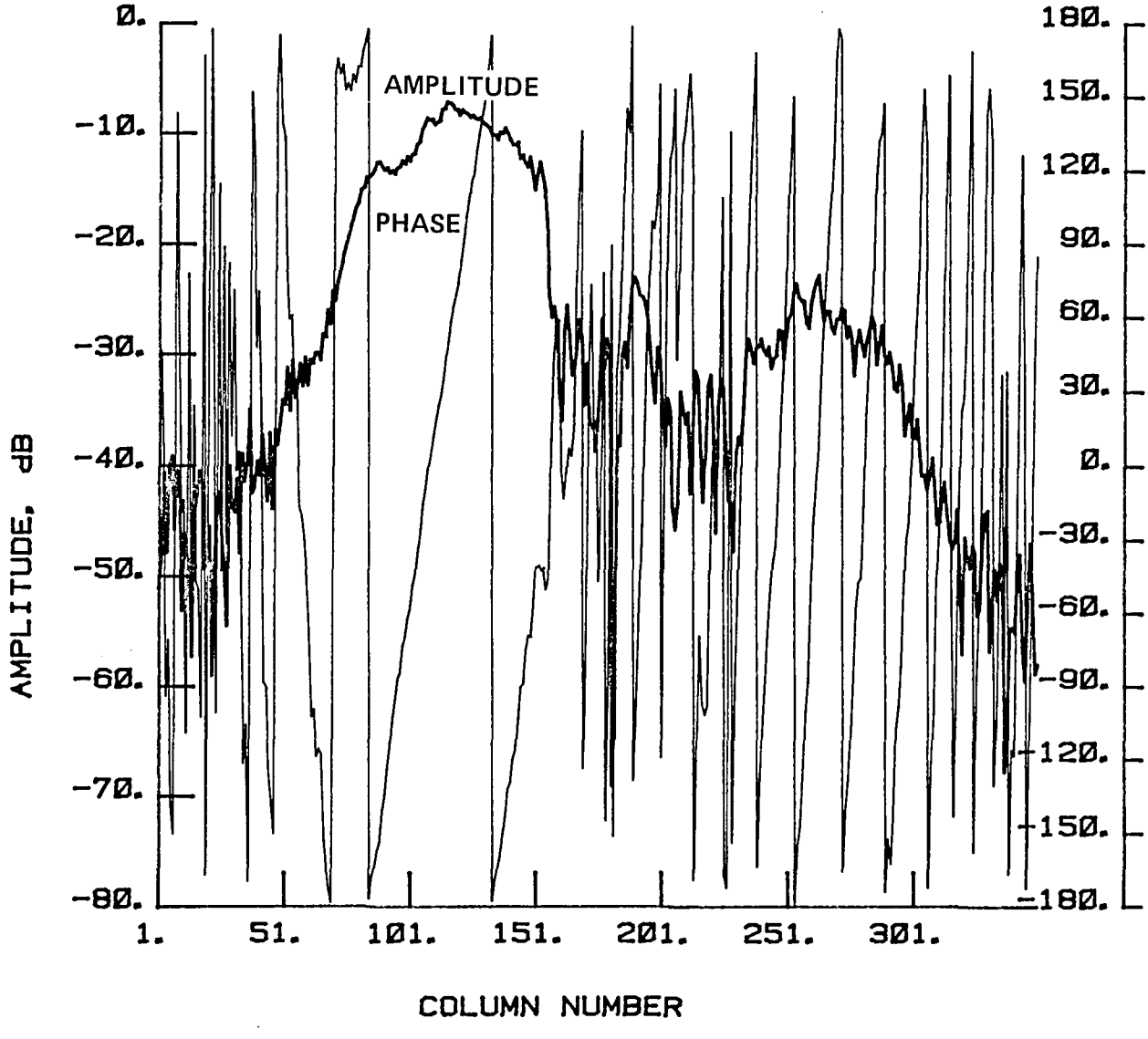

Figure 58 Test 11a, Radial, Port 4, Type 14

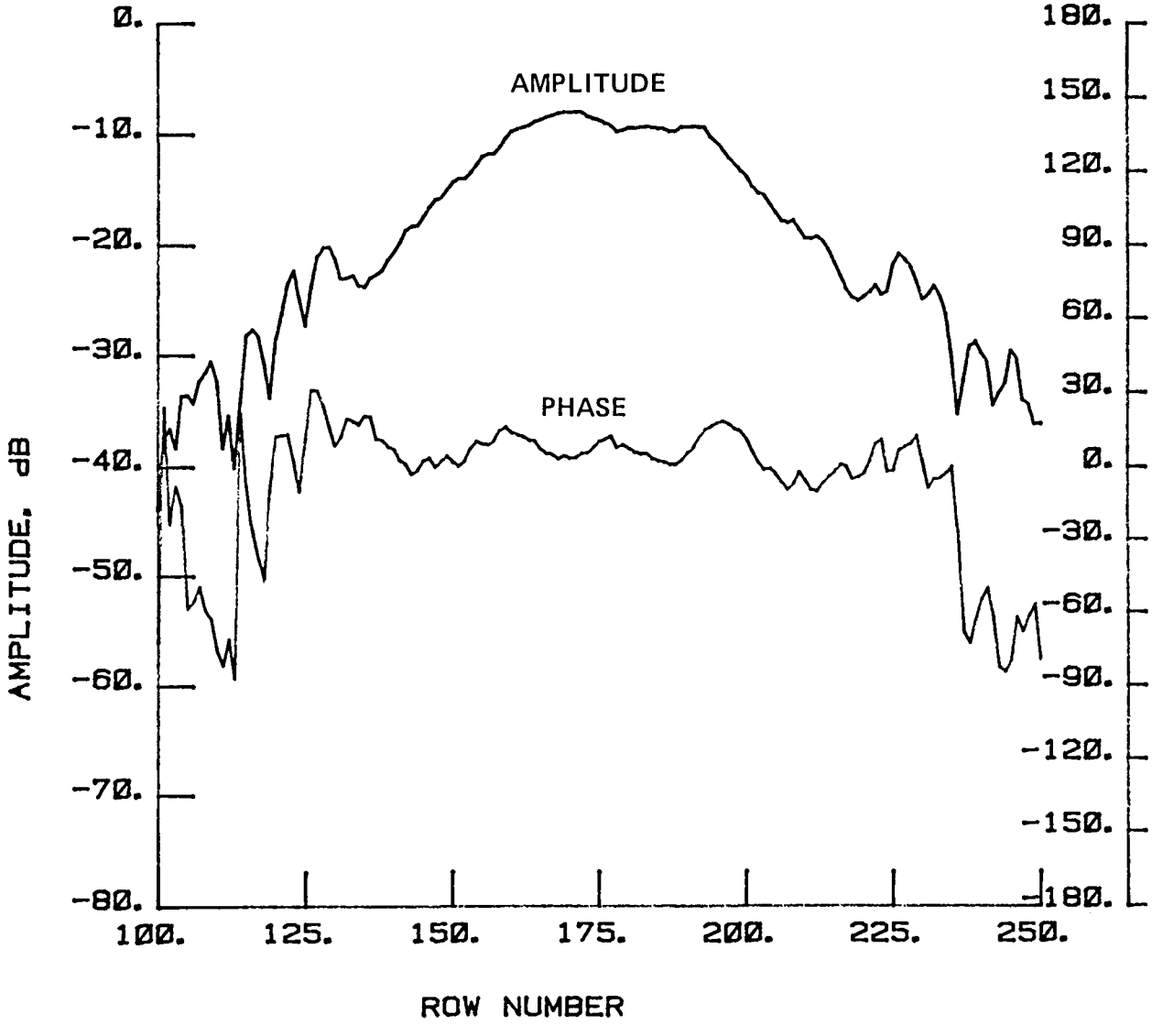

Figure 59 Test 11a, Chord, Port 4, Type 15

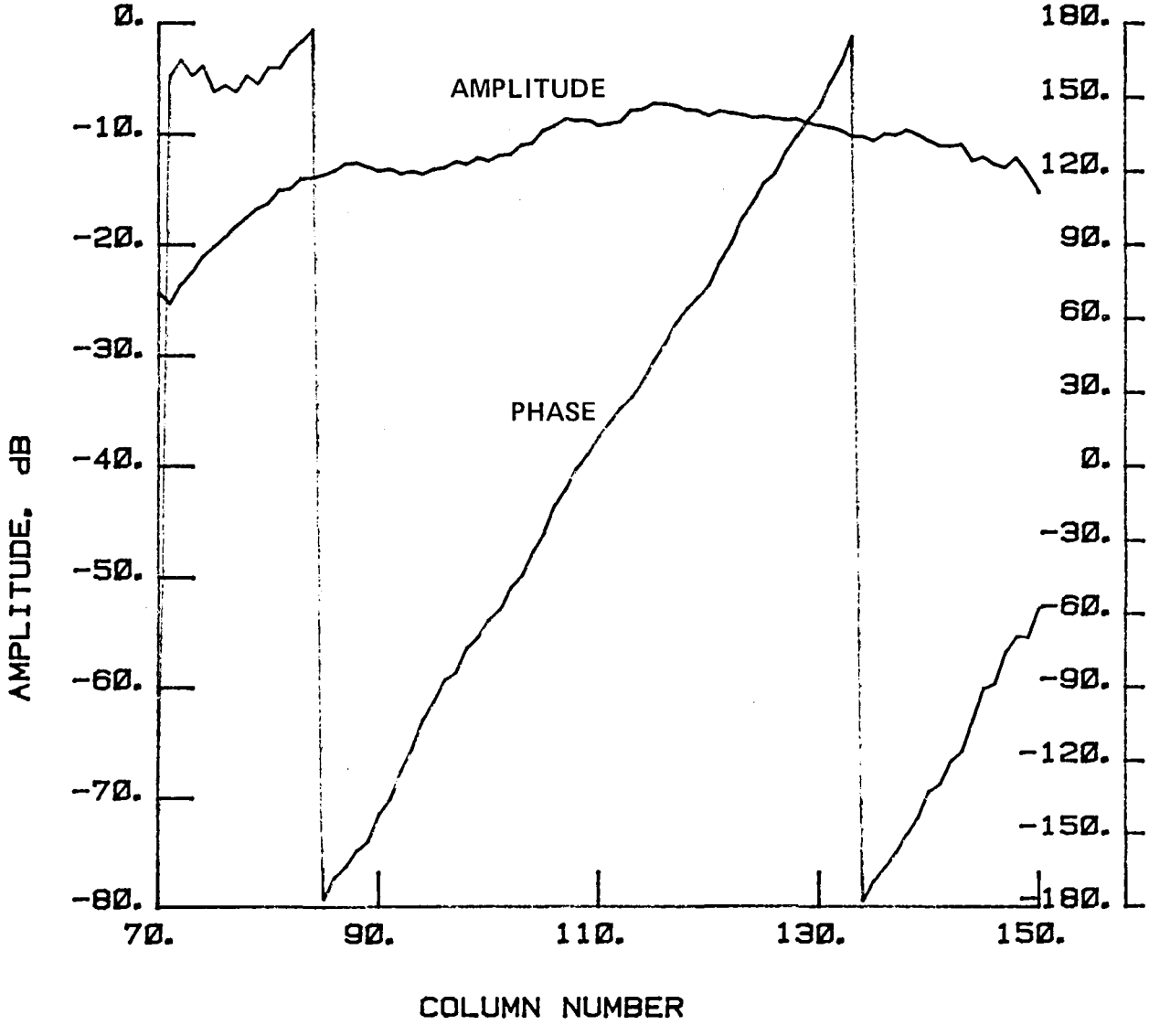

Figure 60 Test 11a, Radial, Port 4, Type 16

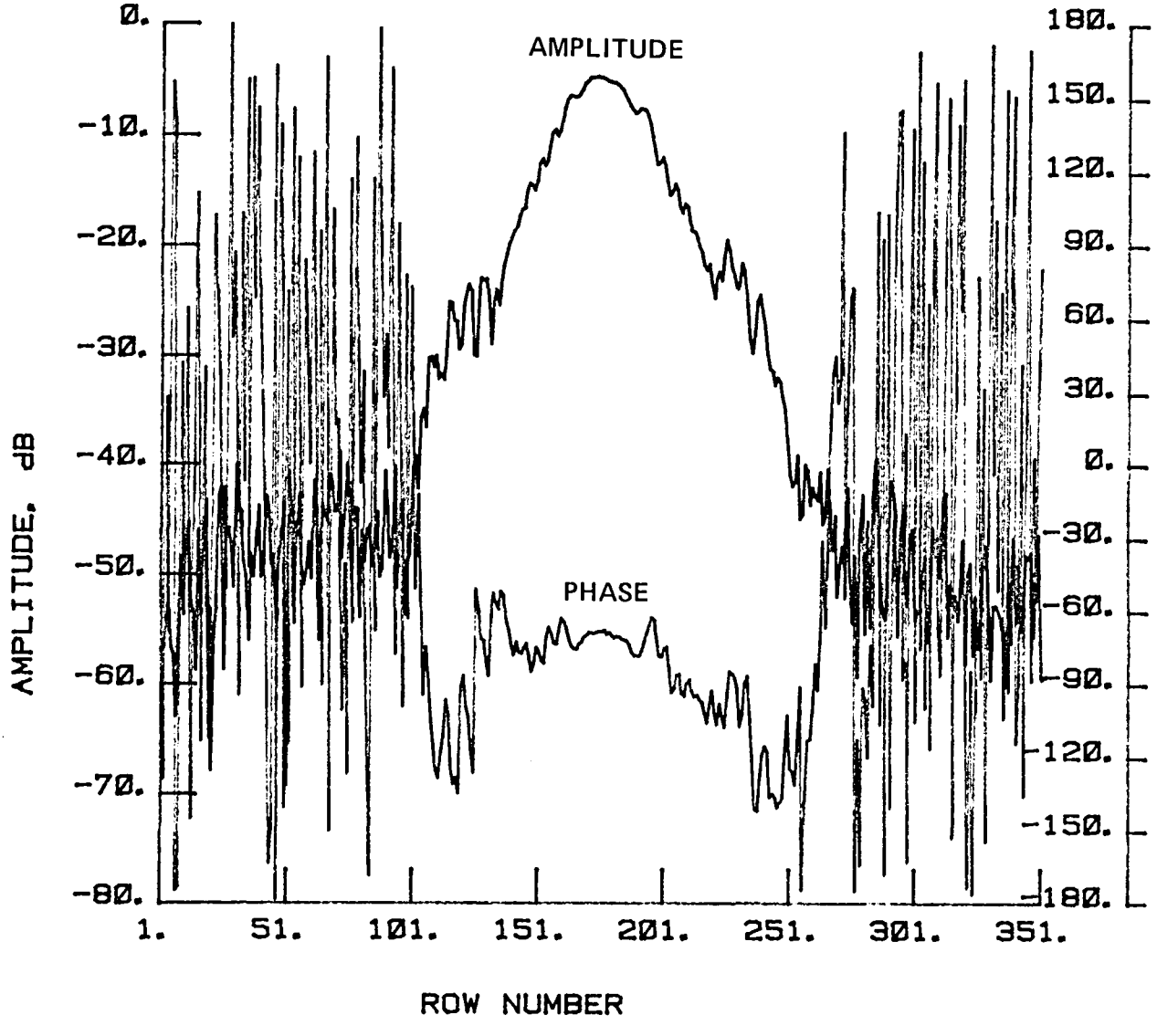

Figure 61 Test 11b, Chord, Port 4, Type 17

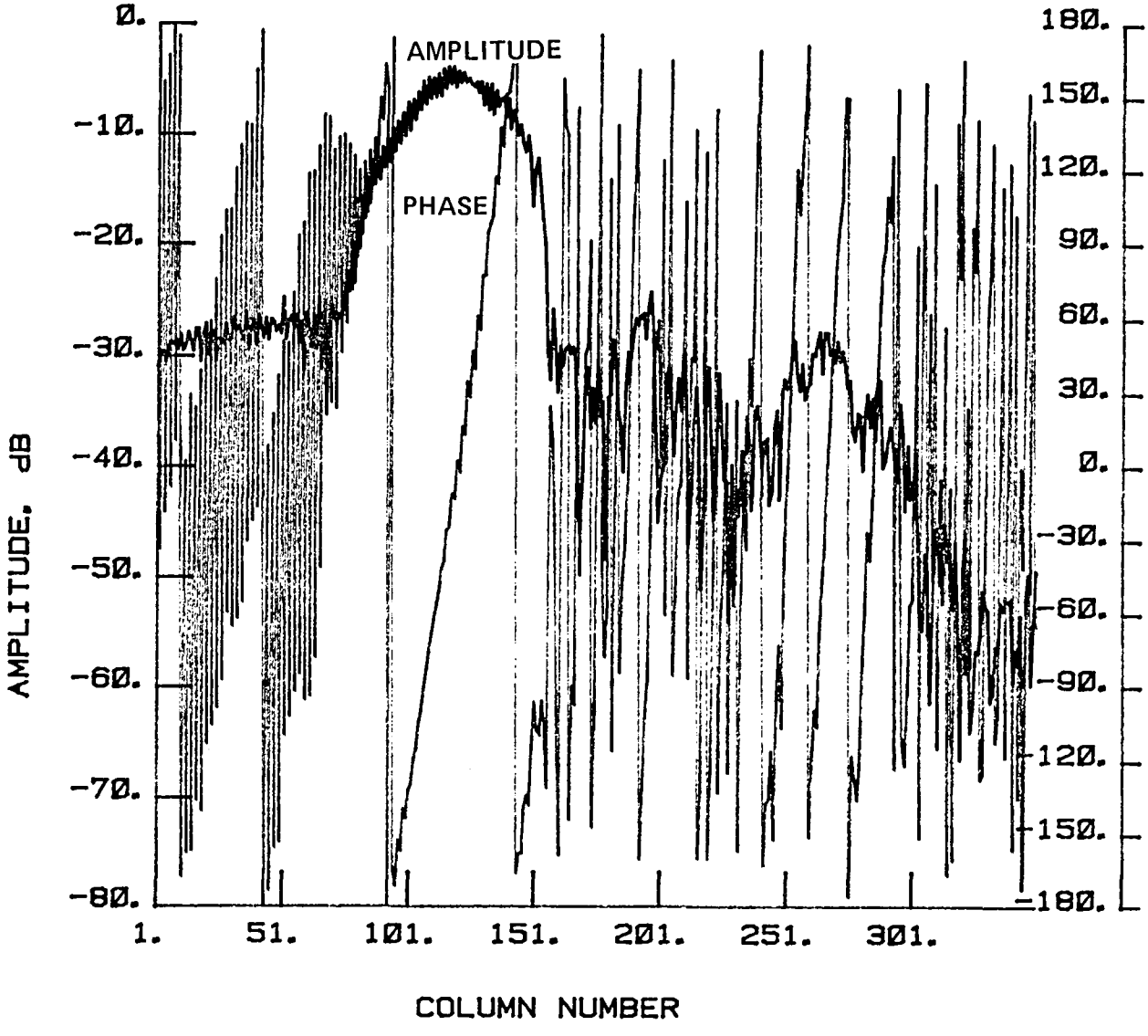

Figure 62 Test 11b, Radial, Port 4, Type 18

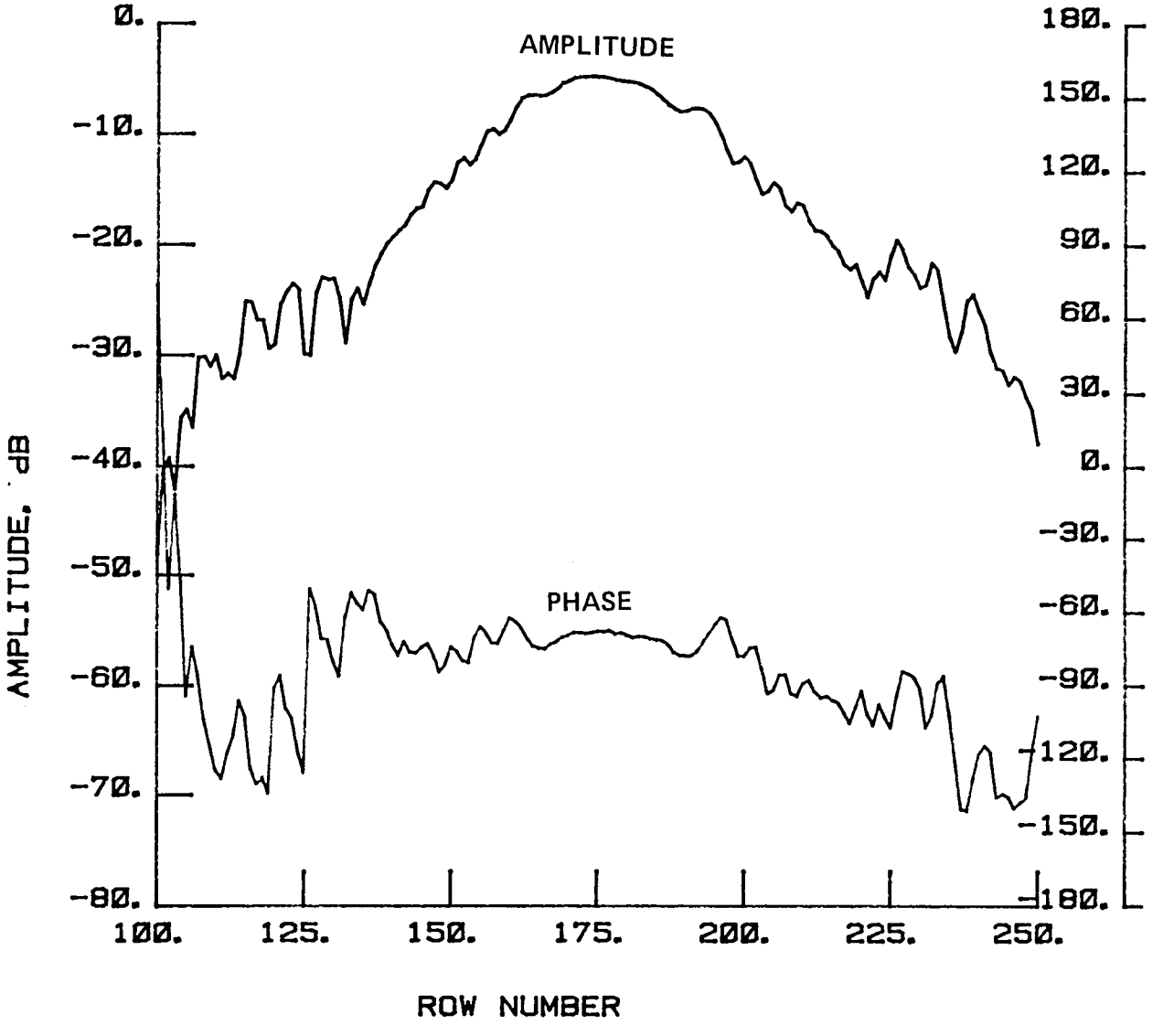

Figure 63 Test 11b, Chord, Port 4, Type 19

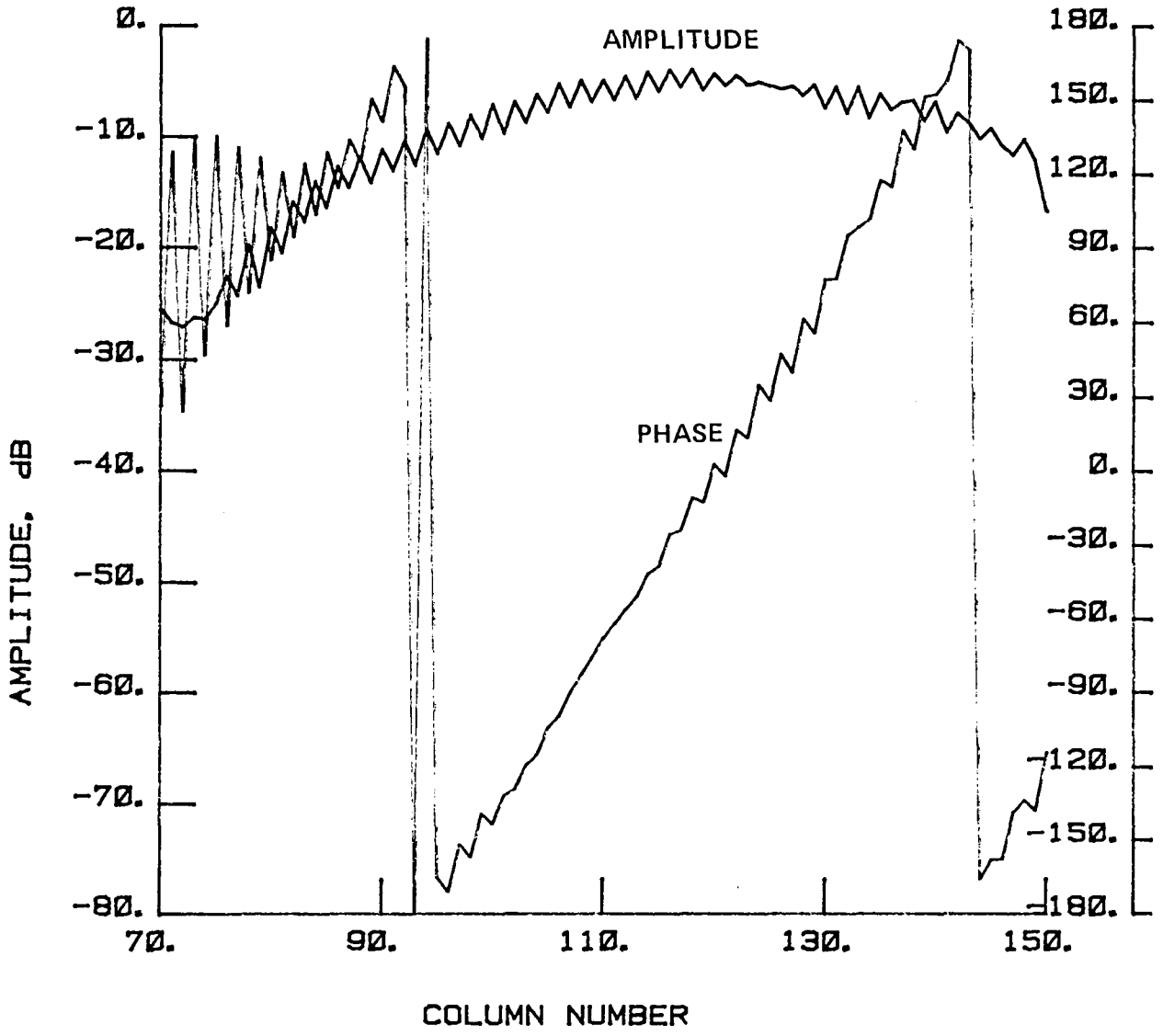

Figure 64 Test 11b, Radial, Port 4, Type 20

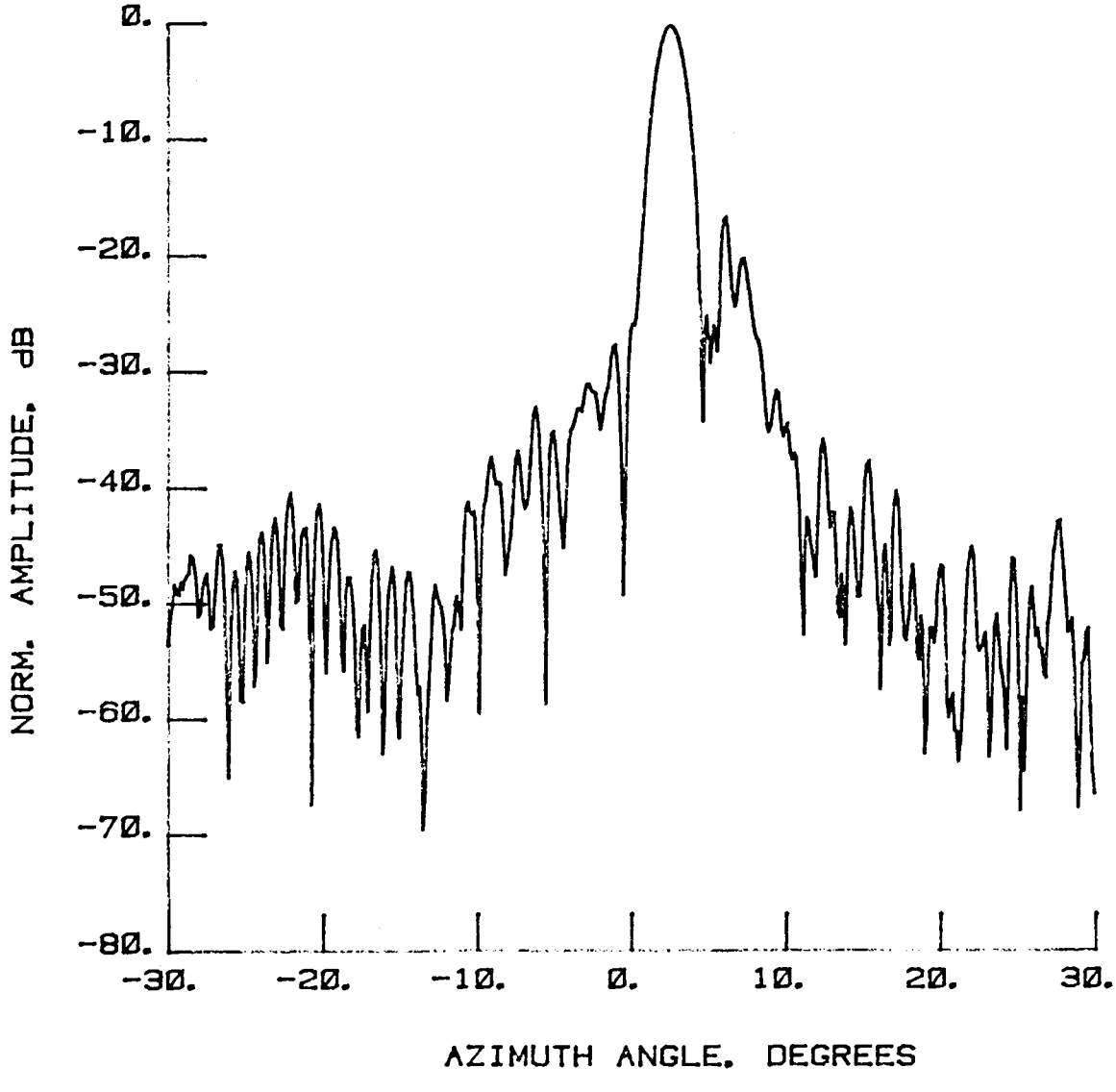

Figure 65 Test 11c, E = 1.6°, Port 5, Type 1

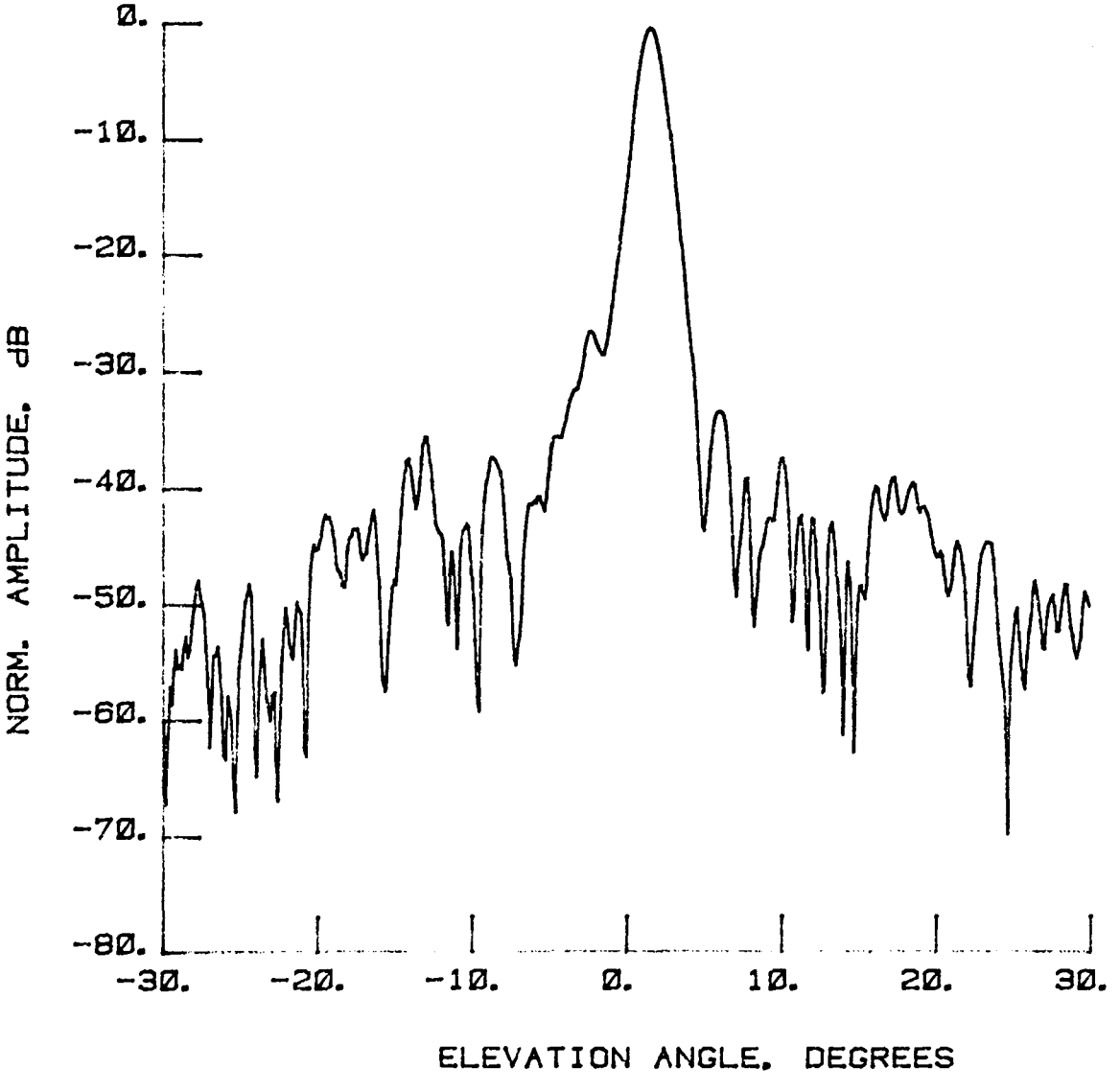

Figure 66 Test 11c, A = 2.6°, Port 5, Type 2

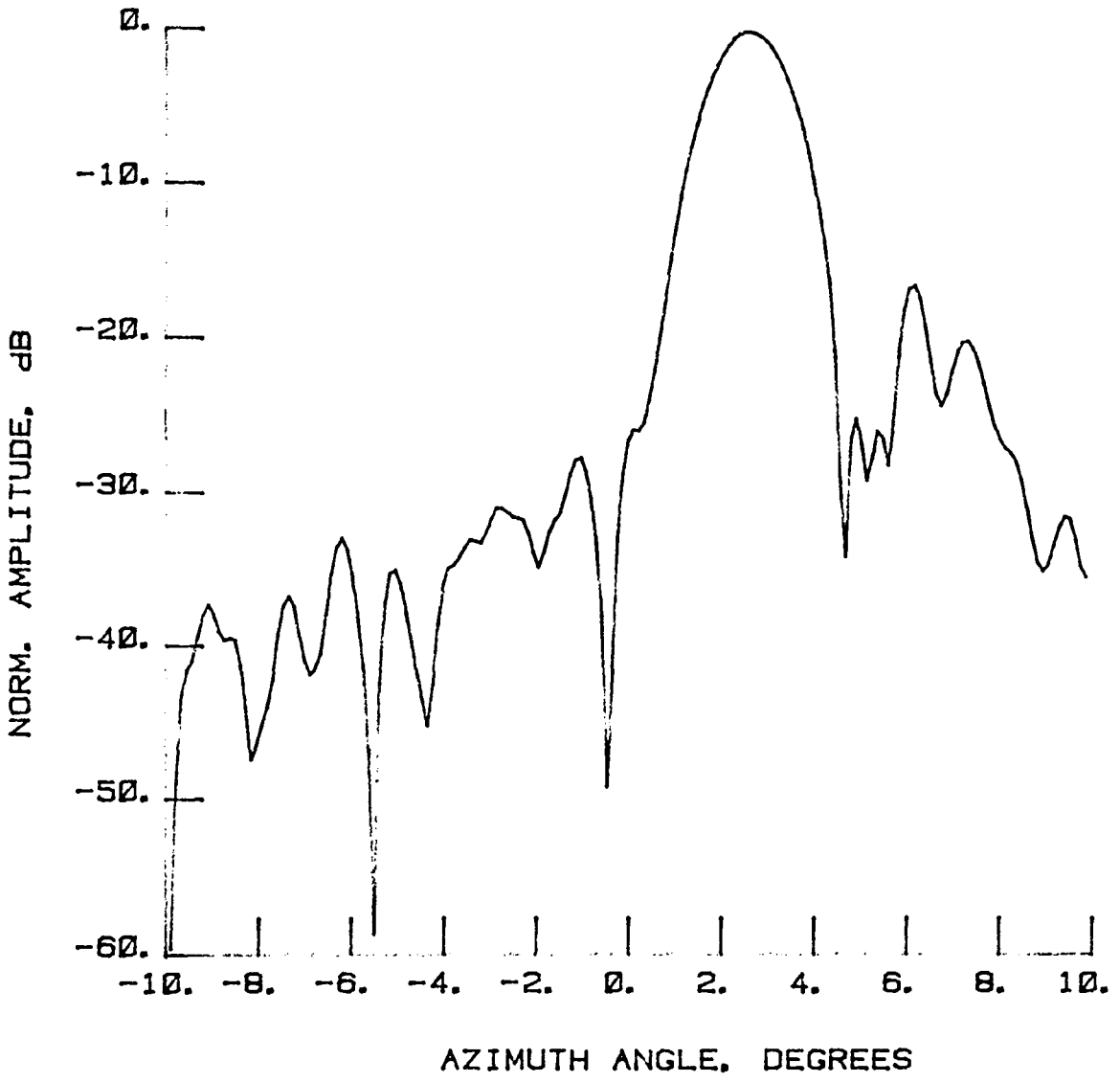

Figure 67 Test 11c, E = 1.6°, Port 5, Type 3

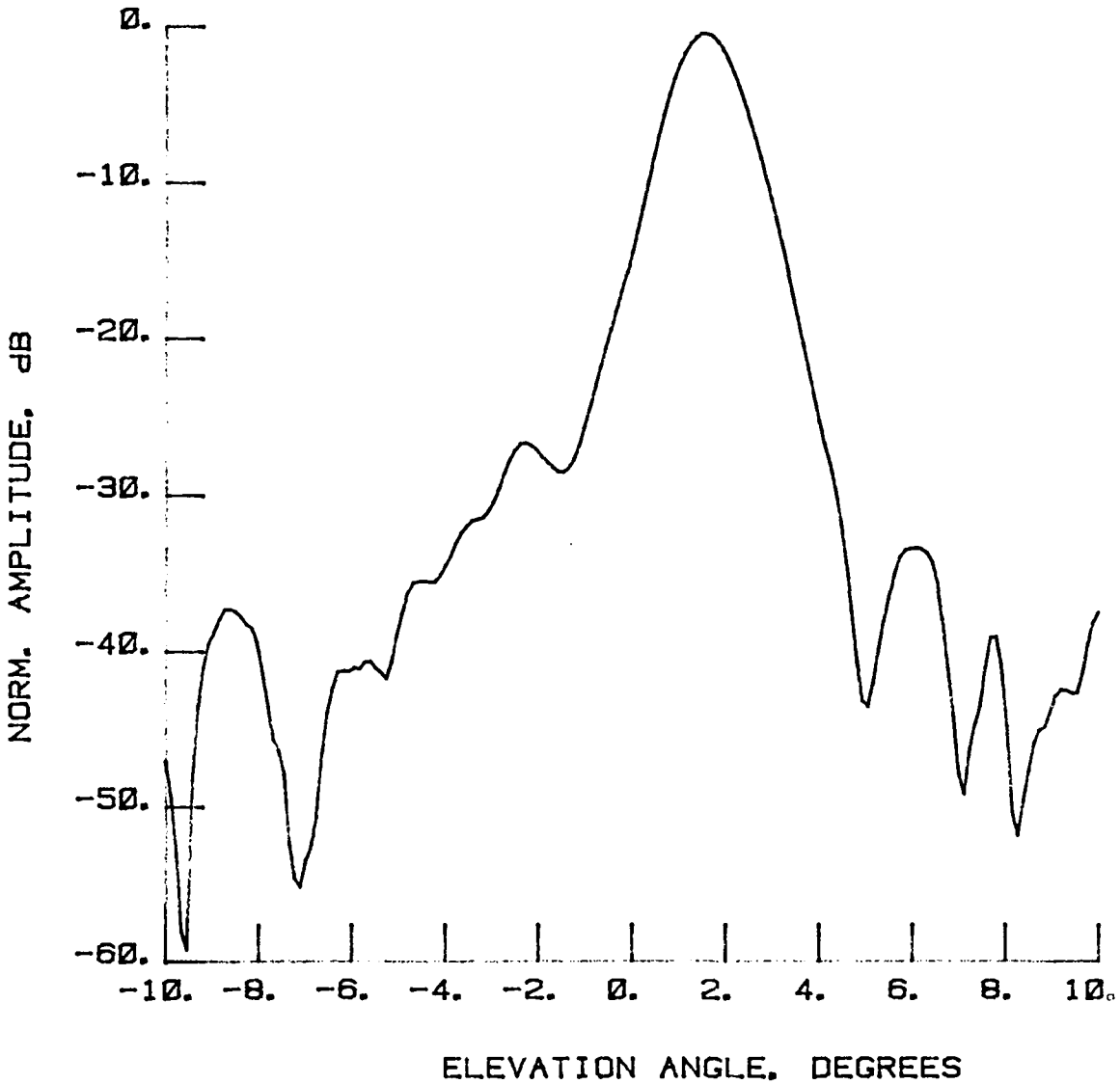

Figure 68 Test 11c, A = 2.6°, Port 5, Type 4

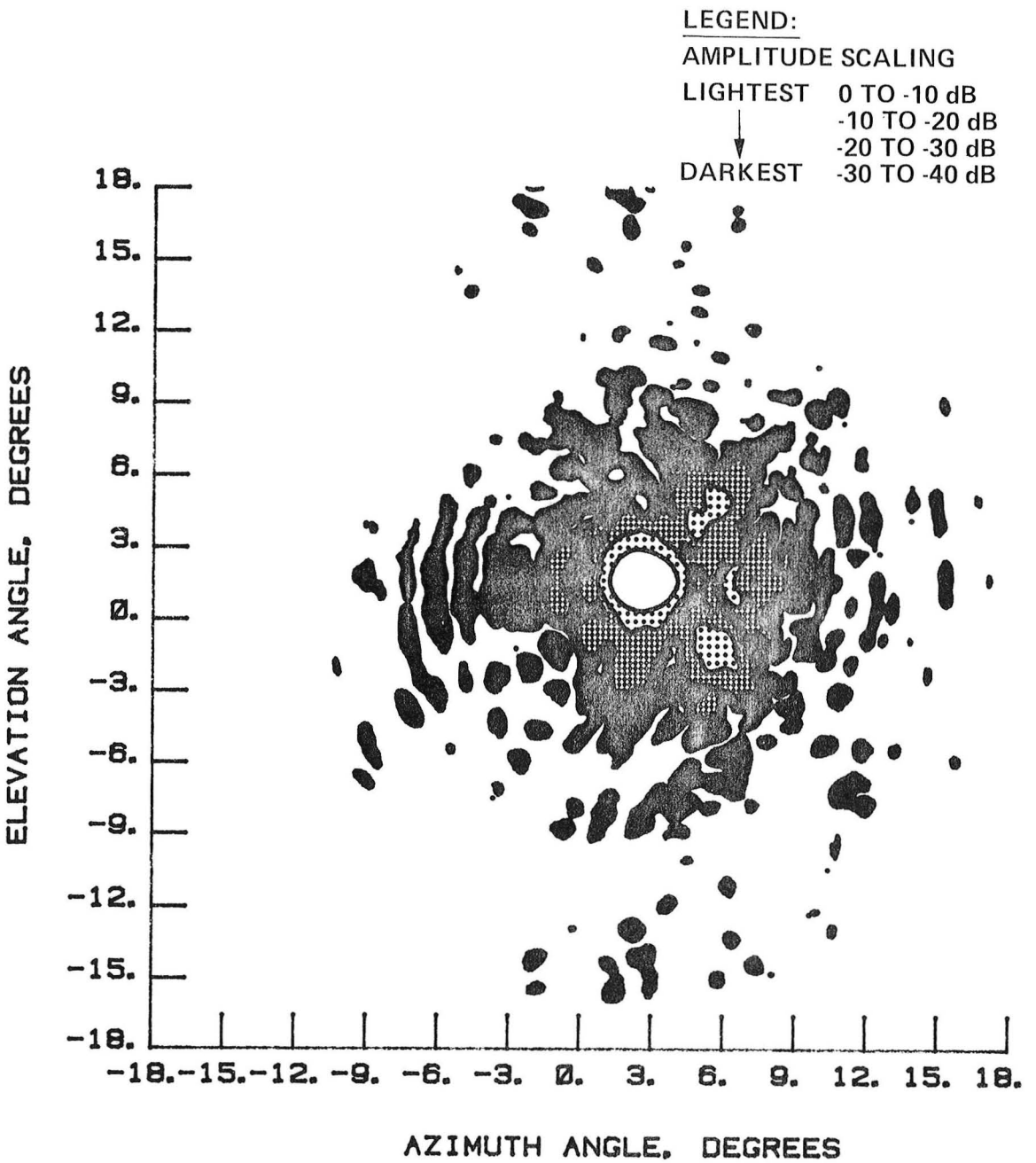

Figure 69 Test 11c, Contour, Port 5, Type 5

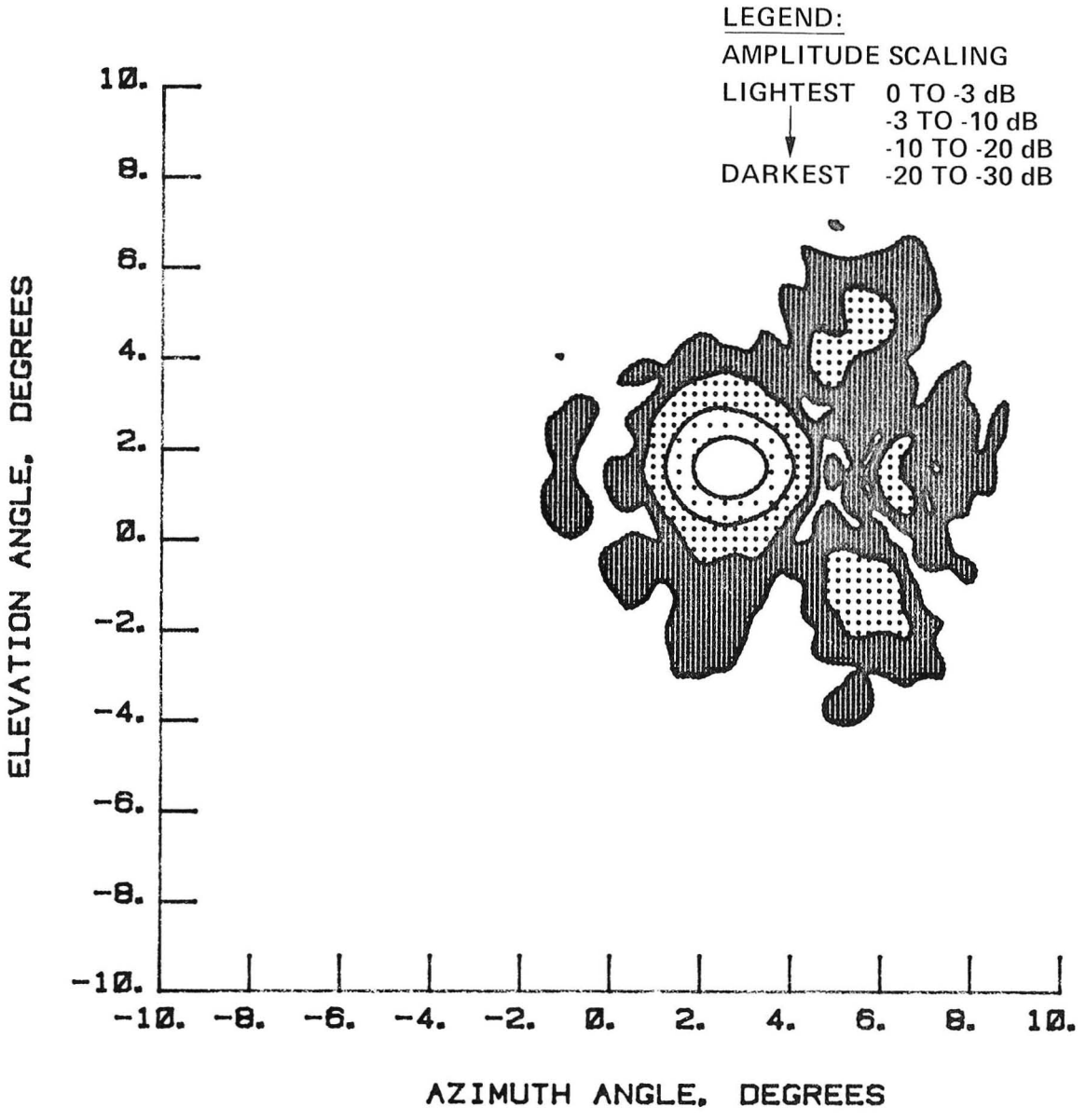

Figure 70 Test 11c, Contour, Port 5, Type 6

This Page Intentionally Left Blank

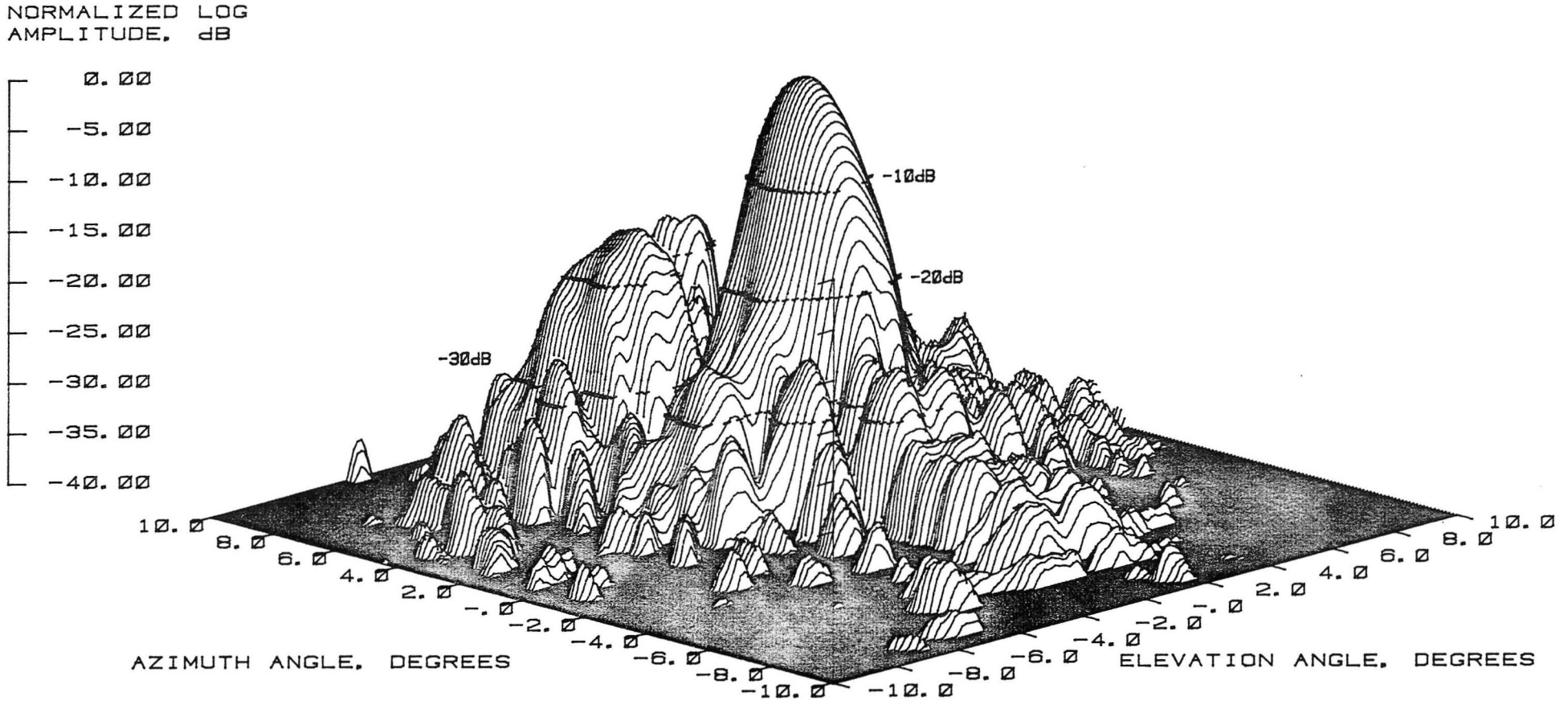

Figure 71 Test 11c, 3-D, Port 5, Type 7

87 and 88

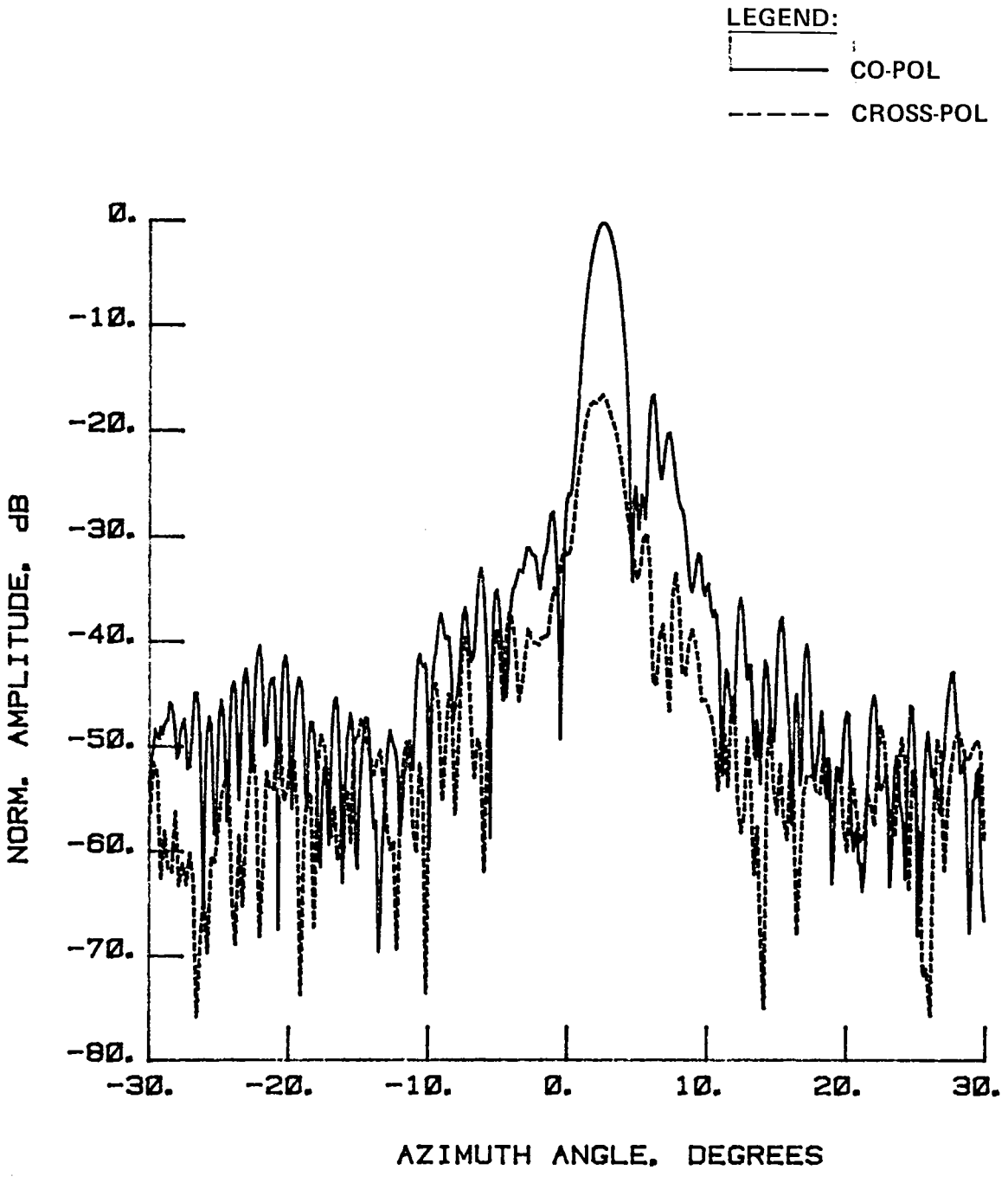

Figure 72 Test 11d, E = 1.6°, Port 5, Type 8

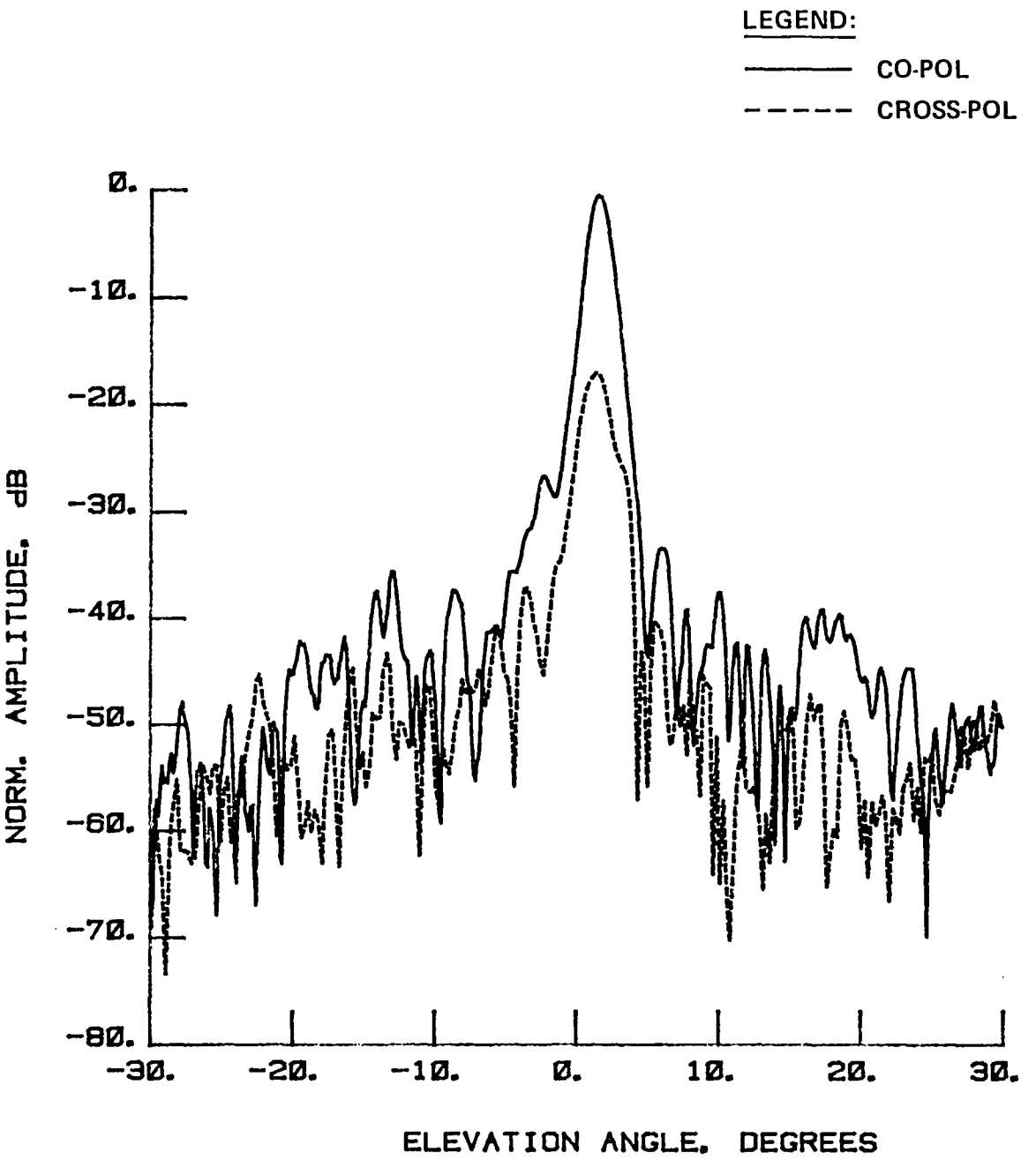

Figure 73 Test 11d, A = 2.6°, Port 5, Type 9

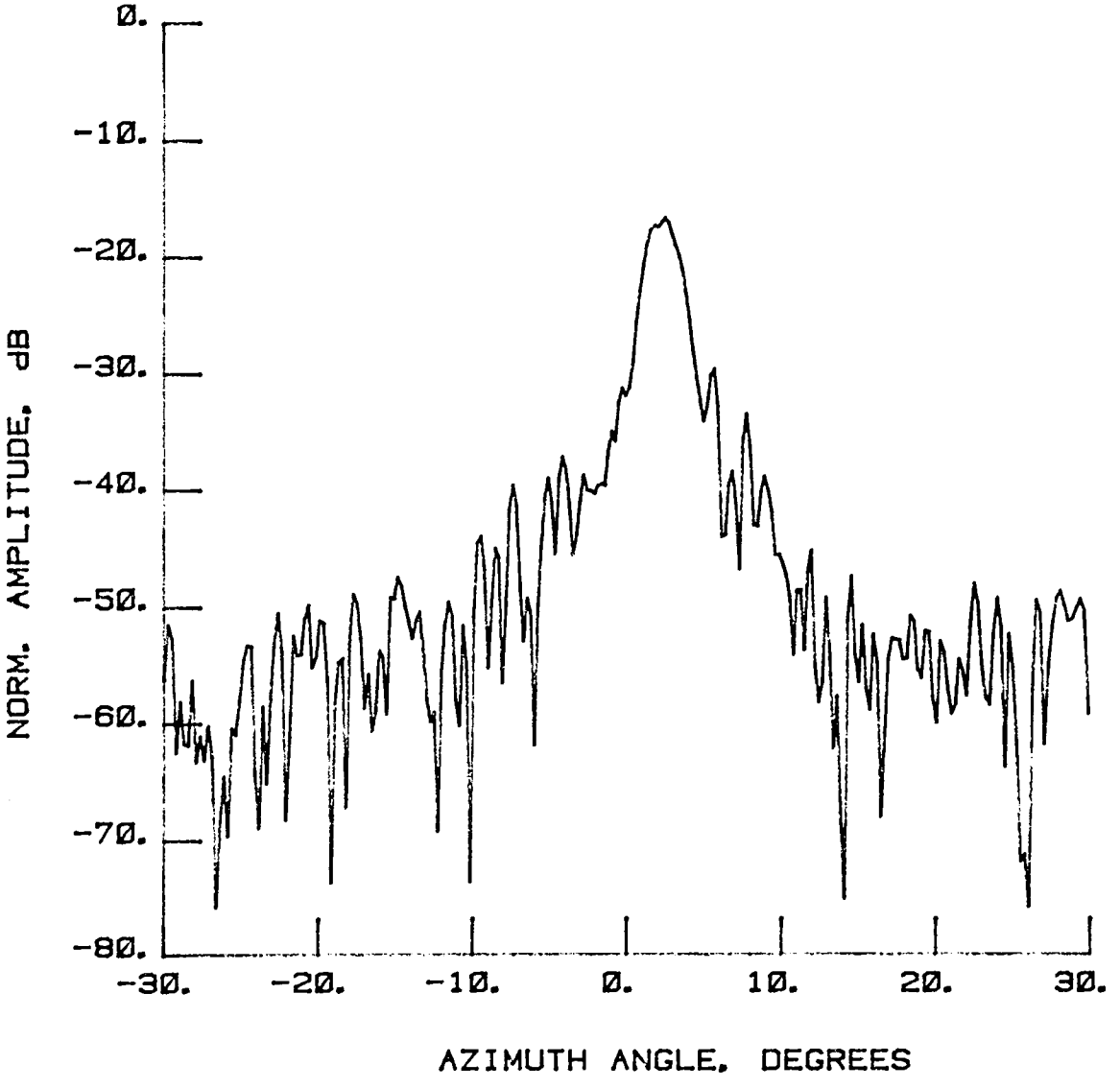

Figure 74 Test 11d, E = 1.6°, Port 5, Type 10

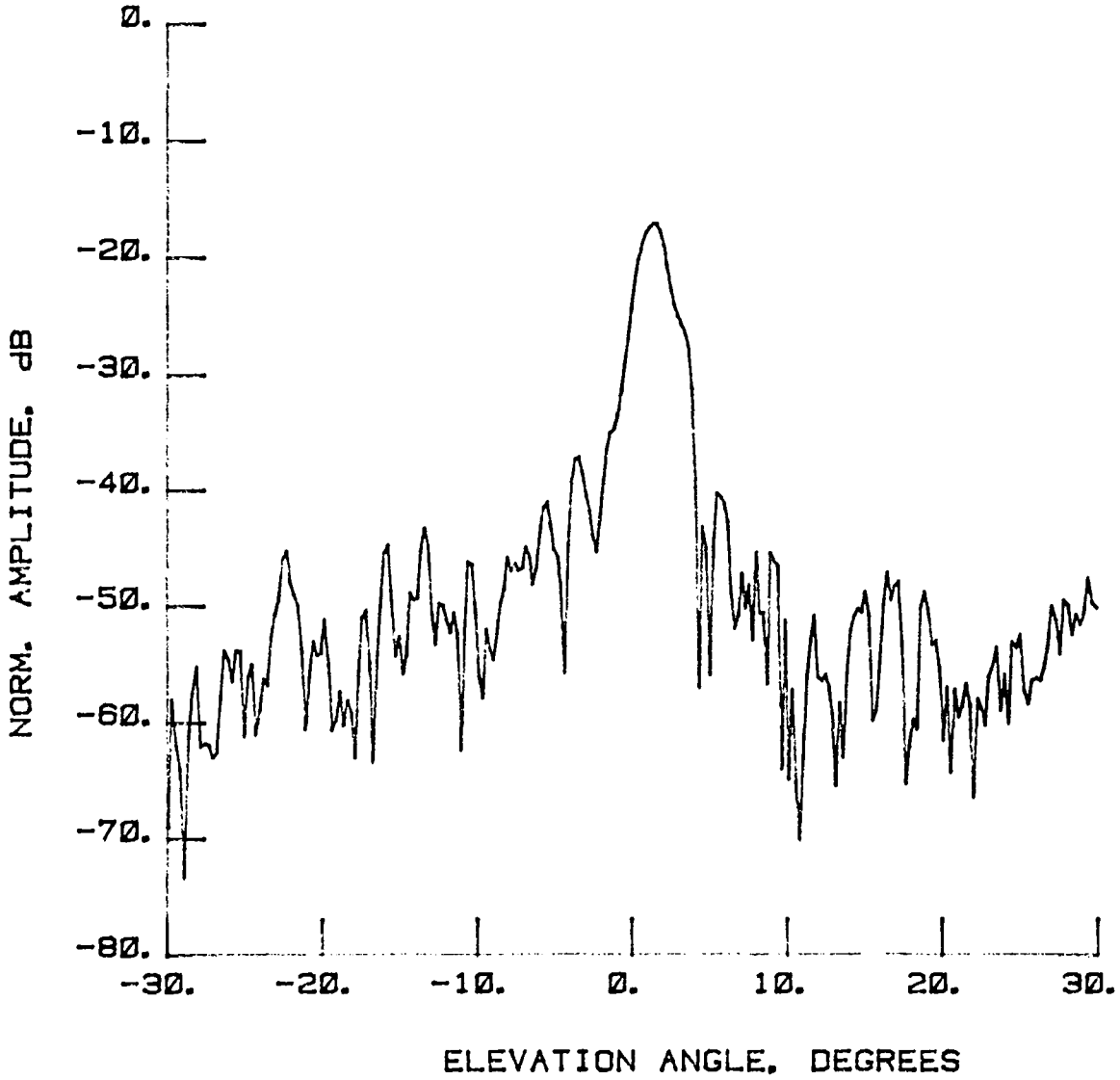

Figure 75 Test 11d, A = 2.6°, Port 5, Type 11

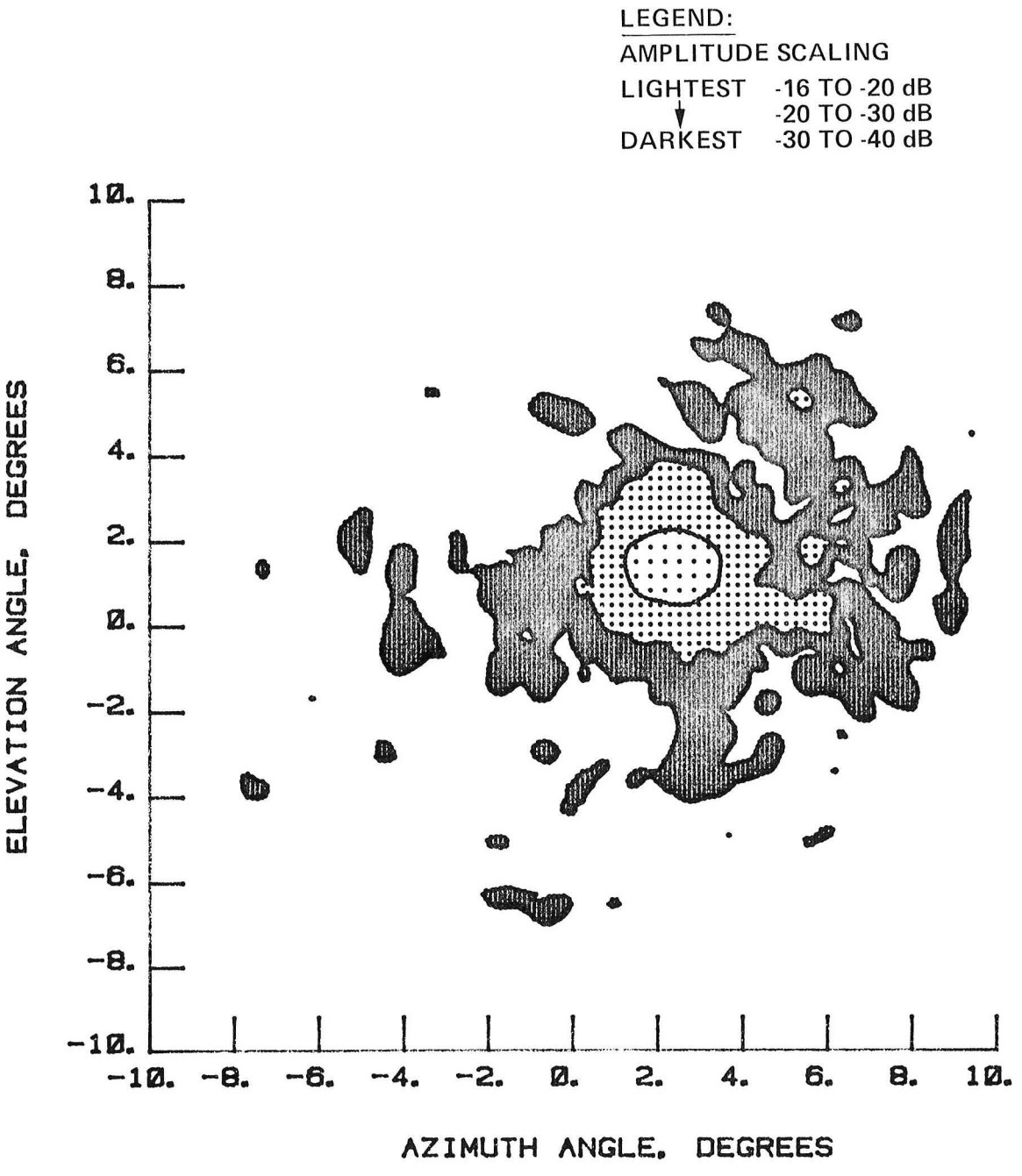

Figure 76 Test 11d, Contour, Port 5, Type 12

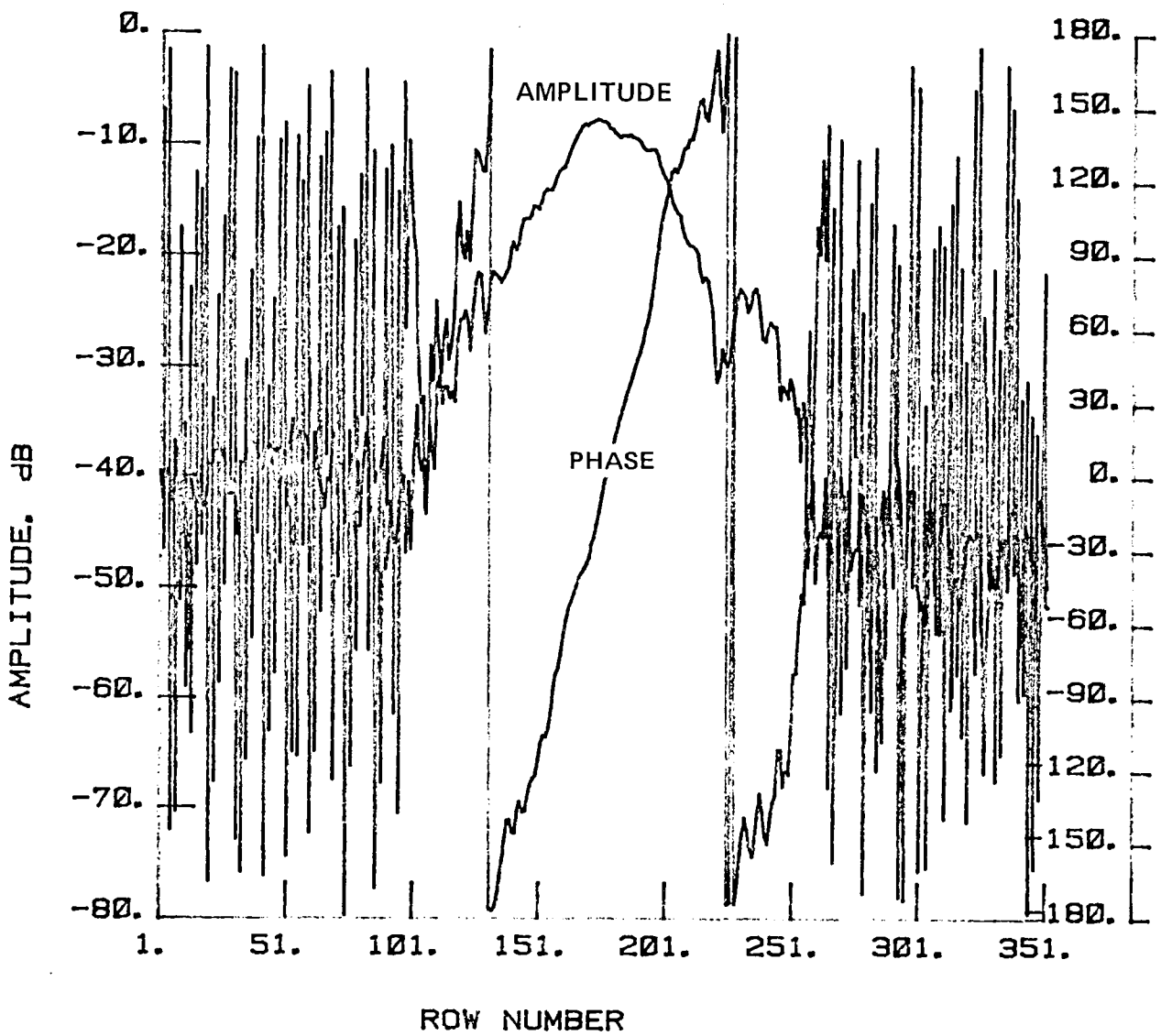

Figure 77 Test 11c, Chord, Port 5, Type 13

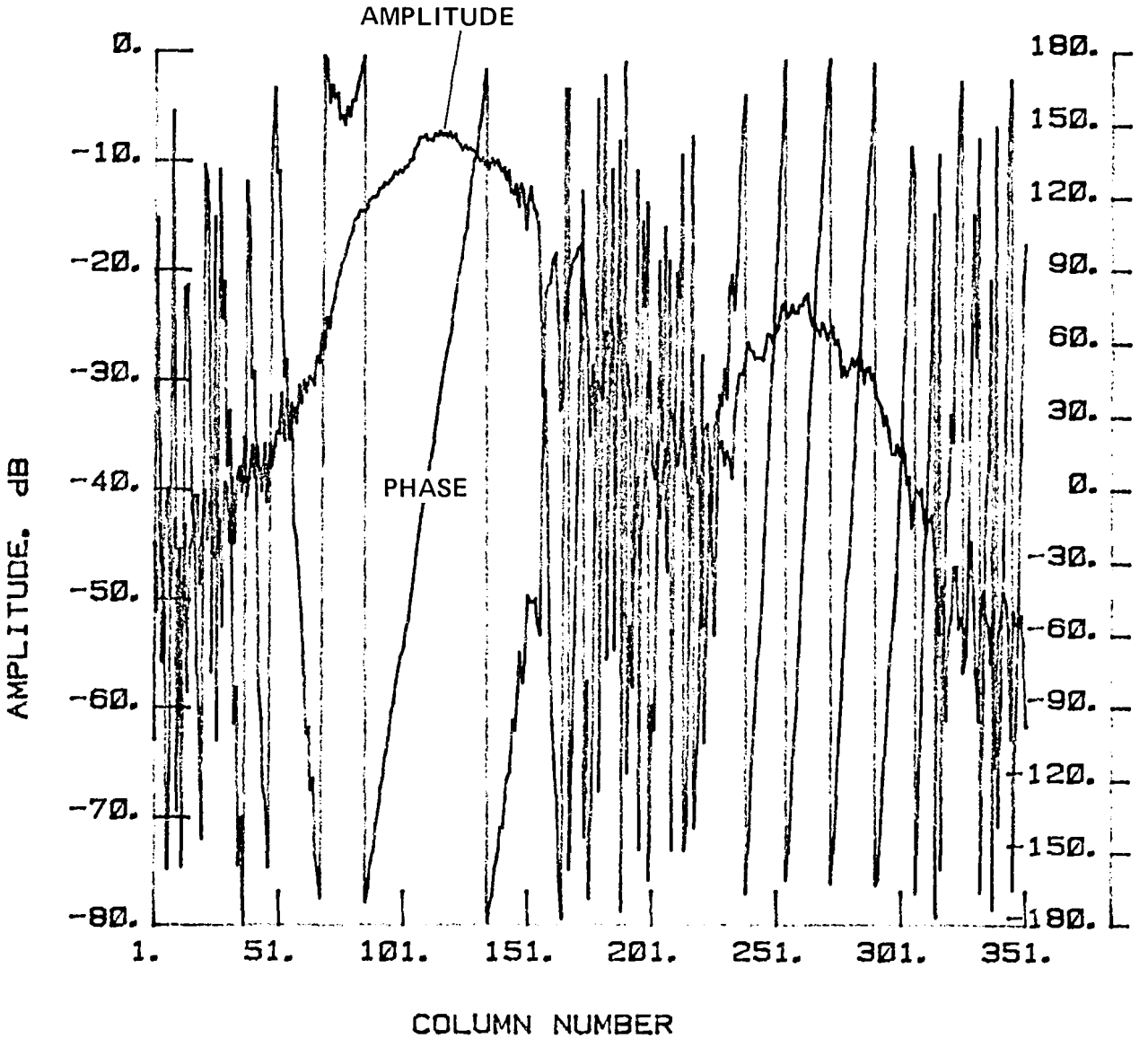

Figure 78 Test 11c, Radial, Port 5, Type 14

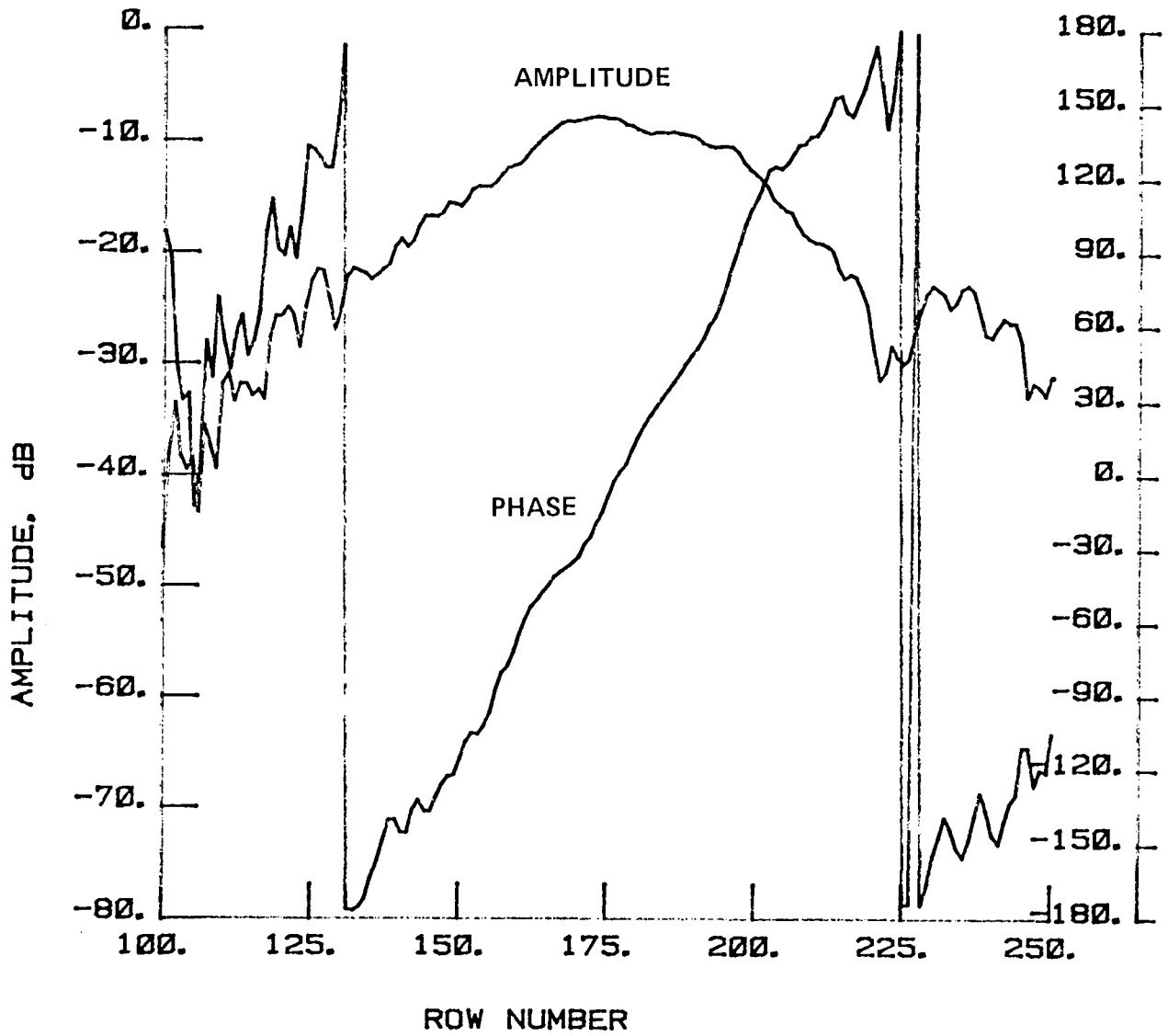

Figure 79 Test 11c, Chord, Port 5, Type 15

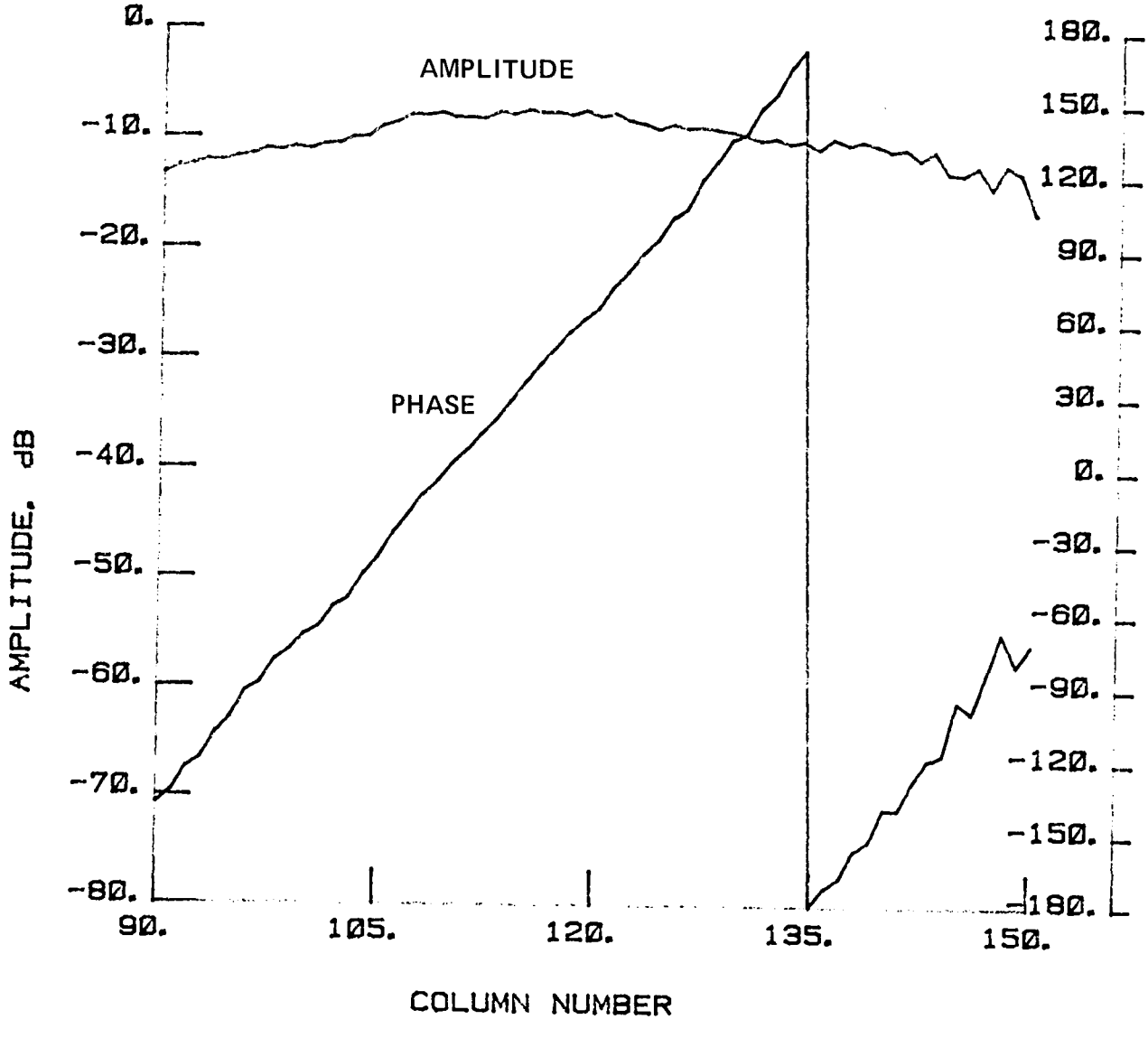

Figure 80 Test 11c, Radial, Port 5, Type 16

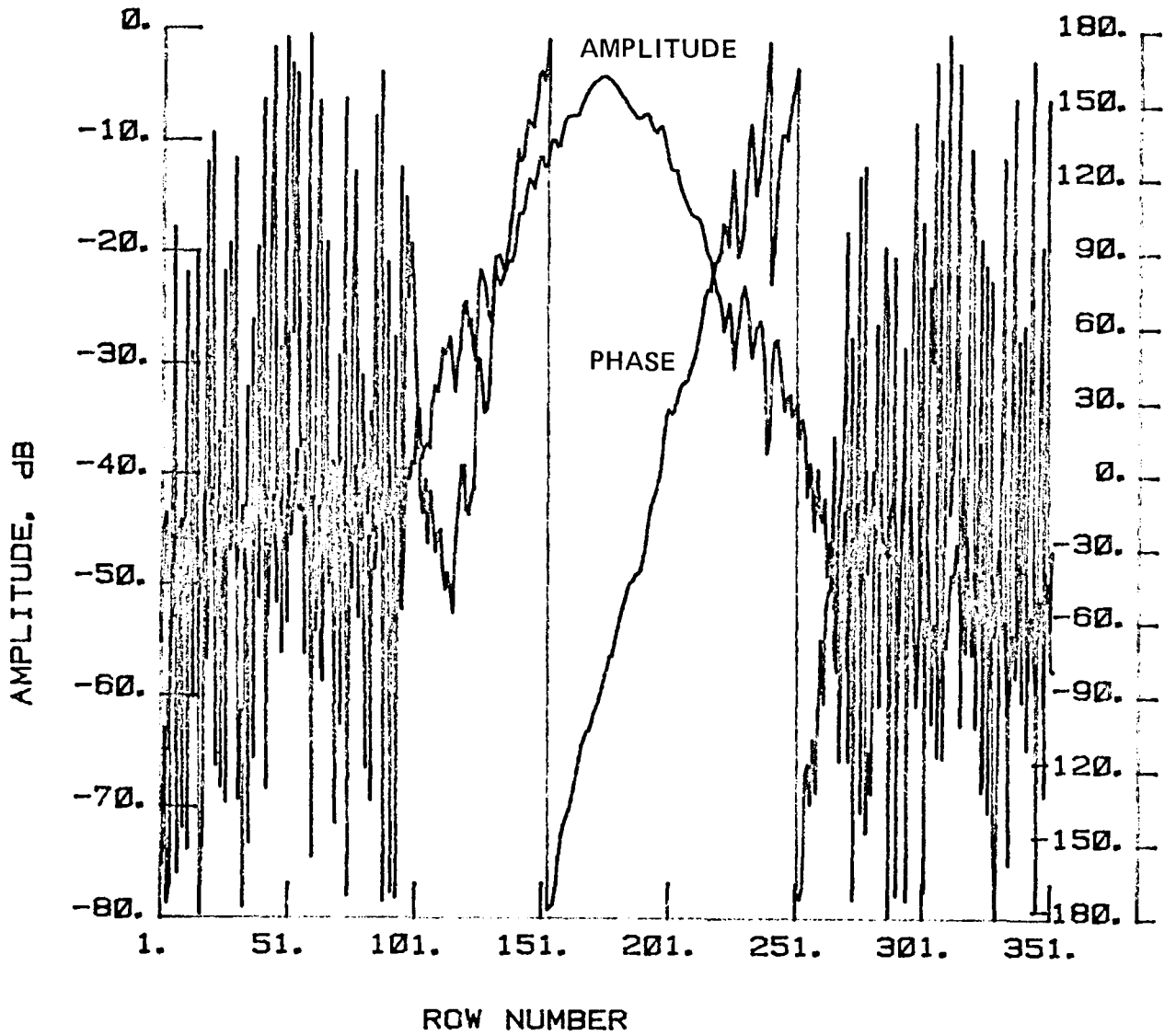

Figure 81 Test 11d, Chord, Port 5, Type 17

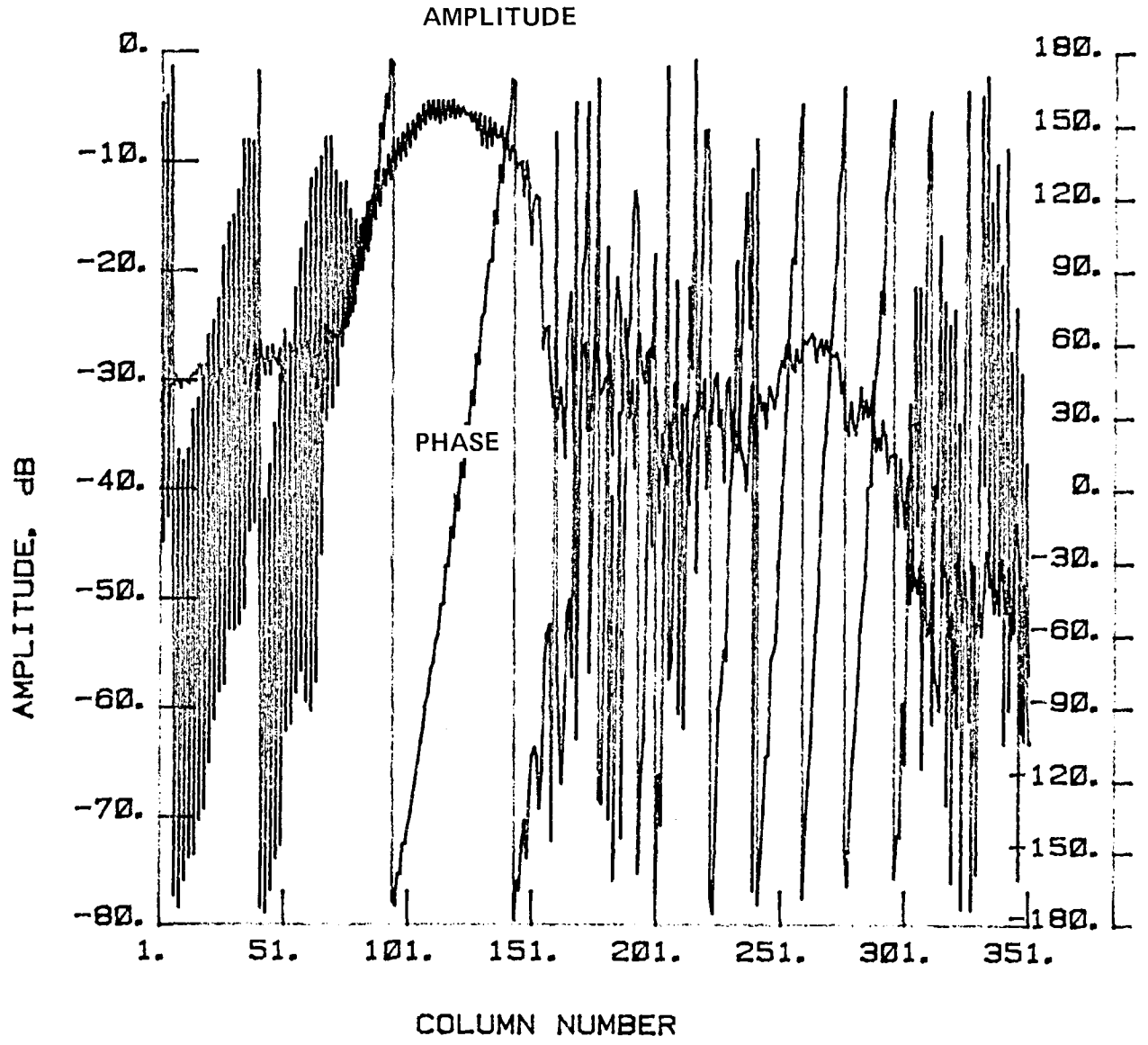

Figure 82 Test 11d, Radial, Port 5, Type 18

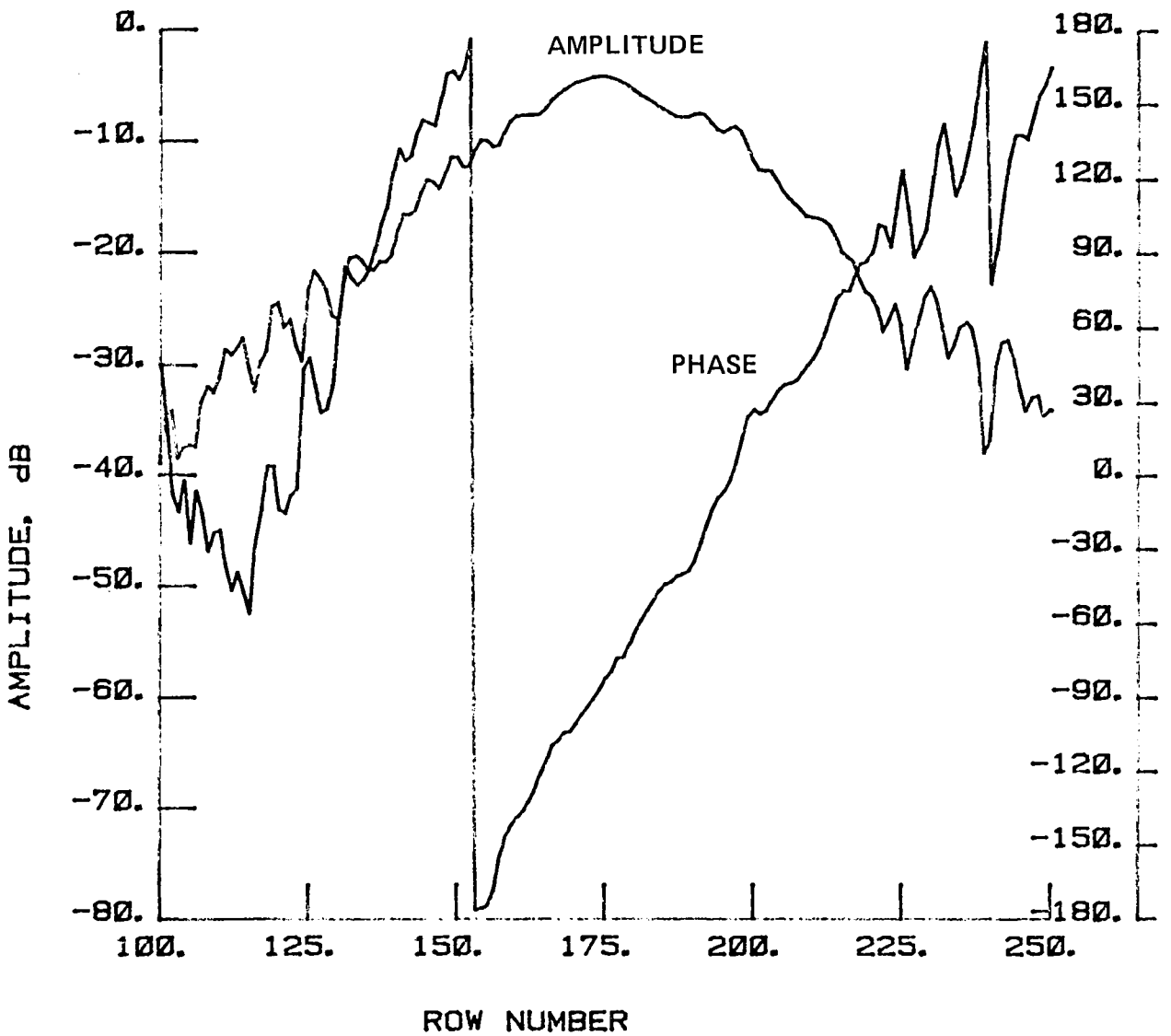

Figure 83 Test 11d, Chord, Port 5, Type 19

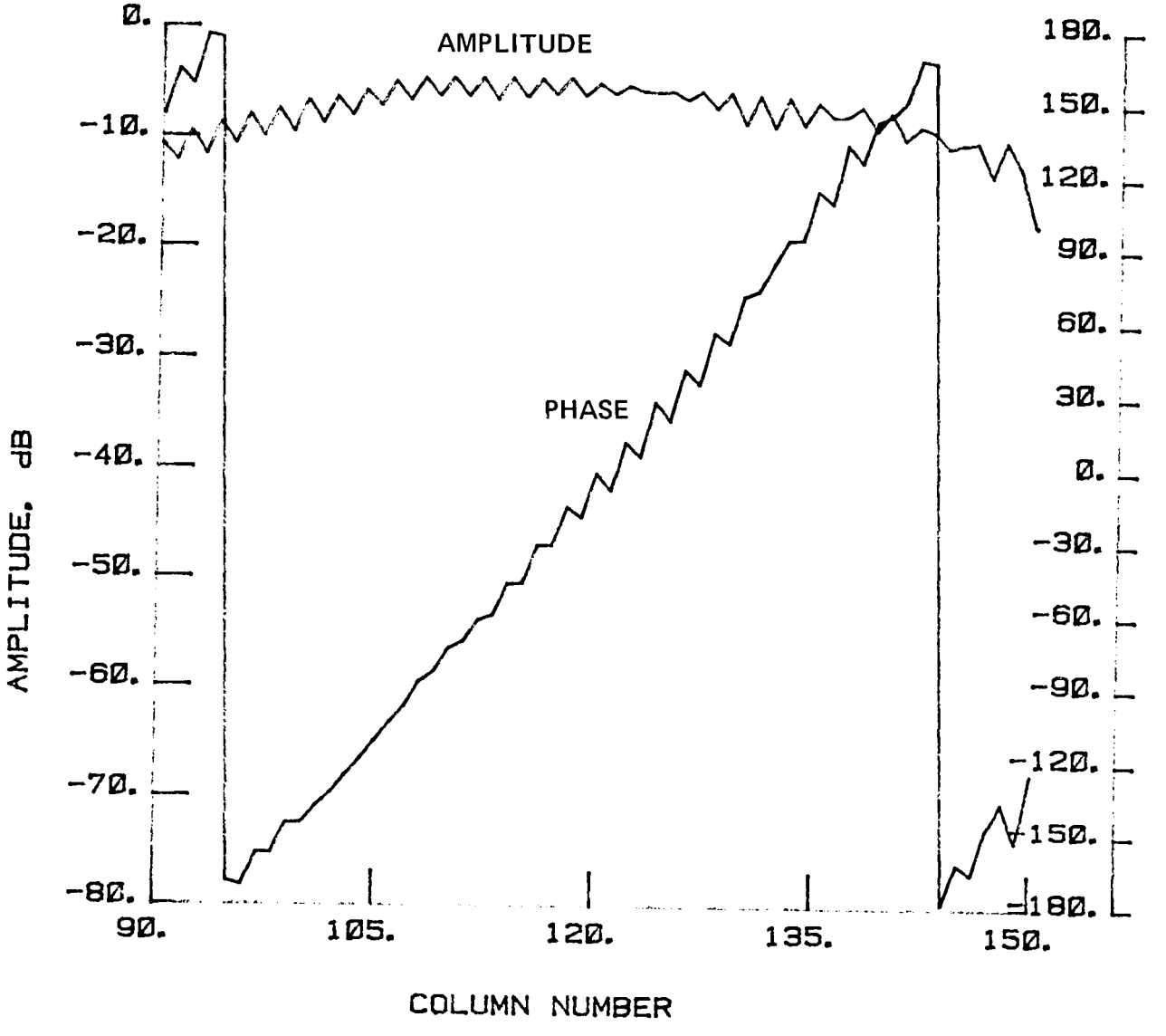

Figure 84 Test 11d, Radial, Port 5, Type 20

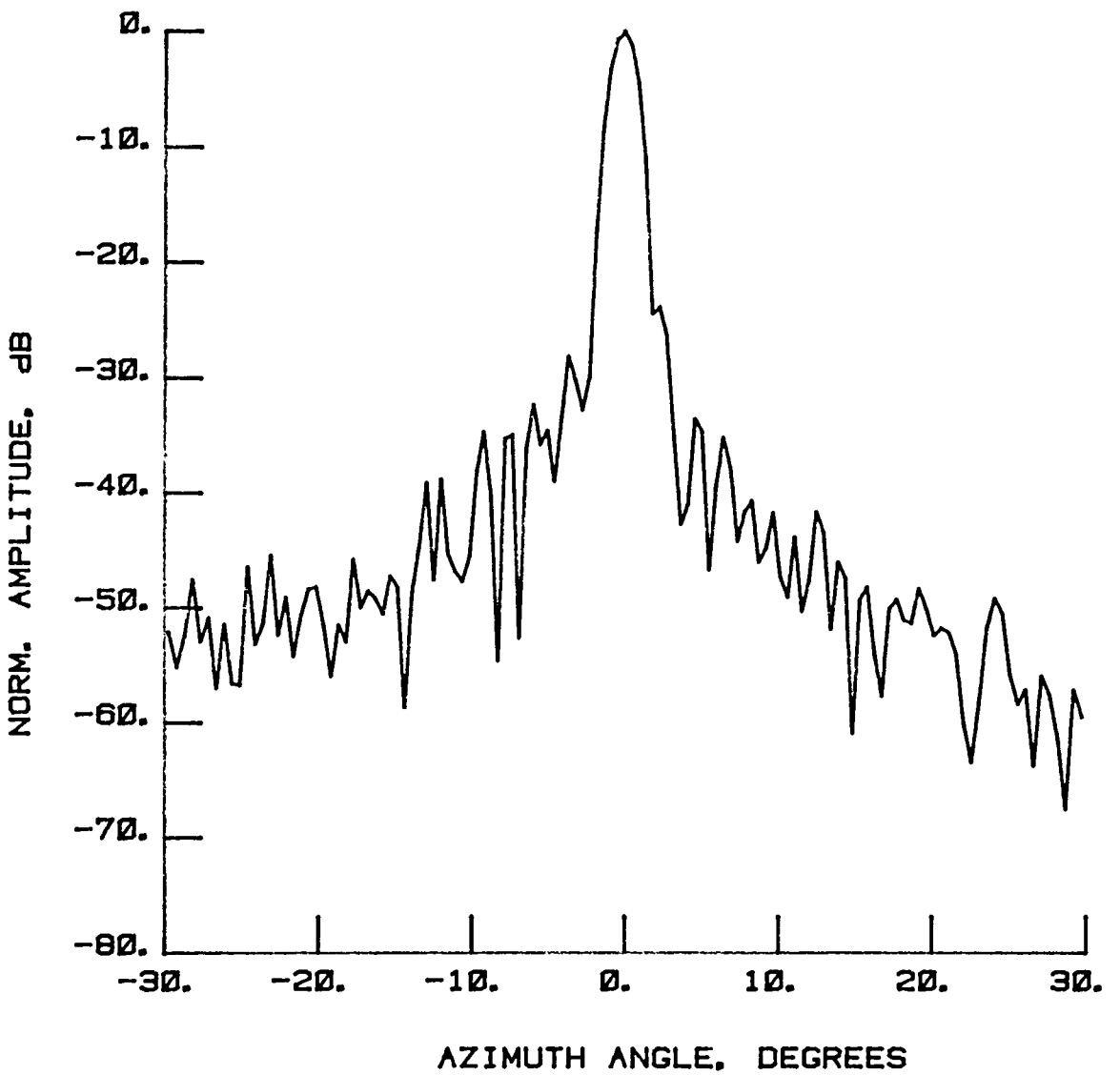

Figure 85 Test 11e, E = 0°, Port 8, Type 1

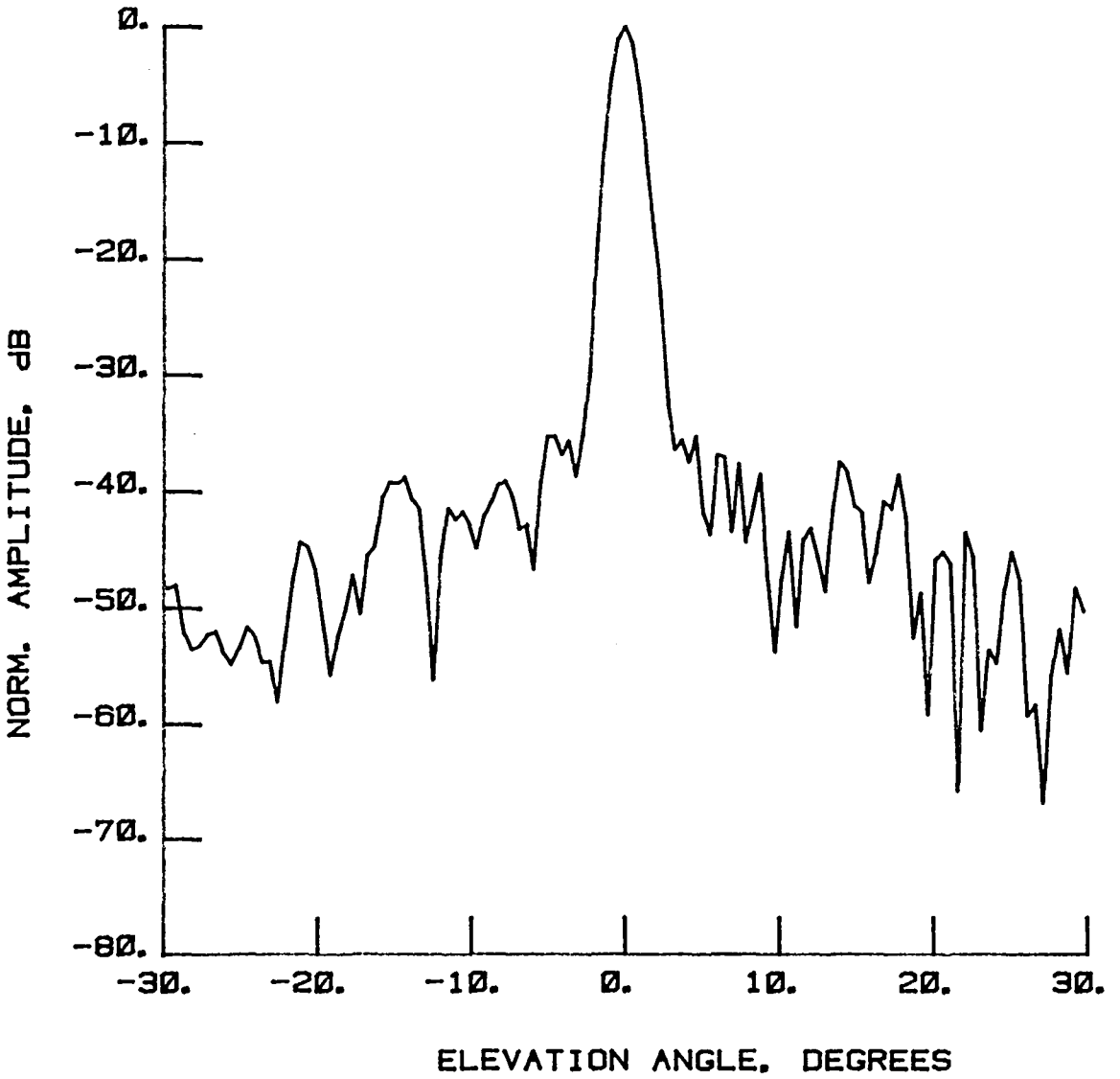

Figure 86 Test 11e, A = 0°, Port 8, Type 2

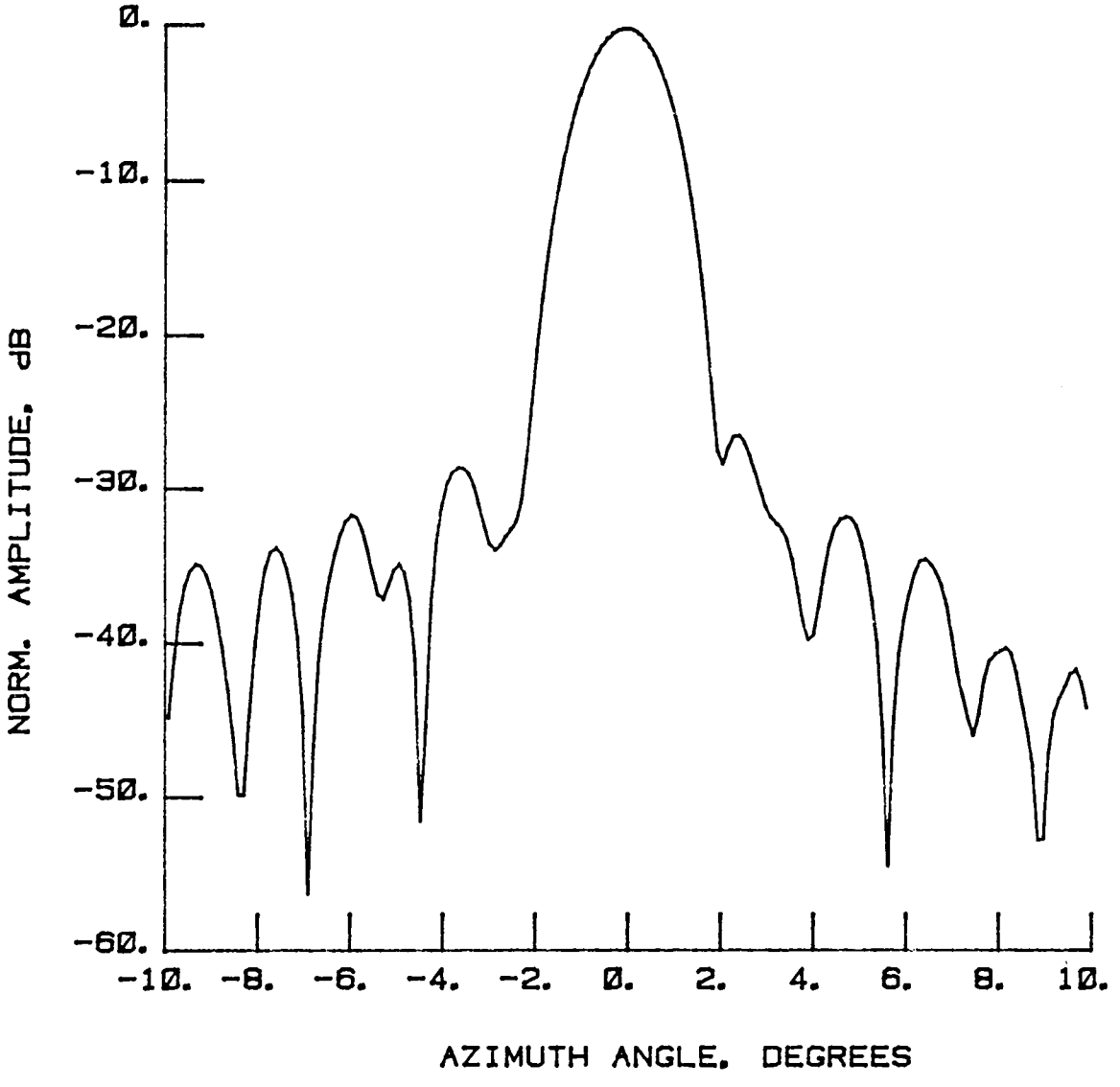

Figure 87 Test 11e, E = 0°, Port 8, Type 3

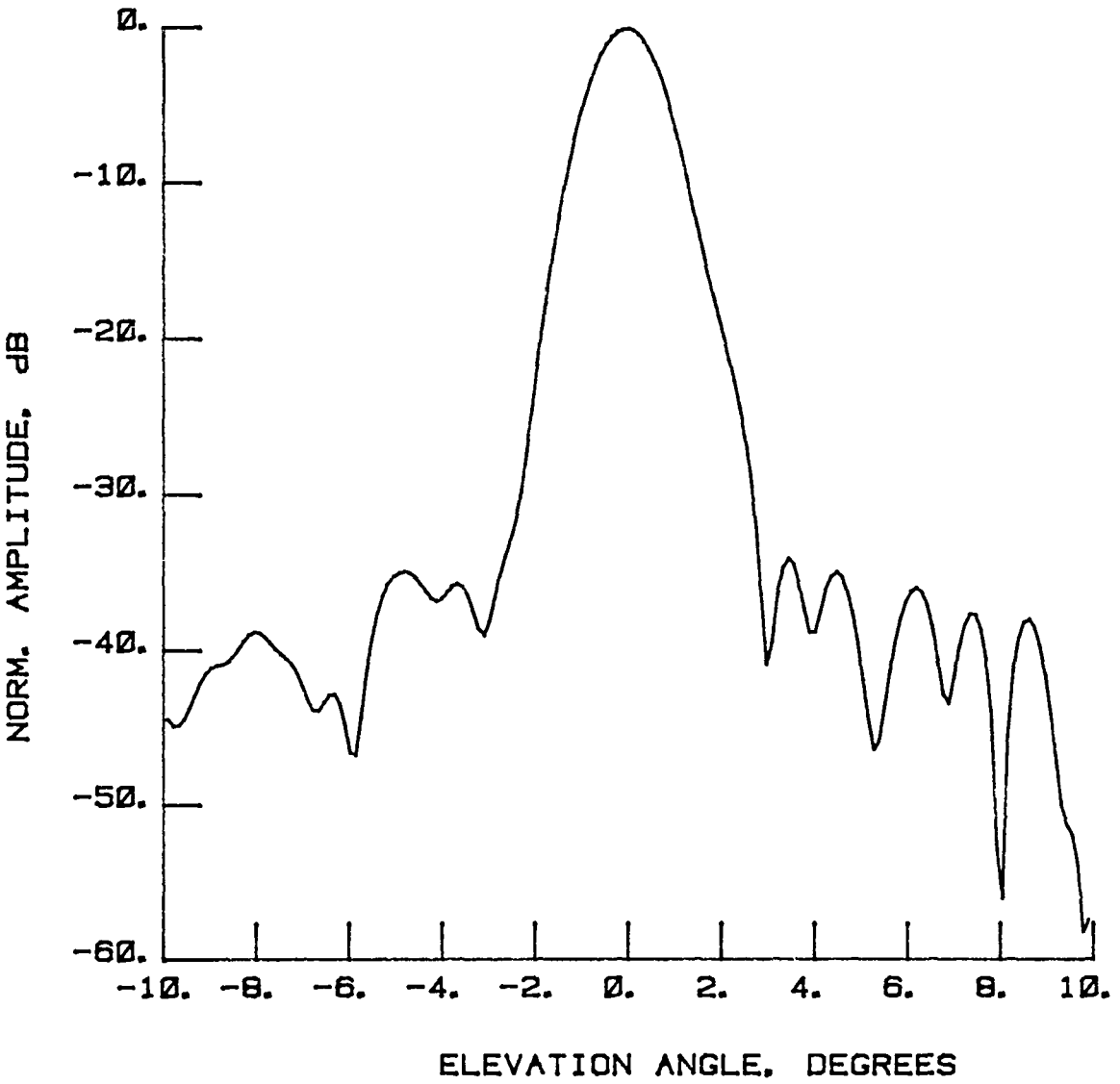

Figure 88 Test 11e, A = 0°, Port 8, Type 4

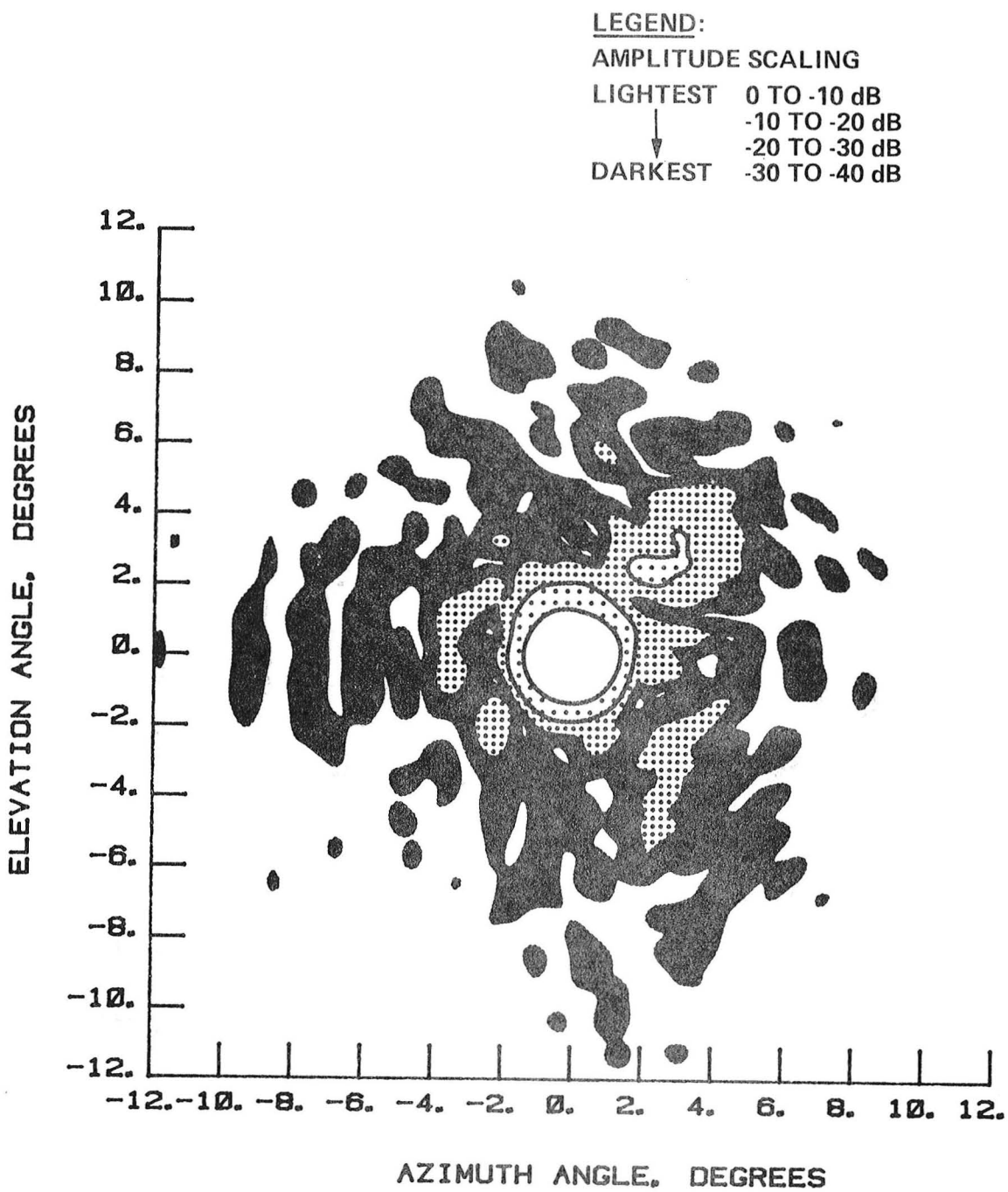

Figure 89 Test 11e, Contour, Port 8, Type 5

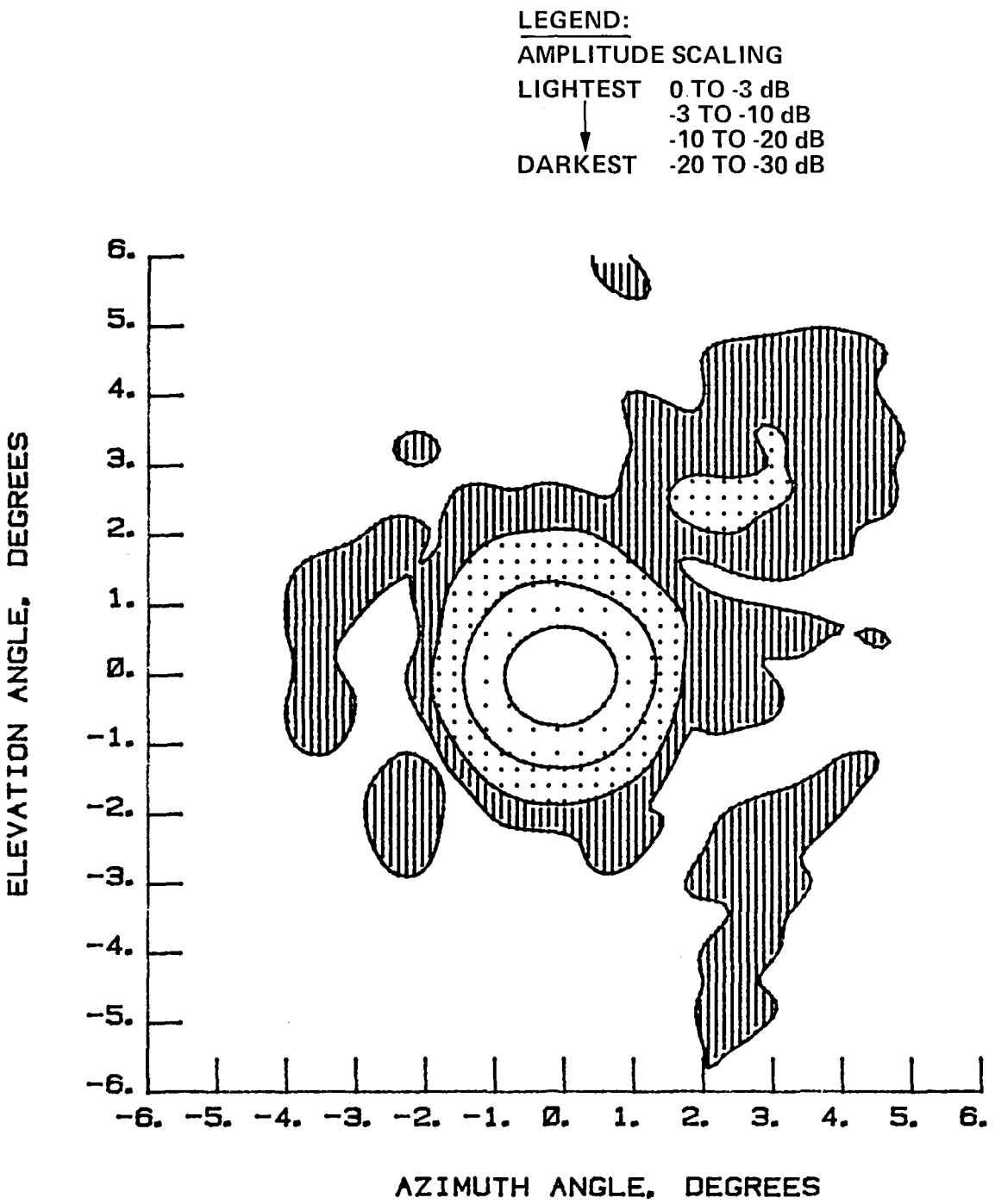

Figure 90 Test 11e, Contour, Port 8, Type 6

This Page Intentionally Left Blank

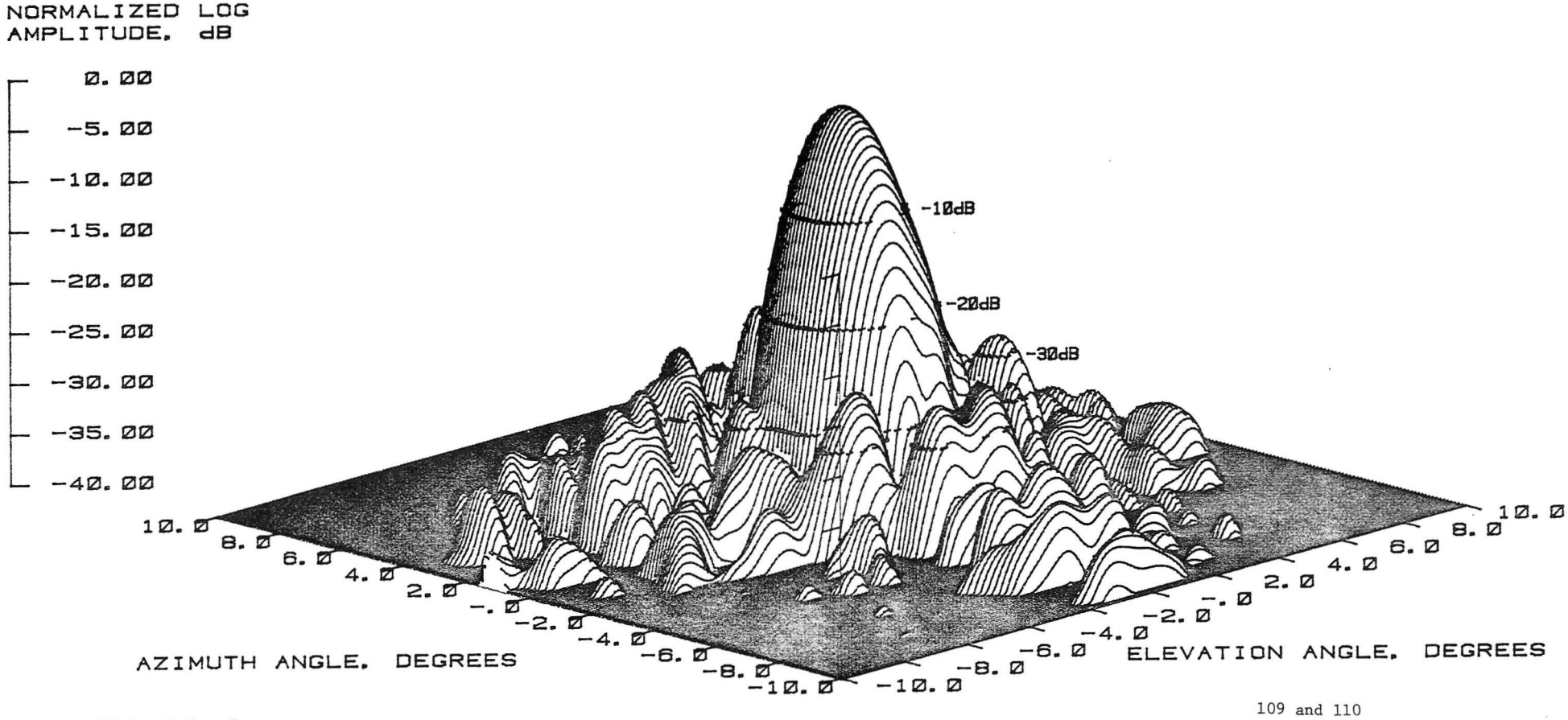

Figure 91 Test 11e, 3-D, Port 8, Type 7

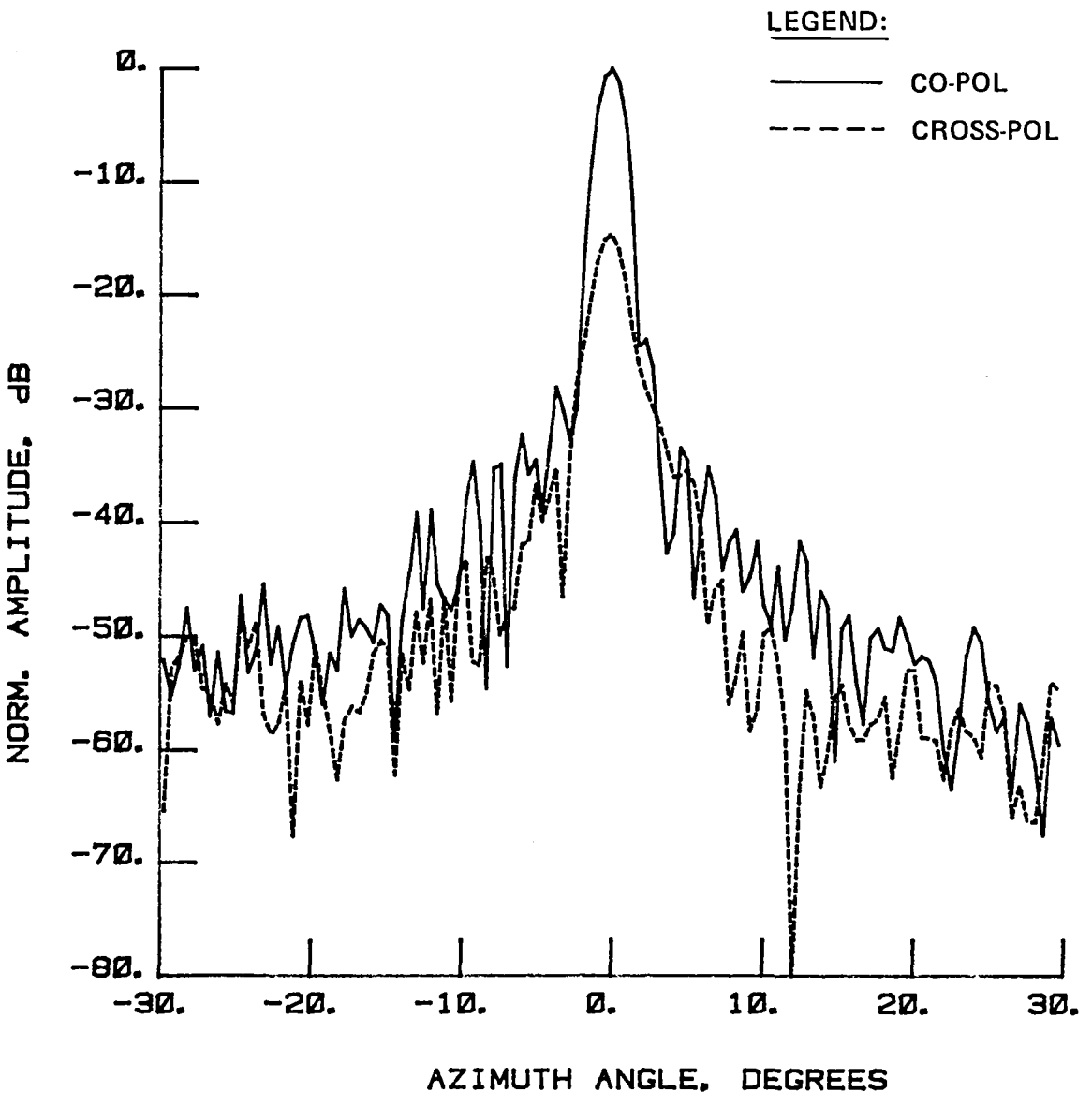

Figure 92 Test 11f, E = 0°, Port 8, Type 8

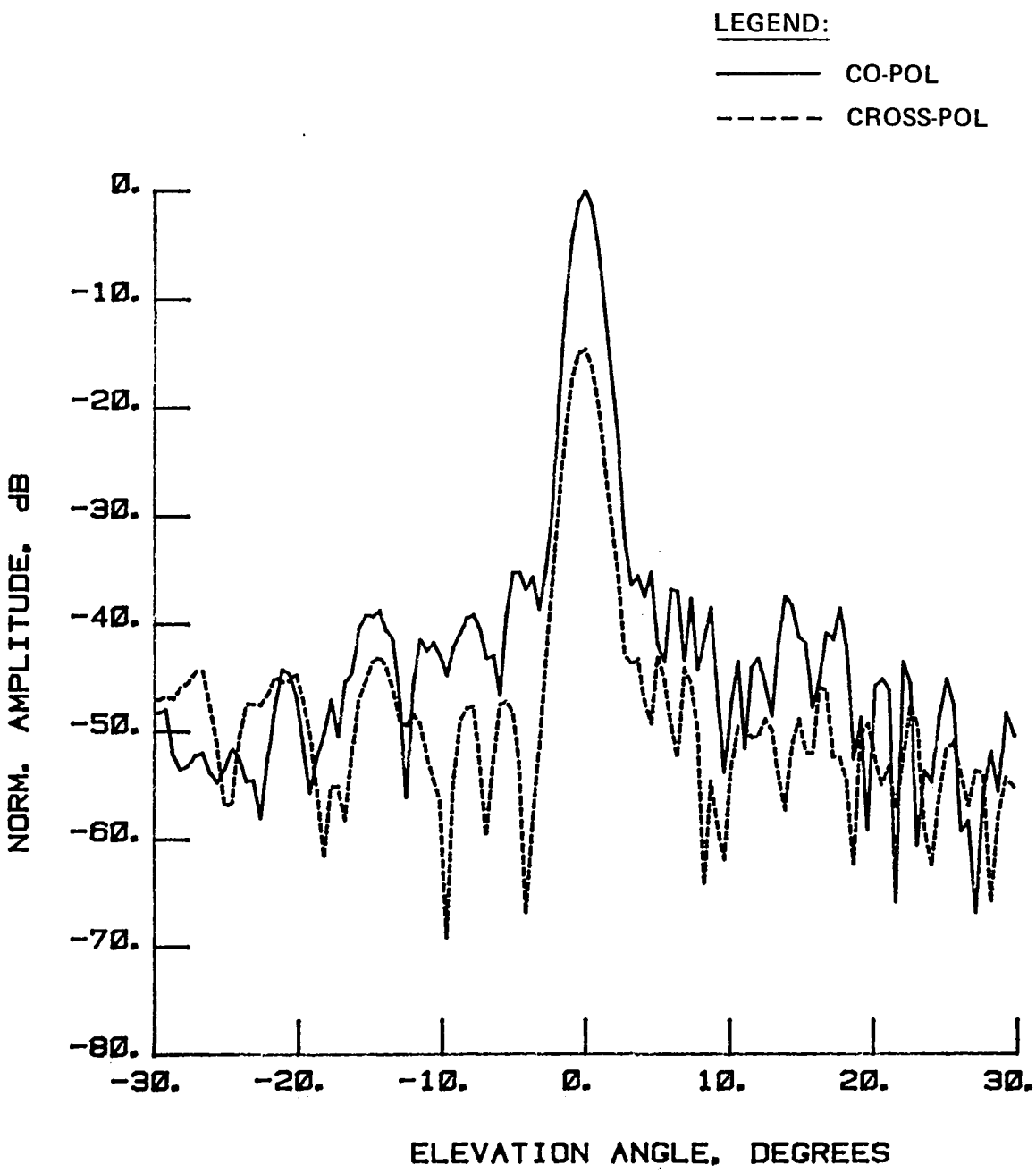

Figure 93 Test 11f, A = 0°, Type 9

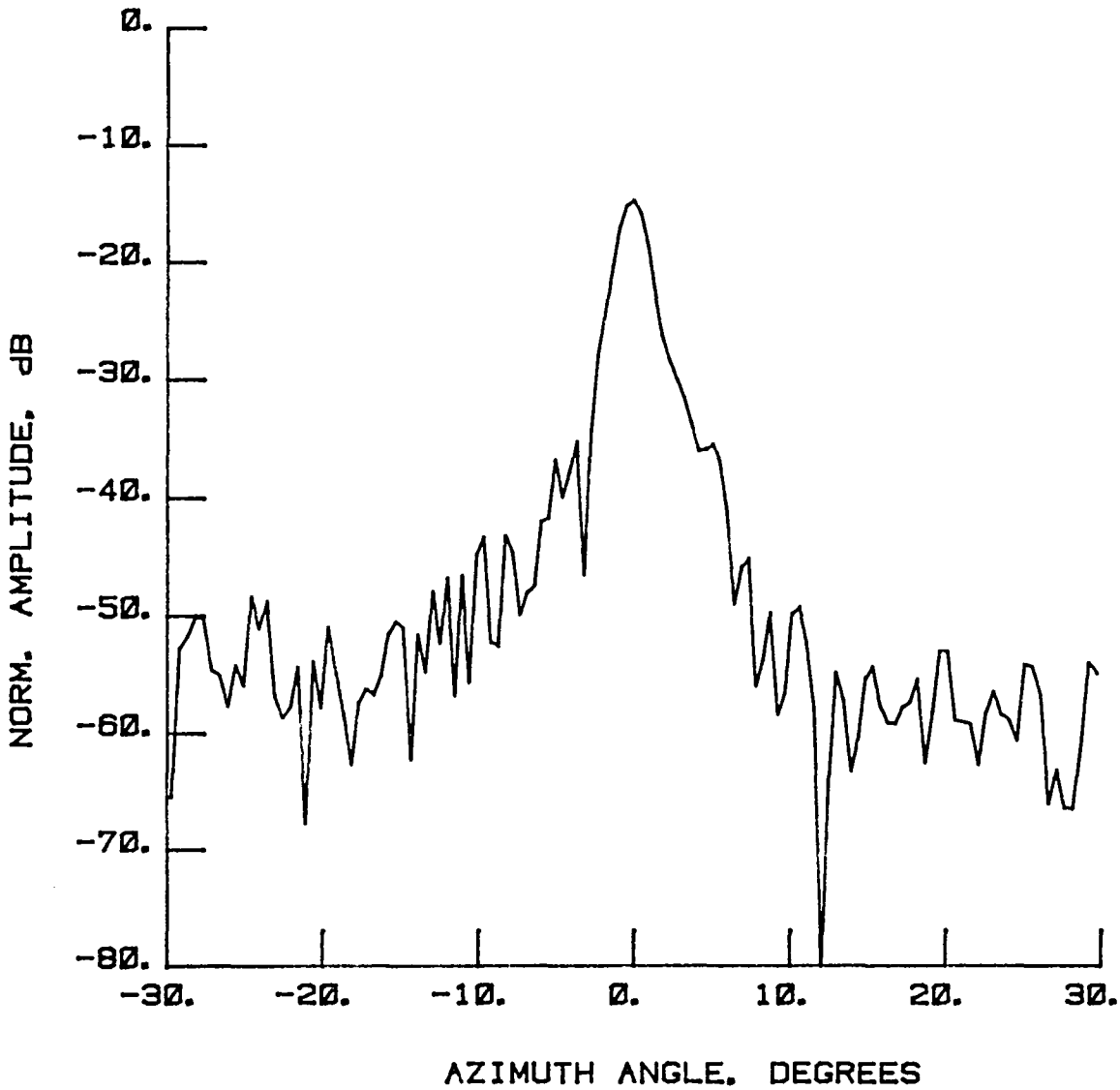

Figure 94 Test 11f, E = 0°, Type 10

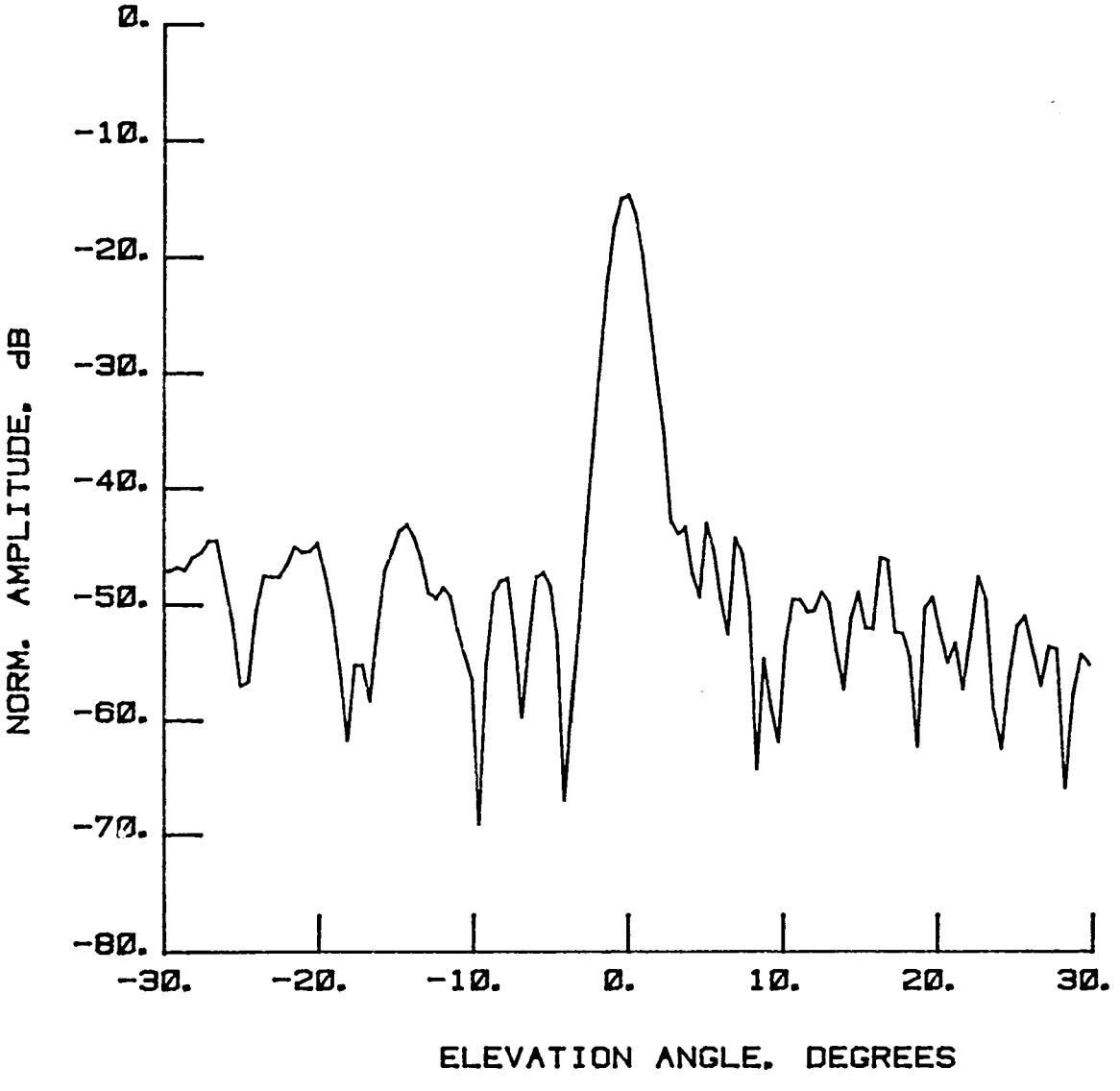

Figure 95 Test 11f, A = 0°, Type 11

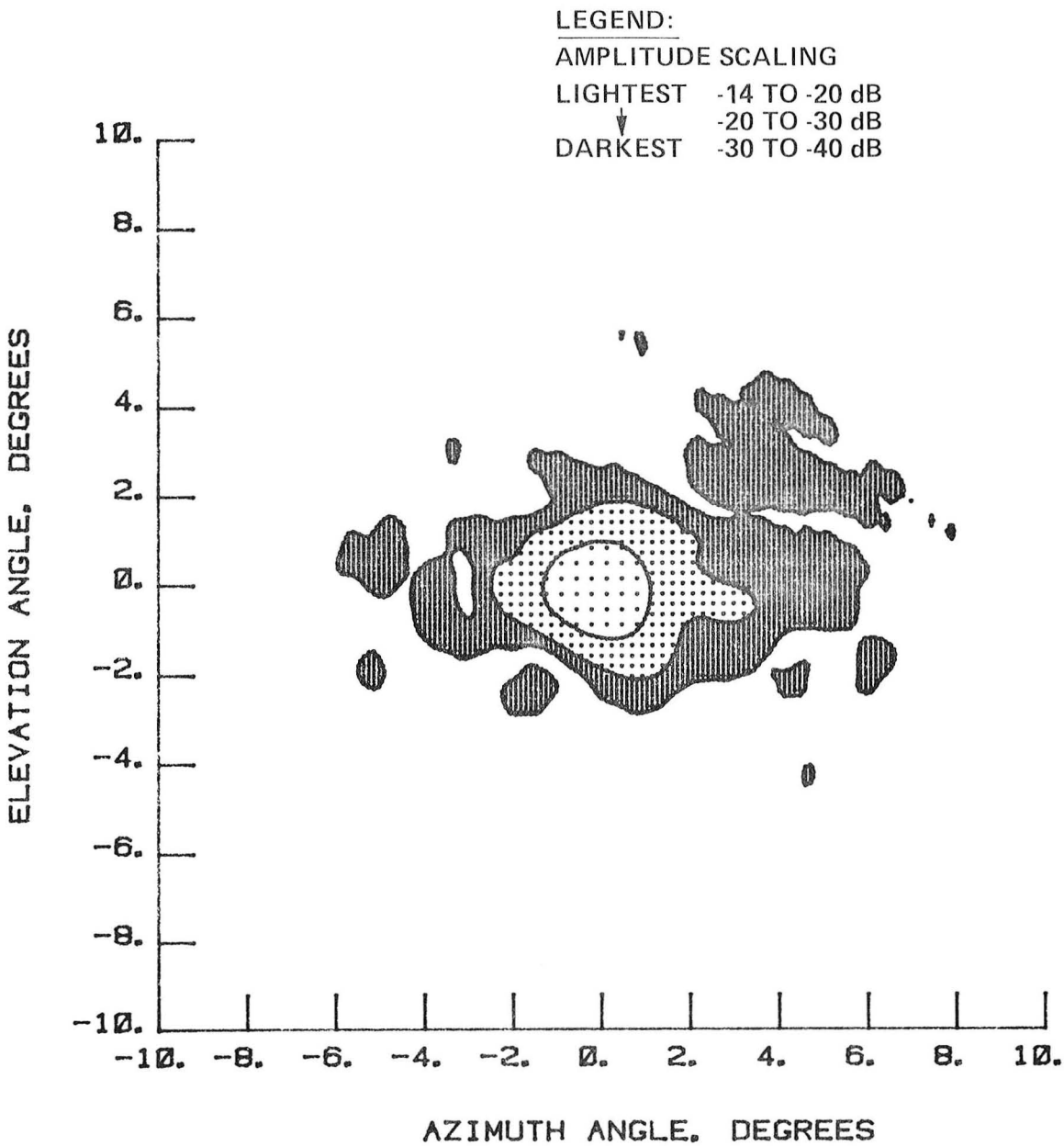

Figure 96 Test 11f, Contour, Port 8, Type 12

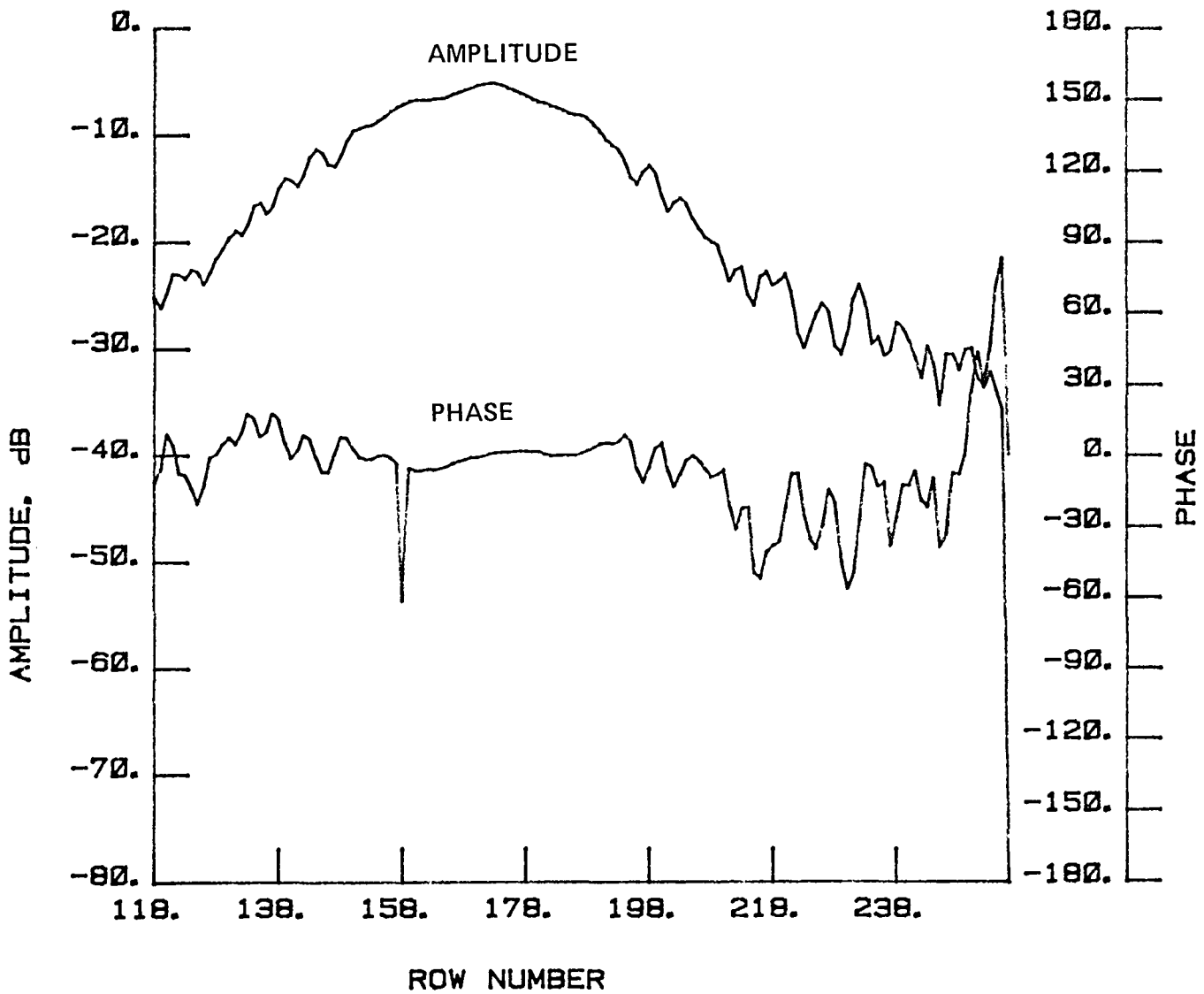

Figure 97 Test 11e, Chord, Port 8, Type 15

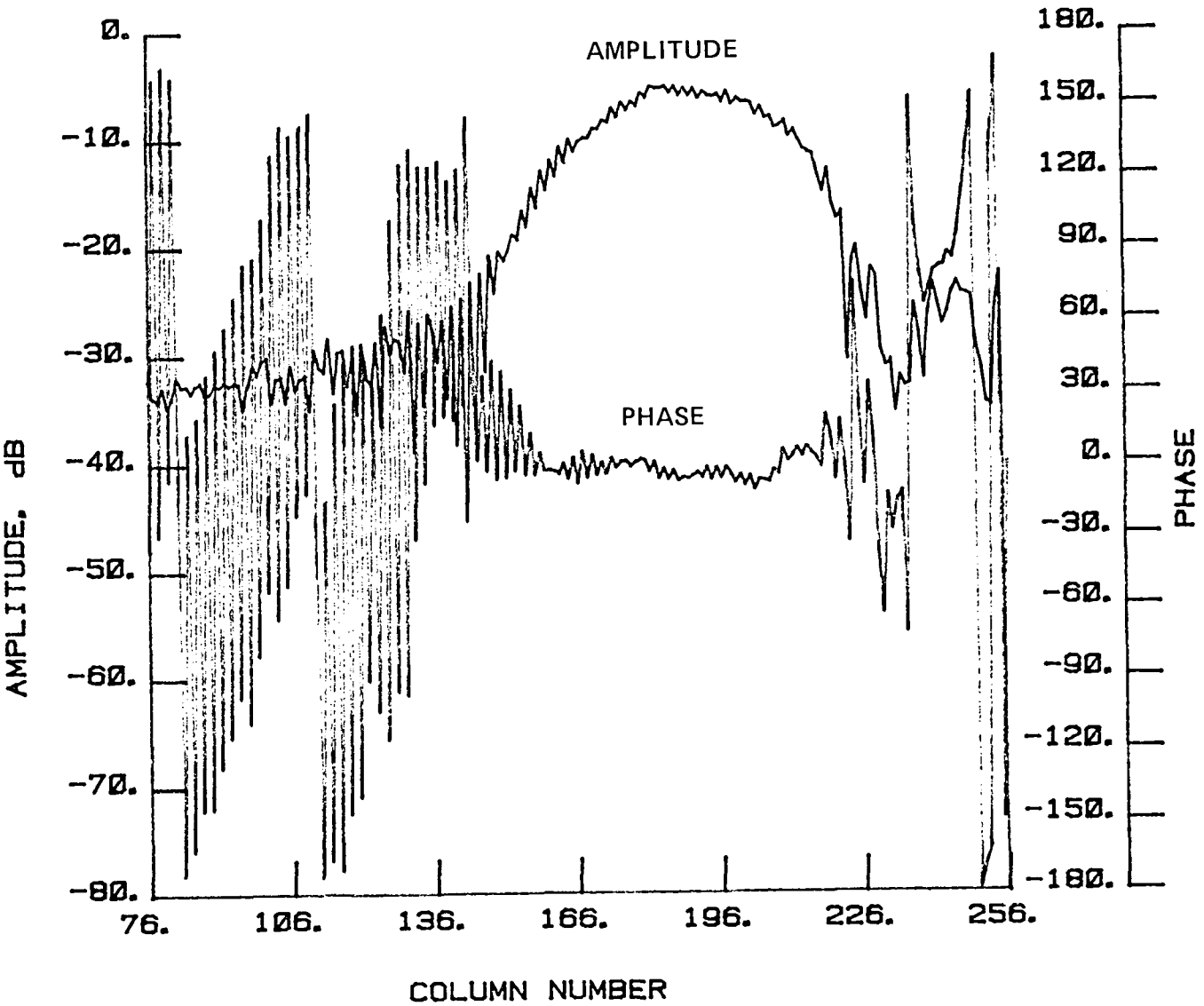

Figure 98 Test 11e, Radial, Port 8, Type 16

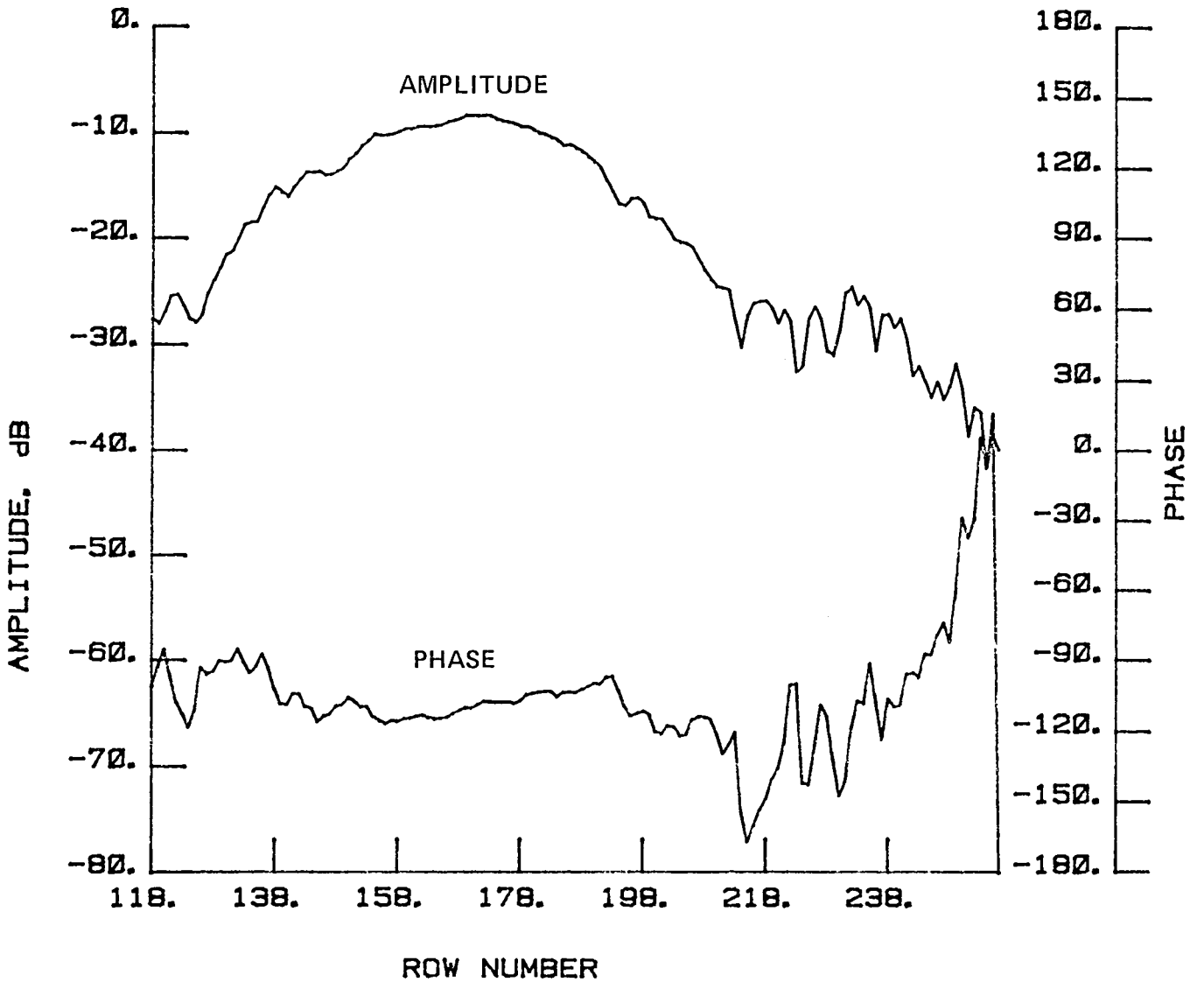

Figure 99 Test 11f, Chord, Port 8, Type 19

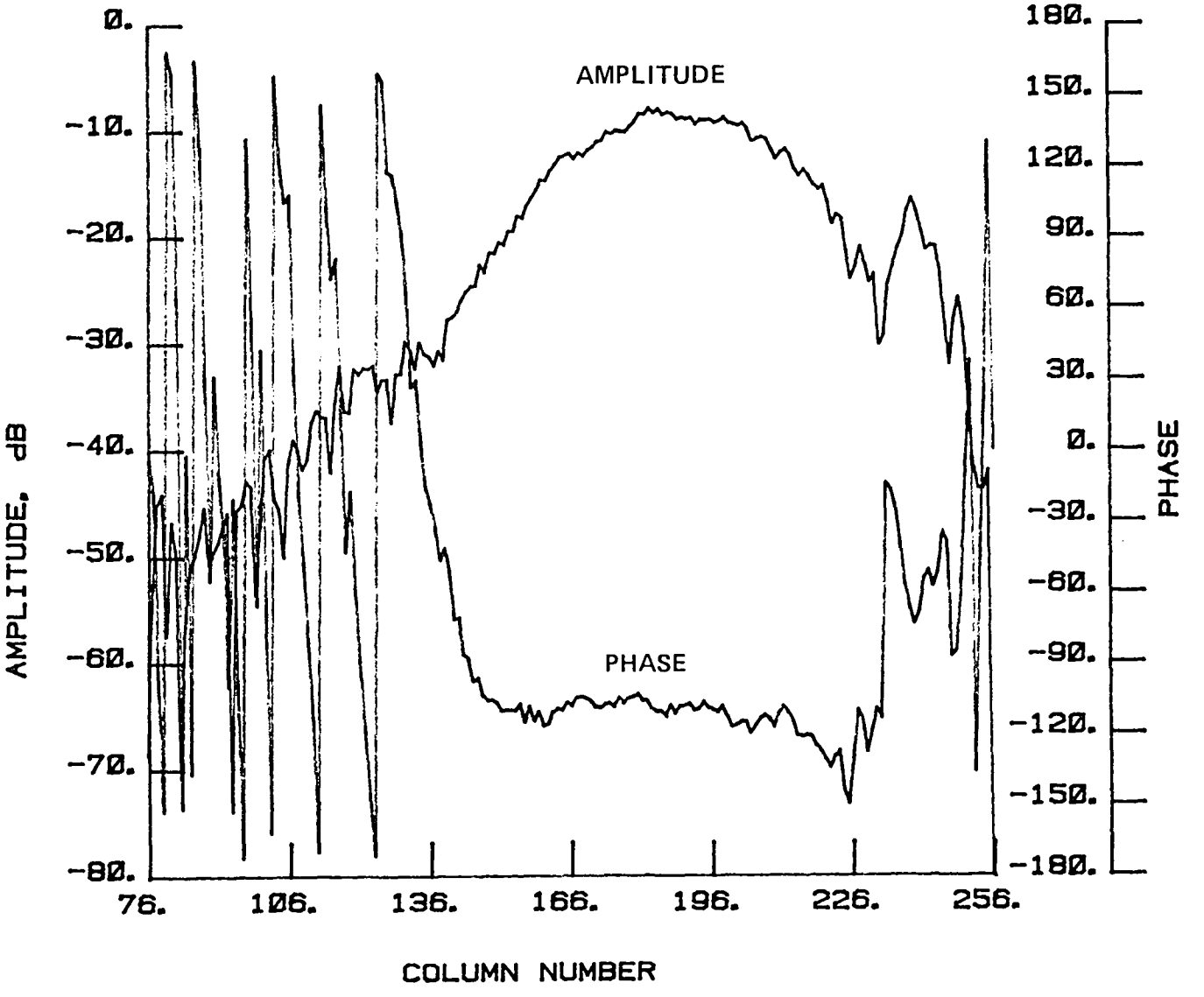

Figure 100 Test 11f, Radial, Port 8, Type 20

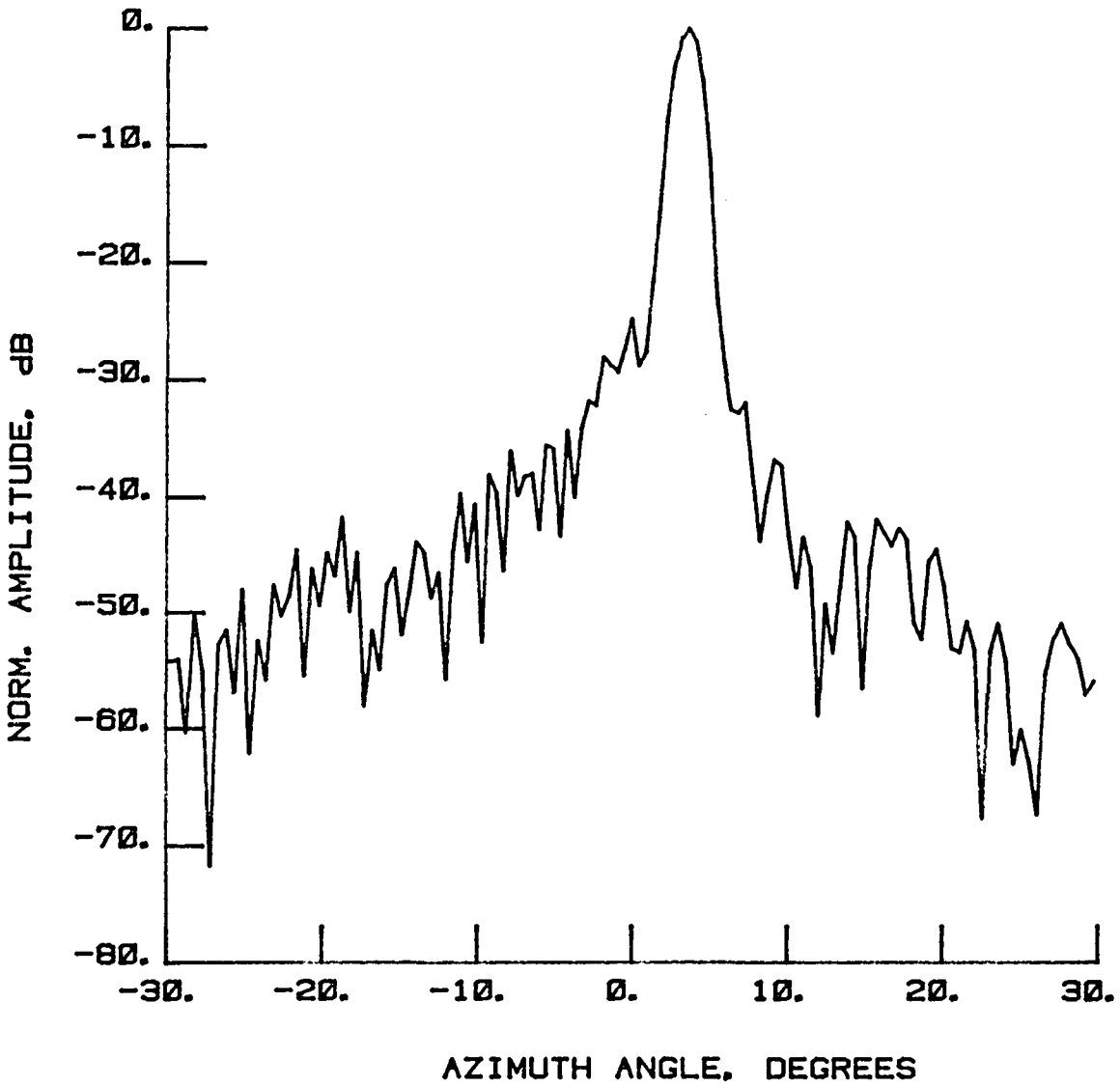

Figure 101 Test 11g, E = 0.5°, Port 2, Type 1

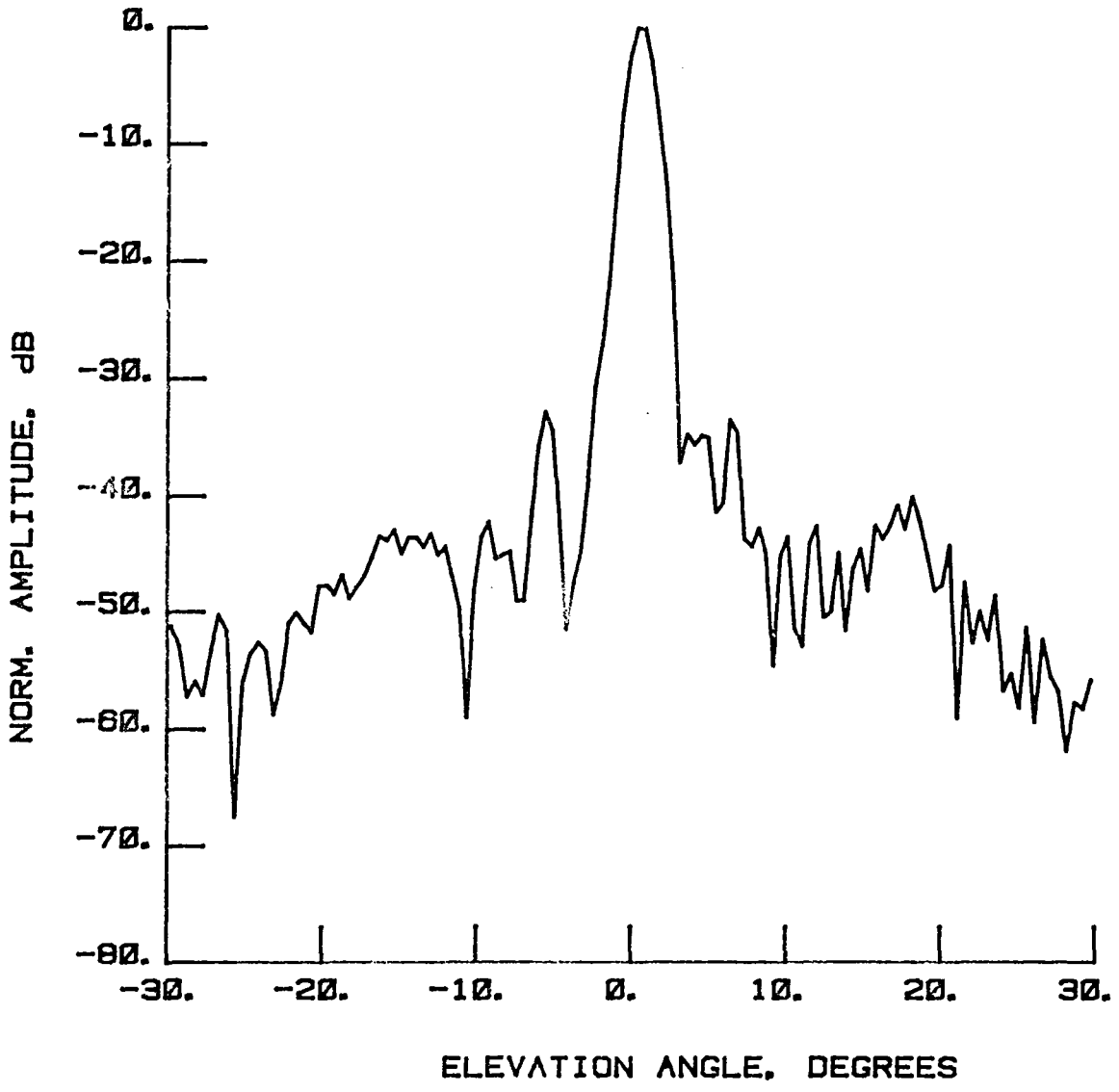

Figure 102 Test 11g, A = 3.7°, Port 2, Type 2

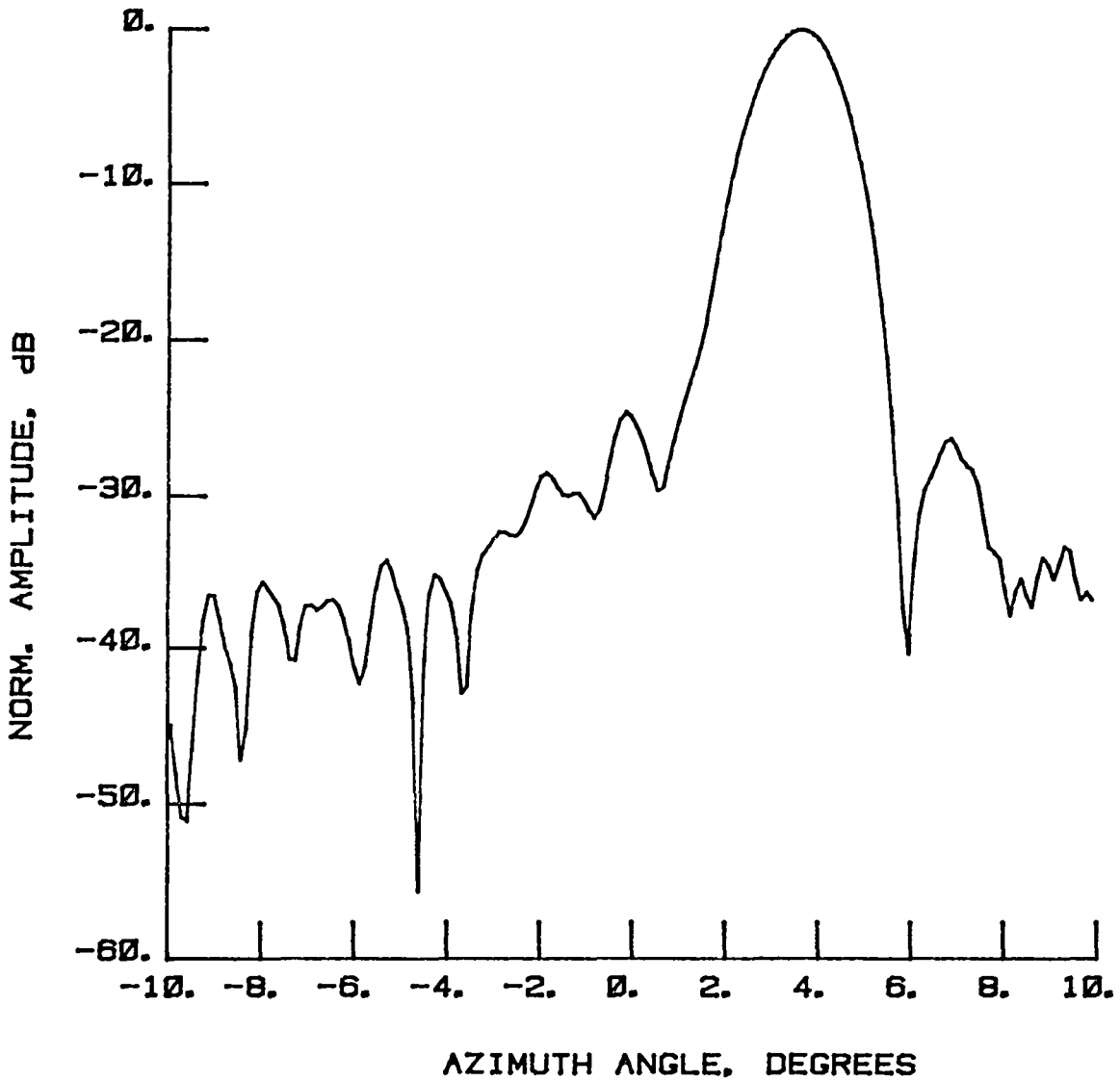

Figure 103 Test 11g, E = 0.5°, Port 2, Type 3

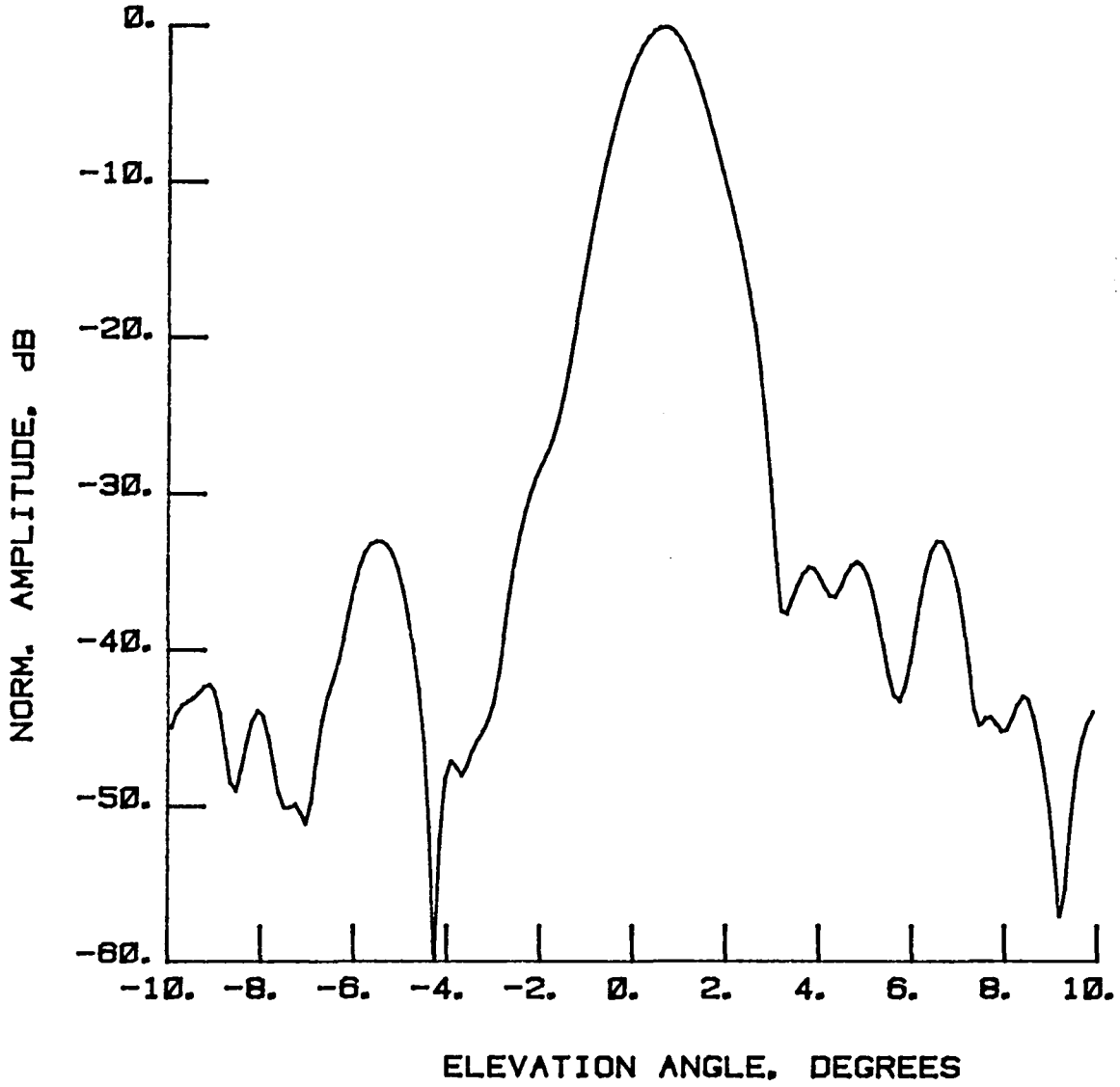

Figure 104 Test 11g, A = 3.7°, Port 2, Type 4

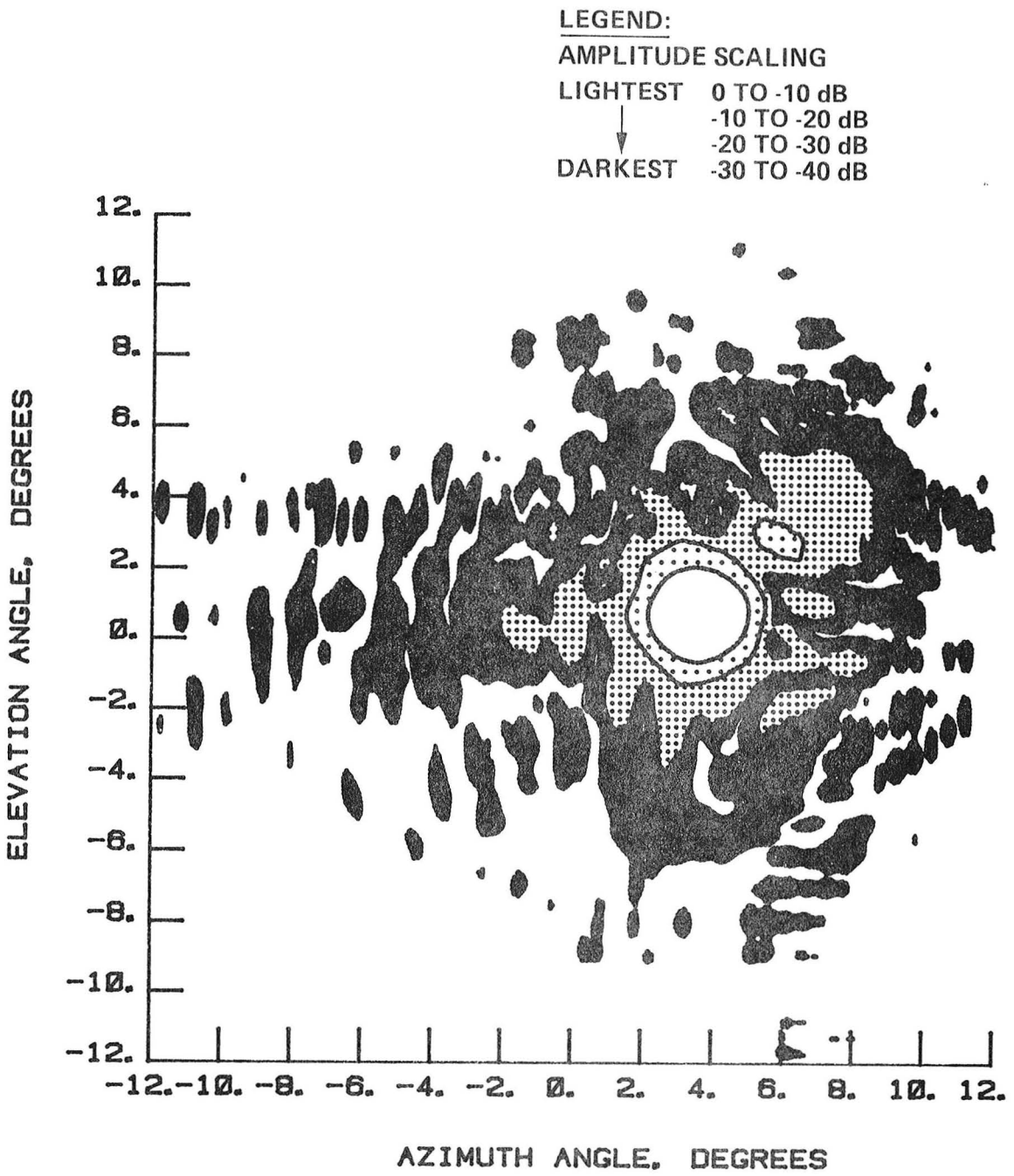

Figure 105 Test 11g, Contour, Port 2, Type 5

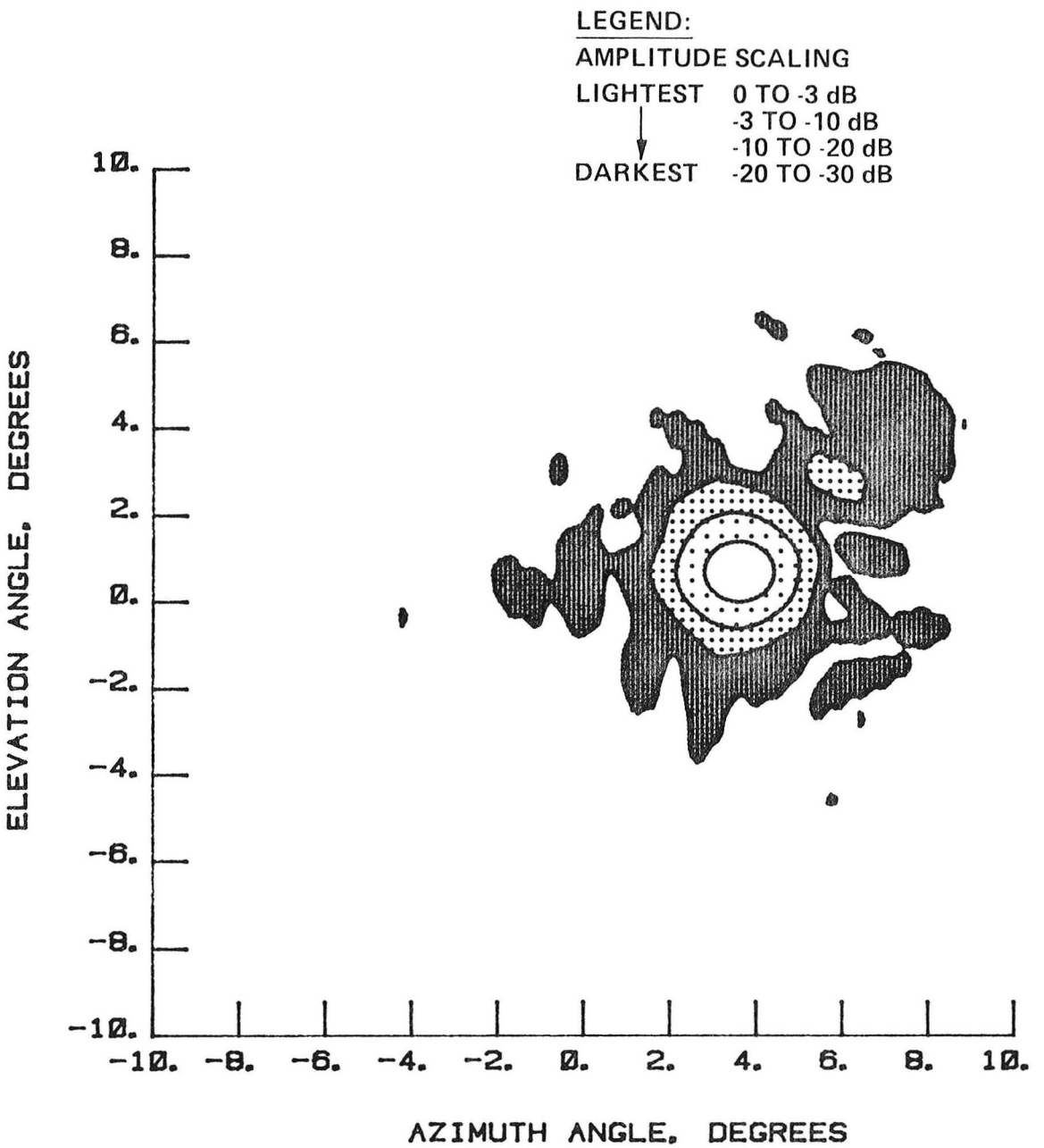

Figure 106 Test 11g, Contour, Port 2, Type 6

This Page Intentionally Left Blank

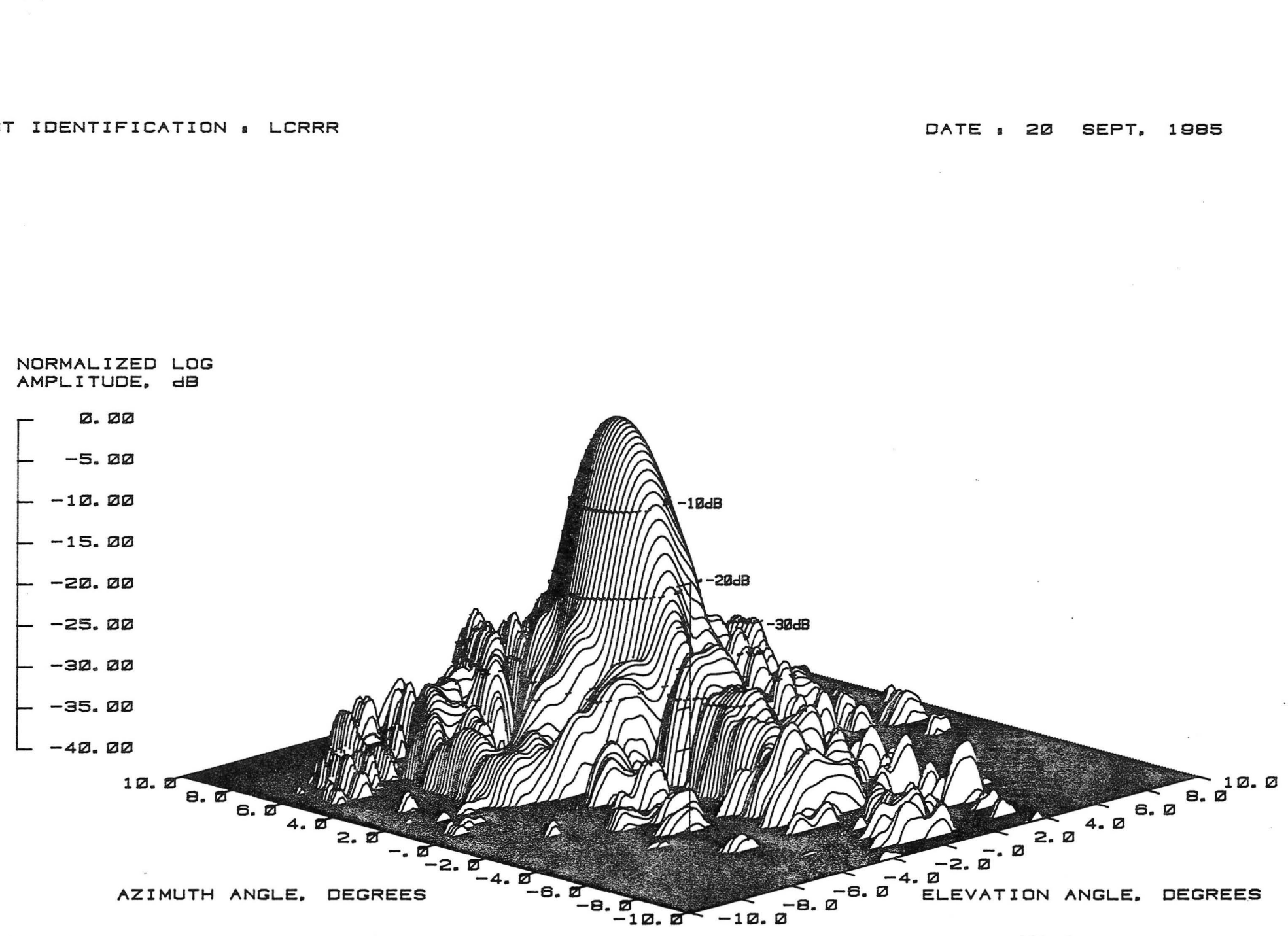

Figure 107 Test 11g, 3-D, Port 2, Type 7

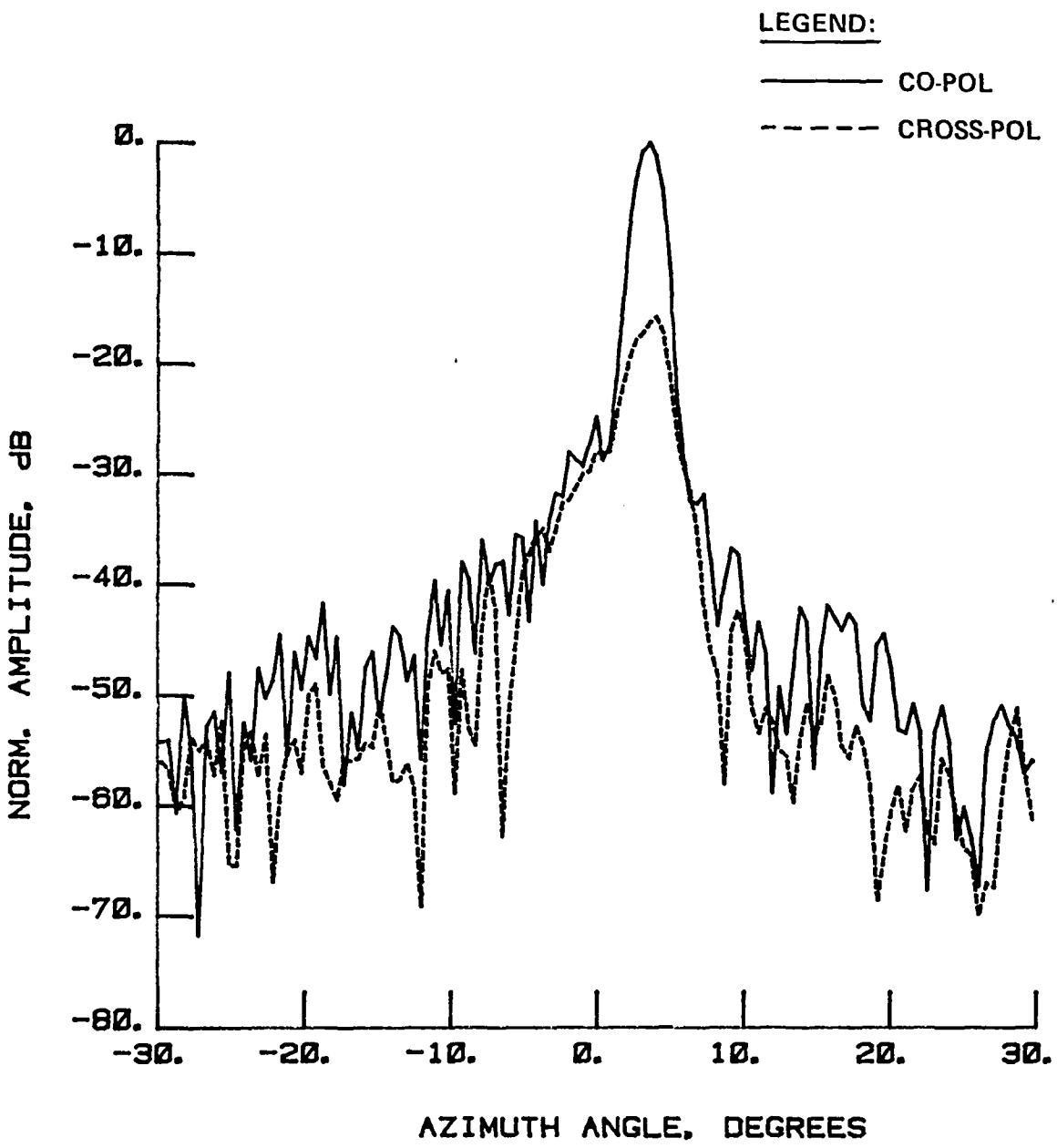

Figure 108 Test 11b, E = 0.5°, Port 2, Type 8

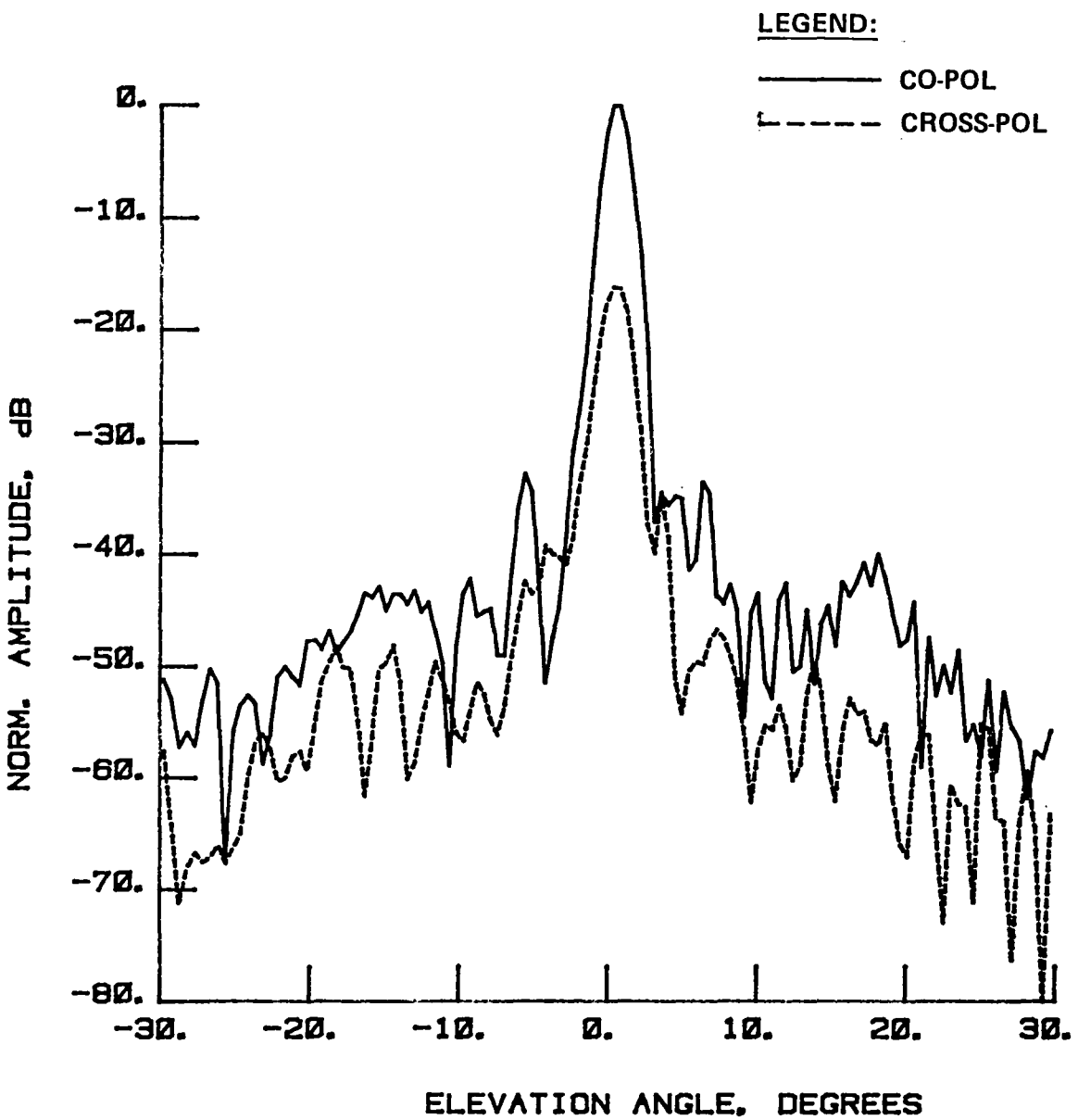

Figure 109 Test 11b, A = 3.7°, Port 2, Type 9

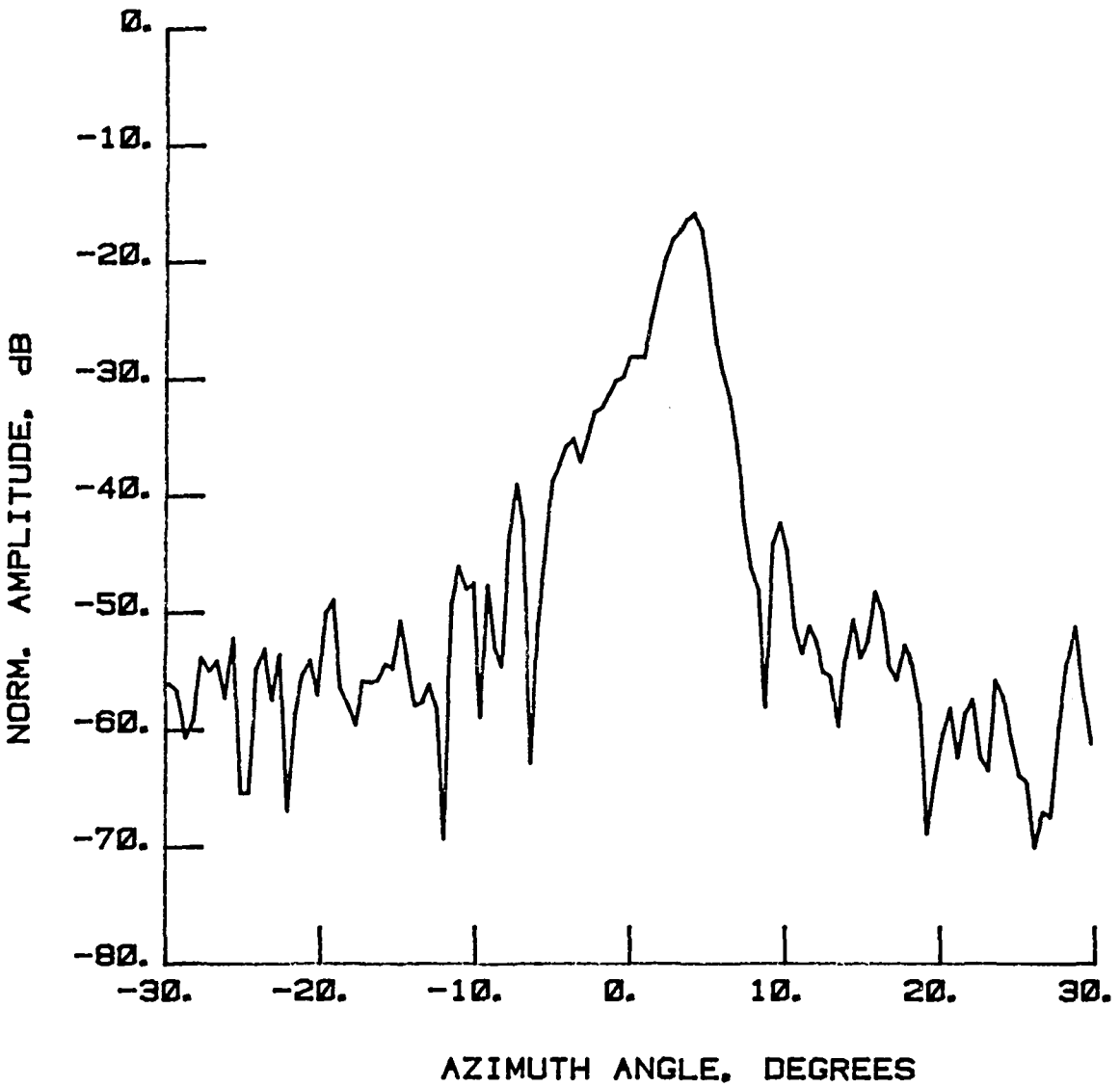

Figure 110 Test 11b, E = 0.5°, Port 2, Type 10

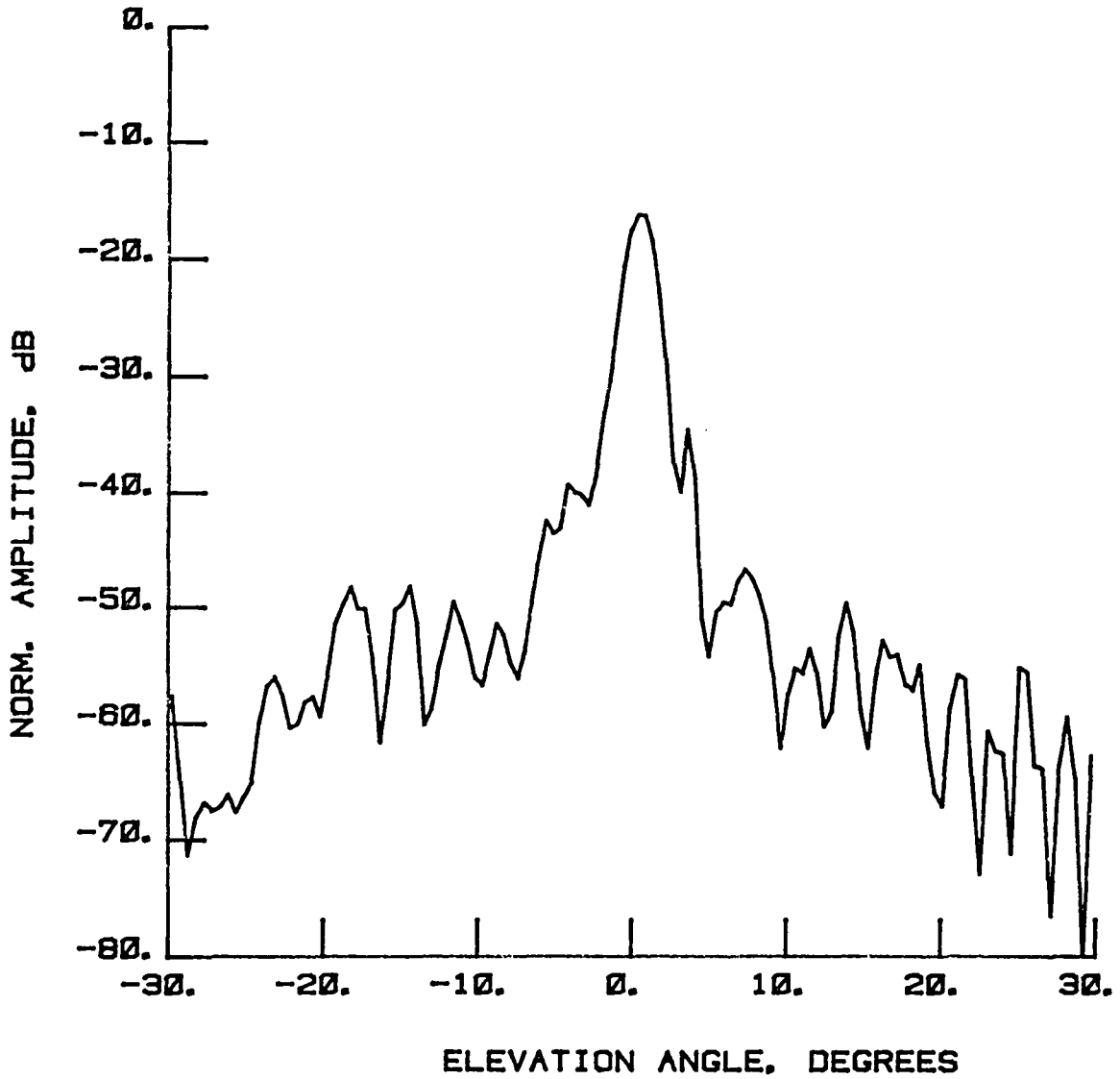

Figure 111 Test 11b, A = 3.7°, Port 2, Type 11

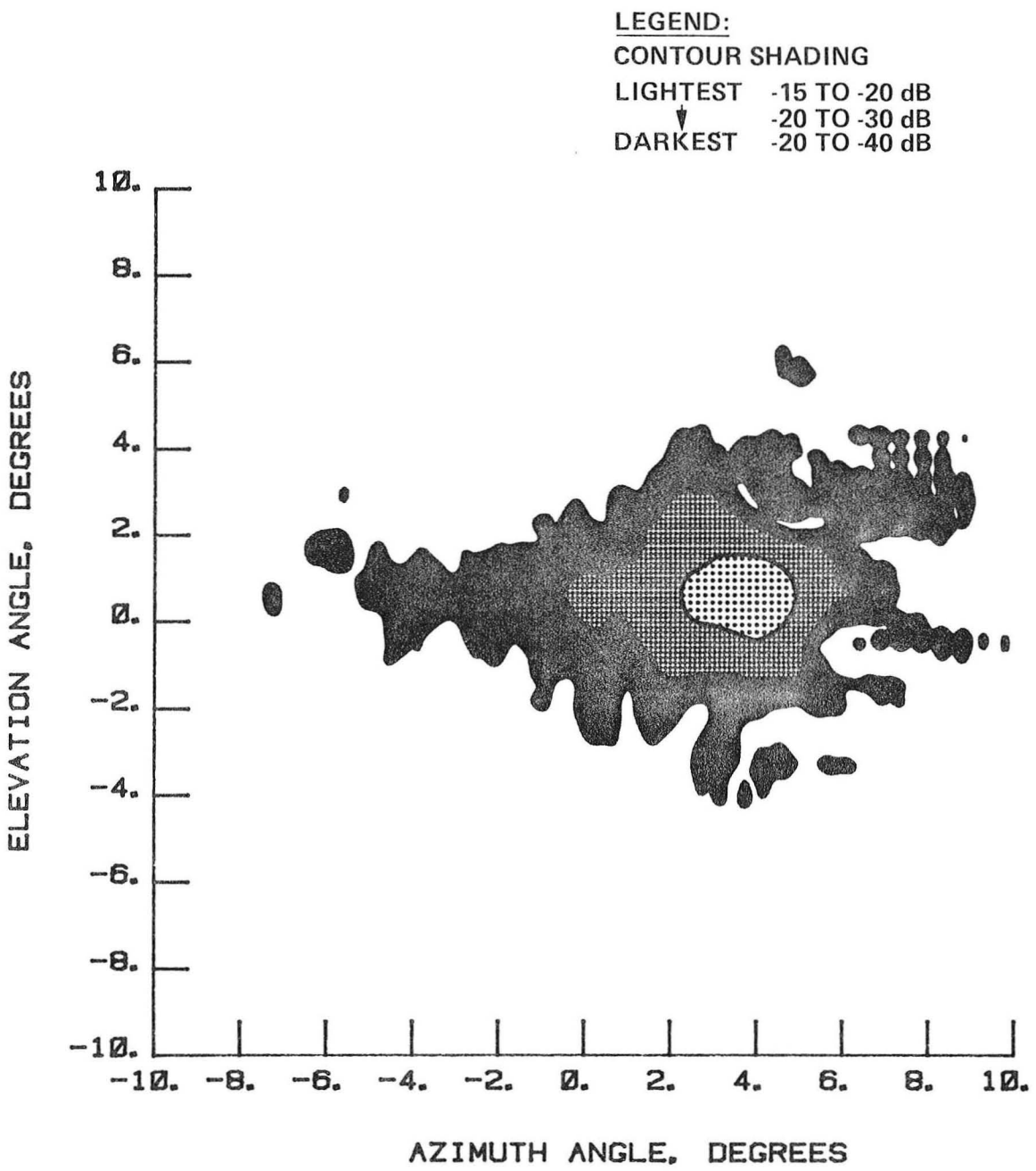

Figure 112 Test 11b, Contour, Port 2, Type 12

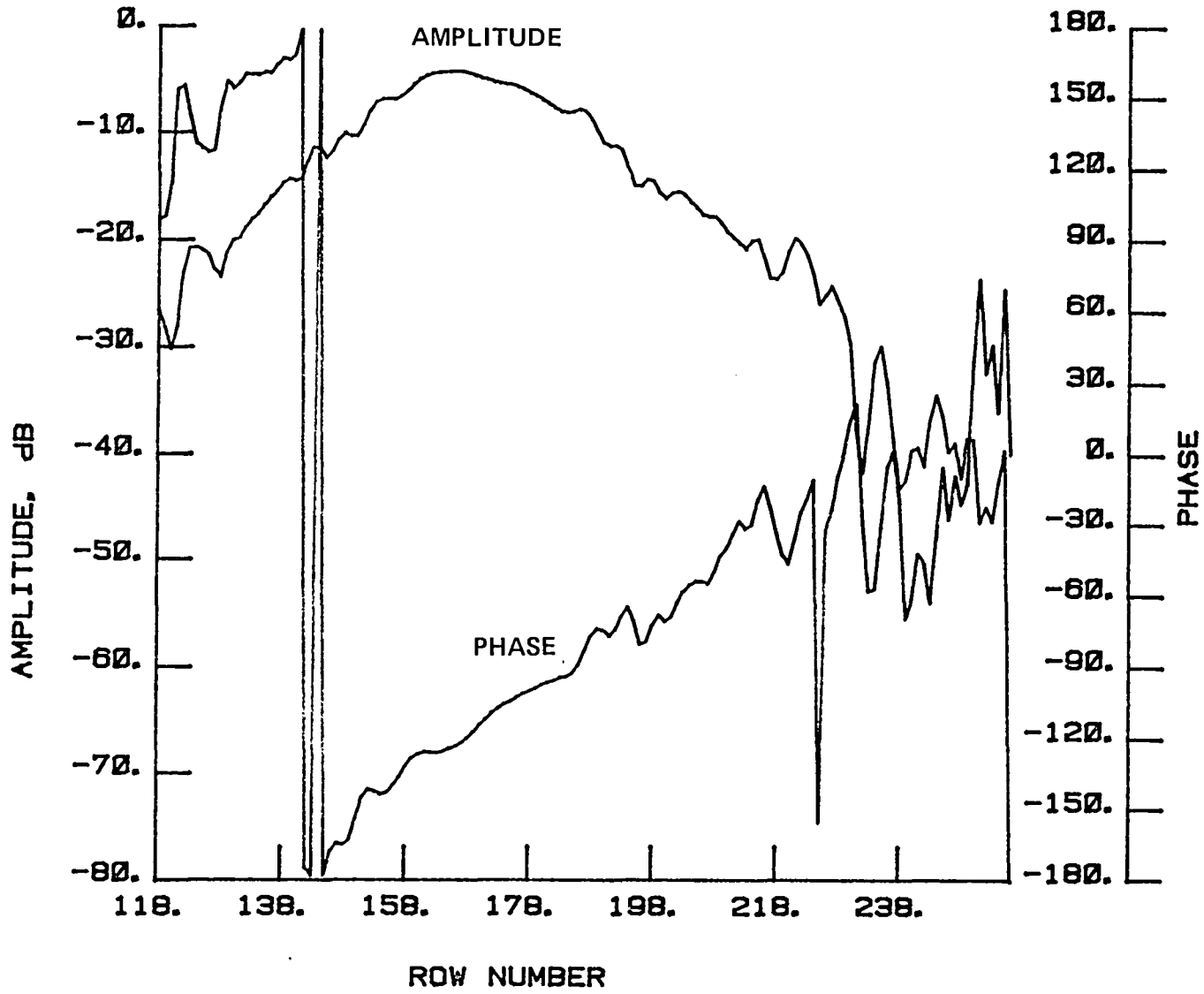

Figure 113 Test 11g, Chord, Port 2, Type 15

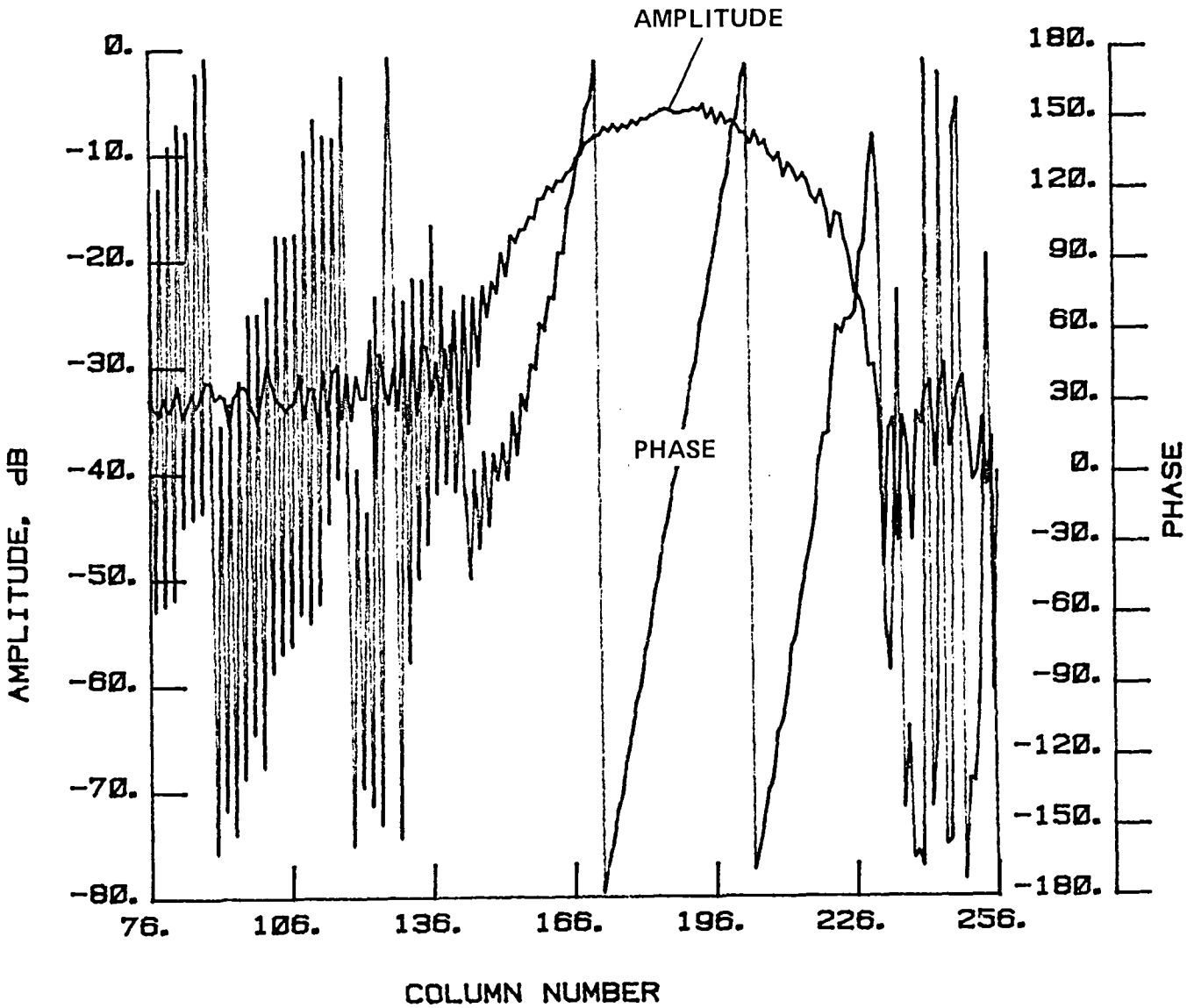

Figure 114 Test 11g, Radial, Port 2, Type 16

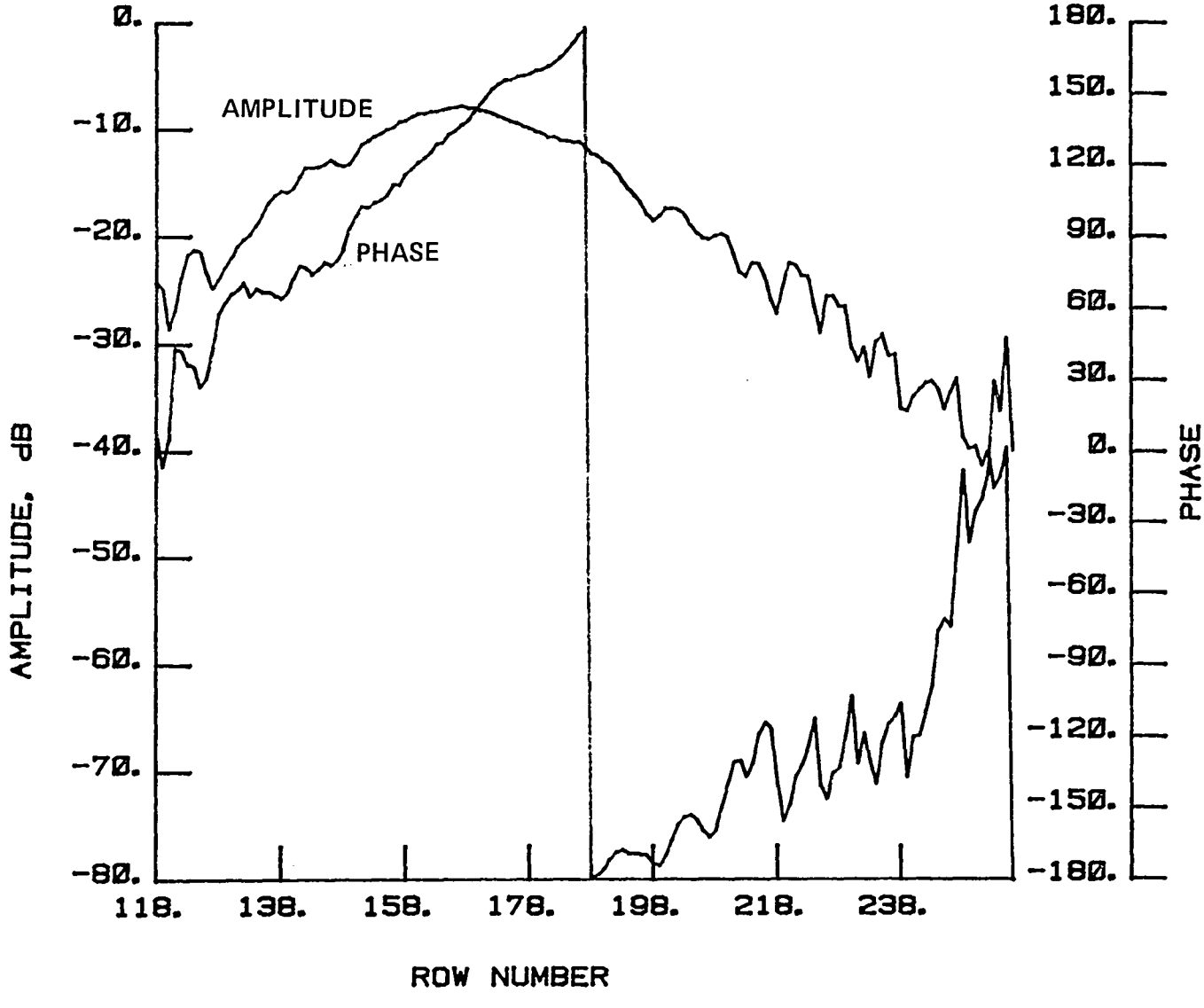

Figure 115 Test 11b, Chord, Port 2, Type 19

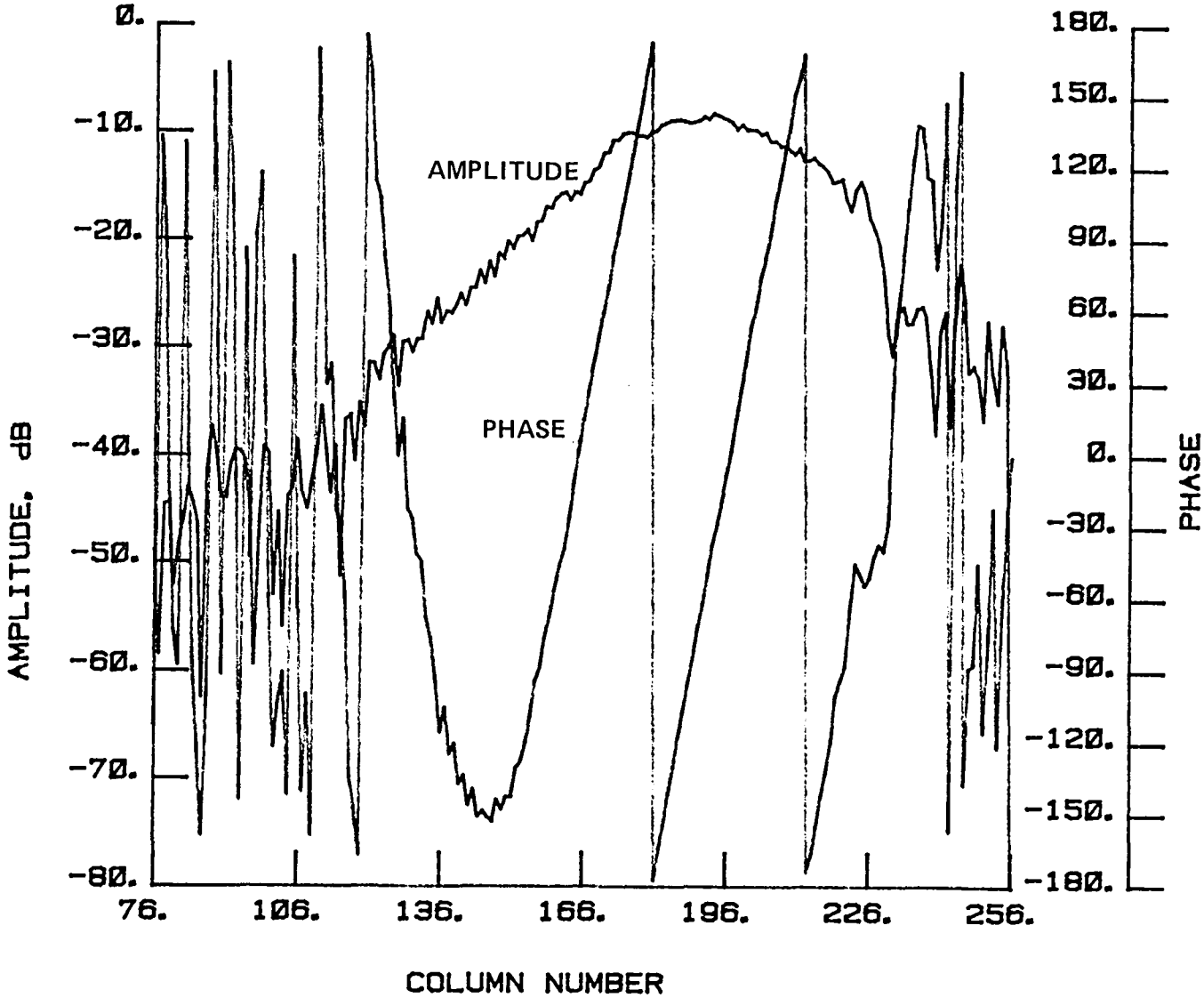

Figure 116 Test 11b, Radial, Port 2, Type 20

This Page Intentionally Left Blank

The gain of the antenna with the JPL feed was greatly reduced from the actual directivity. The components that contributed to this loss in efficiency were, in order of importance, the aperture illumination, the feed losses, and the cross-pol component. Because of the geometry of the reflector and the highly tapered feed illumination, the aperture illumination was responsible for a 3-dB loss in efficiency. The feed had an additional 8.5-dB internal loss in efficiency because of the complex design of the feed. The cross-pol component on boresight represents another 1 dB of gain loss due to impurity of the circular polarization. The remainder of the gain loss was caused by the internal losses of the feed and by the large grating lobes in the feed pattern at 70° off feed boresight. Table 4-1 gives the performance of this feed when combined with the ISM Hoop Column Antenna reflector.

The cross-pol component of the antenna was at the level predicted by JPL, much higher than the linearly polarized LaRC feeds. The sidelobe envelope was higher because the JPL feed was not designed for operation with a quad aperture reflector. Except for the sidelobes caused by the other apertures, the antenna performance was similar to that predicted by JPL.

Table 4-1 Antenna Performance

Test Numbers	Average Half-Power Beamwidth, °	Gain, dB	Peak Cross-Pol, dB	Axial Ratio, dB	Maximum First Sidelobe, dB	Maximum Sidelobe, dB
8, 9	1.50	31.76	-17.7	2.28	-20.5	-15.5
10, 11	1.47	32.02	-17.6	2.30	-22.3	-14.3
11a, b	1.49	31.91	-17.3	2.39	-29.0	-15.3
11c, d	1.48	32.01	-16.3	2.68	-25.0	-14.6
11e, f	1.52		-14.7	3.23	-26.4	-19.0
11g, h	1.49		-15.5	2.94	-24.3	-18.8

This Page Intentionally Left Blank

5.0 SUMMARY AND CONCLUSIONS

The dominant factor in all of the tests performed on the JPL feed was the illumination of the quad aperture reflector, which caused major performance degradation. With a reflector designed specifically for this feed, the co-pol far-field pattern generated by the antenna should improve dramatically. The quad aperture antenna had already shown high performance capabilities with LaRC feeds, especially at this frequency, so the JPL data cannot be considered a measure of optimal reflector performance of an antenna of this design. These tests did show two major improvement needs in the feed design: reduction of the cross-pol level and reduction of internal feed losses. Because the axial ratio represents more than 25% loss in gain as shown by Table 4-1, an optimization of the cross-pol of the array should be performed. However, these losses may decrease when the feed design is scaled to the UHF band, which has the feed design's applications.

Standard Bibliographic Page

1. Report No.	2. Government Accession No.	3. Recipient's Catalog No.
NASA CR-178061		

4. Title and Subtitle	5. Report Date
Near-Field Testing of the 15-Meter Model of the Hoop Column Antenna, Volume III - Near- and Far-Field Plots for the JPL Feed	March 1986
	6. Performing Organization Code
7. Author(s)	8. Performing Organization Report No.
John Hoover, Neill Kefauver, Tom Cencich, and Jim Osborn	MCR-85-640
9. Performing Organization Name and Address	10. Work Unit No.
Martin Marietta Denver Aerospace P.O. Box 179 Denver, CO 80201	11. Contract or Grant No. NAS1-18016
12. Sponsoring Agency Name and Address	13. Type of Report and Period Covered
National Aeronautics and Space Administration Washington, DC 20546	Contractor Report
	14. Sponsoring Agency Code 506-58-23-01

15. Supplementary Notes

Technical Monitor--Lyle C. Schroeder, NASA Langley Research Center
Hampton, VA 23665-5225

16. Abstract

This report documents the technical results from near-field testing of the 15-meter model of the hoop column antenna at the Martin Marietta Denver Aerospace facility. The antenna consists of a deployable central column and a 15 meter hoop, stiffened by cables into a structure with a high tolerance repeatable surface and offset feed location. The surface has been configured to have four offset parabolic apertures, each about 6 meters in diameter, and is made of gold plated molybdenum wire mesh. Pattern measurements were made with feed systems radiating at frequencies of 7.73, 11.60, 2.27, 2.225, and 4.26 (all in GHz). This report (Volume III) gives the detailed patterns measured with the JPL feed (2.225 GHz). Volume I covers the testing from an overall viewpoint and contains information of generalized interest for testing large antennas, including the deployment of the antenna in the Martin Facility and the measurements to determine mechanical stability and trueness of the reflector surface, the test program outline, and a synopsis of antenna electromagnetic performance. A detailed listing of the antenna patterns for the LaRC feeds (7.3, 11.60, 2.27, and 4.26 GHz) are given in Volume II of this report.

17. Key Words (Suggested by Authors(s))	18. Distribution Statement
Large space deployable antenna Near field antenna patterns Cable stiffened hoop/column Quad aperture, offset feeds	Unclassified-Unlimited Subject Category 15

19. Security Classif.(of this report)	20. Security Classif.(of this page)	21. No. of Pages	22. Price
Unclassified	Unclassified	146	A07

For sale by the National Technical Information Service, Springfield, Virginia 22161